IMPROVEMENT OF WEAR AND CORROSION RESISTANCE OF THE H13 TOOL STEEL BY USING THERMAL SURFACE TREATMENT

2020
PhD THESIS
MECHANICAL ENGINEERING

HAMDI ABDULHAMID HASAN RAGHS

Assist.Prof.Dr. M. Huseyin CETIN

IMPROVEMENT OF WEAR AND CORROSION RESISTANCE OF THE H13 TOOL STEEL BY USING THERMAL SURFACE TREATMENT

HAMDI ABDULHAMID HASAN RAGHS

T.C.
Karabuk University
Institute of Graduate Programs
Department of Mechanical Engineering
Prepared as
PhD Thesis

Assist.Prof.Dr. M. Huseyin CETIN

KARABUK
September 2020

I certify that in my opinion the thesis submitted by Hamdi Abdulhamid Hasan Raghs titled "IMPROVEMENT OF WEAR AND CORROSION RESISTANCE OF THE H13 TOOL STEEL BY USING THERMAL SURFACE TREATMENT" is fully adequate in scope and in quality as a thesis for the degree of PhD.

Assist.Prof.Dr. M. Huseyin CETİN .....
Thesis Advisor, Department of Mechanical Engineering

This thesis is accepted by the examining committee with a unanimous vote in the Department of Mechanical Engineering as a PhD thesis. September 2020

Examining Committee Members (Institutions)	Signature
Chairman : Assoc.Prof.Dr. Okan UNAL (KBU)	.....
Member : Assoc.Prof.Dr. Fuat KARTAL (KU)	.....
Member : Assist.Prof.Dr. Nuri SEN (DU)	.....
Member : Assist.Prof.Dr. Abdullah UGUR (KBU)	.....
Member : Assist.Prof.Dr. M. Huseyin CETIN (KBU)	.....

The degree of PhD by the thesis submitted is approved by the Administrative Board of the Institute of Graduate Programs, Karabuk University.

Prof. Dr. Hasan SOLMAZ .....
Director of the Institute of Graduate Programs

"I declare that all the information within this thesis has been gathered and presented in accordance with academic regulations and ethical principles and I have according to the requirements of these regulations and principles cited all those which do not originate in this work as well."

Hamdi Abdulhamid Hasan RAGHS

ABSTRACT

Ph. D. Thesis

IMPROVEMENT OF WEAR AND CORROSION RESISTANCE OF THE H13 TOOL STEEL BY USING THERMAL SURFACE TREATMENT

HAMDI ABDULHAMID HASAN RAGHS

Karabuk University
Institute of Graduate Programs
The Department of Mechanical Engineering

Thesis Advisor:
Assist. Prof. Dr. M. Huseyin CETIN
September 2020, 203 pages

In this thesis, the H13 alloy steel specimens will subject to Thermal surface treatments in order to improve and enhancing wear and corrosion resistance, and an attempt to expose H13 alloy steel samples to different experiments, and improve the length of life of H13 tool steel by increasing the hardness, toughness, impact resistance and its fatigue strength, and the ability to withstand cracking. Thus improving economic viability by limiting early failure and the ultimate goal is economic gain through delaying fail mode. To this end, we will employ a thermal treatment process to stress relieving, for the purpose of decreases stresses in H13 tool steel, which will later be heated and cooled so as to modify their physical and mechanical properties while maintaining the form and without changing the product shape, and examine elemental compositions, surface morphologies and structural properties, and tribology properties of the H13 steel in hot conditions.

In the present thesis, powder boronizing occurs in boriding and, applying boron paste, we develop a shielding layer while treating the samples with heat so as withstand oxidation. In the meantime, boronizing with powder is is carried out under a controlled atmospheric environment to prevent oxidation, and detecting the microstructures in further detail.To determine the phases formed on the surface, all materials are examined. Accordingly, the maximum surface hardness is seen to materialize with boriding process. In this respect, boronizing is shown to offer many advantages in comparison with conventional hardening methods.The boride layer has high hardening value, and maintains this property at high temperatures along with other ideal features, namely, protection against wear, oxidation and corrosion.

Moreover, microhardness measurements are carried out in various cross-sections. Additionally, Wear and corrosion resistance of the specimens was measured and checked alongside metallographic analyses of the boronized samples, later to be tested again for abrasion. The results are compared to determine the economic implications, because abrasion of these kind of materials cause financial costs, which further emphasizes the need to develop wear and corrosion resistance in such tools.

In the laboratory, we used nano-silver-doped lubricants under working conditions. The boronizing process was carried out at 700, 800, and 900 °C for 2, 4, and 8 h in a nano-boron powder atmosphere. Wear tests were conducted under dry conditions and with nano-silver-doped colloidal suspension media prepared with three different ligands. Analyses of the experimental results examined the parameters of friction coefficient, weight loss, microhardness and surface roughness.

According to the experimental results, an average coating thickness of 26.5 μm and hardness value of 2001 HV were obtained under conditions of 900 °C for 4 h. The nano-silver-doped colloidal suspension prepared with gelatin yielded 52% better friction coefficient, 88% better weight loss and 51.42% better surface dryness results than the dry wear conditions. It was determined that nano-silver-doped colloidal suspensions prepared with different ligands exhibited different characteristics in the wear environment, and also the corrosion rate decreases at 900 ° C for 4 hours and the corrosion resistance increases.

We selected AISI H13 tool steel in this research, because it has large application on tools production. Wear of extrusion dies has an important technological and economic significance due to cost to prevent die failure from thermal cracking, erosive wear, soldering and corrosion or a combination of these processes. The hardness, strength of H13 can be enhanced significantly through the application of compressive residual stresses around the surface area.

In our attempts, Structure investigations will have performed by Corrosion test , Hardness test, Wear test , Microstructure view analysis by Scanning Electron Microscope (SEM), Ultra-violet (UV), Transmission Electron Microscopy (TEM),Energy Dispersive X-ray analysis (EDX), and XRD Analysis is used to define the mechanical properties for specimens, and also 3D topography methods were used for visual and elemental analysis of the surfaces. Thus the specimens being compared to study the change of metal, and this will help us to explain properties of the samples so as to detect all variations and changes likely to occur in the course of the experiments, and also the research has made Recommendation for future work.

Keywords: Boriding, Scanning Electron Microscope (SEM), Energy Dispersive X-ray analysis (EDX), Transmission Electron Microscopy (TEM), American Iron and Steel Institute (AISI), Severe Plastic Deformation (SPD), Surface Treatment of Metals (STM), Wear resistance, Stress Corrosion Cracking (SCC),Surface Engineering (SE), Coefficient Of Friction (COF), Mechanical Properties, Surface Mechanical Attrition Treatment (SMAT), Charge Coupled Device (CCD), Corrosion resistance, XRD analysis, surface quality, Composition Structure, Erosion, Corrosion behaviour, Metal matrix composite, Mechanical surface treatments, Tribology properties, Thermal surface treatments, High temperature corrosion, Wear rate, Sliding wear, Tool steel, Micro hardness, Wear behaviour, Corrosion rate. Surface damage, Microstructure, Surface treatments, Toughness, Wear mechanisms, Structural steel.

Science Code : 91419

ACKNOWLEDGEMENTS

I want to thank my God for seeing me through this program successfully despite the all challenges along the way.

The author would like to take this opportunity to thank a number of individuals who have in one way or another made the production of this thesis possible. I would like to gratefully acknowledge these assistances from all those people who offered me their help. This thesis would not be finished without their supports, and for their significant help of this work and for contributions to my academic and professional development:

First, I would like to express my deepest gratitude to my supervisor, Dr. M. Huseyin CETIN, with whose guidance I finished the dissertation smoothly. He not only taught me the useful research methodology, but also has offered me valuable suggestions and criticisms with his knowledge in this topic and rich research experience, and instilled the necessary confidence for success. He was always there to provide encouragement, especially when I needed it most. Thank you for all of the constructive feedback, sharing of your experiences, and for helping me get to the finish line, I do appreciate his great help for this thesis.

I would like to equally express my gratitude to the Mechanical Engineering Department and graduate college for support throughout my study.

Second, I am extremely grateful to Research. Assistant. Bilgehan KONDUL in university. I cannot make this research without her supports and encouragement. In addition, Thanks are also due to my programme friends, who never failed to give me great encouragement and suggestions.

I thank all of my colleagues and fellow students for all the help and guidance throughout my research, whether it was with lab equipment or procedures, or just research questions and discussions, you have all been of great support.

Finally, I am extremely grateful to my parents for their continued faith in my abilities and all forms of support, of which I have been the fortunate recipient throughout my life.

I would like to thank my family for their support all the way during my study, and without whose support, I would have never made it to this stage.

CONTENTS

Page

Page

Page

Page

LIST OF FIGURES

Page

Page

Page

Page

Page

LIST OF TABLES

Page

SYMBOLS AND ABBREVITIONS INDEX

SYMBOLS

Ra : Roughness average

Rp : Maximum peak height

Rm : Maximum peak-to-valley height

D : Density

EW : Equivalent weight

λ : Metric conversion factor

Ra : Roughness average

σ : Standard deviation

ABBREVITIONS

EDX : Energy Dispersive X-ray analysis

TEM : Transmission Electron Microscopy

COF : Coefficient of Friction

AISI : American Iron and Steel Institute

SMAT : Surface Mechanical Attrition Treatment

SEM : Scanning Electron Microscope

STM : Surface Treatment of Metals

UV : Ultra-violet spectra

SPD : Severe Plastic Deformation

CCD : Charge Coupled Device

SCC : Stress Corrosion Cracking

PART 1

INTRODUCTION

A composite comprises two or more substances of various features to form one material that differs from them entirely in terms of characteristics. Such a definition is valid for numerous daily materials in use. To choose the right material in engineering, numerous issues are to be kept in mind. For instance, all producers know that metal alloy are distinct in characteristics and behave differently against mechanical and chemical influences. To optimize effectiveness and reduce finances, hence, it is vital to be aware of these properties and make the right choice of alloys for any given operation [1,2].

In the overall sense, the mechanical characters of metals depend on grain size, heat processing, atmosphere, and temperature. Combined, they determine the response of any metal when put to use by the industry. Producers need numerous tests to see the way these alloys are affected under what settings and up to what critical point before they fail. The criteria important in these attributes vary – among them, yield strength, hardness, the ductile-brittle transition temperature, and susceptibility to the surrounding conditions. All such factors and criteria can, hence, be altered to best fit the purpose. Temperature, for instance, can impact tenacity and elasticity up to a significant degree. Heat and surface processing, in this respect, help achieve ideal results and significantly enhance a given metal's mechanical properties of ductility, hardness, tensile strength, toughness, and shock resistance [3,4].

Quite commonly, these materials are exposed to outside factors once applied which are checked by experts and scientists of the respective fields for derangement or fragility as a function of force, time, temperature, and similar other aspects. Materials scientists, in particular, examine these changes by means of experiments so as to describe the attributes representing the real quality of the metal at issue and the best

way to process it by means of altering those qualities. To this end, the way the metal reacts while in production and while it is being applied can be improved significantly. That is to say, such features in metals can be explained in the way they behave when exposed to outside influence on the one hand, and in the way the can withstand such forces on the other [4,5].

Among these forces, atmospheric wear is a major issue and, thus deserves special attention from producers. In general, all metals can be oxidized when exposed to certain conditions in length; this effect relies on certain parameters such as the metal and its attributes, the type of protection applied to it, agents and their impact against corrosion, and whether there cracks and deformations on the surface. Field stress and tensile strength, in turn, can deteriorate with added heat and so do stiffness and fracture stress. Elevated temperatures can specifically impact steel components by causing a drop in its toughness since, with added temperature; the atomic thermal vibration can increase, in turn modifying the structural properties of metal. Other factors impact metals differently; among them, stress and strain stand out; once different samples of various dimensions are compared, one has to measure the load per unit area, and otherwise known as normalization. Stress can be obtained by dividing the force by the area. Stress and strain can makes alloys behave unfavorably and, as such, these two attributes need through testing [5,6,7].

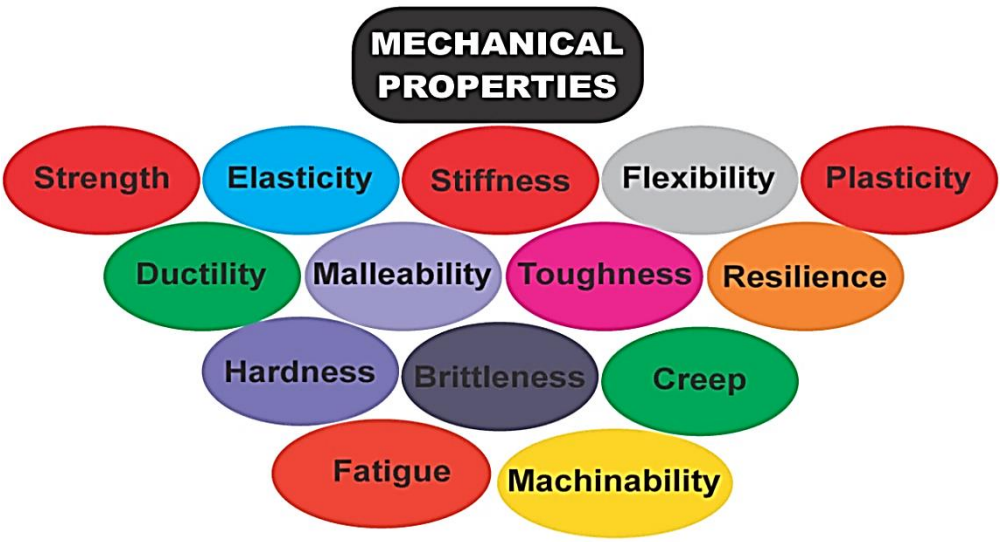

Figure 1.1. Mechanical Properties of materials [9].

Understanding material properties is essential so as to choose the right one as well as to be aware of the sources of these materials appearing in the market. To do this, having a widely-ranged scope of related knowledge becomes indispensable. Along these lines, thermal and mechanical identification of any material at high temperature has been of particular interest to many experts as supervised heating and cooling of a metal can optimize its physical and mechanical attributes and still maintain its shape as a product. Heat treatment is often carried out unintentionally and as part of the usual production line heating or cooling the material by, say, welding or forming processes. These features also play a key role in our knowledge and forecasting ability for behavior within other settings and, in this way, in identifying failures due to shortcomings in the material or in the human-related factors. The necessary changes in design can, then, be made accordingly to further resistance. All such awareness also paves the way toward other aspects of research and, in the end, enhances performance and design qualities for any engineered piece [7,8,9].

Continuous wear and tear caused by corrosion on the surface of the metal in large-scale sites eventually results in reduced productivity and, in worst-case settings, a complete overhaul of operations. Such wear and tear can occur directly as well as indirectly; to make the situations worse the overall impact of such corrosion may eventually reduce the material itself, which can be a bigger impact by itself on the operations and manufacturing. Such consequences point to a synergy that is present throughout the whole process. Despite corrosion likely to happen without mechanical wear, the latter cannot take place without corrosion; that is, corrosion is part of the wearing mechanism up to a degree and regardless of the setting and environment – unless, of course, one is in the absence of air or within inert atmospheres. Usually, these two - corrosion and wear – concur to generate very heavy losses in certain manufacturing activities as in mining, mineral and chemical treatments, pulp and paper industries, and the energy sector. The two procedures comprise numerous mechanisms, whose overall effect multiplies their strength and final impact. One of these consequences is galvanic corrosion in certain areas, including ore crushing and grinding. Wear and corrosion by-products created in this process impact the quality of the product and negatively affect later applications as the chemical and electrochemical properties of the ore are as a whole. Separately, electrochemical

reactions taking place between minerals and the grinder create galvanic coupling effects that end up adding to the corrosion wear [10,11,12].

Given the numerous ideal features it has, steel properly and commonly finds its way into numerous uses and, hence, it is the metal at issue here so as to show the many ways to prevent corrosion. Steel enjoys countless benefits in mechanical terms, among them, strength, toughness, ductility, and dent resistance, not to mention ease of production, flexibility, weld ability, and paint-absorption. Other benefits are abundance, ferromagnetic features, environmental-friendliness, and economics. As this metal is prone to rust when there is humidity, as well as to oxidation in higher temperatures, to take advantage of all these benefits one has to provide some form of coating and resistance. For corrosion, this is done by alloying processes – in other words, applying alloyed and more costly corrosion-resistance steel instead of simple carbon or low-alloy steel, environmental compromises via drying or applying inhibitors, and also monitoring the electrochemical potential through the use of cathodic or anodic currents, also known as cathodic and anodic protection [12,13,14].

Given extreme temperatures and friction in mines, corrosion and wear stand out as prime issues of concern in manufacturing, while vast sums of money are wasted as a result of overhauls, worker accidents and unanticipated fixes due to worn out tools. Despite spare part changes and fixings cannot be done without in mining operations, certain things can be done as well to reduce related losses caused by constant use in unfavorable settings. There are techniques to reduce the counter effects of wear and corrosion, specially in case of major components like heat-resistant steel castings [15,16].

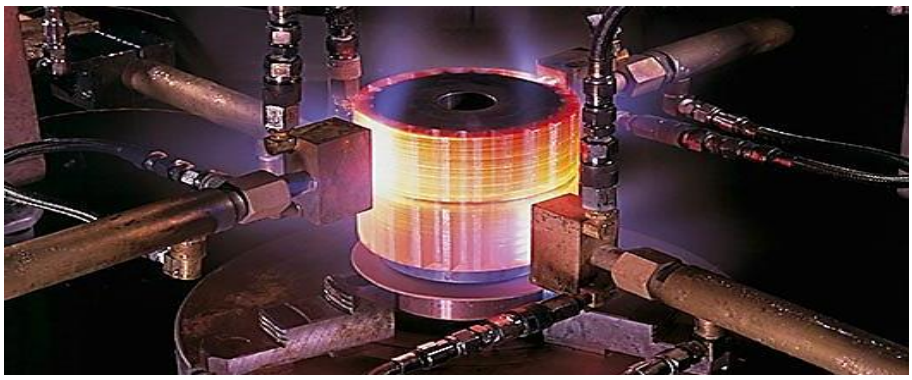

Figure 1.2. Improving wear and corrosion resistance [18].

One ideal method to guarantee component resistance to stress is by using the right material in production in the first place. Apart from strength, dent resistance, toughness and ductility, heat resistance cannot be disregarded and making components with the right materials can add to the level of resistance against cracks and depreciation in harsh settings. To illustrate ideal heat-resistant material, we can point to certain alloys like alloy steel, grey iron and Ni-hard. Changing metals via the process of alloying adds to their strength and resistance against wear and tear. In this respect, steel might potentially possess many good features to qualify for mining operations; it may still experience wearing caused by humidity, oxidation and added heat. To fight this, alloying makes it more heat resistant. Being quite popular, alloy steels are also very economical for mining equipment production, and the use of anti-corrosion layers further reinforces steel castings and related important components against friction and high temperature. Additionally, these coats strengthen the surfaces and act in the form of a defense line against damage and tear [17,18,19].

Apart from making wear-resistant components, an extra protective coat significantly magnifies the operations in unfavorable and wear-prone surroundings of locations like mines. Such application of coating guards all steel casts and many other important components in the machinery against friction and high heat. Proper wear management is held quite high within all manufacturing sectors given the financial implications they have. As stated earlier, corrosion can also cause major repair work and replacement, all part of the anticipated loss caused by overhauls and slowed-down operations. For this reason, engineers are bound to opt for mechanisms and systems that can handle extreme environments and, still, experience the least corrosion. Such an initiative, naturally, calls for an endless endeavor to achieve better material that is corrosion-free as regards certain working environments. A majority of wear-proof metals are, in fact, compounds and, for this reason, costly. Furthermore, corrosion usually takes place on surfaces and its surroundings, which implies that economically treating it simply calls for coating with costly material on other not-so-expensive bulks [19,20,21].

Regardless of what exists within the available literature on the topic, corrosion deals with any alteration of physical, chemical and mechanical attributes caused by

chemical and electrochemical phenomena and owing to the metals' and alloys' inclination toward making new compounds of steadier status. Corrosion or weathering – as the primary reason behind applying metals for use worldwide – can inflict numerous forms of damage; presently, countless methods are available to make corrosion-proof materials to delay such occurrences. Changing the surface properties of materials is long considered by experts at the manufacturing and academic level and, as such, is crucial to designing, to the extent that there are specific disciplines mainly intended for this craft. Among them, surface engineering and tribology stand out. Nowadays, the industry is keeping on expanding the horizon for material applications and, consequently, there is a lot of attention paid to changing surface properties as a pivotal technique in the production line. To compare, material with an altered surface mostly performs better than monolithic materials under the same service environments – in this way, making room for more economical and easily prepared materials to be used with proper surface treatment and cut the associated costs and, yet, maintain high-quality service and operations in the long run [21,22,23].

A vast number of engineering parts depend on not just bulk attributes, but on surface features as well; the case is even more visible among corrosion-proof parts operating within a wide range of service conditions. How any given metal reacts in the presence of other substances is governed by 3 main factors; these are: surface attributes, contact area, and the surroundings or operational environment. Quite often, the surface attributes are not suited against depreciation and certain service conditions, in which scenario one can enhance overall performance in two ways: surface treatment and surface coating. In the former case, there are two additional subdivisions: microstructural changes or chemical changes. Treatments for microstructure within the mass require inductive heating and cooling, flame, laser, electron beam application, and lastly mechanical processing such as cold working. In case of chemical transformations within the surface level, there are techniques such as carburizing, nitriding, carbonitriding, nitrocarburizing, boriding, siliconizing, chromizing, and aluminizing [22,24].

Deliberately applying certain elements to the surface of a given alloy or material has been common practice for long and, more specifically, applied in the industry for many years and in many different variations. Such processes tend to make the surface tough and, hence, are useful in further avoiding corrosion to take place. Considering a certain configuration and loading properties, the level of wear and tear is inversely in proportion to the degree of hardness of the material as such layers on the outer face tend to slow down corrosion rates. A decreased depth of penetration of the counter surface, in this case, offers the benefit of a series of contact points between the surfaces as well, in turn causing the friction coefficient to drop as a result. In a sense, furthering the wear-resistance properties and reducing this coefficient between parts go hand in hand and are extremely useful in adding to service life and reducing the amount of energy required to move the engaged parts. Owing to such enhancements in effectiveness and lifespan of the parts, the topic of surface hardening has been investigated quite significantly [24,26].

Such techniques can further the operational efficiency; whereas, certain operations require more of such modifications so as to reach the ultimate reduced friction and corrosion. The uppermost degree of surface hardness that can be obtained in any material is entirely bound with its chemistry. To illustrate, steel is treatable for added hardness up to 10 GPa. Coating the surface or hard facing does not follow any chemical boundaries since any alternative material may be applied for added surface hardness. Put in simple analytical terms, the best materials for this purpose are those with absolutely advanced degrees of hardness, among them diamond and cubic boron nitride as quite evident alternatives for the task of coating; still, though, these two are highly-stable substances requiring production under extreme pressure and heat, which implies much added expenditure required to make them [25,27,28].

As stated earlier, various techniques are available to reduce wear and tear, such as surface modification, which can work differently depending on the surface it is applied to. At times, the metal can develop a resistant coat such as nickel and stainless steel; whereas in others like mild steel, this possibility does not exist. The way any tool can work effectively relies upon its design, degree of precision in its production, the right kind of material that is, steel and also heat treatment. For tools

with high standards of quality, proper planning, sound production techniques, and the right heat treatment are three major requirements. In this process, supplying added tungsten, molybdenum, manganese and chromium offers the product qualities needed for tough working environments, added dimensional control, and reduced likelihood of fractures once heat treatment is in progress. Tool steel may be processed so as to gain much smaller grain size, the least retained austenite, spheroid, much smaller carbide size, and an even carbide distribution. To achieve the best results, the austenitizing temperature and quenching period need to be proportional; if not, unexpected grain size, added and retained austenite, and carbide separation from grain boundaries can take place, which will greatly affect the working life and cutting efficiency of the tool to be made [23,27,29].

There is common agreement that the final microstructure of steel alloys largely relies on its chemistry and, whatever the alloying elements, a combination of preliminary, middle, and ultimate phases will remain based on the number of rounds for heat treating of the material. Despite the fact that stainless steel alloys offer high resistance against any form of corrosion, these alloys are still prone to local wear regardless of the high degrees of chromium and nickel present in them – the particular case at issue being duplex stainless steels. Stainless steel alloys being resistant against pitting corrosion require a proper oxide coat structure, chemistry and depth. The degree of corrosion in such parts within machinery in use within different industrial settings may at some point result in unexpected stoppage major inadequacies, and considerable costs to be incurred – all of which may, obviously, be alleviated by applying surface treatment [29,30].

1.1. BACKGROUND INFORMATION

1.1.1. Surface Treatment of Metals

For the purpose of avoiding rusting or merely varnishing the outer layers of metal components upon machining and manufacturing, experts commonly employ extra finish techniques, which also improve mechanical or electrical characteristics necessary for general application. Finishing is crucial and numerous methods exist to

either expand or change certain metal properties. These operations also add to the life span of metal components, important in building and automotive sector to mention a few benefits. The approaches employed go back as far as the fourth millennium B.C. – i.e., when humans first began to work with gold as ornaments. Modifying the surface characteristics follows certain reasons, among them better hardness, avoiding rust, decorative and embellishing purposes, and further protection against wear and tear [31,32].

Surface Treatment of Metals (STM) entails processing prior to coating, and includes various techniques. In essence, they all form an obstacle to safeguard the metal in harsh settings – such as those of corrosive nature – so as to add to energy level of the metal. These surface-changing processes include nitriding, carburizing, and induction hardening in case of steel, to further corrosion resistance and fatigue strength. In this way, it can be said that cleaning and surface activation go together to accomplish the purpose. As stated earlier, various approaches exist in this regard, such as electroless plating, vacuum coating, dip plating, electroplating, vapour deposition, sand blasting, painting, coating, anodizing, and surface hardening. Other rather complicated processes are conducted mechanically, metallurgically, electrically, chemically, and physically [32,33,34].

To add to resistance, fitness and appearance, metal components undergo certain procedures common to just about any industry with such treatment equipment; to name a few, we can refer to the electrical industry, industrial equipment, those applying laboratory equipment, the automotive sector, medical manufacturers, container producers, buildings, aviation, and many more. The metal parts used differ, from screws, nuts, and bolts to spectacle frames, gadgets, and numerous other parts. In this respect, steel surface treatment stands out for a series of causes like better reflection and resistance to harsh weather and peeling. Key to this process is, of course, identifying the degree of potential hazard and proper balancing of the measures taken [35,36].

The heavy-duty gadgets, machines, and equipment applied today for different purposes have to last long, thus the main incentive for metal finishing. The process

involves metallic coating on any given part to improve the looks, operations, and practicality. Because of its extended field of application – among them, copper, aluminium, and steel - metal finishing can add value to any field involving these materials. Modern technology has come to the aid of producers dealing with high financial and time costs incurred to equipment caused by wear and tear through the reduction of disruptions and fixings required and adding to performance. Apart from this, the surfaces themselves will have better performance through protection against, abrasion, wear, heat, corrosion, and impact [36,37].

Mechanical properties help in determining material and its behaviour upon exposure to stress. Some of these, in general, can be listed as: strength, hardness, elasticity, toughness, fatigue, ductility, creep, brittleness, impact resistance, plasticity, stiffness, resilience, malleability, and yield strength. Building components are mainly anisotropic and change according to position. Experts investigate these features upon tests, which expose the substances to outside factors as applied in real settings. In turn, they measure these factors and the way deformation or fracture occurs in terms of the energy, time, heat, and other factors. To choose a material for any use, the related features have to comply with the performance and settings needed as per the structure. This is crucial since such performance is decided according to the degree of deformation allowed. Mechanical properties assist in determining behaviour when material is exposed to load, and they are related to the physical aspects associated such as flexibility under pressure [38,39,40].

Figure 1.3. Surface treatment of metals [40].

Nowadays, one cannot see any advanced structures devoid of surface treatments, especially when it comes to automotive and aviation sectors, where work piece surface layers need reinforcement due to extreme loads. Surface treatment primarily develops characteristics like protection against fatigue, rust and wear-and-tear. Many such processes are available with certain features as different technologies require alternative surface layer characteristics affecting the work piece properties directly. A majority of these processes are applied to parts exposed to cyclic loadings so as to extend life span and offer compressive residual stress to both the surface and subsurface of a metallic material [39,40,41].

It can be stated that engineering parts can fail due to such production faults, insufficient maintenance, going beyond the allowed limits, excessive loads, inappropriate choice of material, design shortages, and other causes. For this reason, the performance limits when in operation rely upon many elements, namely specific material characteristics, the settings, maintenance, load and stress factors. Nevertheless, such performance when in use may not be equal to what is anticipated and, for this reason; design factors help experts to reduce failure as much as possible. As a result, there is a need for early prediction and planning. In this respect, plastic deformation can influence the microstructure and improve material strength significantly upon reducing ductility. Apart from this, severe plastic deformation (SPD) can give rise to sub-micron and nano-grained formations with better strength at room temperature and considerable ductility [41,42].

Each material has its own specific characteristics, thus behaving accordingly given the circumstances. Among them are mechanical, thermal, chemical, electrical, physical and magnetic characteristics. Mechanical features are a product of the physical ones specific to any material, and explain the way it counteracts against such forces, hence measured using certain conventional experiments. Metals undergo treatment to alter surface characteristics against wear and tear as well as corrosion, and to better hardness and adhesion of paint and other coats applied. Such treatment impacts, changes, and improves the metal surfaces for a number of purposes, among which corrosion and rust resistance stands out. Mechanical properties refer to the physical properties of a material when it is deformed by elastic or inelastic behaviour

when used mechanical forces, it help us to measure how materials behave under a load, and it is the physical properties of the material which describes its behaviour under the action of loads on it [42,43,44].

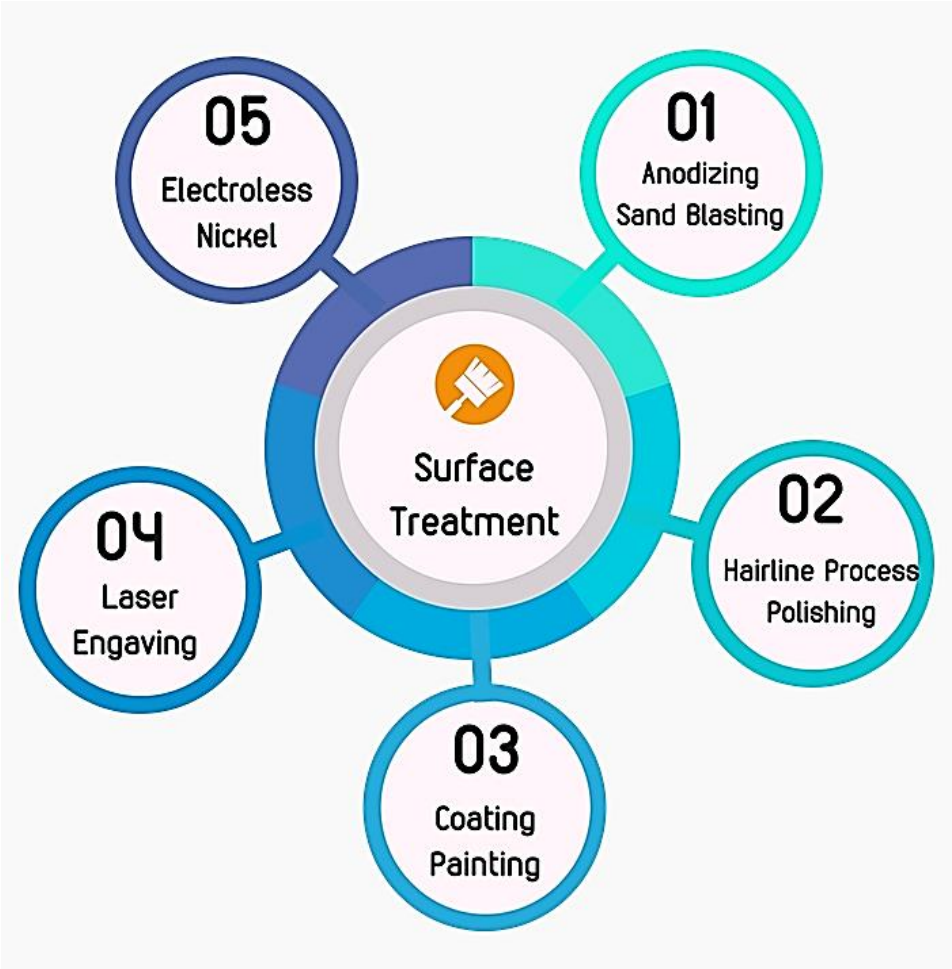

Figure 1.4. Customized Surface Treatment [44].

1.1.2. Heat Treatment of Metals

Commonly, heat causes softness, less strength, and added ductility in metals. The latter characteristic refers to the extending ability of the material to form a wire or identical shapes. Exposure to high heat changes metal structure, magnetism, thermal expansion, and electrical resistance. Heat treatment in general makes metals softer and, thus, easier to work with and adds to its ductility by approaching the equilibrium state. The operations involve heating and cooling the metal to alter the microstructure and improve mechanical and physical specifications. Also, the post-heating cooling

causes major transformations in metals. As a whole, though, heat treatment is done for achieving better hardness, ductility, strength, protection against corrosion and toughness [45,46].

Heating is carried out to obtain the most ideal set of mechanical features in metals, with wide applications in steel industries for improving toughness and hardness and eliminating brittleness. By doing so, more ductile and stable forms are shaped while reducing stress – which process involves heating the metal up to a temperature less than needed for transformation. Next, gradual cooling takes place to remove impurities and achieve additional hardness and strength through changing the grain size more homogeneously in the metal. Gradual cooling also is useful for avoiding thermal stress; once cryogenically processed, the metal is made cooler using liquid nitrogen in a controlled fashion to change the microstructure of alloys and metals – for instance, in the case of aluminium and steel - so as to expand the features ideal to the operational life span of a component [46,47,48].

Owing to added heat and friction in mining operations, corrosion and wear stand out as number-one concerns in this sector. A series of techniques helps reduce these impacts, mainly in case of decisive components as heat-resistant steel. There is excessive loss of finance caused delayed activities, employee issues, and unanticipated fixes caused by work tool wear and corrosion. Though changing parts and fixing them cannot be helped when mining is concerned, one can reduce such incidents brought about as a result of constant application in unfavourable settings. To begin with, corrosion minimizes toughness by both physically and chemically altering the material characteristics, while adding to tough materials' brittleness. Minimizing the thickness caused by corrosion can influence material strength vividly, whereas corrosion impacts ductility and encourages brittleness, in the end bringing about structural failure. What is more, cooler settings considerably reduce toughness, and corrosion and rust deteriorate physical as well as mechanical characteristics in a material [49,50,51].

Figure 1.5. Heat treatment of metals [53].

The degree of heat and the rate of heating, cooling and soaking periods all can change depending upon certain criteria like the size and form of metal parts. These considerations by steelmaker help in conforming the steel specifications for the intended purpose. While heat treatment takes place, certain other factors are to be heeded as work piece transfer equipment and the furnace [50,52].

A major issue still in concern and key to present-day surface engineering is how to develop the corrosion behaviour of metals and alloys in use. Another point is the corrosion factor being a negative and destabilizing one as relates today's fundamental building components and major financial burdens incurred. Henceforth, no wonder extended studies are carried out in this respect within the field of engineering [53,54].

Regarding this issue, the main focus is on the corrosion behaviour of steels since they are most widely employed throughout industries and due to the extent of their resistance in numerous alloys. Steel products are chosen because of corrosion resistance and other major features as strength, ease of production and reduced financial burden; yet, in most cases of use, the products have to be extremely resistant to corrosion. Wear, perhaps, is the number-one reason behind any material replacement in different sectors and an ever-present factor as regards moving

machinery everywhere. This need, hence, gave rise to a certain category of corrosion-resistant steel to meet the demands of the sectors [54,55,56]

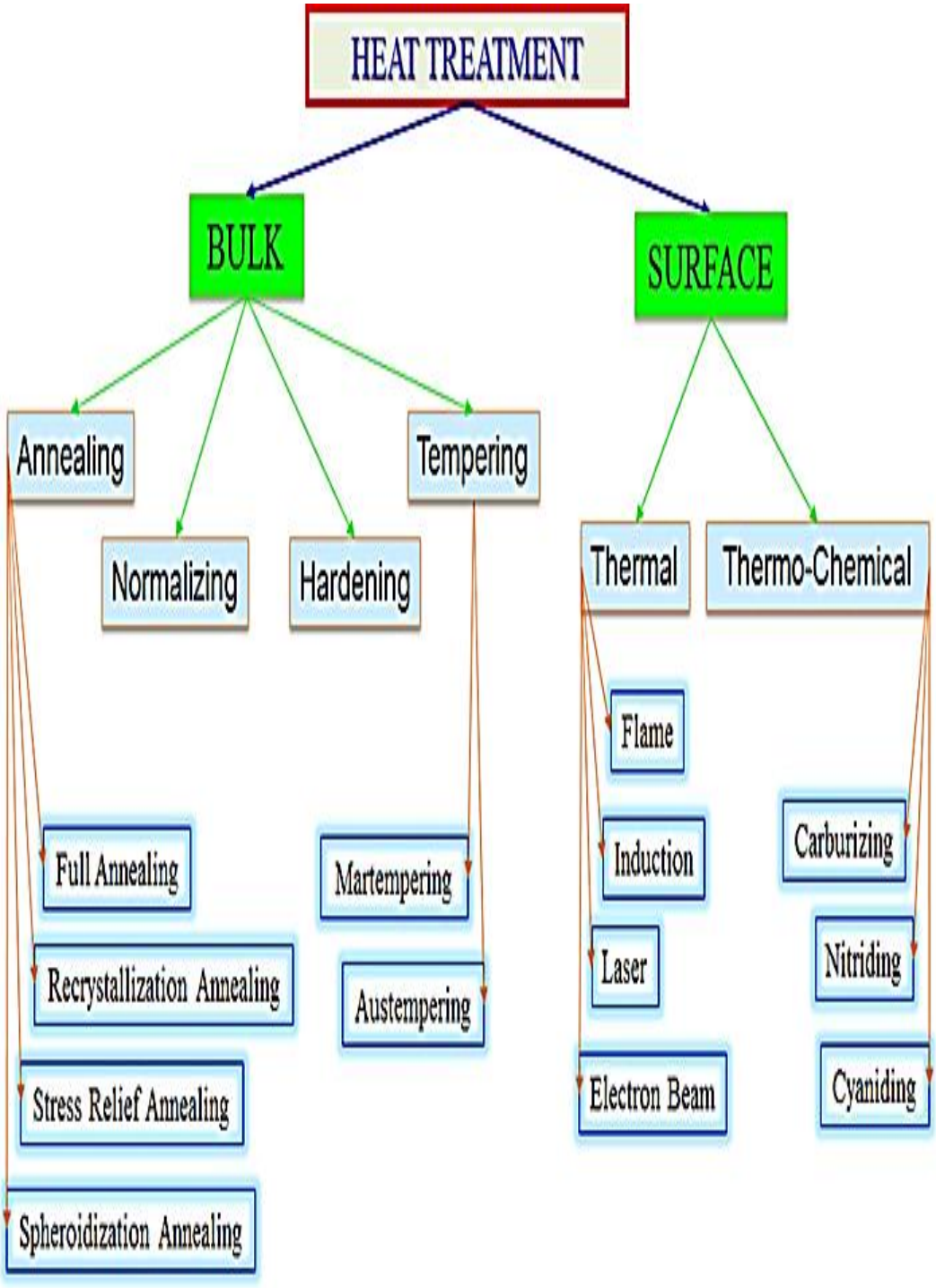

Figure 1.6. Heat treatment process [56].

PART 2

LITERATURE REVIEW

There have been many studies lately in this field, and our review will address the objectives, limits, major points and hypotheses, practical applications and the drawbacks and shortages of these treatment processes for different steels for developing their mechanical properties, reducing wear and corrosion, and other similar purposes, and also several survey papers have been written in recent times. In this literature review, the aim, scope, main arguments, prominent theories, practical application and the knowledge gaps of heat treatment pertaining to the various steels are discussed in relation to the Improvement of properties for materials. Researchers, Improvement of wear and corrosion properties for steel and so on. They have done a lot of research on themes.

The wear factor in steel parts of different machines working under various conditions may lead to unexpected halts, and major mishaps costs. All such occurrences may be prevented using proper steel treatment. However, the common studies conducted in this respect may merely address the wear factor in their experiments, where test factors can greatly influence the outcomes, and the actual wear of a given part can vary significantly under real settings. The corrosion of steel components used on machinery, which is operating in a wide range of industrial circumstances can cause sudden breakdowns, serious inefficiencies, and significant financial losses. These losses can be reduced by means of treatment on steels. The frequently referred scientific literature results, corrosion is not a simple one to measure in the laboratory, where testing parameters significantly affect the results. The actual corrosion experienced by a component may be quite different in practice [4,6,9].

According to previous studies in the field, various degrees of roughness such as bio-based formations and micro surface texturing are also shown to offer promising ways

to develop corrosion resistance and improve tribology. Many of these investigations focus on the impact of surface texturing in particular, and on friction and corrosion, mostly revealing the advantage of applying micro-surface texturing to the substrate [13,16].

At present, surface processing for tool steel remains a very common practice to increase protection against corrosion, with numerous studies detailing all the major developments and important factors involved. As a whole, tool steel is a particular type of material employed for this purpose, and a proper description for this material can be as follows: these types of steel are based on carbon, other alloys, or high-speed steels which can be made harder and tempered even further. Their field of application varies significantly and, thus, calls for satisfactory protection against wear and tear, added strength and toughness, and lastly certain other features specifically chosen for ideal service life [14,25].

In the course of past years, experts in the field of corrosion as well as engineers have come to the realization that this phenomenon can be revealed in various forms of different and, yet, particular likeliness, thus making it possible to categorize them all. Nonetheless, most of these forms though not exceptional, show similar processes with identical features that can impact or entirely lead the beginning and advancement of certain kinds of corrosion [24,29].

As a result, it can be stated that developing the mechanical features of these materials have become a major field. Still, many investigations point to the fact that wear and corrosion are still responsible for almost a quarter of any component failure. There are conflicting reports on corrosion resistance based on alternative kinds of surface treatment. In would therefore appear that Improvement of mechanical properties for materials seems to have taken a more important role in industry. The result of many studies show that wear and corrosion problems account for over 25% of all failures and damage. Different authors report different signatures for corrosion resistance using different types of treatments [27,30].

Several survey papers and Researches have been written in Mechanical surface treatments, and also Thermal surface treatments, some of these researches in the following paragraphs:

Balusamy, Sankara Narayanan et al. (2013) worked on the impact of surface mechanical attrition treatment (SMAT) on the corrosion behaviour of AISI 304 stainless steel in 0.6 M NaCl. SMAT of 304 SS initiated plastic deformation, triggered the formation of mechanical twins and strain induced-martensite phase, added to surface roughness and released compressive residual stress. SMAT also brought about a detrimental impact on the corrosion resistance of 304 SS in 0.6 M NaCl. Double log plots of current–time transients at 25 mV(SCE) reveal the creation of a defective passive film on SMATed 304 SS. A rise in surface roughness, strain induced martensite and dislocations were shown to annul the positive effect of surface nanocrystallization.

Rabelo Menezes,Cristina Godoy et al. (2017) studied the austenitic stainless steels showing superb corrosion resistance, yet lower wear resistance. Former studies had shown that surface treatments using plasma carburizing and plasma nitriding could satisfactorily add to the wear resistance of austenitic stainless steels, and show the effect of a prior shot peening (SP) process on wear and corrosion resistance of sequentially plasma carburized and plasma nitrided AISI 316L austenitic stainless. Triode plasma carburizing (TPC) and triode plasma nitriding (TPN) in sequence form took place under two temperatures: 400 °C and 475 °C. SP processing before sequential plasma treatments, accordingly, caused a major rise in the near-surface hardness. The sequential plasma treatment at 475 °C along with an SP pre-treatment also helped to add to the thicknesses of carburized and nitrided layers, causing additional hardening depth. The most ideal wear resistance using austenitic AISI 316L specimens exposed to SP and sequential plasma at elevated temperatures were related to their additional surface hardness and advanced treatment depth. Yet, such processing in elevated temperatures generated CrN precipitates which disturbed the corrosion resistance in aerated 0.5 M H2SO4 aqueous solution. In addition, electrochemical experiments showed that applying shoot peening before sequential plasma treatments at 475 °C had the potential to somehow neutralize the undesired

loss of corrosion resistance caused by chromium nitride precipitation at such high temperatures. Despite the precipitation of chromium nitrides at higher plasma processing temperatures caused a decline in corrosion resistance in such acidic settings, the outcomes revealed that austenitic stainless steels transformed using shot peening (SP) and later sequential plasma treated at high processing temperatures were able to be essentially applied in places where advanced wear resistance and medium corrosion resistance in certain settings are a necessity.

Haopeng Yang, et al. (2016) studied a nanostructured surface layer made on H13 steel using air blast shot peening (ABSP). A far thicker borided layer on the ABSP specimen may be synthesized by a duplex boronizing treatment (DBT) at 600 °C for 2 h, and then at a higher temperature for a period of time. The borided layer was composed with a monophase of Fe2B with a growth revealing a (002) ideal orientation. The activation energy of boron diffusion for the ABSP sample is 227.4 kJ/mol, which is less compared to 260.4 kJ/mol for the coarse-grained sample. Accordingly, the boronizing kinetics may be increased in practice in case of the ABSP sample with DBT. The high temperature wear resistance of H13 steel with DBT can also be greatly improved. In addition, the H13 steel with DBT assisted by ABSP has far better resistance at higher temperatures when compared to that of coarse-grained specimen with DBT – the reason for which may be the thickness and microhardness of the borided layer being expandable using ABSP. At the same time, the fatigue crack initiation and propagation in the borided layer during the wear test can be avoided by the compressive residual stress and the refined grains in the borides of ABSP sample with DBT.

Lei Wen,Yaming Wang et al. (2010) investigated the nanocrystalline microstructure of the surface of 2024 Al alloy induced by surface mechanical attrition treatment (SMAT) determined by X-ray diffraction (XRD), scanning electron microscopy (SEM) and transmission electron microscopy (TEM). Accordingly, the corrosion properties of 2024 Al alloy after SMAT was tested using potentiodynamic polarization curves and electrochemical impedance spectroscopy (EIS). A pin-on-disk tribometer helped to identify the tribological attributes of nanocrystalline layer in dry sliding conditions. Based on the outcomes, the Al nanocrystalline layer with

an average grain size of 55 nm, when treated for 30 min, began to shape on the surface of Al alloy. Still, a 5 μm thick surface layer containing Fe with the grain size in nanometer scale was also added to the top layer of Al nanocrystalline surface. The iron-rich layer caused the diminution of corrosion resistance of 2024 Al alloy, whereas wear resistance developed thanks to the useful co-formation of efined grains, increased hardness and lubrication effect of iron rich layer.

Aymen Ahmed, et al. (2015) worked on the impact of shot peening (SP) factors on the surface roughness, microhardness, induced residual stresses, wettability and corrosion behaviour of AISI 316L steel. Shot peening took place by applying ceramic shots at three shot sizes (125–250, 450 and 850 μm), two Almen intensities (0.22 and 0.28 mmA) and two coverage degrees (100 and 200%). Corrosion patterns were, then, examined by applying potentiodynamic polarization and electrochemical impedance spectroscopy. The electrochemical tests took place in Ringer's solution at 37 °C. Accordingly, added surface microhardness and initiated compressive stresses took place as the coverage degree and the Almen intensity were added. The rougher surface after SP improved the wettability in terms of reduced contact angle. An added shot size caused reduced surface roughness and better corrosion resistance. Their other studies explained the impacts of hydroxyapatite (HA) coating on the surface layer properties and corrosion behaviour of AISI 316L. This work showed that the Hydroxyapatite (HA) coating used on the shot-peened surfaces can cause additionally develop the wettability.

Run Huang, Yong Han (2013) examined a nanocrystalline layer comprising a pure β phase with high density of dislocations on Ti–25Nb–3Mo–3Zr–2Sn alloy, formed using surface mechanical attrition treatment (SMAT). The corrosion properties of the as-SMATed specimen, along with the solution-treated coarse-grained and 200 °C annealed SMATed specimens, was tested using potentiodynamic polarization and electrochemical impedance spectroscope (EIS) techniques in physiological saline and simulated body fluid (SBF) solutions. Based on the observations, the corrosion resistance of the alloy in both cases substantially improved with declining grain size from microscale to nanoscale – a phenomenon attributed to the dilution of separated alloying elements at grain boundaries and the appearance of more stable and far

thicker passive protection coats on the nanograined specimens. Despite the SMATed grain filtering and disengagements, they both have a constructive impact on the corrosion pattern of the alloy under investigation. Yet, the post- annealing tests show that this improved corrosion resistance is caused by grain refinement.

Biehler, et al (2017) studied two austenitic steel samples 304L and 316L using a solution annealed condition with either polished or shot-peened surfaces. The specimens are tested without plasma nitriding, with plasma nitriding or annealing and a combination of nitriding and post-annealing. The microstructural attributes are studies using optical microscopy (OM) and scanning electron microscopy (SEM), and the phases are analyzed by X-ray diffraction (XRD) and the corrosion properties examined by applying potentiodynamic polarization testing in 5% NaCl solution. Statistical assessments helped to determine major influences between the microstructure and nitriding settngs and the corrosion features. Consequently, the plasma nitriding is shown to enhance the corrosion resistance of both steels with polished surfaces, while shot-peening appears to add to the corrosion rates. Tests for surface hardness revealed an affirmative effect from plasma nitriding on surface hardness. Also, a correlation is seen between specimen treatment and the corresponding microstructures, the nitriding and the annealing process and the corrosion resistance will be presented.

Balusamy, Ravichandran et al (2012) examined the impact related to SMAT on pack boronizing of EN8 steel. SMAT-induced plastic deformation triggered nanocrystallization at the surface, downsized the grain and added to the volume fraction of non-equilibrium gain boundaries, defect formation and disjoints both at the grain boundaries and inside the grains. Such properties caused a rise in boron diffusion. The work is a pioneer one in the sense that SMAT treated EN8 steel can be boronized using moderate a case depth at 923 K for 7 h. Another point is the advantage of double treatment approach to gain the necessary case depth and a dense boronized layer. An FeB phase formation with an Fe2B phase for SMAT-induced EN8 steel is another pioneer attempt in this work. Accordingly to the outcomes, SMAT is applicable in the form of a pre-treatment for boronizing steel on the

condition that needed care is taken as regards boron concentration so as to monitor the volume fraction of the deleterious FeB phase.

Jayalakshmi, et al. (2016) worked on surface changes as well since it is a primary method to establish acceptable mechanical properties and biocompatibility. Also, surface modification is conducted using micro shot peening (SP) with various ceramic shots (850, 450 and 125–250 μm) at 0.22 mmA on two microstructures Ti 6Al–4V alloy with the aim to examine the impact of such a process on the corrosion patterns, surface roughness, microhardness profiles, and residual stresses. Furthermore, the corrosion behavior of the ultra-fine grain of Ti–6Al–4V materials produced by rotary swaging (RS) deformation is taken into consideration and put in contrast with the duplex (DU) and globular (GL) microstructures. In this study, the corrosion behavior is investigated by applying potentiodynamic polarization and electro impedance spectroscopy methods. The electrochemical experiments are done in Ringer's solution at 37 °C, with the conclusion that shot peening caused in near-surface maximum hardness and residual stresses values. A rise in the shot size caused reduced surface roughness and better corrosion resistance. Nevertheless, SP also brings down the corrosion resistance when compared to untreated materials. The globular microstructure reveals advanced corrosion rates in contrast to the duplex and nanostructured materials.

Wang, et al (2008) investigated a duplex reduced temperature chromizing treatment at 600 °C for 120 min, followed by 860 °C for 90 min carried out a low-carbon steel plate with a nanostructured surface layer, generated using surface mechanical attrition treatment (SMAT). Microhardness, wear and corrosion resistances of the chromized SMAT specimens are evaluated and compared to those of the chromized coarse-grained specimens and the as-annealed coarse-grained one. According to test results, these features were enhanced to a great extent, and the significantly improved characteristics of the chromized SMAT specimen compared to the chromized coarse-grained one could be due to its excellent microstructure, a far bulkier chromized surface layer with tinier grains and advanced homogenous phase-distribution, all owing to the applied procedures of SMAT and duplex lower temperature chromizing.

B. Arifvianto, et al. (2012) studied surface mechanical attrition treatment (SMAT) again to develop the mechanical attributes of metallic materials by means of creating nano-crystallites on the surface. The approach changes the morphology and roughness of the work surface. Surface roughening by means of SMAT was also worked on before using a soft sample; though, in the present work the authors began with a rough surface to observe a smoothening process for AISI 316L stainless steel during the SMAT, which is carried out on a sample with roughness at 3.98 μm for 0–20 min. The milling ball dimensions were changed between 3.18 mm and 6.35 mm. Also, changing the subsurface microhardness, surface morphology, roughness and mass reduction of the sample were all examined as well, based on which the enhanced microhardness of the surface and subsurface of the steel occurred thanks to SMAT. The milling balls derange the surface and cause a flat structure at this layer. Surface roughness drops as far as saturation is possible via the SMAT. The decrease in mass among the samples occurs as an indication of material reduction or erosion at the surface level by the SMAT. The milling ball dimension appears to have an important role in terms of the roughness evolution and material removal during the SMAT. Based on this investigation, the authors suggest two main processes concerning the change in surface structure and roughness using the SMAT: indentation and surface erosion caused by numerous impact from milling balls. A comparative investigation of the outcomes related to former tests shows that the original surface roughness plays no part in the hardening process by the SMAT, though such is the case on the saturated roughness figures retrieved from this process.

Nana Li, et al. (2017) examined SMAT employed for making nanostructured surface layers on alloys for nuclear power plant steam generators (SGs). The impacts of surface nano-crystallization are seen on alloy corrosion patterns at room temperature and at 300 °C in a modelled SG setting environment. At room temperature, the polarization curves showed that increasing SMAT periods help shift negatively the corrosion potential of the samples from smaller to larger figures; also, alloy active dissolution rate and passive current density were seen to enhance. Nitriding is applied to further the corrosion resistance. In contrast to the corrosion patterns seen under room temperature, corrosion resistance in the modelled SG settings is

considerably improved due to the nano-sized-grain layer created using SMAT provided advanced density of nucleation sites to generate a passive layer and diffusion paths for Cr, thus creating a quick layer of dense protective oxide.

Wen Lei, et al (2015) looked into the plain as well as Fe-loaded nanocrystalline layers coats created on the surface of 2024 Al alloy using the SMAT technique, ceramic balls and steel balls, respectively. The friction and wear features of the stated alloy prior and post-SMAT are analysed through sliding against a GCr15 steel ball of 5 mm in diameter at a load of 1.5 N. the study shows the surface nanocrystalline layers with average grain sizes of 49.2 and 52.1 nm to be achieved with ceramic balls and steel balls if processed for 30 min. In addition, a 5 μm thick surface layer of Fe was applied to the Al nanocrystalline surface upon treatment with the help of steel balls. Wear resistance in case of the 2024 Al alloy was, consequently, enhanced owing to utilizing grain refinement, added hardness and lubrication impact from the iron coat.

Narayanan, et al (2013) address the effects of surface mechanical attrition treatment (SMAT) on pack boronizing of AISI 304 stainless steel (304 SS). In this case, SMAT of 304 SS is conducted with 8 mm Ø 316L stainless steel balls for 60 min. Unprocessed and SMATed 304 SS specimens are, then, pack boronized using single stage (at 1223 K for 1, 3 5 and 7 h) and duplex (973 K for 1 h and 1223 K for 1 h) processing, with the outcome that that SMAT-induced 304 SS added to the boron diffusion kinetics while creating larger amounts of fraction of alloy borides and enhancing the hardness of the borided layer. Duplex treatment, in turn, is shown to improve the case depth more than the single-stage approach. Based on the results, SMAT is useful as a pre-processing mechanism to boronize 304 SS.

2.1. OBJECTIVES AND SCOPE OF THESIS

The present research attains a number of goals. In detail, we aim to examine the process of thermal surface treatments and to understand the impact of all process parameters on the development of the microstructure, residual stresses, hardness, wear and corrosion resistance.

Furthermore, Boriding processes will be applied in order to investigate how these processes interact, and to assess whether they can be used effectively in combination in order to improve the wear and corrosion resistance, hardness, and the mitigation of residual stresses. Based on this over-arching aim in this research, and given the extent of these aims for the present work, specific objectives and goals have been established, we illustrate in these points as per below:

- Investigate, and study the surface treatment operations in detail to enhance and improvement mechanical properties of H13 tool steel;
- Add to the degree of wear and corrosion resistance, improvement of abrasion strength of the H13 tool steel;
- Study of Friction and Wear Behavior by using nano-silver-doped lubricants under working conditions.
- Examine thermal surface treatment operations to enhance the corrosion resistance of H13 steel;
- Carry out XRD analysis to determination of crystallographic properties of H13 steel, such has crystal structures, as well as gain insight into unit cell dimensions;
- To examine the microstructure and hardness developed under various process settings and parameters;
- Effective understanding of the surface properties of H13 tool steel;
- Assessment of the surface roughness measurement;
- To identify mechanical properties of H13 steel before and after thermal surface treatments;
- Conduct EDX analyses to list the crystallographic features of H13 steel;
- Illustrate the major sources of wear and corrosion of the H13 steel, as well as the way to accurately identify its corrosion;
- Examine the methods to further the properties of toughness, hardness, and strength in case of H13 tool steel, and improve resistance to impact;
- Investigate microstructure view, and measure surface to core hardness in order to increases resistance to penetration, and add to resistance against infiltration;

- Increases resistance to abrasive and attempt reduced frictional energy losses;
- Attempt to reduce residual stresses and increase resistance to mechanical failure for steel; and
- Study in detail corrosion resistance and the status of residual stresses.

2.1.1. Thesis Organization

The thesis consists of five chapters, including introduction.

Chapter 2 is the literature review as information about several papers which have been written, and objectives and scope of thesis, Methodology of Research, Overview of wear resistance, and overview of Corrosion resistance.

Chapter 3 introduces the techniques and methods, and the experimental procedures and test and analysis facilities used in this study, including the specimen preparation, Materials and theoretical background.

Chapter 4 The discussion of results.

Chapter 5 focuses on the conclusions and Recommendation for future work.

2.2. METHODOLOGY OF RESEARCH

This research is based on an experimental approach, where thermal surface processing in elevated temperatures so as to finish the parts and improve fatigue-, stress-, corrosion, and wear-resistance, and add to service life as regards H13 steel.

Failure analysis for future prevention requires a thorough approach to determine the main driving factors; and also needs a systematic approach of investigation for establish the important causes of the damage, hence, it is useful to know these basic factors, and it is worth to familiarize with fundamental causes of failure of mechanical, general approach for the failure analysis, and a common perspective which needed for such analyses. metallurgical failure of a mechanical component can

occurs in many ways, In this regard, metallurgical incidents experienced in mechanical components may take place in a variety of causes curs in many ways, elastic deformation is beyond acceptable limit, excessive and unacceptable level of plastic deformation, complete fracture has taken place and loss of dimension due to wear and tear besides variety of reasons, failure analysis shall be oriented mainly towards the metallurgical failure of mechanical components [57,59].

Steel components mostly need a kind of processing and treatment to add hardness and gain the most possible strength and durability. Along the various stages of such processes, steel characteristics become altered using physical and mechanical means. Among many other benefits of treatment, it can also aid in the manufacturing process. To mention some advantages, we can point to the positive effect in the production line itself; when speaking of mechanical property transformation, we mean shear strength, toughness and tensile strength, all of whose presence make the components more useful and effective in day-to-day operations and lasting against wear and tear even under the toughest settings. Proper processing and treatment changes not just physical and mechanical features, it can improve the production stages, too. A fine treatment reduces stress and creates steel parts that can be worked with easily; namely, welded, machined, and hot formed in conditions otherwise too risky due to high stress [58,60].

It is known that materials perform differently in actual settings and lab settings; for this reason, the design factor often helps experts to reduce failure. Yet, performance at work relies on many other factors, including inherent properties, load and stress, the settings and maintenance. Failure in parts may often be related to: design faults, wrong material selection, production shortcomings, going beyond design thresholds, overload, and insufficient maintenance. Then, once failure happens, these factors are to be looked into to determine the main causes for preventive measures. Among other main factors leading to mechanical failure are: fracture, fatigue, creep, wear and corrosion. the design of a component or structure often asks to minimize the possibility of failure. The failure of metals is a complex subject which can only be dealt with fracture or other relevant phenomenon. Therefore, it is important to understand the different types of mechanical failure. Here, designing begs the

question of how to reduce these incidents. Metal parts failure is complicated and, hence needs to be analysed in terms of the actual type - whether fracture or, fatigue, creep, corrosion, wear, or else among the likely culprits necessitating replacement in industry [61,63].

To guarantee quality, wear and corrosion are prime issues to address. Numerous elements can help alter the steel properties according to demand, the exact ratio of all these elements will affect the steel's properties, varying in ratio and changing hardness, durability, flexibility, and other properties along the way. Engineers can create the correct shape and quality steel they need, and there are many methods used to treat steel. Field specialists offer the right form and quality of material with different treatment methods. This is because steel is quite widespread worldwide all of which calls for proper treatment prior to application. it is one of the most common substances in industry, and all steel has to be treated in order to be used in commercial products [62,64].

Failure mechanisms must be describe and the application of the principles for failure analysis for the steel, and improvement of wear resistance from loss of material from a surface, and increase the ability of materials to withstand any wear from friction, and also corrosion resistance refers to how well a substance and especially a metal can withstand damage caused by oxidization or other chemical reactions, and this after thermal surface treatments for the steel. Metal exposure to high temperatures expands the material and, hence, changes the structure, electrical resistance, and magnetism. This temperature, of course, varies depending on the metal - the so-called allotropic stage, and in this phase the actual structure of metal also changes with heat. The primary cause for metal to receive treatment is to enhance strength, hardness, toughness, ductility, and corrosion resistance [65].

The literature background here covers general information concerning of steel, such as previous advancements and related areas of use. To define the aims to achieve here, we carried out a thorough review of these studies, focusing on wear and corrosion resistance pertaining to metallurgical and mechanical transformations. The outcome of this review helped us throughout the various steps within the present

work, and this information served as a guideline in the course of this study. According to the reviews, most studies have come to the conclusion that thin or thick treatment can result in added wear and hardness resistance. Here, we address the objectives, scopes, prime arguments, major hypotheses, use-related concepts, and limitations concerning surface treatment for different steels [64,65].

2.3. OVERVIEW OF WEAR RESISTANCE

2.3.1. Wear Resistance of Materials

In simple terms, wear is identified as the impairment formed due to resistance or application within contact areas; it is a slow process of eliminating or deranging material on hard surfaces, with reasons being mainly of mechanical nature – such as erosion - or chemical – such as corrosion. Metal wear takes place due to plastic dislocation of the material existing within the surface and nearby areas as well as by removal of pieces that eventually become known as the wear debris [66].

A wear-proof status is achieved by enabling the part to withstand abrasion and erosion due to friction between parts and segments, or due to external factors including scale, grit, and similar other elements. With added amounts of alloy, one can also reinforce resistance since there will be additional carbides within the steel which adds to the degree of hardness and chemical stability. In this vein, wear testing is rather accurate and related to certain conditions that create wear and the method of tool use; a majority of these tests being by moving and contact between two areas within a specimen and another eroding medium. It is common anticipate that harder parts tend to withstand wear more efficiently than softer ones. Yet, another factor is the grade value within similar hardness conditions that can affect the degree of wear resistance. In fact, sometimes lower hardness, but high-alloy grades can be worn out far faster than higher hardness, but lower alloy grades. For this reason, there are other elements at play than hardness when it comes to the wear attributes possessed by any material [66,67].

Commonly, wear can be assessed based on the degree of volume lost and the status of the worn area or surface. The degree of wear can be defined by wear rate, specific wear rate, or wear coefficient. In turn, wear rate can be described as wear volume per unit distance based on the slope of the wear volume curve. Lastly, wear coefficient is the outcome of specific wear rate and the degree of the wearing material hardness [68].

Wear-resistance in any material is the most important property when it comes to machinery and tools exposed to extreme and harsh conditions involving sliding contact. There are numerous factors at play in wear resistance; in detail, they are external – based on relative speed, contact pressure, lubricant, and others – as well as internal – based on the material attributes themselves, including hardness, density, and rigidity. Wear takes place once different parts and tools operate, leading to significant financial burdens and making it a hot subject designing machinery for different purposes. Due to rthe presence of contact areas, friction results in wasted power and energy, not to mention issues associated with machining tolerance – all, once again, making friction a formidable force to be tackled and accounted for in design [69,70,71].

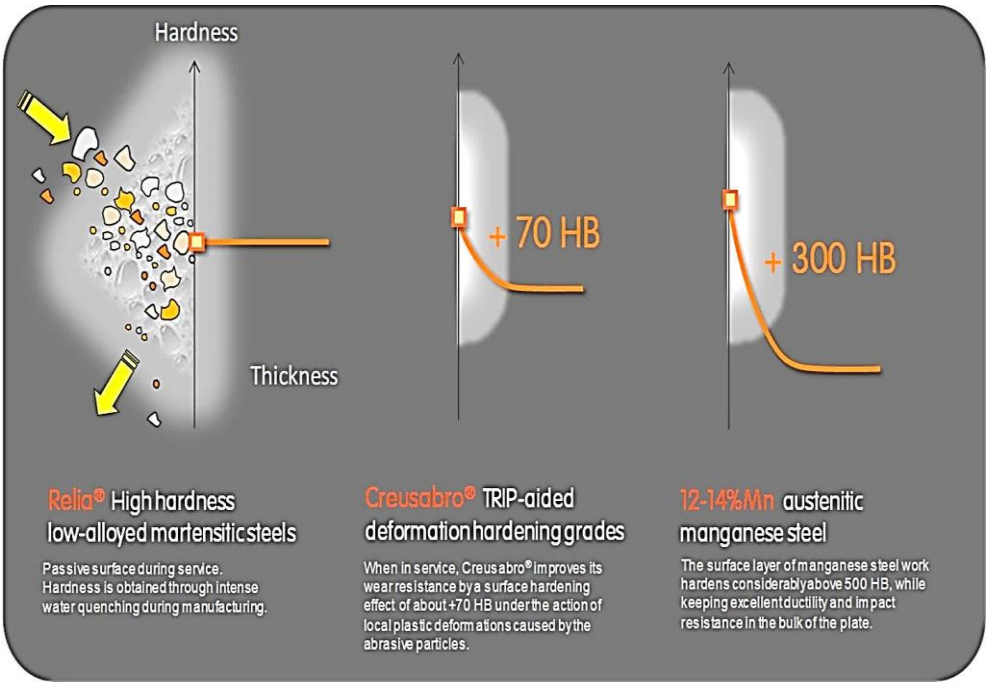

Figure 2.1. Wear resistant steels [68].

2.3.2. Wear Mechanisms of Metals

It is hard to precisely understand the wear and frictional characteristics of metals as they are so varied and the working conditions can be greatly at work in different settings and with various degrees – all resulting in different forms of wear and frictional patterns within, for example, dry or wet (lubricant) conditions. Numerous studies have reported on these properties and behaviors; still, though, we do not seem to have sufficient information as to metal behaviour in many unknown tribological circumstances. Lately, some reports have targeted such performance within certain kinds of metals, namely aluminium, steel and brass.

It can be argued that wear is the number one reason behind material replacement within different manufacturing sectors. To provide some examples, bushings and bearings are typical parts to make up for metal-to-metal wear resistance. Wear is, in plain terms, a universal constant when it comes to moving parts and regardless of the field of use. Against this backdrop, it is useful to address certain kinds of wear so as to have clear view of the reason behind our choice of material, further understand wear mechanisms , it is important to understand wear types, and types of wear as per below: [72,73,82].

2.3.2.1. Adhesive Wear

Adhesive wear is a product of two metallic surfaces having insufficient lubrication upon exposure to one another when in motion, in particular with a cyclical load. Upon contact, the pressure in the area forces them to bind and small pieces of one simply sticks to the other. When taking place in extension and repeatedly, such transfer of material causes surface depreciation and development of wear debris. Adhesive wear is a function of the compatibility of the metals exposed, while the parts comprising similar material have a tendency to adhere to one another far more frequently. Those able to dissolve in others or to generate a new alloy given the working conditions demonstrate even more wear caused by adhesion. The degree of material compatibility is quite evident and well-studied, hence its application as a factor in design processes [74,82,83].

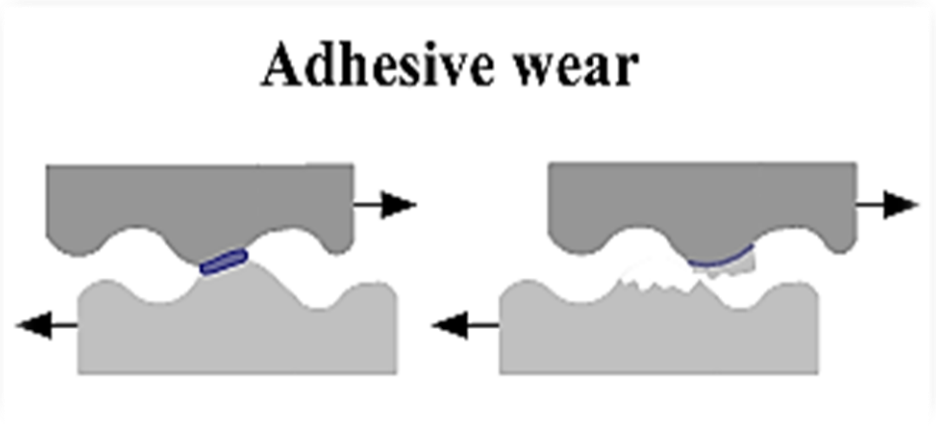

Figure 2.2. Adhesive wear [82].

Adhesive wear is commonly visible everywhere, though it is not detrimental in cases of failures. Broadly speaking, this type of wear is caused by particles detached from an area, moving elsewhere and adhering to other surfaces once certain parts are in contact or work together as part of a system. Such surfaces in contact due to pressure become bond given the added temperature caused by friction and cold welding. The resulting bondcan be much more stable compared to the inter-granular bond strength. When this occurs, particles tend to detach from the weakest points and, in such cases other than welding zone, there is a movement of these particles to other spots. this cycle, when occruing in the course of time and repeatedly, generate adhesive wear and major operational malfunctions [73,82].

2.3.2.2. Abrasive Wear

This kind of wear takes place once hard particles from one surface are pushed toward and alongside another surface. The material removed in the course of such occurrence is also named abrasive wear. Such hard material can be seen in two settings: one is on the surface of another material – known as two-body wear – and in the form of loose substance at the interface – known as three-body wear. Other material as dust from the surroundings and exhaust from working engines are also good examples of this kind of particle. There are two elements that can impact abrasive wear: the hardness differences between materials and abrasive particles, and the pressure creating such contact. An ideal condition at times, perhaps, such settings can at the same time generate unanticipated settings that call for

replacements at an early stage, or filtering mechanisms to be added so as to eliminate pollutants and residue. In case of particles moving and rolling, a rolling or three-body abrasion can take place [75,82,83].

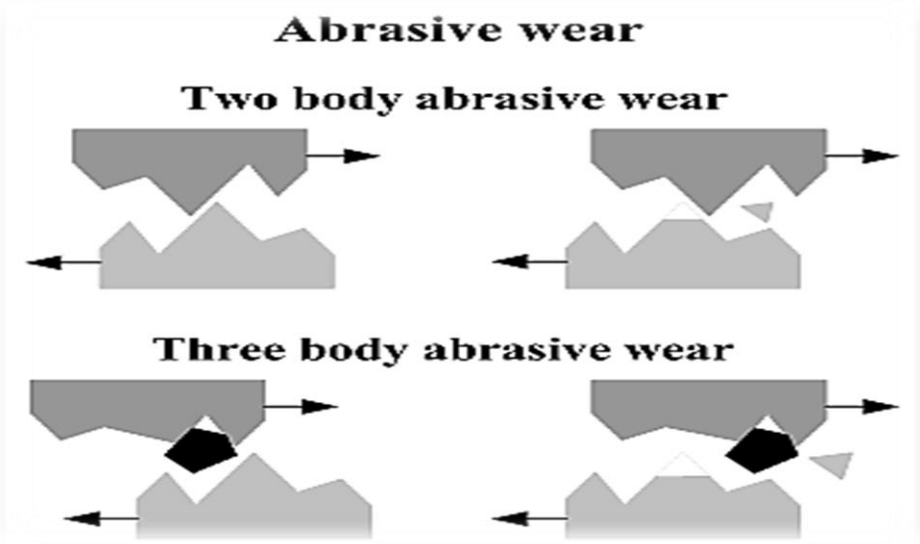

Figure 2.3. Abrasive wear [82].

2.3.2.3. Erosion

Erosion is a product of suspended material within gases or fluids hitting solid surfaces. In this scenario, the actual material begins to be eroded as a result of such interaction. Erosion can be especially seen in conditions involving valve trims with excessive flow and in the presence of other contaminants. The added impact of numerous such exposures constitutes a major force, which is intensified once the particlesare edgy and sharp ion shape [82,83].

2.3.2.4. Corrosive Wear

This type of wearing occurs in the presence of either chemical or electrochemical corrosion alongside wear induced by friction, abrasion, or deformation. Among examples, one can refer to machinery to move slurries in mine operations. When material is degraded due to corrosion and wear, it is referred to as corrosion wear,

with the entire loss caused by a mixture of these two phenomena affecting operations far more heavily than in cases when just one of them is at work [76,82,83].

2.3.2.5. Galling

Metal adhesion can also take shape as galling, where material from one surface in motion against another surface under load starts to blend or fuse to gradually separate particles from that surface. The most common incidents of galling are seen in bearings, bushings, seal rings, and wear rings, or any other places where two metals have to move against each other. In these occasions, alloys containing copper have been chosen as the right material thanks to reduced tendency to gall [82,83].

2.3.2.6. Spalling

Otherwise called deformation wear, spalling occurs once a surface is exposed to deformation caused by continuous, to the extent that small cracks appear and wear particles begin to form, eventually to become visible on the metal part in the shape of sizeable pits [82,83].

2.3.2.7. Fretting

Fretting is a product of tiny amplitude oscillatory movements; in other words, vibration. Fretting is surface-to-surface and in cases when lubrication is flushed out due to added load, leading eventually to further contact between the metals. Other instances include bolted joints and couplings not supposed to be in motion within a system. Almost any machinery is likely to have vibrations, all the more reason for failure due to wearing caused by eventual exhaustion within high-stress parts – the most well-known examples being shafts [77,82].

2.3.2.8. Surface Fatigue

This phenomenon is a product of repeated loading at the time of friction, and in cases where this load exceeds the value of fatigue strength. As a result, cracks appear on

the surface area and gradually proceed downward to the subsurface zone. Often times, these fractures join and separate an entire section of the material from the parts. Fractures and flakes are the main cause of such wear form, coming to shape as constant and shifting cycles of stress are at work, such as in rolling processes, and rail or wheel mechanisms. The main results are tiny fractures at the surface area or below, leading to an overall failure of the engaging parts caused by constant tensile and shear stresses. In other words, fatigue wear is a product of continuous stressing from the moving surfaces. In this regard, the tribological strains are also mainly caused by mechanical stresses on these surfaces [78,82,83].

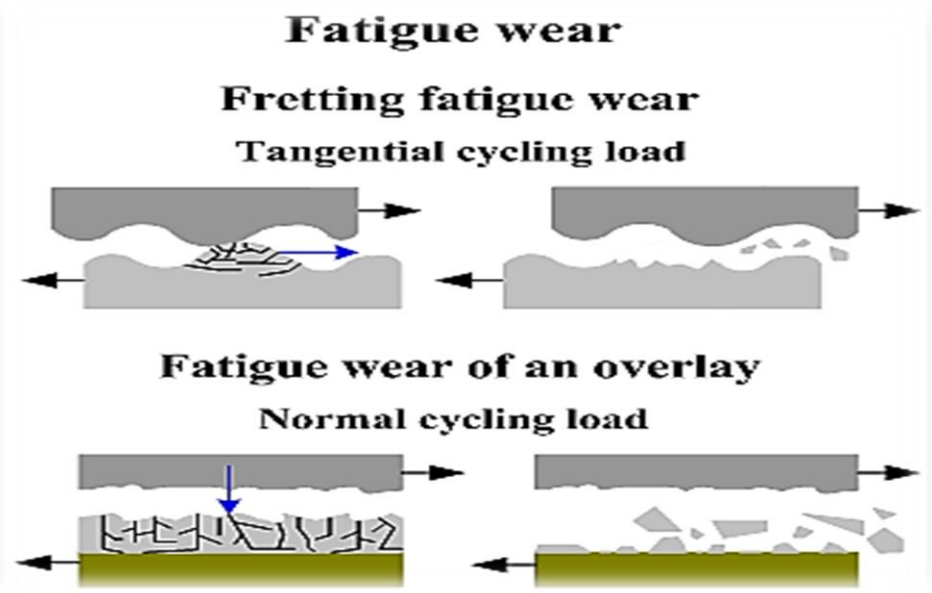

Figure 2.4. Fatigue wear [82].

2.3.2.9. Cavitation Erosion

Thus referred to as bubbles or cavities are formed as a result; the resulting damage owes itself to vapour generated and collapsing within liquids in the proximity of metals. Such impairments are mostly seen where velocity takes a role in operations - hydraulics, pump impellers and trailing faces in propellers, to mention a few. These circumstances call for rushing flows of liquids as well as fluctuations in pressure values, generating bubbles of vapour that quickly collapse after formation [82,83].

2.3.2.10. Methods to Control Wear

The following are some of the applications to bring wear under control:

- Almost soft solids moving on similarly soft solids.
- Hard and sharp material moving on smooth surfaces.
- Fatigue of surfaces by repeated stressing (usually compressive).
- Fluids with or without suspended solids moving against a solid surface.

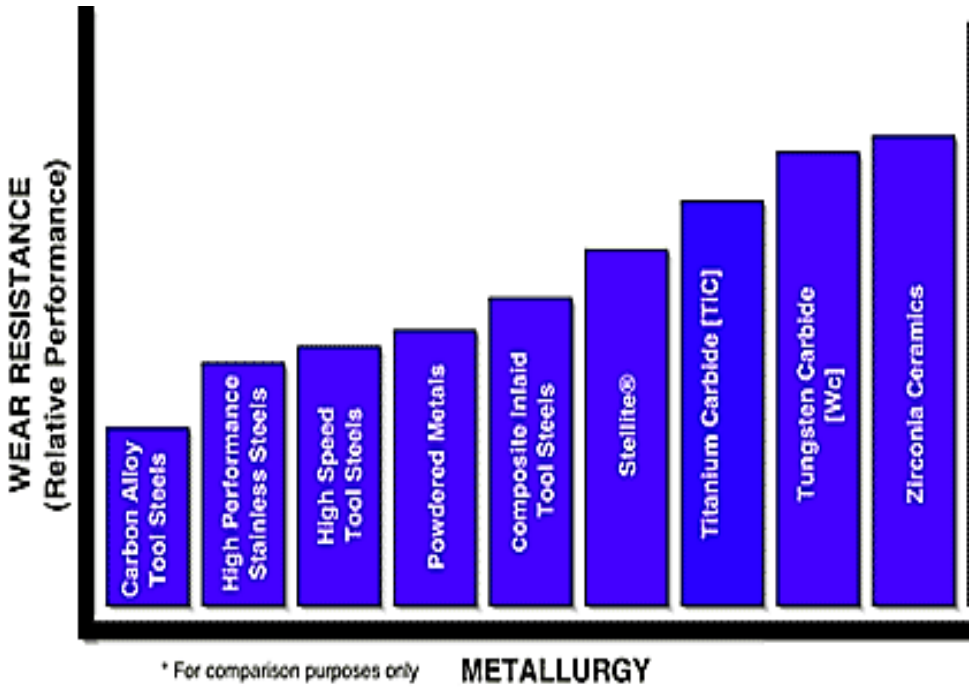

Figure 2.5. The relative wear resistance [83].

2.3.3. Wear Models

Wear investigation is a major concern in tribology, wear being described as a mechanism through which material is continuously lost from the solid parts in motion as a result of contact, gradually reducing the size of both body and mass. Wear is formed in various ways; to begin with, cracks in material cause wear due to different stress factors at play during friction. Such common forms of wear are grouped as being of mechanical nature, also understood by simply the term "wear".

Other alternatives reasons are chemical factors as well as electrochemical interactions, exemplified well by the phenomenon of corrosive wear within the fractures and very well documented among components in motion and servicing within highly chemically-active settings [79,80].

Next come certain physical factors that give rise to wear. To illustrate, we know that relatively any amount of energy lost during friction actually becomes heat, which gradually alters the aggregate status of the material in use. Under such circumstances, wearing is likely to take place due to the melt and flow within the interface area – regarded as ablation wear as well – or due to vaporizing – with examples clearly visible in break systems, high-velocity guides, plane wheels, and others. Heat can speed up diffusion and, henceforth, impact the wear mechanism in many events such as in cutting tools. In these settings, wear becomes an atomic and molecular phenomenon and, let us bear in mind that once we have a system in motion, contact wear is possible through a variety of other factors that take place concurrently. These generate settings that are ideal for wear and rolling contact fatigue – mostly the outcome of friction. Certain studies point out to the use of Archard's wear pattern relating the ratio of the wear volume to the sliding distance multiplied by the normal force and divided by the hardness of the material – the reason behind this formula being its its popularity and high degree of precision. Certain experts also refer to the energy approach and taking wear as an explicit function of the released energy by friction in contact – a good example being the model proposed by Zobory. The main hypothesis is that the contact zone can be classified into two: adhesion and sliding; plus the wear factor being considerably reliant upon the velocity of motion or sliding. Consequently, the wear occurrence is at most within the sliding area. Yet, a different energy perspective has been offered by Pearce and Sherratt, who forecast wheel flange and rail tread wear by assessing wear loss as the zone within the cross-section lost based on the travelled distance as mm2/km [81,84,85].

Given that such forms of contact involve two failure systems, it is not always easy to find the models applicable in many other dissimilar cases. Consequently, there have been other approaches to improve our forecasting ability of wear patterns as well as

rolling contact fatigue. In these cases, limited studies have worked toward assessments where the experts incorporate wear and rolling contact fatigue rail with wheel forecasting simulations upon deciding on the required contact settings necessary to estimate the wear volume as well as the likelihood of fracturing. Concerning Archard's approach, the problem is that the wear coefficient is extremely reliant upon contact settings. Lewis and Dwyer-Joyce examined the creep influence on the wear rate, and other contact settings affecting certain wear rates including pressure, linear velocity, and creep ratio so as to develop a new forecasting approach for the exact extent of wear [86,87,88].

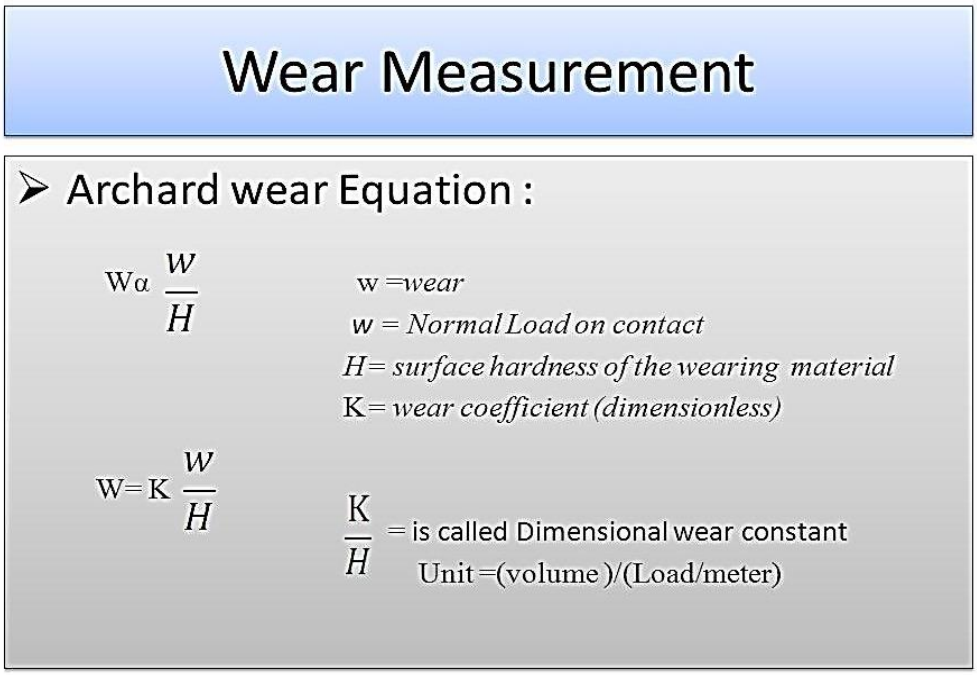

Figure 2.6. Measurement of Wear Model [91].

Naturally, wear and tear is not favored as it generates friction and, subsequently, leads to system malfunctions. Similar to friction, wear can also be reduced by means of lubrication so as to create a space between the two moving parts and avoid direct contact. To this end, it is of course vital to apply the right substance and guarantee the prevention of unexpected structural failures. Whereas steel commonly enjoys high levels of resistance against abrasion, its variations do not share the same properties and, in fact, many of them are engineered to withstand wear in particular; they are simply called abrasion-resistant steels [89,90].

The chemical mix prevalent within such steel is the reason behind its resistance against wear and tear as numerous alloys are available to add to these ideal attributes; for instance, carbon is useful in preventing displacement by adding to hardness and strength. Additional carbon content, at the same time, makes steel create microstructures with added hardness once exposed to heat and quenching regimes. Among the other elements for this purpose, one may refer to chromium and manganese, primarily to decrease wear-generated consequences and effects overall [91,92].

2.3.4. Wear Analysis Strategy

It is paramount for the industry to supervise and manage possible issues causing potential machine corrosion and wear and tear by means of objective analytical methods. Monitoring and controlling problems that lead to active machine wear are critical to an effective wear analysis strategy. As regards such efforts, numerous applications have already been proposed stretching from basic experiments like elemental spectroscopy, all the way to advanced ones like comprehensive analytical ferrography. These all have certain benefits and drawbacks, as matter of course, as far as identification and analysis of active wear mechanisms are concerned. Popular and conventional methods include elemental analysis, ferrous density, particle counting, X-ray fluorescence, and analytical ferrography [92,93,94].

All mechanical machinery can depreciate in the course of time and, based on the nature of their activities and the surroundings in the working periods, internal depreciation is commonly seen as fatigue, rubbing, sliding, abrasion and corrosion. A macroscopic view of these occurrences show that the debris formed might look like negligible specks mainly in the same shape and behaviour; nevertheless, from the microscopic perspective, such debris possess a peculiar structure in terms of shape and size, as well as surface topography in terms of roughness, texture and surface pattern, all depending on the type of depreciation or wear mechanism at play [94,95]. Wear stands among least favoured of all machining phenomena because of its negative impact on the service life of equipment, in turn affecting the degree of size accuracy, surface status and, lastly, the financial aspect of operating any machinery

as a whole – all giving rise to the necessity to monitor such status as wear. Owing to proper supervision, worn out parts can be replaced periodically and prevent the loss of time and reduce component waste. monitoring signals analysis is most crucial role in development of tool wear monitoring during hard turning, because it helps to achieve effective results [93,94].

In reality, this mechanism can address all forms of wear processes, but in general only one is targeted so as to create new mechanisms for others, eventually leading to an integrated system. Put differently, it is not safe to consider only one form of wear and disregard the rest; plus, one has to be aware of the numerous other factors at work in each mechanism. This requires thinking in unconventional terms to have a thorough perspective and come up with numerous choices, such as concerning load, system, materials, and lubrication to state a few. Obviously, certain interventions can be improved when put in contrast with other alternatives, thereby offering the best of all after analysis and comparisons for a given purpose [95,97].

The wear rate can be estimated followed by the equation for adhesive wear and abrasive wear. Next, we can determine erosive wear and fatigue wear using the right equation, eventually leading us to the overall wear rate. Evidently, variations exist among all these equations, such as numerous undefined variables or very few of them, as well as very limited number of variables to properly define one specific system. Complex situations may rise when the system is not thoroughly defined or once the variable are simply too many to be accounted for and estimated, thus requiring numerous other tests to be carried out [98,99].

In all, merely applying wear equations cannot always provide definitive solutions, and other aspects require consideration as well because most of the available equations have been drawn for mild wear rates in components. At wear rate if it is on the mild domain mild regime then only can be predicted. In severe wear case, it cannot be predicted or can say if we are rejecting some component. It is because of severe wear, because of the high wear rate that is why we are rejecting mild wear. In major wear scenarios, the situations differ as the wear rate is high and, on top of all, severe wear may come with a number of combinations of wear mechanism [98,100].

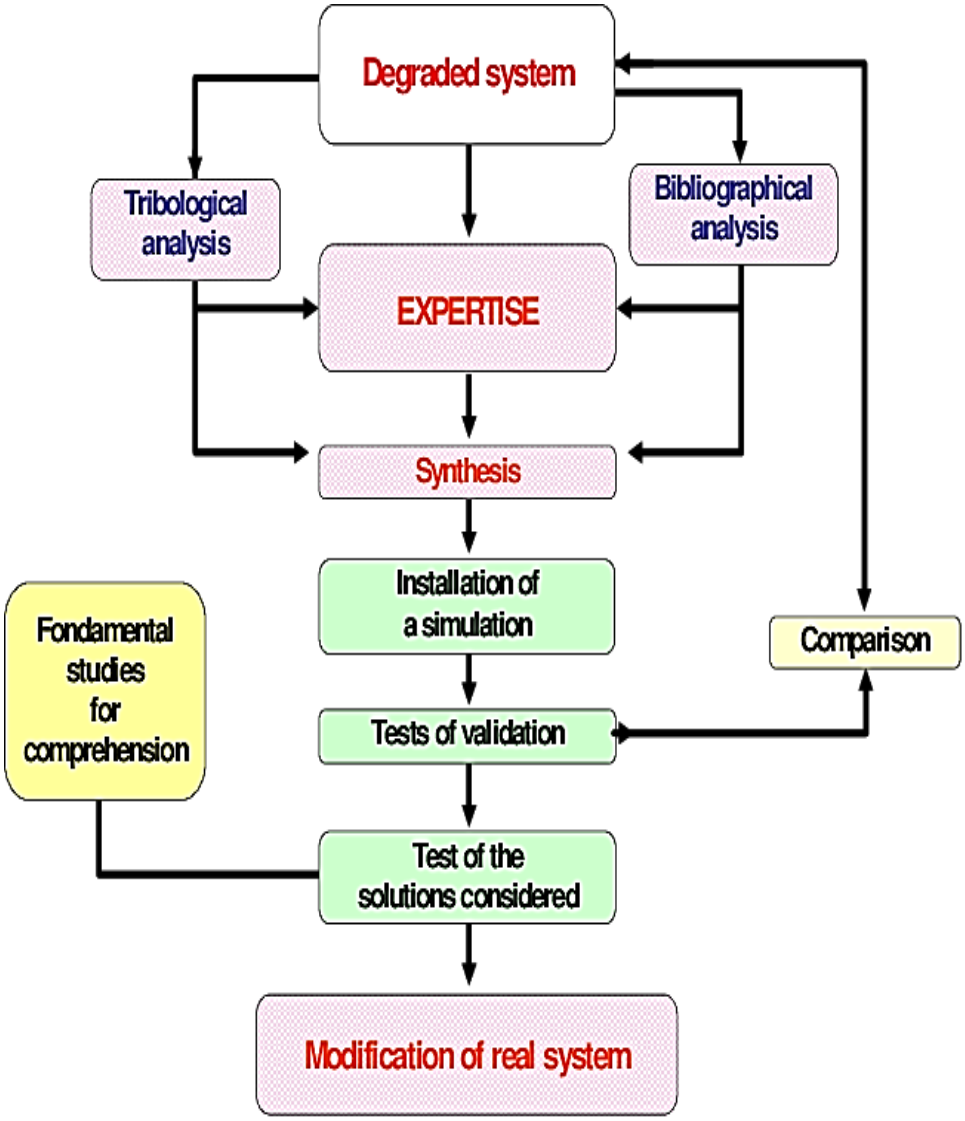

Figure 2.7. Flow chart for identification of wear mode of surfaces [101].

2.3.4.1. Factors Affecting the Wear Performance of Materials

The patterns pertaining to wearing of any material follow specific attributes, and Wear behavior of a material depends on many factors, such as the following:

- It considerably relies on the type of surface material, form of contacting areas, and operational settings, and also on the type of material of which the components are made. For instance, wear varies in case of tool steel on tool steel, and between tool steel and aluminum.

- Solid surfaces, such as bulk surface distortion and regional microscopic deformations, can change wear significantly.
- Added surface roughness increases wear.
- Alloying elements influence both wear and friction.
- Wear patterns and behaviors highly rely on crystal structures, and on grain size and boundaries, which – in case of polycrystalline substances – affect both friction and wear patterns. With sliding motions, surface dislocations are obstructed due to grain boundary, thereby gathering at point of boundary and causing strain-hardening within the surfaces. In the end, sliding becomes hard, adding to friction, and causing wear.
- Harsh atmospheres accelerate oxidizing of corroded areas. Loading, separately, is another issue when two surfaces collide against one another as opposed to merely one surface in motion.
- Heat, velocity, and lubrication can intensify wear [95,96].

Wear comprises surface damage due to erosion or movement of material caused by mechanical action within a contacting solid, liquid, or gas. The result is major surface depreciation often considered as slow deterioration.
The primary characteristics of wear failure are:

- Material elimination and shrinking in size due to mechanical action; and
- Plastic deformation and material separation in the course of time.

Generally defined, adhesive wear is also known in the form of galling or seizing. On the other hand, abrasive wear – otherwise called abrasion – occurs due to material removal from solid surfaces as a result of hard debris moving on the surface. Erosion - erosive wear as it is called – comprises material removal from such solids caused by relative contacting motion against lubricants having solid particles in them. A given component may experience many forms of such wear and tear at the same time [101,102].

2.3.4.2. Coefficient of Friction

Friction is decisive throughout all industrial activities, not to mention our daily lives, and it is responsible for energy waste in equipment, triggering as such major initiatives to reduce it as much as possible. Through studies, the limiting frictional force between two surfaces is shown to rely upon the actual type of the materials on surfaces and the normal reactions between them. The friction force is that made upon a surface once a component moves across it or attempts to do so, the frictional force can be written in the following manner:

$$F_f = \mu F_n$$

with F_{f} representing friction force, μ being the coefficient of friction and reliant upon the type of materials, and F_{n} being the normal force existing between the surfaces and the same as **W** in the following diagram.

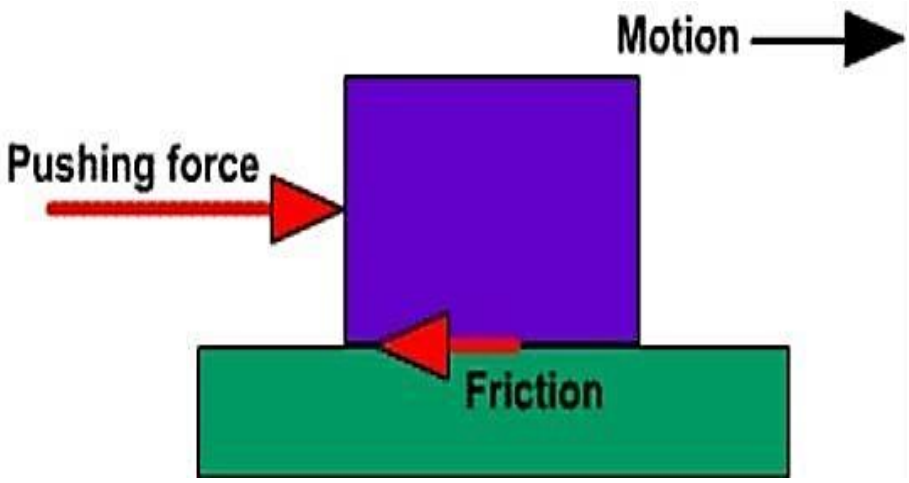

Figure 2.8. Friction force [102].

The coefficient of friction is a scalar value, thus of no unit. Owing to being a ratio between two forces, the coefficient of friction it defines the ratio of the force of friction between two bodies and the force pressing them together. This value, given the type of material, is based on factors as the coupling materials, surface roughness, and operating circumstances [103].

2.4. OVERVIEW OF CORROSION RESISTANCE

2.4.1. Corrosion Resistance of Metals

Such corrosion occurs electrochemically and entails certain changes in the metal as well as the surrounding environment in contact with it. With corrosion processes being virtually identical at microscopic scales, different such structures, configurations, and mechanically-related design factors can cause the corrosion to unfold in various forms. Not only the kind of metal, but also the state surroundings especially, gasses are detrimental to the shape and degree of depreciation. The degree of resistance of metals and alloys is a primary attribute and in conjunction with the degree of their interaction with an assumed set of outside elements. Corrosion occurs inadvertently and decreases the amount of binding energy in the material, eventually causing the atoms to become oxidized by losing one or more electrons and detaching from the bulk. As stated before, the process can volatile and highly burdensome in financial terms; structures have been known to fail and bridges collapse, pipelines shatter, chemical plants start to release toxic material, bathrooms flood, and many other instances. Worn out electrical appliances spark fires and other dire events, medical implants bring about toxic effects within humans, and air pollution has been known to help depreciate artistic works across the globe. Corrosion is an impediment against proper removal of radioactive material to be kept in containers for millennia. Pure metals have even more bound energy, virtually signifying added energy states compared to other elements in the environment like sulphides or oxides [104,105,106].

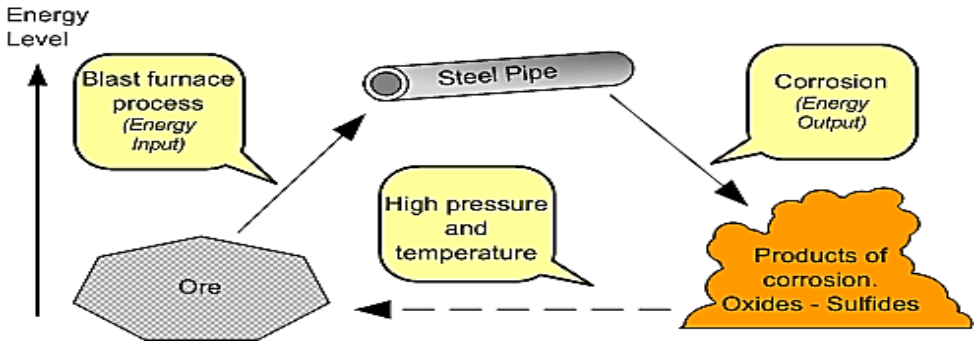

Figure 2.9. Energy state of metal in various forms [105].

There are many working conditions that help wear out tool steel. Resistance in this respect can be gained by applying a shallow oxide layer on the steel – otherwise called a passive layer because it practically helps to neutralize toward electrochemical impact of corrosive factors. Resistance is best achieved with plain steel exposure and deposit-free surface. With the removal of passivity within circumstances unfavourable for passive film replacement, steel is likely to wear off similar to carbon or other low-alloy steels. Given the right conditions, this passive coat deteriorates at certain points on highly exposed surface areas. Once this occurs, corrosion takes place on those very areas – a process referred to as pitting. A major factor contributing to this type of corrosion, can be contact with humid surroundings with chloride. To illustrate, we can name seashores and coastal areas, road salt mixed with rainfall, and water utilities at home with chloride-rich content [106,107,108].

2.4.2. Corrosion Fatigue

Fatigue particularly entails failure processes triggered by cyclic stress and corrosive settings. Once cracks appear due to fatigue, corrosion can naturally add to their spreading. Quite often, corrosion fatigue leads to numerous parallel cracks on the surface; though, in certain cases these formations are circular, in particular around welded joints. To see cracks, proper and non-destructive experiments are needed with the help of ultrasound and magnetic particle testing, and these the most common methods in particular to inspect for corrosion fatigue. Added to the issue of stress corrosion cracking (SCC) caused by static stress, the exerted forces are mostly cyclic and generated by mechanical or thermal factors. Given non-corrosive settings, such cyclic or differing stress values lead to damage on the surface and, eventually, further expansion and complete failure of the component [109,110].

In corrosive environments, cracks appear inside corrosion pits far in advance within the operational life of a component, only to advance thanks to the suitable settings. Corrosion alongside fatigue, in this way, cause failure once only a few stress cycles have occurred and much earlier than in non-corrosive settings. Such fatigue generates a series of advancing cracks and not just one - as is the case without the added influence of corrosion. Corrosion fatigue fractures might or might not get

covered with debris, and this is subject to the relative impact of corrosion and stress. Additional signs of corrosion can be found under reduced stress values and cycling frequencies as exposure time elongates. Different from cracks caused by stress corrosion, corrosion fatigue is widespread and goes beyond any given alloy-environment factors and requirements [110,112].

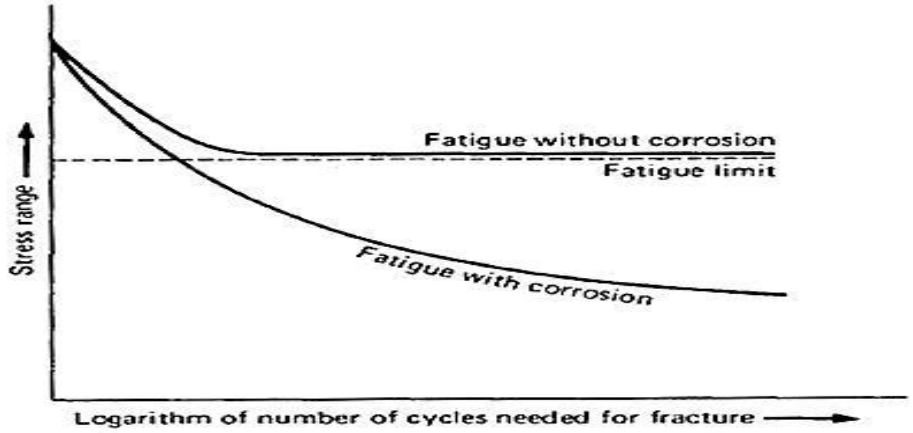

Figure 2.10. Curves for fatigue behaviour of a steel [112].

2.4.3. Corrosion Rate

Corrosion rate is the corrosion effect on a metal at each unit of time, and it is reliant upon system and the nature of the effect. In this way, such a rate can be defined as a spike in corrosion depth within each unit of time – that is, the speed at which metals can depreciate within a given setting. Corrosion rate may also be explained as the degree of corrosion loss from the thickness within one year. The related rate is subject to environmental settings as well as the nature and circumstances of the metal at issue. Roughly 85% of the entire steel manufactured is of carbon nature and, hence, subject to natural oxidation and galvanic corrosion, whose rate can be properly defined within typical atmospheric settings. However, as far as experts are concerned, the exact local or micro settings deserve thorough investigation so as to come up with guaranteed and definitive durability concerning the intended design [111,113].

Both alloy and carbon steels corrode in micro-settings that are rather intricate. To illustrate, the pH, humidity, and chloride values are merely three factors that impact

the corrosion rate. Related charts are hard to form given the numerous factors involved in such settings. Corrosion in water, for instance, involves oxygen values, agitation levels, wave motion, heat, chloride values and others, thus making chart preparation exhaustive and expensive – and, hence, the reason why these charts exist merely for very specific spots and settings and not for general purpose [114,115].

The average rates pertaining to carbon steel in various atmospheres, it should be noted corrosion rates in micro-environments can greatly exceed the corrosion rates given in the next table:

Table 2.1. Corrosion rate of steel in different atmospheres [115].

Atmosphere	**Corrosion rate (µm/ year)**
Rural	4-60
Urban	30-70
Industrial	40-160
Marine	60-170

Here, the approximate uniform wastage is explained in the absence of pitting or other local attacks. With uniform corrosion, the material life may be forecast based on tests that offer the rate of corrosion. These rates are often written in the form of "inches per year" or "melts per year (MPY)", with a melt equalling 10-3 inches. As a result, the equation is expressed using a sample within corrosive settings for a specified period as:

$$ipy = \frac{12W}{TAR}$$

Here, W represents mass loss in time (T) in lb; T stands for time in years, A is the surface area in ft2, and R is the density of material in lb/ft3.

Primarily, corrosion rates are based on the tasks, the working life of a plant, the cost to supply material, and the degree of safety of the environment. This is the case for more general-purpose and less expensive materials like carbon- and low alloy-based

steels. Added heat often accelerates corrosion as well whose rate relies on numerous other elements – as stated earlier – along with design and final conditioning procedures including for air gaps, thin & intersection of the ranges, and source location, and surface processing [115,116].

Metals corrode differently and in different ways. Malfunctions caused accordingly are of great importance in terms of safety and economics. These various forms of corrosion occur in general, galvanic, crevice, pitting, inter-granular, or stress forms – all manageable by means of galvanization, inhibitors, proper choice of materials, protective layers and following certain design principles. As stated before, corrosion is a chemical process leading to material depreciation and loss of attributes, eventually causing component failure. For this reason, many issues are to be borne in mind when analysing failure factors and investigating the impacts, for instance:

- Kind, and corrosion type,
- Rate of corrosion,
- Extent of corrosion,
- Relations present between corrosion and other failure-inducing processes.

Given its natural nature, corrosion is hard to remove entirely; though reduction and management is possible via the right choice of material, design, protective layers, and at times by transforming the environment or relocation as a last resort. Numerous metallic and non-metallic coatings help prevent corrosion of metal components [116,118].

2.4.3.1. Methods to Control Corrosion

Thanks to numerous desired properties, steel has been chosen at a popular level for many an application within engineering, and hence addressed in this study to show the many stages involved in corrosion-control. Steel enjoys numerous ideal mechanical attributes, namely in terms of strength, toughness, ductility, and dent resistance. It has acceptable degrees of manufacturability, formability, weldability, and paintability as well. To refer to other ideal characteristics, we can name

accessibility, ferromagnetic features, environmental friendliness, and expenditure. Due to its likelihood of experiencing corrosion in humid environments and oxidation with heat, properly taking advantage of these ideal features often calls for some kind of coverage and protection among them appearing a list as proceeds below:

- Changing the metal through alloying; in other words, applying other highly alloyed and costly stainless steel instead of simple carbon-based or low-alloy versions;
- Using natural, metallic, or inorganic – that is, glass and ceramic – protective layers;
- Modifying the surroundings through desiccation or applying inhibitors; and
- Managing the electrochemical properties through cathodic or anodic currents; in other words, cathodic and anodic protection [117,119].

2.4.4. Corrosion Monitoring

To control corrosion entails an assessment and viewing of the respective parts within the system, fabrication, operational units, and plants to identify the tell-tale signs of corrosion. Such monitoring schemes attempt to determine such specific settings so as to add to service life of the components and machinery and, in the meantime, increasing secure measures while eliminating replacement costs. These programs deal with any form of depreciation and materials, and involve the assessment of process stream conditions through the application of the so-called probes positioned inside the process stream and ever in contact with the same conditions as the process itself. These probes are either of mechanical, electrical, or electrochemical nature as a form of equipment [119,120,121].

Such probes make up a key part of the corrosion control mechanisms, with qualities relying upon different and independent monitoring methods; as a whole, though, they can be considered as mechanized vouchers. In the past, electronic sensor leads were more common in these applications and for sending information to signal-processors. Yet, with improvements in the field of microelectronics, the sensors have adopted a

microchip-like feature which is a primary part of the sensor units. Certain corrosion assessment mechanisms are also on-line.

Implementations and, as such, in continuous contact with the processing flow; others are off-line, among them laboratory-based analyses. There are also methods that make it possible to directly estimate the amount of metal loss or the degree of corrosion, whereas others simply predict or make inferences as to the existence of corrosion and its required settings. There are many real-time mechanisms in use in many fields across the industry, pointing to the notion that the degree of corrosion damage can hardly be proportionate with the time factor. For this reason, additional information from other places as process parameter logging and inspection reports are needed to be used alongside the existing data as input so as to accurately provide and manage the information system [120,122,123].

An important benefit of monitoring corrosion is advanced preparation should there be any indication of corrosion, in a way that the pace and parameters causing it can be all predicted. Some of these parameters subject to later adjustment are temperature, pressure, and pH. On top of these, the practice of monitoring can tell us about the degree of effectiveness related to preventive mechanisms employed and see if additional or different methods to examine and treat the issue are necessary or not [123,124].

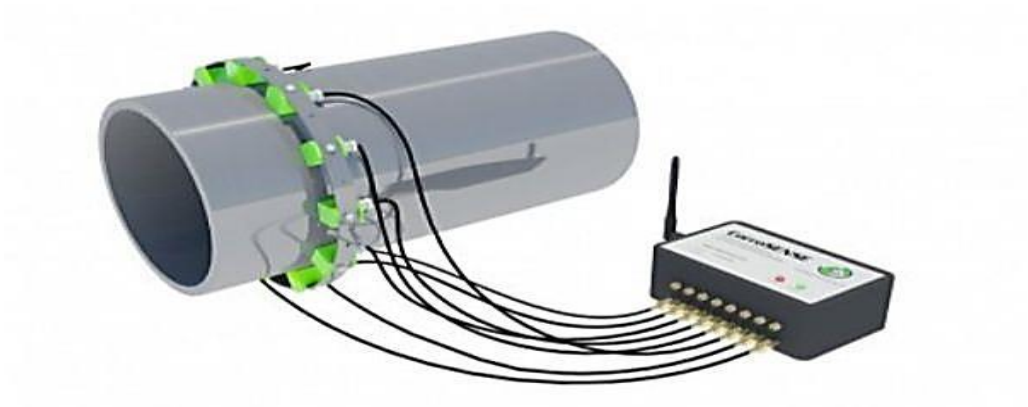

Figure 2.11. Corrosion Monitoring System [118].

Corrosion causes damage to countless sensitive procedures and, as a result, brings about major financial costs for repair works. Apart from this, there are machinery

that get old and, hence, become more likely to corrode easily and operate inefficiently in harsh settings such as in increased heat or pressure. In this respect, a functional monitoring scheme is also responsible for adding safety, decreasing repairs and monitoring expenditure, and increasing effectiveness. Corrosion monitoring encompasses a large array of methods related to measuring, inspecting, and preventing corrosion. The related methods are, generally speaking, of two kinds and related to either inspection or monitoring, as described below in detail: [124,125].

2.4.4.1. Inspection Techniques

Prior to any inspection, one has to record all related operational parameters in the machinery likely to trigger corrosion; namely, these are in brief: pH, flow rate (velocity), pressure, and temperature. Next, non-destructive experiments and inspection is carried out to pinpoint and determine the kind of place of the damage caused by corrosion. The conventional NDT techniques to carry out detection are: ultrasonic tests, radiography, and magnetic flux leakage. Risk-based inspection and fitness-for-service evaluations can be the other approaches to guarantee added accuracy within the scheme – among them, qualitative and quantitative techniques to obtain data related to the status quo within the equipment and the anticipated service life ahead [120,122].

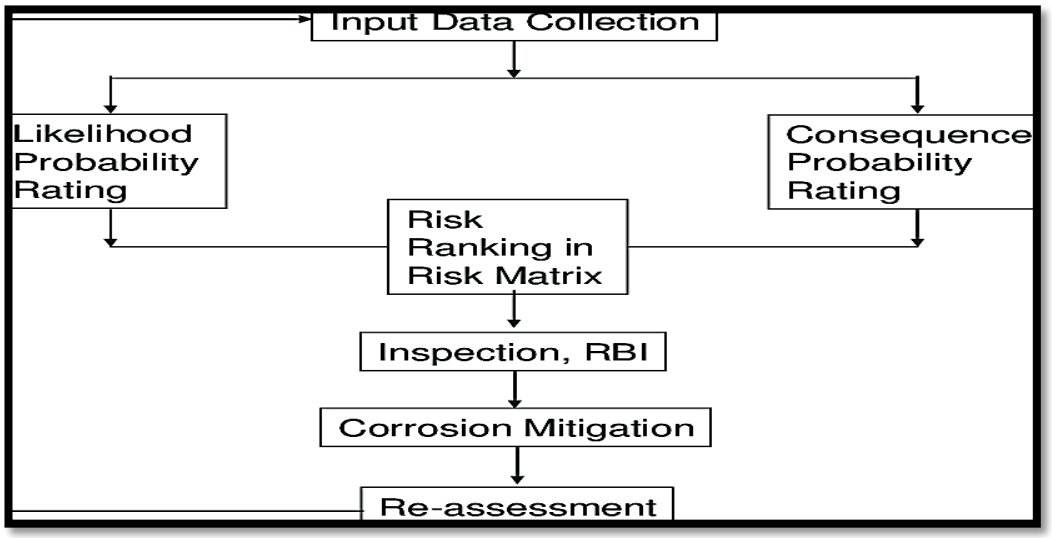

Figure 2.12. Flow chart of various inspection for detecting corrosion [123].

2.4.4.2. Monitoring Techniques

After determining the presence of corrosion, certain evaluations are used to identify the exact corrosive conditions. To do this, probes of mechanical, electrical, or electrochemical nature basically survey the changes in the degree of corrosivity when the equipment is at work. Additionally, other methods are applied for out-of-operation status of the equipment. The pH levels are determined alongside other microbiological tests. These methods offer direct assessments with the process unit at work; standard monitoring involves the so-called corrosion coupons or vouchers as stated earlier, with electrical resistance, linear polarization resistance, and galvanic monitoring. More sophisticated approaches involve the assessment of biological, ultrasonic thickness, and hydrogen penetration factors and figures. Monitoring throughout the service life of any piece of equipment is key to its operation, and the related methods are subject to change depending on the number of years of service and the overall conditions of the equipment. Henceforth, they need to be carried out routinely [124,125,126].

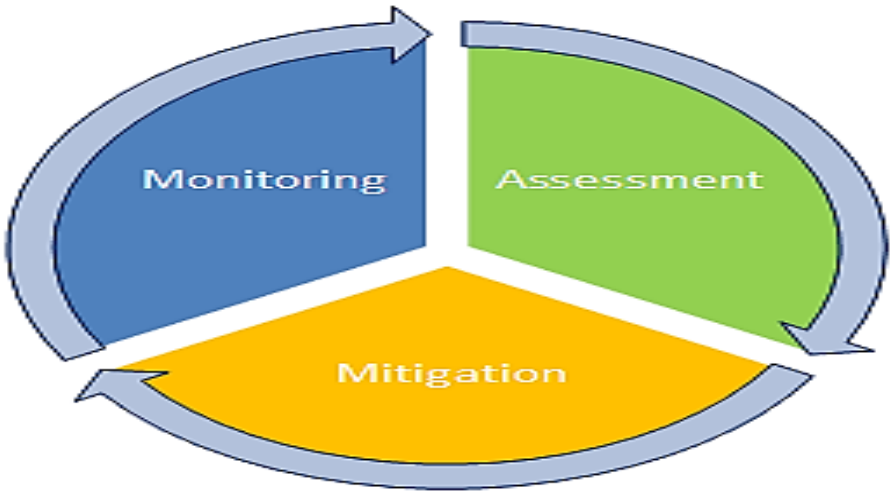

Figure 2.13. Corrosion Management [124].

2.4.5. Atmospheric Corrosion of Steel

For long, atmospheric corrosion in iron and steel has remained within the spotlight of electrochemistry and other experts given its abundance in nature and being the

leading factor in material depreciation – all part of the industrial movement. Chemical and electrochemical processes take place upon oxidation, and iron in any form can be found in numerous environments. Given its extreme reactivity with other material to generate iron oxide, it develops a thin protective layer by mixing with oxygen, leading to rust-resistance by up to 99% RH; however, other material as acidic rainfall can easily deteriorate this layer and make the way for further rust. Deeper layers of iron oxide can add to protection and, within the first few years behind, are likely to decrease the chances of corrosion far more significantly as shown in the following graph: [123,125].

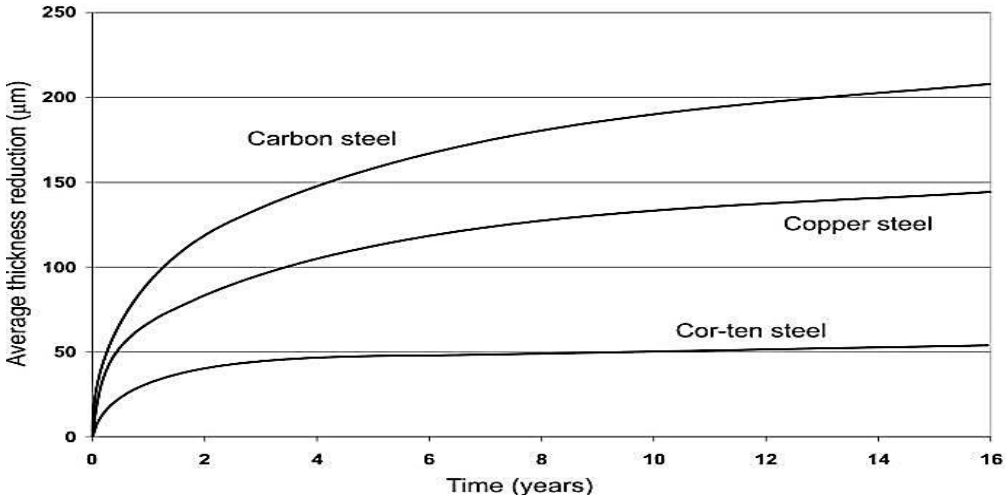

Figure 2.14. Time-corrosion curves of three steel in industrial atmosphere [125].

The atmosphere remains the number one cause of corrosion for most metals. Upon exposure, steels mix with air humidity to form oxides. Metals oxidized in this way are subject to five key elements as regards performance: heat, moisture, rainfall, sulfur dioxide present in the atmosphere, and salinity. These are all independent elements and act individually toward oxidization. Lengthy tests concerning metals have provided us with forecasting abilities pertaining to the rate of corrosion for different types of metal. For instance, carbon steel corrodes once the relative humidity reaches 70% to 80% at over 32 F. The rate of corrosion can speed up depending on pollutants within rain drops and in the form of dust and dirt on the surfaces, some micro structure of oxided steel samples are shown in next figure [126,127].

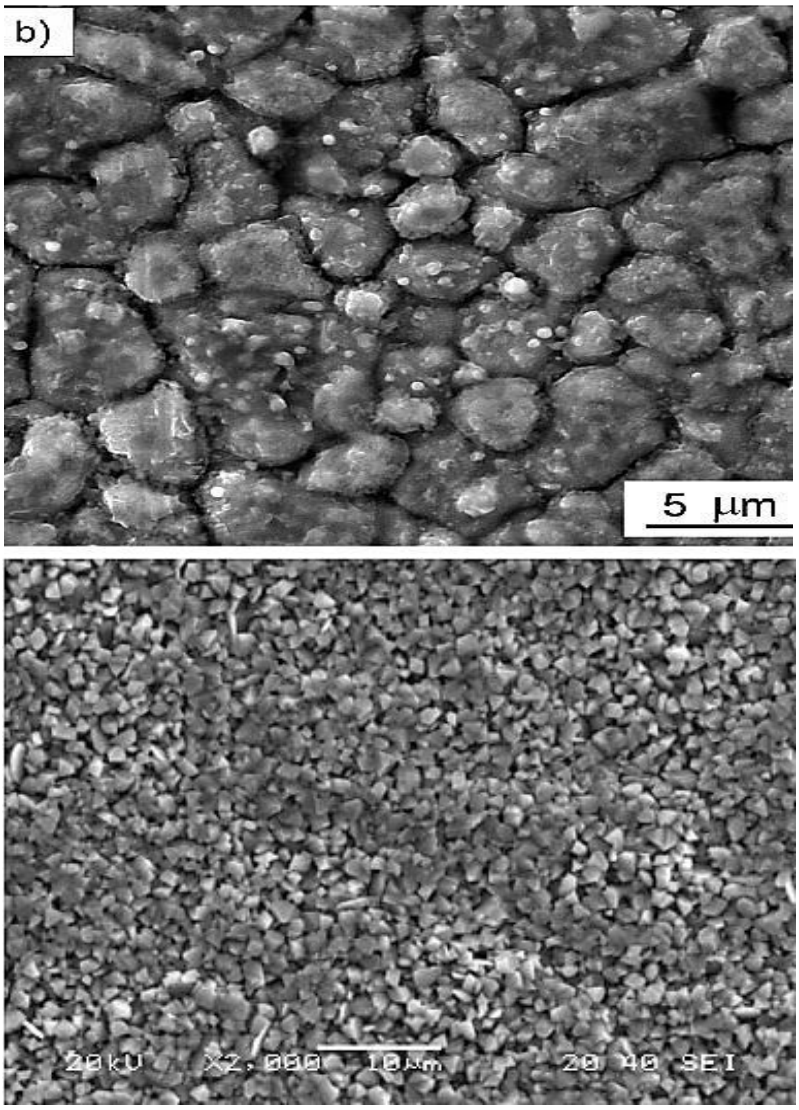

Figure 2.15. Microstructure of oxided steel samples [126].

2.4.6. Mechanism of Steel Corrosion

Steel corrosion is electrochemically induced with various steps. The primary invasion takes place within the anodic regions on the surface over ferrous ions becoming dissolved. Electrons escape the anode and travel along the metallic structure toward neighbouring cathodic regions to mix with oxygen and water and generate hydroxyl ions. In turn, these ions mix with ferrous ions from the anode and form ferrous hydroxide, thus additionally oxidizing in the presence of oxygen and creating hydrated ferric oxide – in other words, rust. These interactions can be represented by the following equation:

$$F_e + 3O_2 + 2H_2O = 2F_{e2}O_3H_2O$$

(Steel) + (Oxygen) + (Water) = Hydrated ferric oxide (Rust)

Nevertheless, as time goes by, certain polarisation impacts like corrosion-related products within the surface can hinder corrosion itself. Other reactive anodic regions can, then develop and add to corrosion. With time, metal loss can be relatively uniform across the surface region, commonly regarded as 'general corrosion'. The event calls for water and oxygen elements to exist simultaneously, in the absence of either, corrosion does not occur. Below, a schematic representation of the corrosion mechanism is shown [123,125,127].

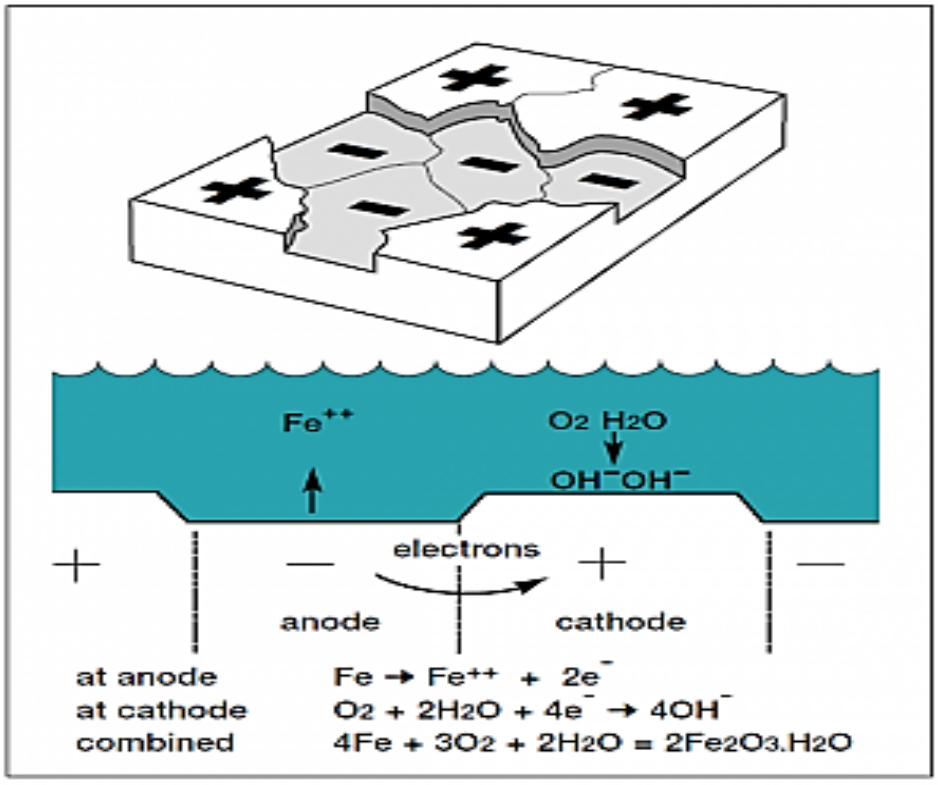

Figure 2.16. Schematic representation of the corrosion mechanism for steel [127].

There is more concern toward the corrosion behaviour among steel types given their wide application in engineering and also given the relatively low resistance among the different alloys. Mostly, this choice is made not in relation to resistance, strength, ease of production, or low expenditure, but other applications that need improved resistance toward corrosion.

2.5. MEANING OF HARDNESS

An attribute within all materials, hardness is not inherently a physical value and can be explained as resistance to denting or influence caused by abrasion, puncture, strokes, scratches, and wear and tear as a whole. The way to measure hardness is by calculating the ultimate extent of the indentation. In a way, this attribute represents the degree of resistance to local deformities, hence applicable to cutting or bending for the same purpose as well. Such deformity is of plastic nature occurring at the surface layer when it comes to metals, ceramics and a majority of polymers. As to elastomers and other polymers, hardness is obtained as resistance to elastic deformation – again at the surface level. Therefore, it can be stated that not having a clear-cut description is an indication of hardness being a non-essential and composite feature depending on yield strength, work hardening, true tensile strength, modulus, and a few other elements. Evidently, any assessment in this respect is mainly intended for quality assurance to yield fast results based on nondestructive experiments that apply only minor indentations in zones having reduced stress levels [128,129,131].

In easier terms, once a definite amount of force or load is employed along with a specific marker or indenter, a minor indentation signals more hardness. Indentation hardness can, then, be assessed based on the estimation of depth or the area of indentation in different ways. Considering the absence of conventional criteria for hardness, every experiment is bound to announce the outcomes as a unique and random measure. Certain materials as steel have shown that hardness and tensile strength can be practically in relation to one another. As for pliable materials, like varieties of plastic and rubber, hardness is determined using durometers. To reveal the degree of hardness, mechanical tests are required for attributes according to design, structural details, and material formation – the ultimate goal being to see if a given material is appropriate for certain use or processing. Given its simplicity, hardness tests have proved to be most applied when examining metal and alloy qualities [130,132].

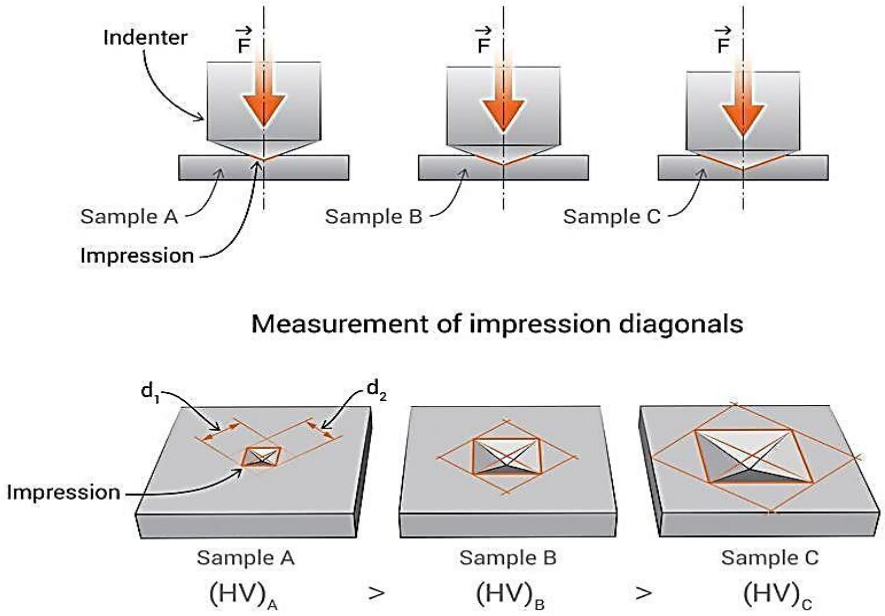

Figure 2.17. Measurement of Hardness [133].

2.5.1. Material Hardness and Hardness Analysis

As stated earlier, considering the number of definitions and equipment for assessing hardness, as well as the absence of clear-cut methods, one can claim that hardness is secondary attribute. that relies on factors such as true tensile strength, modulus of elasticity, work hardening, yield strength, and others. Mineralogy defines hardness as resistance against scratch - the ability for which is measureable in accordance to the Mohs scale on relative hardness. As to macro hardness, it can be easily assessed by means of reference to the information concerning the mechanical attributes for bulk material and based on minor-size specimens. This approach is common for quality assurance as well when it comes to surface processing; yet, the degree of macro indentation can be over-extensive when compared to surface attributes once related coating or coverage is considered vital to withstand friction and wear. For this reason, the process of calculating exact macro hardness values can greatly change and, hence, may not necessarily represent each single attribute in isolation for materials with intricate microstructures, multi-levels, and non-homogeneous or easily fracturing property. Under these conditions, it is better to apply micro hardness measurements [132,134].

Micro hardness is established through the insertion of an indenter (Vickers or Knoop) within the outer layer at less than 15 grams to 1 kg load. The resulting puncture is very tiny, requiring micro-scale assessment that offers insight into micro-level composition and shear gradients available for case hardening. The obtained figures are, then, convertible to tensile strength and similar scales as Rockwell in case of numerous metals and alloys. A micro indenter is constantly pushed inside a specimen while, at the same time, calculations are made related to load, insertion depth and the cycle duration. As for nano-indentation, the experiments are conducted by forcing at very minute amounts as 1 nano Newton to calculate the depth. Such operations require advanced know-how for accuracy and proper control over the forces and depth parameters. Such depth will indicate the continuous degrees of force required for a given specimen, thereby establishing the upper-most indentation values permissible prior to material failure or the film falling out of the testable scope. In addition, a full control can be made of whether hardness is stable post-indentation. Various forms of hardness testing are abound depending on the accuracy anticipated. Considering the close descriptions offered for ultimate strength and hardness, one may assert that as whole, strong metals are hard in the meantime – for which, experiments are designed to establish the degree of tolerance against penetrating non-destructible balls or cones. These tests show the degree to which these utensils can penetrate within the metal based on a given load and duration. Among the highly popular methods, one can find the Rockwell, Brinell, Vickers, Knoop, and Shore methods [134,136,137].

Upon part design, hardness is bound to be determined; still, most experts are unaware of the full scale of this concept and the ways to measure it, naturally due to a number of causes as follows: The issue of hardness is rather ambiguous and, hence, countless methods have been suggested for its assessment, making it even more confusing. There has been more attention paid to these evaluations for metals at higher temperatures due to initiatives toward making alloys that are durable as such. Hot hardness – as it is referred to – is a mark of likely applicability for alloys, sharing no similarity with stiffness because components can be of high or low hardness and still have equal stiffness. A titanium part, for instance, can be as hard as a steel part, with half as much stiffness. Also, hardness alone is different from brittleness or ductility

as two materials sharing equal hardness may still have different values of the two latter properties [135,137].

Hardness in steel is vital in many applications and defines the degree of resistance against plastic deformation, indentation, penetration, and scratching. Within the sector, this concept is key as the intrinsic resistance against friction or erosion caused by oil, steam, and water can be multiplied relatively – that is, added steel hardness means added surface resistance and, hence causing challenges in terms of cutting and machining. The properties that affect hardness work in unison, for which many practical tests exist. Brinell has been the standard method for softened steels, while Vickers is popular for application in general. The two approaches estimate the dimensions of the indentation formed at the surface. As for the Rockwell approach, hardness is determined based on the depth of such indentations[138,139].

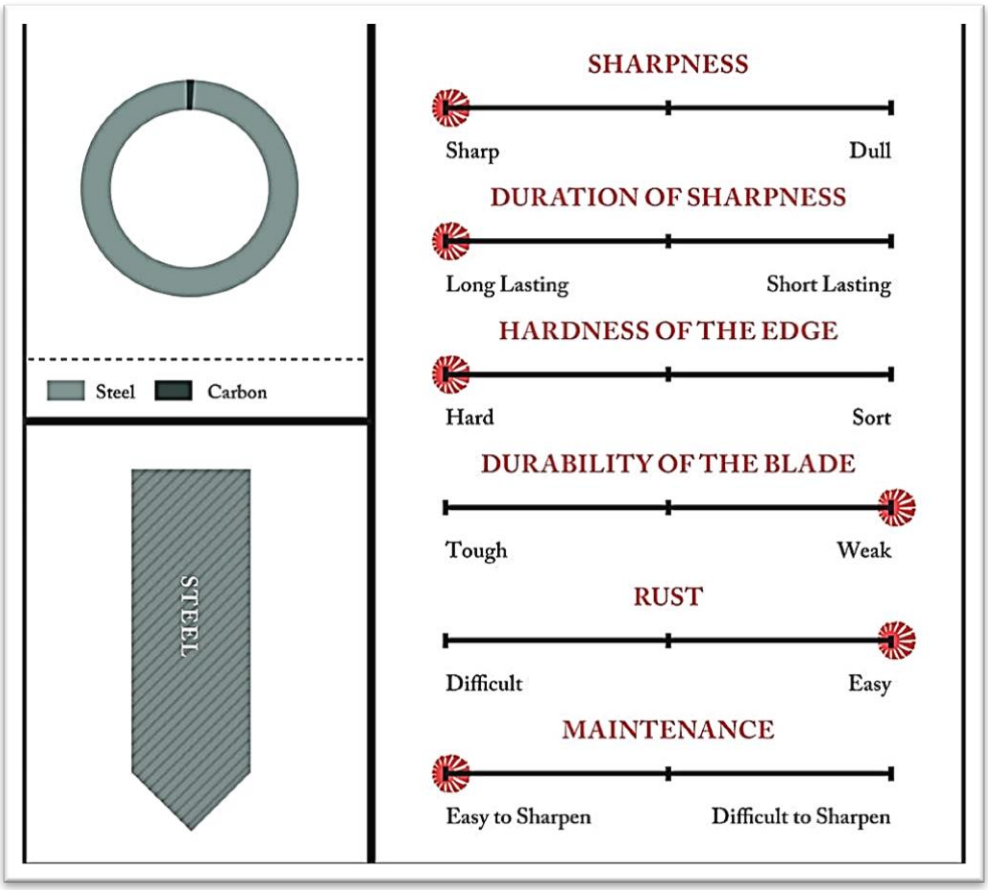

Figure 2.18. Hardness of steel [139].

Vickers estimates hardness based on the dimension of a dent made with load by means of a pyramid-like diamond tip. This is a conventional approach in case of metals, specifically the ones that are quite hard. There is a fixed amount of pressure applied to the surface for a given time, at the end of which the diagonal shape can be judged using a microscope to produce the Vickers value upon conversing. The Vickers indenter takes a square-based pyramid with facing sides joining at the apex at 136 degrees. The diamond is pushed inside the surface using a load of approx.120 kg, to determine the dimension of the dent – commonly, lower than 0.5 mm – with standardized microscopes. The Vickers value (HV) is gained as per HV = 1.854(F/D2), in which F represents the load in kg, and D2 the dimension of the indentation in square mm. The applied load accompanies the HV figure oftentimes. The Vickers equipment employs an indenter of square shape and tipped at one corner, thus looking like diamonds on typical playing cards. Of diamond material as well, the indenter is preferred due to its durability, leaving a dark square mark on bright backgrounds which can be identified with more ease as opposed to, for example, the round mark by Brinell equipment. Also, the Vickers number is determin by division of the load by the surface area of the indentation (H = P/A), with the load ranging between 1-120 kg [140,141,142].

Hardness in metal parts is also representative of durability against wear and abrasion. Any material capable of resisting puncture and impact has to have a certain level of hardness and ductility. To achieve this, tempering can be done – an operation intended for cold-rolled and cold-worked pieces. Once experiencing cold forming, grains can elongate and change in shape. As hardening involves stretching and cold treatment, pieces are bent or strained constantly to decrease plasticity and improve ductility. The properties highlight hardness at room temperature, and some alloys like nickel-titanium are exempt from such practices as they possess strain-relieving attributes that force them to regain the former shape they had. Hardness does not constitute a physical attribute; it is more complicated and relies on strength and plasticity, not to mention the assessment approach. Described in measurable terms and as a value, it is subject to transformations within the metallic structure. Owing to these changes that are similar to the yield point altering based on heat or post-thermal and mechanical processing, any transformation in mechanical attributes post-

treatment can be examined based on hardness – a property that is measurable instantly. As to micro-hardness calculation, it is conducted to examine the mechanical features of each grain type and the building blocks of multiple-component alloys. To roughly estimate a given metal's resistance against heat, experts often employ the long-term hardness or micro-hardness values which can be assessed in higher temperatures and within extended durations as minutes and hours [143,144].

It is not quite as easy to explain metal hardness because it is dependent on each individual material. To begin with, given the elements comprising an alloy, the term "hard" often applies to anything that does not bend, take shape, work or feel the same as other metals do in relative terms. Hardness is a varying property, which means that all alloys can become hard or soft in various forms. Metallurgy regards hardness testing in different fashions – possibly, the most common and vital assessment that there is. The outcomes of such assessments decide the applicability of a material for an intended task or the type of processing it may require. As a surface hardens, resistance increases against deformities. Tempering heats the worked metal up to degrees that disintegrate the grains. Conventional methods for tempering are available depending on specific alloys and the type of grains once being re-crystalized. Temper arrangement, in this respect, is carried out according to grain size and not yield strength [145,146,147].

High-temperature hardness tests today are even more prominent due to the necessity for material to withstand harsher conditions and be more mechanically durable. As opposed to traction tests, these experiments are better, more standard, and more complicated so as to cover the issue of deformability at the surface level and within certain working conditions. Let this not be forgotten that high-temperature hardness tests, up to now, remain non-standard – be it locally or at the EU or other union levels. Certain works have been focused on relating the concept of hardness with other mechanical specifications that surface in elevated temperatures; among them are the correlation between hardness and traction resistance and resilience at elevated temperatures. Once we are to select the right approach for high-temperature testing, we have to take into account certain variables as whether the surface of the resistance

element is observable as regards the marks of hardness, the type of material being studied, the range of hardness likely to obtain, the degree of accuracy of testing, and finally methods of heating and its monitoring, such as the use of ovens and thermometers [143,145,147].

2.6. TRIBOLOGICAL BEHAVIOUR OF STEEL

Tribology is concerned with the study of surfaces in motion and relation to other surfaces. This discipline cuts across numerous daily events that take place around us, and comprise 3 main areas: friction, wear and lubrication. The first area is about resistance against relative movements; the second addresses lack or absence of material caused by such movements; and the last, lubrication, hovers around applying other materials such as fluids so as to reduce the first two factors - friction and wear. The discipline of tribology is crucial in making new and more technologically and financially compatible devices that may have to be operated against many external forces, including wear and friction. Tribology aims to ideally remove or reduce as much as possible any inflicted damage caused by friction and wear within any stage of operations that may entail contact between surfaces. Such studies help pave the way toward improving performance, effective manufacturing practices, supervised and controlled replacement overhauls, and most importantly reducing the added financial burden to promote further growth [148,149].

Specifically, this field stands out in present day operations worldwide since a lot of energy is being wasted merely caused by friction within different parts of machinery. To reduce energy consumption, it is better to reduce such waste in the first place. Sliding faces, in particular, lose a lot of energy and, for this reason, it is paramount to find new ways to reduce friction and wear using more modern approaches in tribology and attain more environmentally friendly solutions for the world. Numerous topics in this regard overlap one another as to the three aspects of tribology; yet, these topics have separate definitions – to mention a few, surface roughness, contact mechanics and nano-tribology. The main problem is that friction is often explained as being a subdivision of physics and mechanical engineering, wear being a part of material science and metallurgy, more specifically, and

lubrication being a field within chemistry. All of these intricacies generate a quite complicated scene as far as the discipline is concerned and, as such, through designing is a must so as to triumph over the difficulties caused by added friction or wear. On average , friction tends to consume or deplete a certain amount of energy which has been generated by humans; whereas a significant degree of manufacturing potential is set aside to replace certain parts that become depreciated over time due to wear and tear [149,150,152].

Investigating the topics of friction, wear, and lubrication – hence, tribology has, consequently, major implications since most mechanical, electromechanical, and biological systems operate in accordance to a level of friction and wear. Over the past decades, this area has been within the spotlight, thus making it a fact that depleting our valuable sources of energy due to unnecessary friction and wear accounts for over 6% of the Gross National Product (GNP) figures in many countries. For this reason, the gains that are likely to be obtained can be major on the condition of adding to our knowledge of tribology [151,152].

This area of expertise circles around testing and hypothesizing certain operations that vary between atomic and molecular levels all the way to micro scales. While adhesion, friction, wear, and thin-film lubrication occurs within sliding surfaces, a solid surface, or more precisely a solid–gas or solid–liquid interface can constitute a complicated form and have such attributes as well – all relying on the nature of solids, the method of surface preparation, and the interactions taking place between the surface and the surroundings. in this respect, the specific attributes pertaining to solid surfaces prove to be vital to surface interaction given that such attributes impact the actual contact zone and – in this way – factors as friction, wear, and lubrication. On top of these tribological features, surface characteristics find their way into other alternative implications, namely optical, electrical and thermal operations, painting and appearance [151,153,154].

Other forms of production also depend on tribology; these are rolling, turning, stamping, grinding and polishing. In addition, transportation at large requires the use of this discipline both in terms of mechanical and moving parts and the contact

between the wheels and the areas where they move or roll on. Other cases include machinery used for buildings and search efforts, namely excavators, oil fields, mine slurry pumps and tunnel drills. In short, the mechanisms related to friction and wear, and applying lubrication so as to manage such phenomena is all inherent within a large number of sectors [152,155].

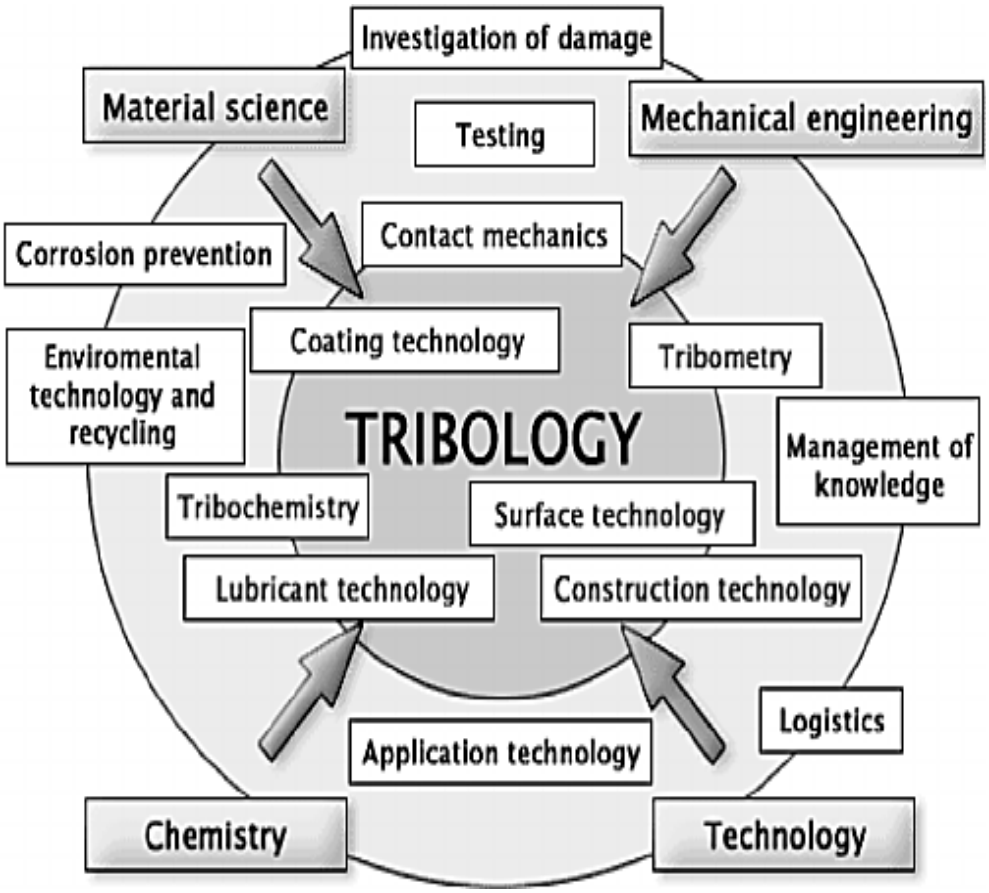

Figure 2.19. Description of Tribology [156].

2.6.1. Role of Tribology in Surface Properties

The present world of technology has many applications for tribology due to the vast amounts of energy being wasted in the form of friction within moving parts. To tackle the problem, it is vital to reduce wastage, in particular within processes involving sliding interfaces. To find the solution against friction and wear, other considerations come into the picture, such as environmental and recyclability concerns for future generations [153,155].

When assessing the right materials to be used for certain purposes, the tribo-test selection criteria is the tool for the purpose. For this, one has to be most realistic in terms of carrying out tests by careful attention to factors as time, expenditure, and control of experimental settings. With more realism within these settings, more reliability can be achieved when listing the implications of the obtained results, hence much safer implementation of the solutions. The less such rankings are, on the other hand, far more attention has to be paid to guarantee that friction and wear within the implemented tools are precisely modelled in the experiment; all of this leads to the studies of the surface damage gaining even more criticality in tribo-testing. Apart from these considerations, as regards the test parameters, one has to opt for the as much similarity to real-life settings as they can – which can be accomplished via copying the exact loading conditions, contact pressures, sliding velocity, contact frequencies, ambient heat, atmospheric factors, and lastly the applied lubricants. The degree of such resistance is a function of the materials, geometries and surface properties of the contacting surfaces, along with the service environment [154,156,157].

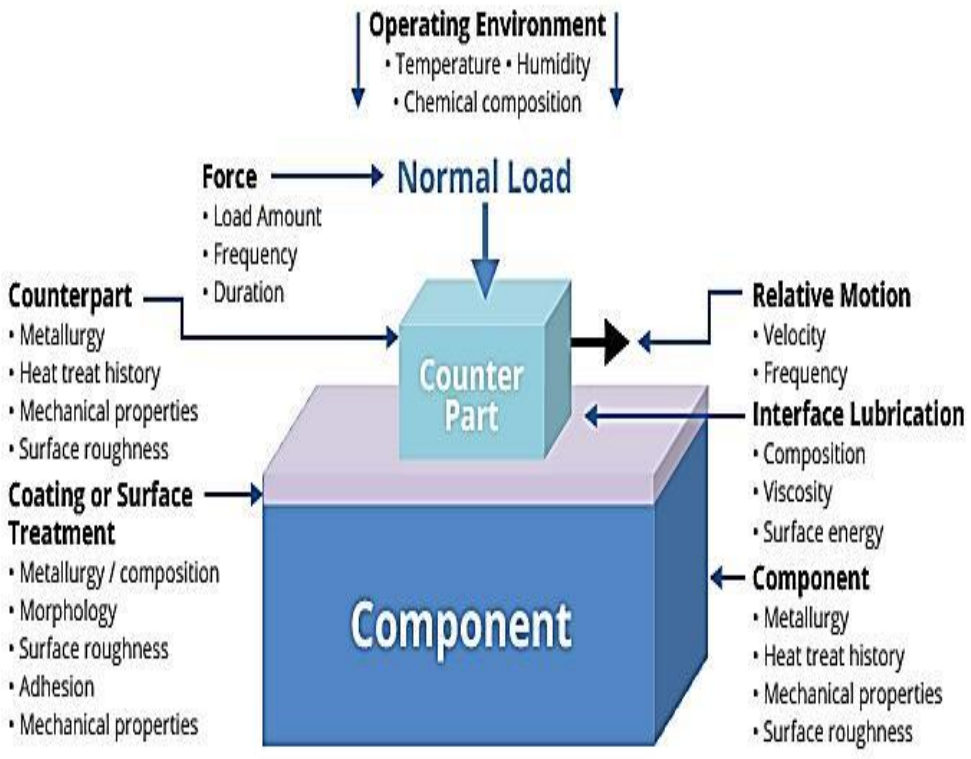

Figure 2.20. Tribological System [158].

2.6.2. Phase Transformation Mechanism in Tool Steel

Phase is a part with a system with attributes as composition and continuity being consistent and unique compared to the rest of the system. The components within a system constitute the system; while the composition of a phase or the system is presentable in accordance to the relative values of these components. In the field of metallurgy, steels are regarded as a combination of numerous phases. In this respect, phase changes in them occur once one or more phases alter to form a new phase or a combination of phases [158,159].

Thermodynamics define the activation process involved and, within a steady temperature and pressure, the relative stability of a system can be explained by Gibbs free energy (G) which is defined by the equation:

$$G = H - TS$$

where H represents enthalpy, T stands for absolute temperature, and S is the entropy of the system. Enthalpy is a unit of the amount of heat within the system and is written as:

$$H = E + PV$$

Here, E represents the inner energy within the system, P represents pressure, and finally V stands for volume. The inner or internal energy, E, is subject to the total kinetic energy and potential energy of the atoms in the system. The total kinetic energy may be increased by means of speeding up the atomic vibration in solids or liquids and adding to the translational and rotational energies of the atoms or molecules in a liquid or gas. Potential energy is the interaction or joints within the atoms in the system [157,159].

The equilibrium of a system is may be explained as the most durable state, in which there is no tendency toward any transformation as time passes. Given fixed

temperature and pressure, a closed system with a definitive mass and composition is in equilibrium on the condition of the least possible value of the Gibbs free energy as:

$$dG = 0$$

According to the Gibbs free energy definition, maximum stability occurs with low enthalpy and high entropy. As such, in solid phases at low temperature, those with more stable atomic bonds are so due to low enthalpy; on the other hand, given more elevated temperatures, the $-TS$ term becomes dominant and the atoms within phases are more likely to be in motion, which means a weaker atomic binding, become most stable [158,160].

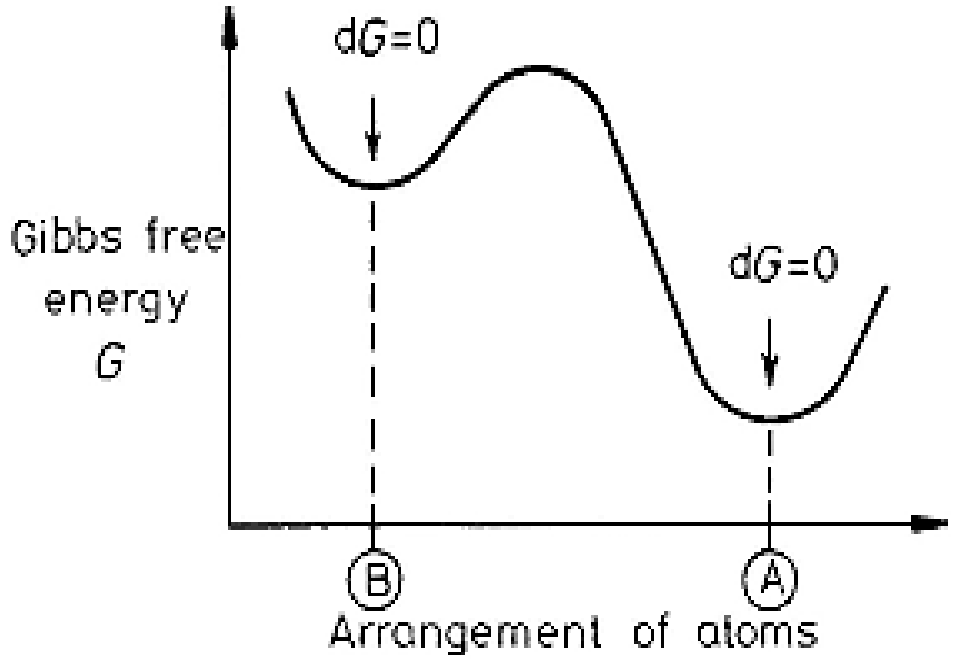

Figure 2.21. Schematic variation of Gibbs free energy [161].

Often, there is a minor degree of local and free energy within metastable equilibrium states. Based on the previous figure, configuration A possesses the least free energy, thereby establishing the arrangement for a steady equilibrium. Yet, configuration B has obtained the least local and free energy, thereby considered a metastable equilibrium. The intermediate states, in which $dG \neq 0$ remain unsteady and, should

the atoms form such a state, then they are likely to re-organize as one of the free energy minima. Once a system changes from steady to metastable, it also gains a new stable equilibrium within time. It is likely for any change to occur, causing a decline in the Gibbs free energy, with the pre-requisite being:

$$\Delta G = GA - GB < 0$$

Such a transformation, of course, cannot straight away reach an equilibrium state, and is subject to numerous intermediate metastable ones in advance [160,161].

PART 3

THEORETICAL BACKGROUND

3.1. MATERIALS (TOOL STEEL)

3.1.1. Steel - A Definition of the Term

This metal encompasses an extended group of alloys, where iron combines with carbon and other elements. Steel varieties come as mild, medium- or high-carbon depending on the carbon levels, which scarcely exceeds 1.5%. The addition of nickel, molybdenum, cobalt, vanadium, chromium, and tungsten adds to this variety, such as stainless steel and high-speed steels. Iron remains crucial in this material along with carbon levels of less than 0.2% up to 0.5% according to grade. Metal alloys are otherwise regarded as cast iron due to carbon levels that impact melting point and offer ease mold-filling [162,163].

Steel is abundant in buildings and other structures like bridges, tools and gadgets, machines, vessels, transportation parts, and firearms, the reason being its mechanical attributes of ductility that make it ideal in terms of arrangement and cost-effectiveness, hardening rate, yield strength, resistance to impact loading, and surface structure. Tests have been conducted at deeper levels of grain refinement to improve both yield strength toughness. On top of the stated benefits, stainless steel possesses advanced temperature properties, making it applicable where oxidation resistance in such circumstances is an utmost necessity. Tool steel falls into 6 groups: high-speed, cold-work, hot-work, water-hardening, shock-resisting, and special purpose – according to which purpose, choice is made based on the economics, shock resistance, surface hardness needed, working temperature, strength, and toughness [164,165].

There are two main reasons for the popular use of steel:

- It is widely available in the earth's crust as Fe2O3, requiring minimum conversion effort; and
- It may be transformed easily and significantly in microstructural terms to possess different mechanical properties.

Though steel features are countless in every sense, plain carbon steel takes up 90% of all its derivatives due to its toughness, ductility, economics, and acceptable casting, working and machining. The latter requires only basic heat treatment to generate numerous and different properties [165,167].

Various approaches and efforts have been shown to improve the performance of low-carbon steel to guarantee expansion to other more advanced use cases. Adding to strength or high-performance material, the carbon in steel has to be minimal for toughness and weld-ability.

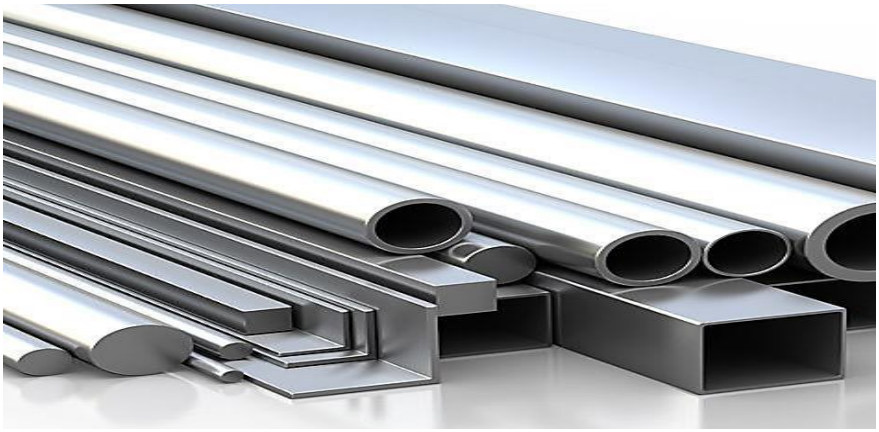

Figure 3.1. Stainless Steel [166].

3.1.2. General Characteristics

The attributes associated with steel come from certain chemistry, mechanics, and heat treatment factors. The chemistry, to start with, is key to the mechanical aspect and the supply of alloys like carbon, manganese, niobium and vanadium adds to its

strength – though costs can also exceed and also negatively impact other features like ductility, toughness and weld- ability. Reduced sulphur improves ductility, while nickel adds to the toughness. The chemical configurations for every type of steel are intended for the qualities expected from that product – among which, one may refer to corrosion resistance, strength and formability, and also high and low temperature service. For this, certain elements are supplied on purpose to achieve certain qualities; whereas others appear by chance in the mix and may not be eliminated in any form – otherwise known as trace or residual elements [166,168].

Table 3.1. Chemical Composition of Medium Carbon Steel [169].

Component Elements	**Content (%)**
Carbon, c	0.34
Iron, Fe	0.60
Manganese, Mn	0.44
Phosphorus, P	0.21
Sulfur, S	0.03
Chromium, Cr	4.78
Copper, Cu	0.08
Nickel, Ni	0.15
Molybdenum, Mo	1.61
Vanadium, V	0.51

Steel alloys abound with intricate groups and families depending on the main components. In general, there are: Plain Carbon Steel; High Strength Low Alloy (HSLA) Steel; Alloy Steel, Ultra Low Carbon (ULC) Steel; High Alloy Steel, including Tool Steel and Stainless Steel; and Electrical Steel. Advanced High Strength Steel (AHSS) is among the latest additions to this categorization. Alloying elements, as stated before, are used for different functions; such as manganese, which adds to strength and hardness in rolled form, and also to the hardening ability as a major point in heat treatment [167,169].

Stainless steel varieties are ideal in terms of corrosion resistance, though they may lack strength, hardness and wear protection. Adding the cost factor, these products are limited in use and, henceforth, call for surface modification approaches to

achieve corrosion resistance as well as satisfactory strength, hardness and wear protection. These varieties are optimally applied in many areas calling for robust performance, namely aviation, oil and gas industries, energy supply, petrochemical sector, building material, automobile and household equipment and utensils [168,170].

3.2. H TOOL STEEL

H-steel is formed using a hot-rolled steel strip and high-frequency resistance welding to generate thinner plate thickness and added accuracy in cross-sectional sizes as opposed to hot-rolled H sections. In this way, the material is applicable in different sectors like prefabricated housing compartment, temporary housings, structural steel frames, pre-engineered structures and hothouses, not to mention other sophisticated designs based on durable quality. In this respect, chromium hot-work tool steels fall within this category as well based on the AISI, beginning from H1 all the way to H19 with the most widely applied materials being H11, H12, and H13 – easily air-hardened in 150 mm thick sections. These are then exposed to minimum distortion when hardening takes place based on their balanced alloy content. Tools made using this steel are then safely cooled with water because of low-carbon and alloy contents [163,164].

Figure 3.2. Hot tool steel [172].

In the industry, it represents hot working steels and, henceforth, such tools are expected to possess added strength and hardness when employed in higher degrees of heat. In them appears a significant degree of alloying elements and a certain grade value that is Cr-, W-, or Mo-based. H1 to H19 comprise Cr up to 5%; whereas, H20

to H39 have a W value of 9-18% and a Cr content of 3-4%; H40 to H59 are Mo-based. The common applications for H-grade tool steel are in cold heading die castings, die casting in hot settings, hot extrusion, hot gripper, hot forging, hot swaging, and hot work knives [171,172].

The present thesis concerns the H13 Tool Steel, and we selected H13 Tool Steel because H13 was designed as hot work steel, and also it has solved many cold work applications where extra toughness could be gained with some sacrifice of wear resistance. Apart from this, H-13 can tolerate rapid cooling – even early and premature heat checking – characterized by satisfactory machining, welding, and ductility properties and a wide range of use in both hot and cold work tooling. More specifically, the H13 tool steel is chosen for its superb mixture of increased toughness and fatigue resistance, and H13 chromium hot-work steel is widely used in hot and cold work tooling applications, not to mention its applicability more than others for tooling purposes as it brings together good red hardness and abrasion resistance with resistance against heat checking. Another reason is the common use of this steel in extrusion press tooling as it can safely undergo extreme cooling after being used in high temperatures [171,173].

Table 3.2. Modulus of Elasticity of H steel [174].

Temp °F	**Modulus psi x10^{-6}**	**Temp °C**	**Modulus GPa**
70	30.0	21	206.8
200	29.0	93	199.9
400	27.0	204	186.2
600	28.5	316	196.5
800	27.5	427	189.6
1000	23.0	538	158.6

3.3. H13 TOOL STEEL

H13 Tool Steel is a versatile chromium-molybdenum hot work steel (5% chromium and 1.30% molybdenum), intended for maximum toughness and satisfactory red-hardness. It has chromium, vanadium, manganese, molybdenum, silicon, and carbon,

among which molybdenum and vanadium account for strength whereas chromium for softness when applied in heat. As stated earlier, H13 can tolerate sudden cooling and early heat-checking, rendering its good machining and welding properties along with acceptable ductility and formability using any standard method. The hot hardness (hot strength) of H13 resists thermal fatigue cracking which occurs as a result of cyclic heating and cooling cycles in hot work tooling applications. Due to advanced toughness coupled with good resistance against thermal fatigue cracking or heat checking, H13 is the preferred material over all other alternatives in hot conditions [174,175,177].

Figure 3.3. H 13 tool steel [178].

Table 3.3. AISI H13 Steel Mechanical Properties [175].

Properties	Metric	Imperial
Tensile strength, ultimate (@20°C/68°F, varies with heat treatment)	1200 – 1590 Mpa	174000 – 231000 psi
Tensile strength, yield (@20°C/68°F, varies with heat treatment)	1000 – 1380 MPa	145000 – 200000 psi
Reduction of area (@20°C/68°F)	50.00%	50.00%
Modulus of elasticity (@20°C/68°F)	215 GPa	31200 ksi
Poisson's ratio	0.27-0.30	0.27-0.30

There are numerous cold work tooling uses for this steel as it offers improved hardening ability in large section thicknesses and advanced protection against wear compared to conventional alternatives like 4140. Another benefit is improved toughness and high stability in heat treatment. The steel is of air hardening chromium die with added vanadium to make for improved resistance against cracking and overall advantage in other features required for extreme temperatures. These tools can be cooled using only water and with no concern for checking. Upon routine heat processing, nitriding at 0.30mm (0.012") of depth can be done. This type of steel is popular for die casting for zinc, white metal, magnesium and aluminium, not to mention extrusion dies, gripper dies, trimmer dies, casings, hot shear blades, and identical hot-work uses. The table below offers a glimpse into the chemical composition of H13 tool steel:

Table 3.4. Chemical composition of H13 tool steel [175].

Component Elements	**Content (%)**
Chromium, Cr	4.75 - 5.50
Molybdenum, Mo	1.10 – 1.75
Silicon, Si	0.80 – 1.20
Vanadium, V	0.80 – 1.20
Carbon, c	0.32 – 0.45
Nickel, Ni	0.3
Copper, Cu	0.25
Manganese, Mn	0.20 - 0.50
Phosphorus, P	0.03
Sulfur, S	0.03

H13 brings together good red hardness and abrasion resistance and resistance to cracking. AISI H13 is common in extrusion press tooling given the potential tolerate sudden and major cooling after working in hot conditions. Making H13 by using vacuum degassed tool steel helps – alongside scrutinized hot working conditions – to achieve ideal uniformity, stable response to heat treatment, and extended working life in tools. In H13, the molybdenum and vanadium serve to add strength, whereas chromium helps with die steel H-13 against softening in heat, H13 die steels have a very good shock resistance and, as for AISI H-13 tool steel, it demonstrates steady

and high degrees of polish ability and minimal distortion during hardening. As commonly known, AISI H13 steel is often chosen for tool manufacturing along with anit-wear dies because of their applicability and economic benefits by protecting them against cracks, erosion, soldering, rust, or all of such impacts [177,178,179].

Table 3.5. Thermal conductivity of H13 tool steel [174].

Temperature °F	**Btu/hr-ft °F**	**Temperature °C**	**W/m °C**
80	10.17	27	17.6
400	13.52	204	23.4
800	14.50	427	25.1
1200	15.49	649	26.8

Apart from these qualities, H13 is an excellent die steel for die casting aluminium and manganese. Being applied for zinc in extended manufacturing rounds, as well as for slides and cores in tool assemblies. The hardness of H13 stands somewhere around 45/52 RC. In addition, plastic molds use H13, which enjoys high polish and, thus, is convenient for lens and tableware molds [180,181].

In hot work applications, H13 is applied within a hardness of HRC 38 and 48. Ordinarily speaking, this scope for die casting dies varies between HRC 44 and 48 with tempering needed at roughly 1100°F. to gain better shock resistance, the steel is often tempered at temperatures approaching, H13 steel has very high harden ability and should be hardened by cooling in air [181,182].

Table 3.6. Coefficient of Thermal Expansion (47 – 48 HRC) for H13 steel [174].

Temperature °F	**in/in °F x10^{-6}**	**Temperature °C**	**mm/mm Cx10^{-6}**
80-200	5.8	21-93	10.4
80-400	6.3	21-204	11.3
80-800	6.9	21-316	12.4
80-1200	7.3	21-427	13.1
80-1500	7.5	21-538	13.5

3.4. EXPERIMENTAL TECHNIQUES AND METHODS

3.4.1. Boriding Process (Thermal Surface Treatments)

Boriding, also known as boronizing, applies boron to metals or alloys as surface transformation for steel, cast iron, and nickel alloys to improve surface hardness and wear resistance. The method applies boron atoms onto the surface, which practice is grouped according to chemical processes. In detail, an element with a small atomic radius (such as N, C, or B) enters into the surface at high temperature via the interstitial locations of iron lattice, eventually creating a hard layer. Boriding is done on various steels and cast irons like tool steels, case hardened steels, stainless steels, structural steels, cast steels, or sintered steels (known as well by powder metallurgy) [183,184].

Figure 3.4. Boron powder [185].

As a thermos chemical operation employed to harden surfaces, boriding requires material heating up to 700-1000°C for 1 to 12 hours with a boronaceous solid powder, paste, liquid or gaseous medium. Among the main benefits, one may refer to definitive and major improvements in surface hardness of the processed material minimizing the friction coefficient – that is to say that surface wear drops to low levels and, given the operations carried out within the austenitic scope, air-hardening steels may be both hardened and borided at the same time.. Water-hardening grades are exempt from boriding due to the threat of thermal shock. Likewise, re-sulfirized and leaded components are inapplicable owing to case spalling or cracking potential [185,186].

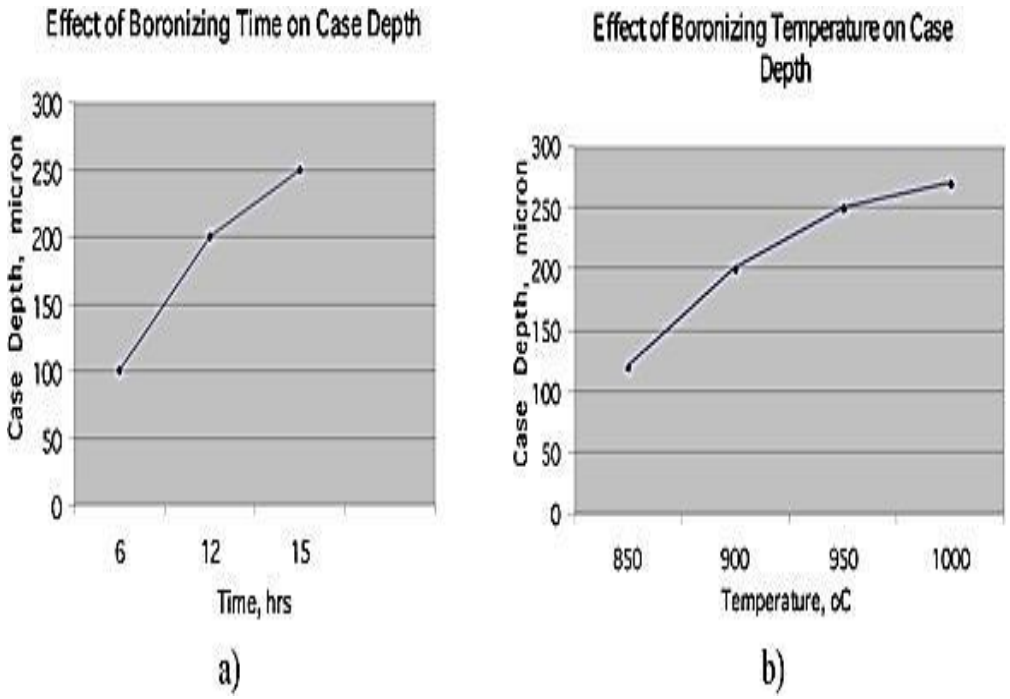

Figure 3.5. Boronizing process flow chart [187].

Boronization entails a dual stage: the initial reaction occurs between the boron-yielding material and the metal surface with a particle nucleation rate being a function of the boronization time and temperature. This produces a thin, compact boride layer. Next comes the diffusion-controlled stage, the subsequent second reaction is diffusion controlled, and the total thickness of the boride layer growth at a particular temperature can be calculated by the simple Formula: $\boldsymbol{d = k\,t}$

Here, d stands for boride coat thickness in cm, k as a constant based on temperature, and finally t for time in seconds within an assumed temperature. Accordingly, Boron dispersion at 950°C is estimated to be 1.82×10^{-8} cm^2/s for the boride coat and 1.53×10^{-7} cm^2/s for the dispersion area, thereby stretching this area over 7 times the thickness of that layer within the substrate. Experts state that concentration gradient is the main factor behind the advancement of dispersion-controlled boride coat. Such degrees of diffusion case intensity stand around 0.13 mm for ferrous alloys pending their content and structure. Less case depth is needed in case of steel with more carbon and alloy, while more depths are necessary in case of reduced or average carbon tools. Once between 320 and 350 μm, no further heat treatment is needed for these depths [187,189].

Though old and still quite unfamiliar for many experts, boronization allows for specific feature formation appropriate for settings likely to cause a lot of wear and tear. The technique is not merely coating, and involves surface transformation; hence, the form and content of of the final coat can be greatly affected pending material and alloys employed. Also, this method involves thermal dispersion to create coats that are immune to wear. For different steel materials, the boron coat hardness may achieve 1600 to 2000 Vickers. Nickel-based alloys may utilize the method, too, to reach up to 2800 Hv. In case of common austenitic steels like 304, 316 and 904, the degree of hardness varies between 1600 and 2200 Hv on average [188,189,190].

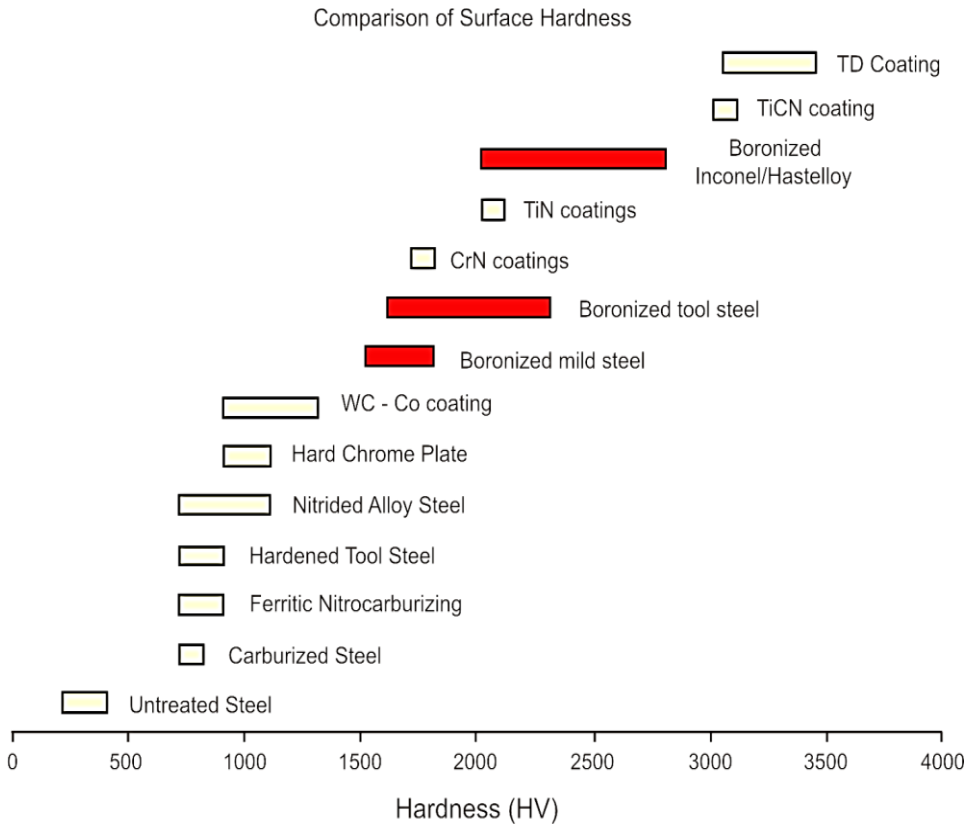

Figure 3.6. Layer hardness of boriding process [192].

Being a diffusion process, the outcomes of the method for thickness are subject to temperature and alloys used. On average, 10µm to 100µm is possible, even going further up to 150µm and more given the right conditions. The principal remains that the more alloy, the thinner the layer and the less tooth-looking the form. In case of moderately and little-alloyed products, acceptable figures are roughly 30 to 100µm,

and 200μm for extreme wear resistance – given the fact that boronizing, similar to many other approaches, can vanish as time goes by, The method, apart from all these advantages, enhances substantially the corrosion resistance of mild steels and low-alloy steels, making it useful in areas of advanced wear and tear due to corrosion – namely pumps and valves. Boronizing and boron steel differ in terms of the level of diffusion; in the former case, the surface layer is covered with an agent to merely alter exterior side, implying the core remains intact. Tiny amounts of boron, though, have substantial effects on hardenability, and values of approx. 0.0015% to 0.0030% have been considered as maximum, though still changeable as per the hardening method [191,192,193].

The latter case - boron steel – holds this material throughout the whole of the texture and not just superficially – which implies there is boron in the core, too. Boron levels supplied to a given material may change according to the hardening needed. Conventionally speaking, boron steel possesses low forging as well as ductility properties as opposed to bopron-free steel. To choose between the two approaches, consequently, is rather a challenge relying upon the purpose and application. Whereas the two offer better hardness, boron steel is rather brittle given to through and through hardness. Boronized steel maintains a mild core, assuming that original material would count as such and display better ductility. Also, in boron steel, boron needs insertion into the material in the form of an alloy, ideal in this way for work pieces to be made and formed. As for already existing steel parts, boronizing is superior given that merely extra diffusion layers would be required and no more in-depth processing than a few micrometers is necessary. Boron may be supplied to mildly-alloyed or unalloyed steel for added hardenability, and may be seen in austenitic steel as well for better strength in hot conditions and avoiding pearlite and ferrite formations, thereby adding to hardness and strength. A common boron steel is ferroboron, which is an alloy containing ferritic steel and a significant amount of boron varying from 12% to 24% as per the common industrial routines [193, 194,195].

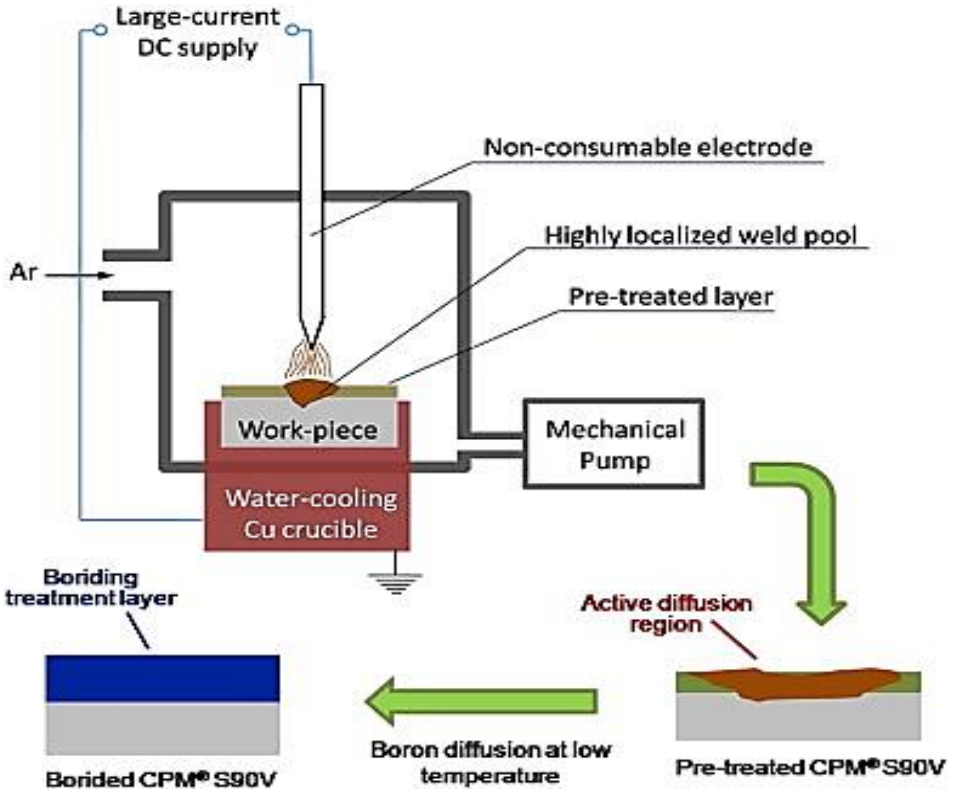

Figure 3.7. Schematic flowchart of low-temperature boriding process [187].

Like all other coating practices, boriding involves two stages: initiation and growth:

1. Initiation: Here, potassium fluoborate is disbanded at temperatures exceeding 530 °C to free the boron trifluoride (BF4) as gas, using the following formula:

$$KBF_4(S) \xrightarrow{T > 530\ ^\circ C} KF(S) + BF_3\ (g)$$

Next, BF4 reacts with boron carbide on the surface of the steel substrate, creating iron boride (Fe2B):

$$\mathbf{2F_e(s) + \frac{1}{13}\,BF_3(g) + \frac{3}{13}B_4\,C(s) \xrightarrow{T > 570\ ^\circ C} Fe_2B(s) + \frac{3}{52}CF_4\,(g) + \frac{9}{52}\,C(s)}$$

Fe2B is vital for boron layer formation and, upon seed formation, no other initiators like (KBF4) will be necessary. With oxygen from the atmosphere, potassium fluoborate is oxidized to oxygenyl boron fluoride (O2BF4) – itself ineffective as an initiator andh, hence, the main cause for the operations to be carried out within an inert atmosphere [197,198,199].

2. Growth: At this stage, the iron boron layer expands upon reaction between boron carbide of the gent) and iron boride coat on the surface as per:

$$\boldsymbol{B_4C(s) + Fe_2B(s) \xrightarrow{T > 600\,^{\circ}C} 4B[Fe_2B\ or\ F_e\ B\ ](s) + C\ (s)}$$

The boron in atomic form disperses within the boron layer, causing it to expand. The boron content of the agent is decisive in the boride layer formula. Should the boron values on the steel surface be high – that is, elevated B4C values within the agent – the FeB can form and develop over the Fe2B layer; In other cases, Fe2B becomes the main component in the boride layer. Given Fe2B's common place as layer, SiC is supplied to the boriding mix to decrease boron activity at the surface – hence, the term 'diluting agent' for SiC [197,198,199].

In the same way as other thermos-chemical procedures like carburizing or TD, the rate of the growth stage is subject to boron atom dispersion within the steel structure and boride layer. The boride layer thickness at a given temperature is obtained according to this formula – otherwise known as the parabolic law:

$$\boldsymbol{D = K\sqrt{t}}$$

Here, D represents the layer thickness, t as the time period, and K for growth rate constant as a function of temperature. K is written using an Arrhenius-type format:

$$\mathbf{K = A.exp}\left(\frac{-\boldsymbol{Q}}{\boldsymbol{RT}}\right)$$

Here, A stands as a pre-exponential constant, T as temperature in Kelvin, R as universal gas constant (8.314 J/mol.K), and finally Q as the activation energy of boron dispersion within the boron layer. The activation energy relies upon the substrate and boride layer, but within the range of kJ/mole. The figures obtained from studies on various steel types appear as follows:

Table 3.7. Activation energy of boron diffusion in different types of steels [195].

Material	Q (kJ/mol.k)
AISI H13	186.2
AISI M2	240
AISI W1	171.2
P20	200
Fe-10%Cr alloy	147
SS 420	222
SS 304	199

3.4.2. Characteristics and Properties of Boride Layer

Alloying elements decrease the boride layer dimension by creating a diffusion barrier and limiting boron penetration; in particular, nickel and chromium cause morphological flattening. Henceforth, the tooth-like formations are common in reduced-carbon and mildly-alloyed material, whereas high-alloy steel gains a more even interface of boride layer. Such common tooth-like formations are also abundant in pure iron, unalloyed low-carbon steel, and also mildly-alloyed steels. Once the alloying agents and carbon values of the substrate steel elevate, this reduces the boride layer density; furthermore, an even interface is achieved instead of tooth-like formations – excluding the cases of nickel, cobalt, and manganese as they impede and postpone boron penetration within the substrate – thus adding to FeB values. To illustrate this phenomenon, in boronized stainless steel, alloying elements create a rather trim and even interface of about 100% FeB phase of the boride layer [196,198,200].

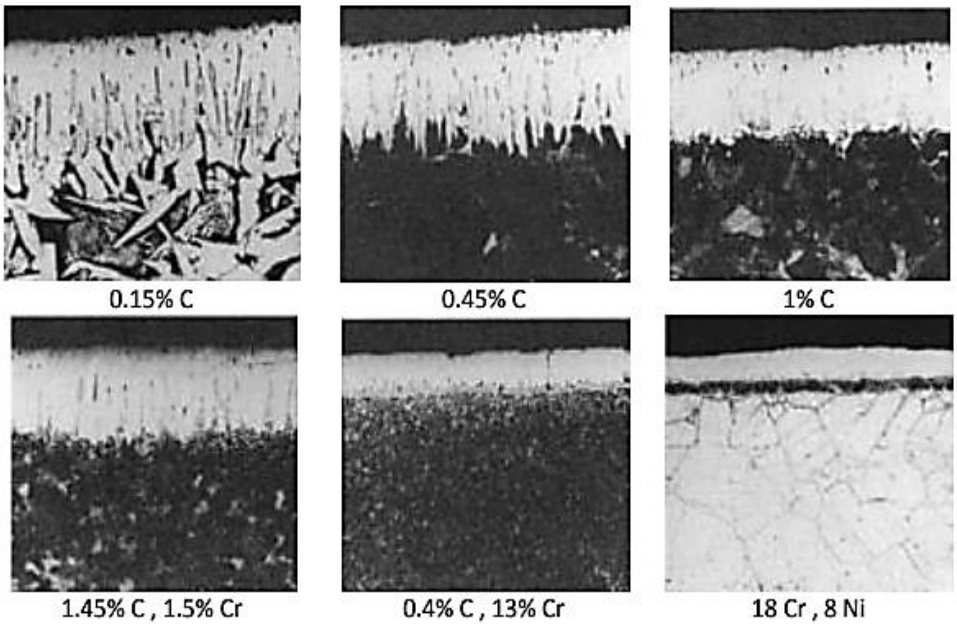

Figure 3.8. Effects of steel composition on morphology of boronized layer [198].

3.4.2.1. Properties of Boronized Steels

Boronizing, steel results in favourable attributes on the surface, such as added wear resistance, corrosion resistance, and useful life span of up to 3 to 10 times the normal conditions, and properties of boronized steel as per following:

1. Toughness: A boride layer offers better bonding with the base metal, thus preventing under-load flaking and peeling; nevertheless, the boronized steel toughness also relates to the boride thickness, the cross-section zone, and other mechanical attributes. During experiments on bending, boronized samples of boride thickness between 150 and 200 μm exhibit 4% stretching without any cracks.

2. Adhesion Resistance: The boronized surfaces demonstrate no accretion or wear and also no tendency toward cold weld. As a result, this feature is applied in cold metal working. In the absence of the lubricant, the boronized layers do not have an appreciable change at 300 °C in order to protect the environment by reducing the lubricant.

3. Abrasive Wear Resistance: Advanced micro hardness offers additional wear resistance to the material.

4. Corrosion Resistance in Acids**:** Boronized carbon and alloy steel add to the corrosion resistance in HCl, H2SO4, and H3PO4. Also, boronizing austenitic stainless steel furthers such resistance in HCl [201,202,204].

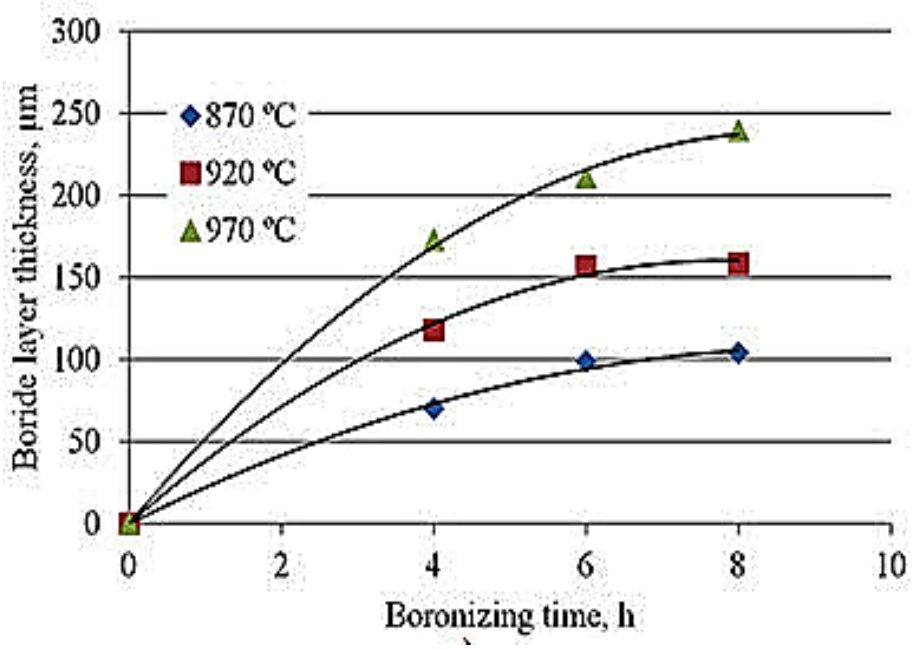

Figure 3.9. Boride layer thicknesses as a function of boronizing time for steel [204].

3.4.2.2. Operational Conditions for Solid Boriding

- Temperatures arte conventionally set between 850 and 950°C. In case of cemented carbides and hard metals, over 900 °C of heat is advised against for the possibility of boride separation from hard carbides.

- The processing period, often, is decided at 15 minutes to 30 hours relying on the expected outcomes. Yet, between and 1 and 8 hours is common. For steel varieties, a combination of high temperature and short duration is preferred to low temperature and long duration.

- In solid boriding, one needs a vacuum or inert gas atmosphere, and boronizing relies on the kind and quality of such atmosphere. Ideal outcomes are best achieved using high-purity argon [198,200,203].

3.4.2.3. Advantages of the Boriding Process

These benefits include:

- Boride layers hardness achieved on carbon steels exceeds that of standard methods;
- Superb adhesion appears through dispersion with no grinding or finishing necessary post-process;
- Boriding, owing to its major improvements in corrosion-erosion resistance of ferrous materials in non-oxidizing dilute acids and alkali media, is gaining more attention from various sectors;
- Borided surfaces demonstrate average oxidation resistance at about 850°C with considerable resistance against molten metals;
- No increase in surface roughness in most cases, and can be selectively processed to target areas.
- Advanced surface hardness coupled with reduced surface coefficient of friction for borided layers allows for resistance against major wear mechanisms like adhesion, tribo-oxidation, abrasion, and surface fatigue;
- A high surface hardness coupled with low surface coefficient of friction for borided layers allows for resistance against major wear mechanisms like adhesion, tribooxidation, abrasion, and surface fatigue;
- Boride layers show absolutely high hardness figures of around 1450 and 5000 HV along with a high melting points of the constituent phases;
- Major improvements are visible in terms of abrasive wear resistance and case depth compared to nitriding and nitro-carburising;
- The boride layer hardness is retainable at elevated temperatures compared to nitrided cases;
- A wide variety of steels, including through-hardenable steels, are compatible with the processes.

- The operation is possible on blind holes and internals, not to mention its convenience for small-size parts; and
- Borided segments show better fatigue life and service life in oxidizing and corrosive environments [201,202,203].

Table 3.8. Properties of boronized steel [204].

Property	**Boronized steel parts shows**
Wear (Adhesive or Abrasve)	increase the lifespan more than 25 times
High Temperature wear	Excellent after 650 **°C**
High Temperature Oxidation	Good resistance up to 1000 **°C**
Corrosion resistance	İncrease by a factor of 200 %
Fatigue Strength	İncrease by a factor of 25 %
Ultimate and Yielding strength	İncrease by a factor of 10 to 20 %

3.5. SCANNING ELECTRON MICROSCOPE (SEM)

A scanning electron microscope (SEM) is an instrument to generate views of samples for the surface areas using a focused beam of electrons, which interact with the atoms in the piece to form different pulses of information regarding topography and composition. The electron beam scans the work piece in a raster pattern, while electrons are formed at the top of the column by the electron source, later to be released once heat energy takes over the work function of the source material. The electrons gain added speed and become absorbed by the positively-charged anode. Once generated at the top of the column, they are sped along to pass through some lenses and apparatus, creating a centralized beam to strike the sample surface. The sample itself is positioned on a stage within an area, and the pulses released by such electron-sample exchange offer a glimpse into exterior texture, chemical mix, and crystalline formation as well as orientation. A majority of cases involve information accessed using a sample zone within the surface, along with 2D pictures showing spatial alterations. These areas vary between 1 cm and 5 microns in width, viewed by a standard SEM method of enlargement between 20X and 30,000X, and a spatial resolution at 50 to 100 nm. This tool can carry out assessments related to choice

locations, in particular beneficial for qualitative and semi-quantitative evaluation of chemical mix, crystalline form, and crystal arrangement [205,206].

Figure 3.10. Scanning Electron Microscope in the lab [207].

Key to SEM are the electron source, electron lenses, sample stage, signal detectors, monitoring and data output equipment, power supply, vacuum system, cooling system, steady stage, and a room devoid of ambient magnetic and electric fields. Accelerated electrons contain high levels of kinetic energy, which is released in the form of pulses upon electron-sample exchange once the incident electrons are slowed in the solid sample. Such signals carry secondary electrons to generate the images, backscattered electrons (BSE), diffracted backscattered electrons (EBSD) to reveal the crystal form and mineral arrangements, specific X-rays intended for element studies and continuum X-rays, visible light (cathodoluminescence--CL), and finally heat [207,209].

All of the electron column has to remain in vacuum conditions and, similar to all other such microscopes, the source is securely within a custom chamber to maintain vacuum and safeguard against contamination, motion or other disturbances. Vacuum also makes room for obtaining high-resolution pictures, and without it different atoms and molecules may find their way into the column, interacting and resulting in deflection and poor image quality. Increased vacuum further improves the degree of electron collection by the detectors [208].

Lenses guide the electron paths and since electrons are unable to move through glass, electromagnetism in lenses is important. There are wire coils within metal pole pieces in lenses and once a current moves along them, magnetism is achieved – a feature to which electrons show sensitivity and, hence, allows for their direction to be guided by mere changes in the current. Electromagnetic lenses commonly appear in two forms: the condenser lens initially receives the electrons moving in the direction of the work piece, converging the beam prior to the cone's re-opening; convergence occurs once more by the objective lens prior to striking the work piece. The condenser lens determines the beam size whereas the objective one centralizes it over the work piece. SEM lenses hold scanning coils applied to raster the beam onto the sample. Often, apertures join these lenses to restrict the beam size [209,210].

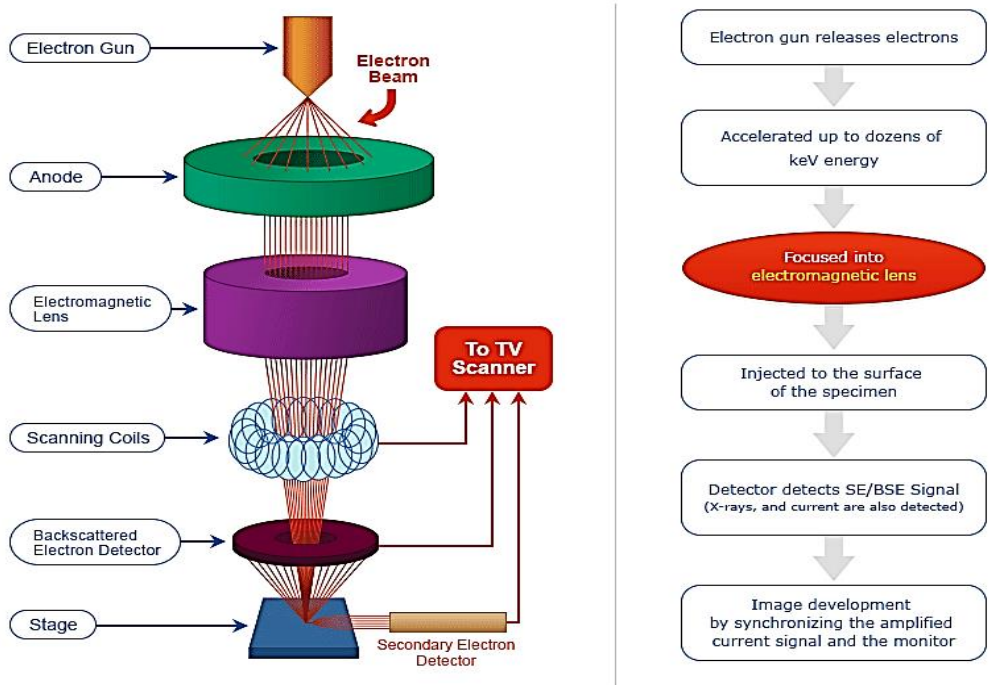

Figure 3.11. The basic SEM components [210].

Electron-sample exchanges yield electrons, photons or irradiations of different form. For the SEM, two main electrons types are – as stated earlier- BSE and SE; the former are of the initial group within the beam and sent back upon elastic interactions between the beam and the sample; the latter, though, comes from sample atoms as a consequence of inelastic exchanges between the electron beam and the sample. In essence, BSE belongs to more in-depth sample sections, whereas SE is

from the surface; hence, the change concerning the information contained. In more detail, BSE pictures are more sensitivity as regards the atomic number – the more this number, the brighter the material [211,212].

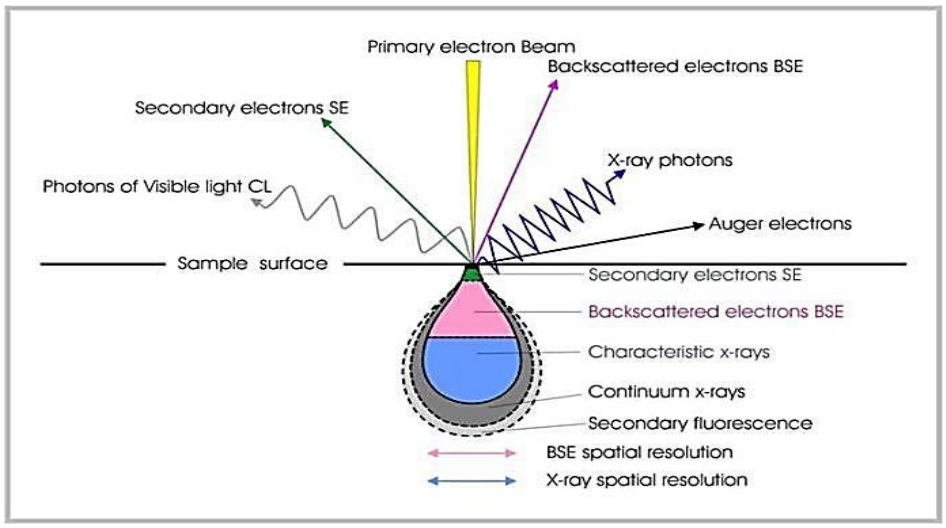

Figure 3.12. Different types of signals used by a SEM [212].

In most microscopes, X-ray detection based on the electron-sample exchanges plays a role in elemental analysis as all substances have differing X-ray energy values – in a way, serving as fingerprints and, as such, allowing for thorough determination of all elements present in a sample [211,213].

3.5.1. Applications of Scanning Electron Microscope (SEM)

- It helps to extend our knowledge of the surroundings, regardless of qualifications and age. Enlarged pictures of different things offer context to our living environment;
- It assists biology experts in examining in more detail the microscopic organisms such as bacteria and viruses. In turn, geologists employ SEM to study crystalline formations;
- Many areas of use are available, such as in trade, microelectronics, semiconductors, medical equipment, production lines, insurance, law, and food industries.

- With SEM, one can determine the stages according to qualitative chemical studies and crystalline formations, and accurate calculation of tiny segments as small as 50 nm - with BSE, in particular useful for quick phase differentiation in multi-phase specimens;
- Phases may also differentiated as per the mean atomic number generally associated with relative density, along with configurational maps according to trace elements and activators, transition metal, and rare earth elements;
- Common applications to make high-resolution views of sample shapes to reveal spatial changes in chemical mix, making elemental maps and specific spot chemical studies with EDS.
- SEMs using diffracted backscattered electron detectors (EBSD) help with micro-fabric and crystallographic orientation of numerous substances. Sectors applying microscopic parts for manufacturing apply SEMs, e.g. for fine filaments and thin films.
- Apart from standard secondary electron imaging, 3D surface recreation is possible using the information obtained from four-quadrant backscatter electron detectors;
- Fields such as cosmetics, dealing with small particles apply SEMs to learn more about the shape and size of the small particles they work with;
- Structural faults like cracks and contaminants on coated surfaces are easily located; and
- In general, all businesses producing parts can use SEMs for composition and topography tests of products [208,213,214].

3.6. WEAR TESTING

Wear experiments forecast the related performance and working mechanisms of this feautre. In terms of material, these experiments are carried out to see if it is suitable for certain uses; in terms of engineering, though, they assess the likelihood of applying specific methods to decrease wear for certain usage and see the impact of treatment – i.e., parameters – on wear performance to improve the process. Wear is the deformation and disappearance of surface material due to physical movements

against opposite surfaces. Numerous elements alter this process, namely rolling, reciprocating, unidirectional sliding, impact loads, temperature, and speed, to mention a few [67,70,71].

These experiments are conducted at three stages of laboratory, simulation, and in-service. Wear refers to material removal caused by movement. Separately, lubrication refers to fluid application against friction and wear. To economize on energy, one way is to reduce waste as a great deal of it goes to no use as a result of friction in interfaces. Consequently, there is a need for reducing friction and wear using modern approaches. To assess the wear factor, we use a tribotester or tribology. “Tribo” means to wear, friction and lubrication. There are various configurations and processes to test wear in labs. Wear testing apparatuses commonly have two segments loaded against while slightly moving one another. Such motion comes from an engine or electro-magnetic sources. For the sake of convenience, a part under study is called specimen, an the other counterface [72,73,74,75].

Figure 3.13. Wear Testing Machine [69].

To assess the wear factor, weighing and size transformation evaluation is mostly applied, with the former being rather a challenge given minute quantities in relation

to the part under study. Also, wear often occurs disproportionately on surfaces, causing hurdles in in local assessments in comparison to total mass loss. Lab simulations register constant changes in this respect, but they lack actual component and settings. As a result, it is better to assess wear scar sizes using microscopy [76,77,78].

Determining wear mechanisms and surface damage is what tribotesting operations are for, and so they require calculating the respective wear and friction figures. Examining worn surfaces is, then, done using microscopy or surface topography as an inseparable part of the whole process. Once studying such surfaces, attention to damage type is paramount to compare with component life span. The signs, in particular, may not necessarily be out there to identify easily [80,81].

3.6.1. Wear Measurement

These assessments are conducted to see how much material is lost after tests and, in effect, after working for a given life span. The lost material is defined in weight (mass) loss, volume loss, or linear dimension changes based on the objectives, the kind of wear, geometry and dimensions of samples, and also upon whether accurate assessment equipment is being used. In general, measuring employs a precision balance apparatus for mass loss, profiling surfaces, or alternatively microscopes for defining wear depth or its cross-sectional parts of wear track for volume loss or alterations in linear size [79,81,83].

These evaluations are appropriate, in particular once the area subjected to wear is disproportionate or lacking symmetry as far as shape is concerned. The work piece needs thorough cleaning at first, followed by weighing both pre- and post-test to gain the weight loss in gram (g) or milligram (µg). Commonly, wear volume can be determined based on the wear track or scar dimensions as well as geometric profile by applying a profile-meter of stylus type or, optionally, a scale-equipped microscope in mm^3. This value helps for contrasting of wear throughout materials with varying densities; yet, wear track irregularities can make evaluations challenging – under which circumstances mass loss is calculated and the volume loss

determined provided uniformity and exact knowledge of the density values [84,85,86,88].

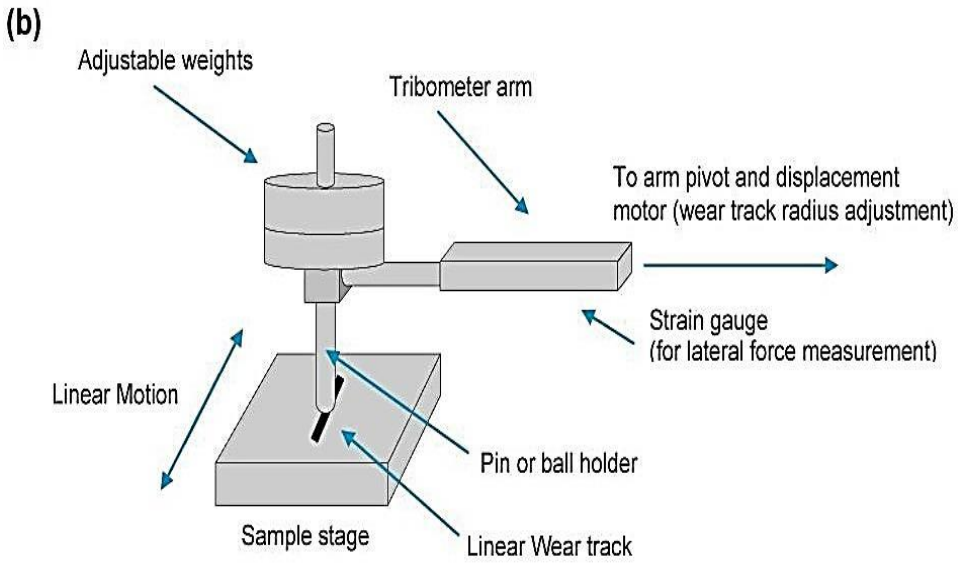

Figure 3.14. Schematic of linear wear tests [97].

In most cases, it is beneficial to assess wear according to linear size fluctuations as length, thickness or diameter can be more decisive against the normal function of the system – all possible again by employing stylus-type surface profile-meters, a micro-meters or microscopes with the unit in μm or mm. Wear resistance refers to the anti-wear attributes of any given material; though, as a scientific term, it is rather vague and devoid of any particular unit. Despite all this, the reverse of mass loss or volume loss can often be applied as the relative wear resistance. The ratio of wear loss in a reference material against that of the material being studied in identical circumstances is another way to determine relative wear resistance. At any rate, provided a numeric value of wear resistance, one has to assign clear meanings to it [87,89,90,92].

The resistance of materials to wear in parts can be assessed using bench experiments and within the settings based on the operational period to a preset level or maximum wear. Wear resistance is expressed as a standard indication of materials while experiments are carried out using custom devices modelling actual wear settings. The rates stand for wear mass loss, volume loss or alterations in linear size within unit

applied normal force and unit sliding distance. Wear rate is also written in various forms, some of which appear in next table.

Table 3.9. Wear Measurement Methods [71].

	Measurement Methods	**Units of wear**	**Units of wear rate**
Mass loss	Direct measurement by a precision balance. Calculated from volume loss for known density material.	µg g	µg/m, g/m, µg/N, g/N, µg/(N.m), g/(N.m).
Volume loss	Calculated from depth, width, wear profile and other dimension data of wear track. Calculated from mass loss for known density material.	mm^3	mm^3/m mm^3/N mm^3/(N.m).
Linear dimension	Direct measurement by surface profilometry, microscopy and other dimension measurement techniques.	µm mm	µm/ year mm/ year

Wear is a product of friction between materials in time. Certain such abrasions are purposefully applied – among them, sanding, grinding, and blasting. Other accidental ones, nonetheless, can lead to part failure, hence the need for the right material to avoid unexpected mishaps. Whereas steel commonly offers superb abrasion-resistance, not all steel behave as such and many types are custom-made for this purpose as a result. While choosing the right material, it also matters to adjust the degree of such properties: excessive resistance, for instance, causes an upward spike in costs [91,93,94].

Steel that is abrasion-proof needs a microstructure suited for advanced hardness, which can be gained to an extent upon supplying the right elements. Still, alloys by themselves cannot guarantee the right structure, and heating and instant quenching is

required for martensite and bainite as examples to add to hardness. Welding or heating abrasion-proof steel, on the other hand, is a delicate operation and extreme temperatures can anneal the part, thus reducing hardness and abrasion resistance [95,98].

Further in this regard, two-body abrasion wear refers to two kinds of sliding abrasion, where wear debris cannot be found and coupling surfaces wear out upon direct contact. Abrasion wear results in various scratching effects and, micro-ploughing, micro-cracking, micro-fatigue or micro cutting; whichever is abrasive at most is relative to exposure of the material[99,103].

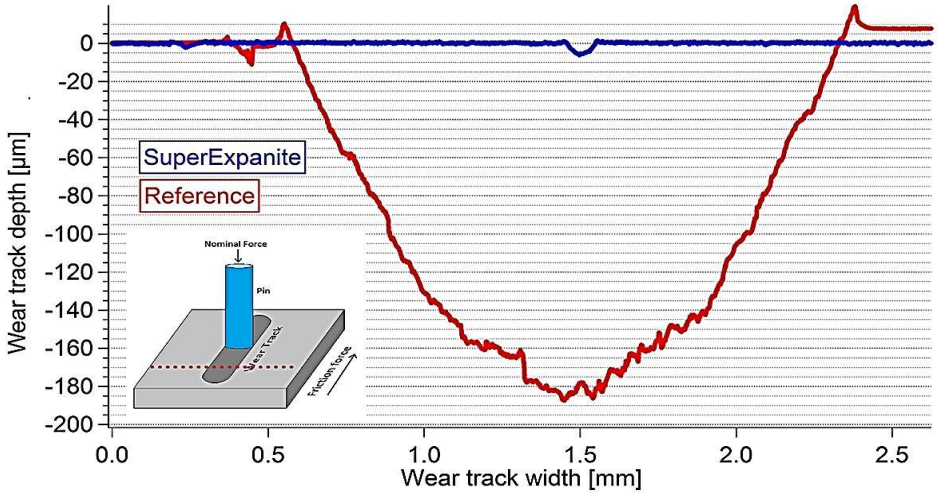

Figure 3.15. Wear resistance on steel [75].

3.7. CORROSION RESISTANCE TESTING

Corrosion is a process in which a material is oxidized by substances in the environment that cause the material to lose electrons. Corrosion resistance accounts for the ability to maintain the binding force and tolerate deterioration and chemical breakdown caused by exposure. Tests in this regard show resistance against corrosion in specific settings such as temperature, humidity and saline water. Labs commonly carry out these experiments to tackle, avoid, or help solve corrosion issues by employing procedures for industrial materials and infrastructure products – commonly referred to as failure analyses. In this way, additional data is accessed to

support decision-making for material, process and treatment purposes. Proper choice of material and corrosion tests remains vital to ensure a robust service environment as there are irreversible damages possible in case of material, tools, other properties and pipelines. Such threats, apart from high costs, can give rise to later malfunctions and, finally, halts in manufacturing, safety issues and notoriety loss for businesses and their stakeholders. Corrosion testing plays a key role in designing, creating, and life span metallic materials, parts and goods and based on studies conducted by prominent global leaders in the field to the most common tests for oil & gas, aviation, medicine, and transportation, these tests significantly decrease the dangers in complicated or extreme corrosive environments [104,105,108,110].

Figure 3.16. Corrosion Testing Laboratory [113].

Corrosion testing is widely applicable in cases conventional methods fall short, or in sensitive scenarios calling for sophisticated procedures. Passivation and similar modification approaches can help add to corrosion resistance and assess efficiency in production and handling operations to remove unwanted residue from parts. Apart from this, tests are able to make comparisons among numerous secondary processing impacts and their influence on corrosion attributes. A natural phenomenon, corrosion takes place everywhere given the settings. In a broad sense, it is metal loss caused by reaction with the surroundings and assessed as the percentage of weight loss or

corrosive penetration rate, degrading the material and, later, resulting in major equipment, product, or property failure [112,114,116].

In operational environments where common pass or fail exposure testing cannot be enough, these tests are a higher initiative and materialize via monitored electrochemical exchanges between two materials, or between an exposed surface and the environment. Adding a current to the system quickly speeds up the impact of watery mixture; hence, electrolyte solutions are an option for modelling extended settings, make forecasts, and identify corrosive attributes of the part. Many labs offer various modelling conditions for signs of cracking, fatigue and similar faults, with naturally varying prices given the method [113,117].

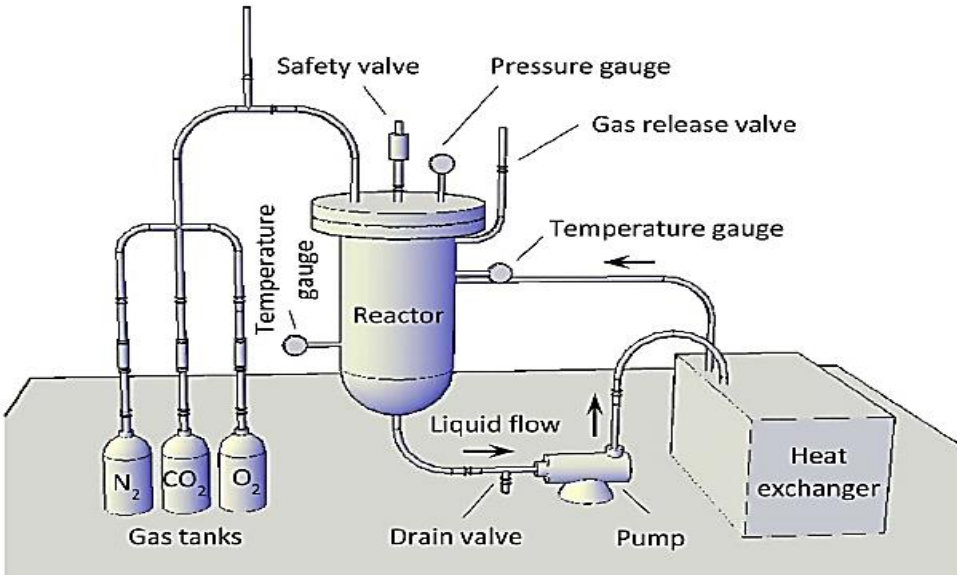

Figure 3.17. Schematic for corrosion testing in steel [117].

Corrosion resistance is behaviour against reacting with other elements leading to corrosion and the extent to which materials – mostly metal – are able to endure oxidization or similar formations. Many materials are naturally corrosion-proof, while there are certain techniques that can enhance this property. Steel is partly corrosion-proof – a passivity caused by a thin and hard-to-detect oxide coat formed due to metal and oxygen reaction and significantly increasing resistance. One can say, then, that steel is passivated or minimally affected by outside elements like air and water [120,122].

Adding a protective coat is the most popular way to achieve corrosion-resistance, employing substances that separate areas subject to attack. The degree of resistance is, hence, a main factor when the choice of material is made; thermodynamics, in this context, is a decisive factor as certain metals by nature possess sluggish reaction kinetics while thermodynamically susceptible to corrosion. Often times, corrosion resistance can be written as a rate and calculated in millimetre per year or mils based upon a specific environment and determined working conditions, pressure, temperature and fluid velocity. Apart from natural resistance, this factor may be strengthened upon using other techniques; the rates are calculated to see the degree of sustainability under given circumstances [123, 126].

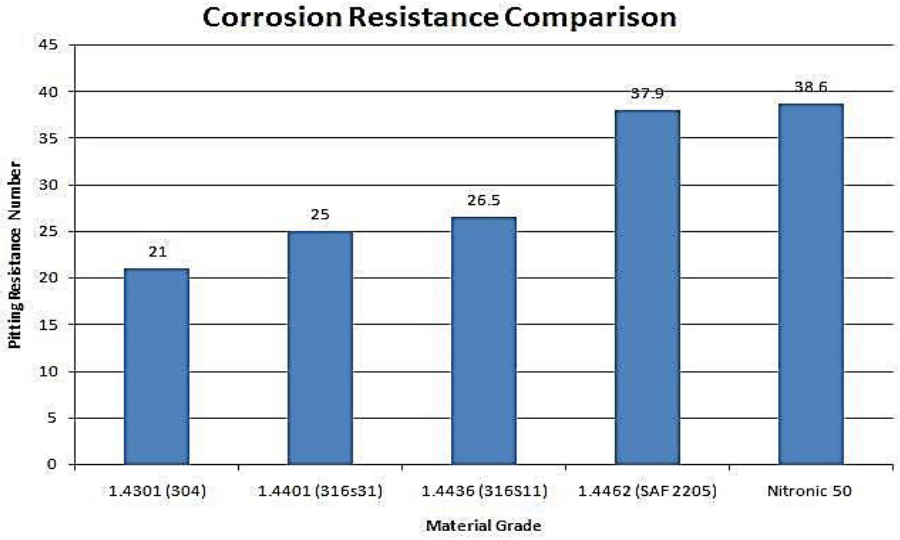

Figure 3.18. Comparing of corrosion resistance for stainless steels [120].

3.8. MICROHARDNESS TESTING

Microhardness tests have been found to be very useful for materials evaluation, quality control and R&D. Despite being naturally experimental, hardness is related with tensile strength in man cases to address wear resistance and ductility. This is a mechanical experiment to determine attributes needed for design, analysis, and development of material and structure with the main goal of identifying appropriateness for given applications or treatments. Easy to carry out, these tests are widely employed for metal and alloy inspections. A material feature, hardness is not

a major physical characteristic, explained as resistance against cracking and finalized by calculating the permanent depth of indentation. In other words, once fixed loads are applied along with indenters, the smaller the indentation, the harder the material. Indentation hardness value is determined by calculating the indentation depth or area [128,130,132].

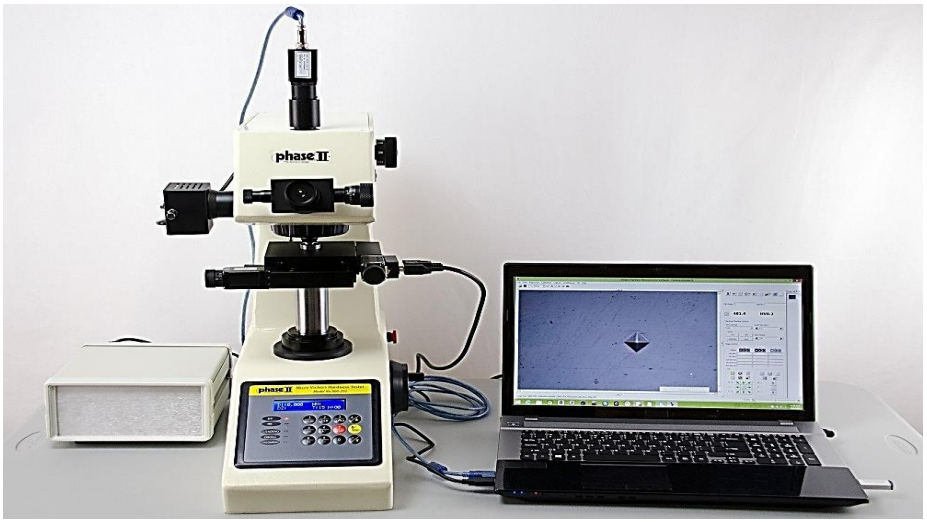

Figure 3.19. Microhardness Tester [130].

Microhardness testing offers us clues as to resistance against penetration in the case of small or thin samples or areas within them or within plating. In this way, correct and thorough data is obtained for surface attributes with minute microstructure, multi-phase, non-homogeneous or susceptible to indentation. This test involves loads exceeding 10 Newton (N), under which level the tests are often for small-size specimens, plating, or films. The test also allows for assessing surface-to-core hardness on carburized or case-hardened segments and case depths, not to mention grinding burns, carburization or decarburization. During microhardness evaluations, a diamond indenter is pushed into the surface using a penetrator and mild loads of 1000 grams to form an indent or permanent deformation based on the indenter shape. These tests incorporate certain evaluations of the indent by employing equations, and the operational accuracy calls for certain microscope equipment given the small indent sizes. This test is carried out at micro as well as macro levels using max.50 kg as the load and controlled pressure for a determined period and applying a square-based diamond pyramid indenter. The diagonal of the created indention is, then,

assessed using a microscope, whose measurement along with the load are applied in a special equation to determine the Vickers hardness value [133,134,135,136].

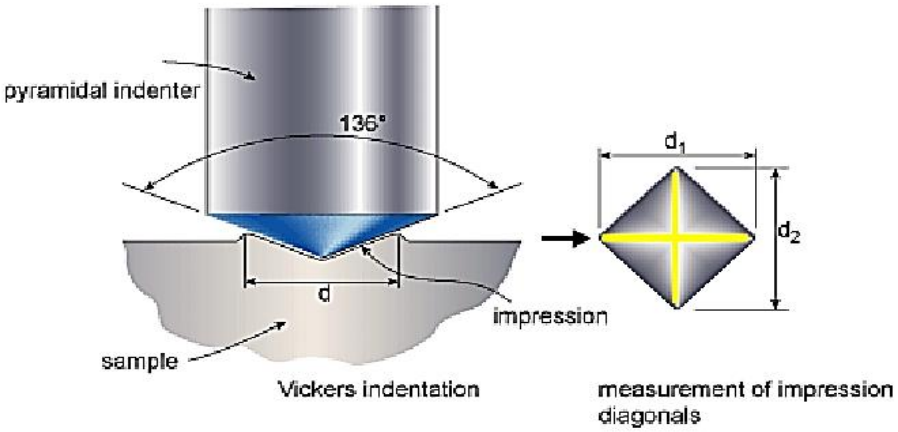

Figure 3.20. Schematic of a Vickers indentation probe [138].

Better and reproducible outomes call for these tests to also consider sample size, preparation and environment. Specimens, to begin with, have to be well positioned on the stage, perpendicular to the indenter tip. Highly rough surfaces cause the data accuracy to drop, thus calling for proper sample polishing. The tester itself is to be free of vibrations. Furthermore, specimens containing numerous phases or grain size variety need additional statistical data. Vickers indenter is applied for pushing into a surface using determined amounts of force for 10 seconds on average. The created indent is examined optically to calculate the lengths of the diagonals for the impression size. In numerous cases, contact depth (h_c) is dissimilar to the displacement depth (h) caused by the surrounding material deflecting elastically while indentation takes place as well as environmental issues, thus also influencing accuracy and precision in the final data [137,138,140].

The Vickers method is an optical measurement approach. The test process known as ASTM E-384, determines a series of light loads with a diamond indenter to indent, the result of which is calculated and expressed in hardness value terms. Test pieces require thorough polishing to measure the impressions accurately. A square base pyramid shaped diamond is applied for the Vickers scale. The Microhardness tests are commonly conducted on metals as well as ceramics and composites [141,142].

Because of the insignificant dimensions of the indentation in Vickers mode, many advantages abound; e.g. for positioning in a plastic medium to make facilitate the process. These marks are to be sizeable enough to enhance resolution. The process, however, may experience operator-related issues. In the Vickers hardness machine, loads are implemented to the indentor using basic lever systems; whereas, more advanced machines carry out the same task electronically. Also, surveys are possible on welded joints regarding each round as well as areas influenced by heat. Small marks require flat surfaces that are also perpendicular to the indentor with over 300 grit finish. There are many factors that can affect the accuracy of the hardness test such as flatness and surface finish but it is worth re-emphasising the point that flatness is most important - a maximum angle of approximately ± 1° would be regarded as acceptable [140,144,145].

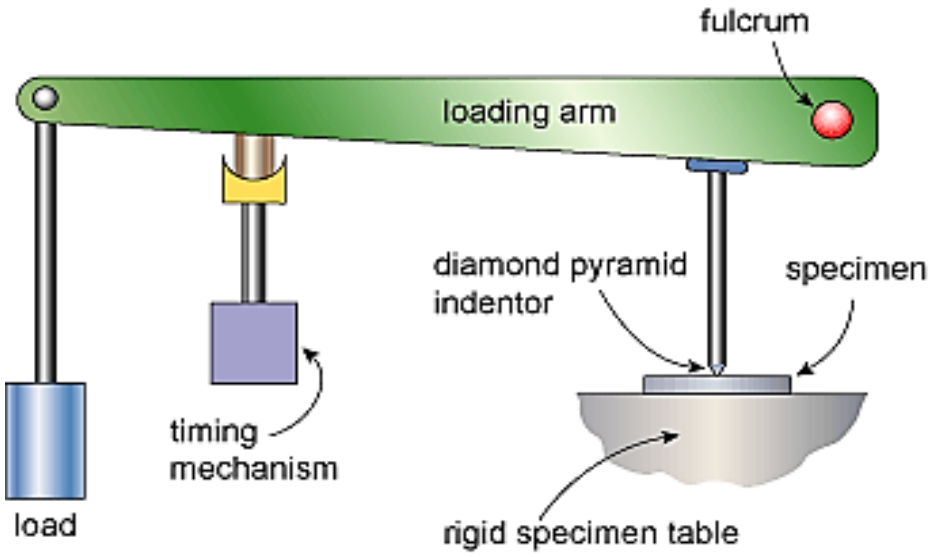

Figure 3.21. Schematic principles of operation of Vickers hardness machine [138].

For ideal flatness tolerance and surface finish, grinding or machining is crucial, with the right load implemented without friction within the system; or else, only small and insufficient dents may be formed. Apart from this, a sample size exceedingly thin or hard tables may also change the the outcomes. In the latter case, firm support and good conditionr are key; burrs or raised edges underneath the specimen can reduce the quality of the readings. There should be no impact loading as the indentor may be forced without any difficulty into the surface once the table is elevated to the

expected level, thereby generating pressure on the equipment and harming the indentor. Lastly, frequent validation and calibration provides precise and repeatable results [142,144,146].

3.9. XRD ANALYSIS

X-ray Diffraction (XRD) is a technique used for determining the atomic and molecular structure of a crystalline material, in which the crystalline structure causes a beam of incident X-rays to diffract into many specific directions. Powder XRD is also applied widely to determine the phases through assessing the beam diffraction angles and intensities and contrasting the outcome pattern against reference databases. The analysis offers an insight into unit cell dimensions, with the subject material finely ground, homogenized, and evaluated in terms of average bulk composition. In XRD, the material interacts with X ray beams of certain wavelengths. As the beams are spread according to the crystal structure, they form plots with intensity as a function of 2theta, thus identifying both the phases and the amounts of relative intensity. Likewise, the approximate crystallite size can be obtained since the shapes are often preferred in development – contrary to amorphous material because they possess clear-cut features including melting point and solubility factors detrimental for controlling the end product [215,216].

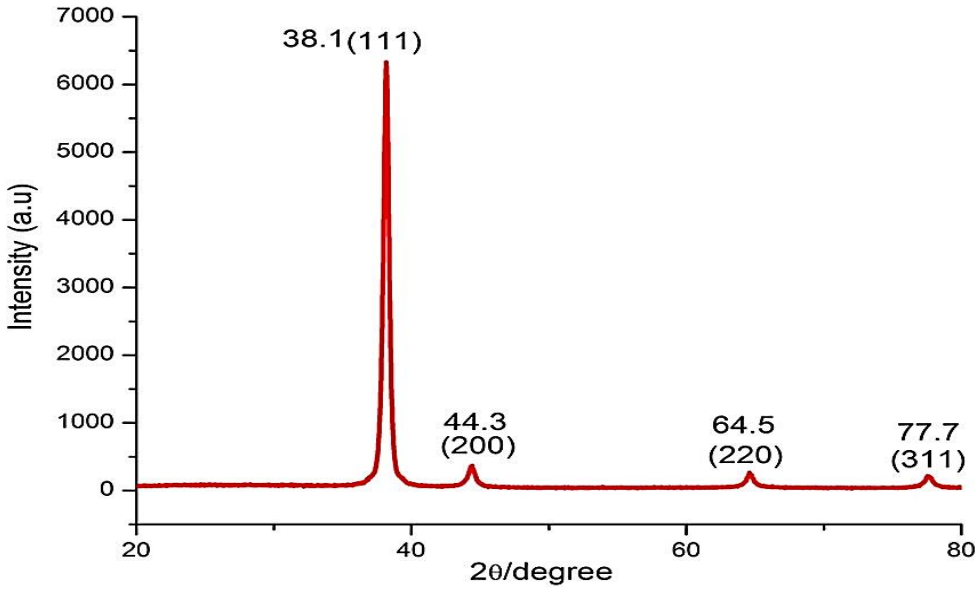

Figure 3.22. The graph for XRD analysis for characterizing crystalline [215].

The XRD analysis is also applied for determining the crystalline phases within materials to further shed light on their chemical configuration. This is done upon comparing the obtained information to corresponding databases. The method proves beneficial in the assessment of minerals, polymers, corrosion products, and unknown materials. Generally speaking, specimens are examined using finely ground powder diffraction. Apart from this, XRD can identify strain, preferred orientation, crystallographic structure, and grain size of crystalline materials. When applied in a glancing angle mode, these structures are visible as a function of depth. Organic material analysis is another area of application; for instance, for identifying the degree of crystallinity within polypropylene fibres as a function of annealing time. The differences are, then, correlated to tensile strengths and elasticity data [216,217].

XRD is a space-consuming equipment requiring a lot of power; apart from this, a majority of standard machinery employ parafocusing Bragg-Brentano geometry to provide high-resolution and high beam-intensity analysis that might need accurate alignment properly prepared specimens. Plus, such geometry calls for the source-to-sample distance to remain constant and identical to the sample-to-detector distance. Hence, any faulty occurrence can bring about dire consequences in phase identification and quantification. Incorrectly placed specimens, not fully transparent specimens, and coarse ones lead to dissatisfactory results. Specimen flatness, roughness, and positioning errors often avert in-line measurements. A parallel incident X-ray beam can prevent these obstacles [217,218].

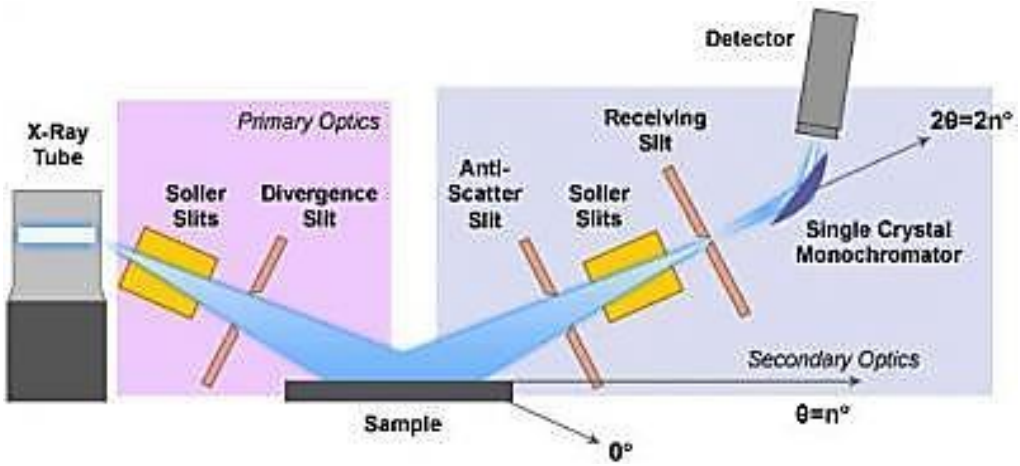

Figure 3.23. X ray Diffraction [216].

3.9.1. Principles of Operation

X-ray is produced in a cathode ray tube by heating a filament to generate electrons, speeding them in the direction of a target using a voltage, and hitting that target material using electrons. With adequate energy to dislocate the inner-shell electrons on the surface, these electrons help to generate X-ray spectra of the target comprising numerous components –among them Kα and Kβ. To an extent, Kα comprises Kα1 and Kα2. Kα1 possesses a rather shorter wavelength and is double the intensity of Kα2. These wavelengths are indicative of the target material (Cu, Fe, Mo, Cr). Filtering with the help of foils or crystal monochrometres is necessary to generate monochromatic X-rays for diffraction. Kα1and Kα2 are in close proximity, thus a weighted average of the two is applicable. Copper stands as a widely used target material for single-crystal diffraction, with CuKα radiation = 1.5418Å. Such X-rays are combined and released toward the specimen. As the specimen and detector are turned, registration takes place of the X-ray intensity. Upon the incident X-rays geometry satisfying the Bragg Equation, constructive interference takes place along an intensity peak. At this point, a detector monitors and processes the X-ray signal, changing it to a count rate to become the output upon a print or screen [217,218,219]. Using parallel-beam geometry, the specimen placement may be changed and there is no need for precise distancing of source-specimen and specimen-detector. The geometric flexibility makes room for any production settings given the larger scope of specimen forms and dimensions. Parallel beam geometry, immune toward displacement errors, can essentially tackle any common error functions causing asymmetric peak broadening, non-flat or rough specimens, axial divergence, and sample transparency. Due to this advantage, not much preparation is needed; apart from this, applying poly-capillary collimating optics, the target parallel beam XRD system may be used in conjunction with a low power X-ray source, thereby decreasing equipment size and power consumption. Parallel beam XRD applying X-ray optics is effectively applied for thin film analysis, specimen texture analysis, examining crystalline phases and configurations, and specimen stress and strain studies. An X-ray diffractometer geometry operates with the specimen turning in the direction of the combined X-ray beam at an angle θ with the detector positioned on an arm to gather the diffracted X-rays and turn at an angle of 2θ. A goniometer

controls this angle and moves the specimen. For typical powder patterns, information is gathered at 2θ from ~5° to 70° as predetermined angles [218,220].

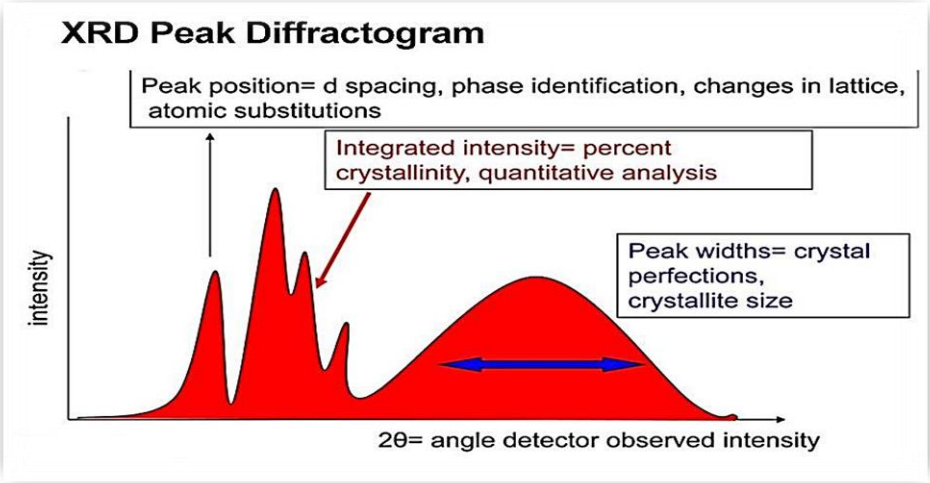

Figure 3.24. XRD peak diffractogram [218].

The Bragg equation, $n\lambda = 2d\sin\theta$ is among the determining tools to comprehend X-ray diffraction where n represents an integer, λ stands for the characteristic wavelength of the X-rays released onto the specimen, d represents inter-planar spacing between rows of atoms, and θ is the angle of the X-ray beam against the planes. Once the formula is satisfied, X-rays spread by the atoms in the plane of a periodic structure are in phase and diffraction takes place in the path determined by the angle θ. In the most basic settings, an XRD test comprises a series of diffracted intensities and observation angles. This diffraction pattern can be thought of as a chemical fingerprint, and chemical identification can be performed by comparing this diffraction pattern to a database of known patterns [216,219].

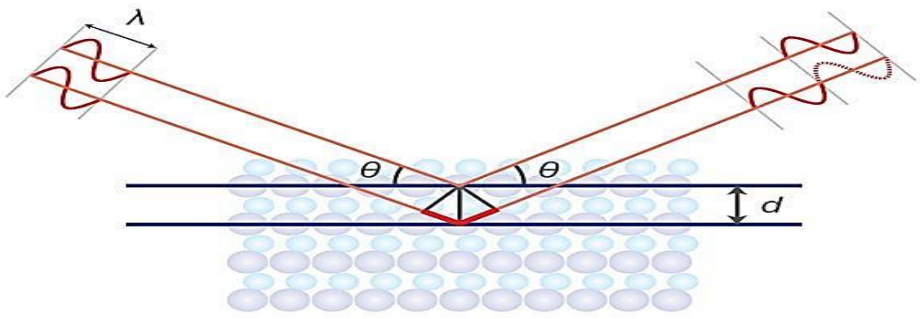

Figure 3.25. Diffracted intensities and the angles [219].

3.9.1.1. Applications for XRD Analysis

- Identify crystal formation with Rietveld refinement;
- Identify modal quantities of minerals – a.k.a. quantitative analysis;
- Examine production hydroxyapatite to determine Calcium:Phosphorus proportions along with comparing the percent HA, Beta-tricalcium phosphate and Calcium oxide;
- Reverse engineering and competitive analysis;
- Identify thin film specimens by:
- Establishing lattice mismatch between film and substrate and to inferring stress and strain;
- Establishing dislocation density and quality of the film using rocking curve analysis;
- Identifying film thickness, roughness and density by means of glancing incidence X-ray reflectivity tests;
- Textural measuring, including grain orientation, in polycrystalline specimens; and
- Calculating super-lattices in multilayered epitaxial formations [216,218,220].

3.9.1.2. Strengths and Limitations of X-ray Powder Diffraction (XRD)

- A robust and quick (< 20 min) method to identify unknown minerals;
- Clear and final conclusions in most cases;
- Least preparation needed for specimens;
- Large scale of availability; and
- Significantly plain and unambiguous data interpretation.
- Standard reference databases for inorganic compounds must be available;
- For mixed materials, detection limit is ~ 2% of the sample;
- Homogeneous and single phase material is best for identification of an unknown;
- For unit cell determinations, pattern indexing for non-isometric crystal systems is a challenge;

- Peak overlay is a possible occurrence, deteriorating with high-angle reflections; and
- 1/10 of a gram of material needed to be ground into a powder [215,217,219].

3.10. ENERGY DISPERSIVE X-RAY ANALYSIS (EDX)

Energy Dispersive X-Ray Spectroscopy (EDX) helps to analyze the chemical compositions material at the micro level alongside SEM. This utility identifies the x-ray released by specimens while projecting an electron beam onto it for thorough elemental analysis, which is possible for features measuring 1 μm or even smaller ones. Upon SEM's projections, electrons leave the atoms present on the outer layer of specimens, and their empty places are taken up by electrons from a higher state, resulting in the release of x-ray to maintain balance in the amount of energy in these states. In this way, an x-ray is a typical representation of the element it originates from [221,222].

Commonly made of lithium-drifted silicon and solid state, the EDX evaluates the average availability of the rays released against the energy they possess. Upon contact with EDX, an x-ray forms a charge pulse in ratio with its energy which is transformed to a voltage pulse – again, in proportion to the amount of energy - by a charge-seeking pre-amplifier. Next, the signal travels to a multichannel analyzer for pulse classification according to the amount of voltage. Accordingly, the amount of pertaining to each ray appears on the computer to be shown and assessed further. The x-ray energy-counts range is estimated to establish what constitutes the specimen in the form elements [222,223].

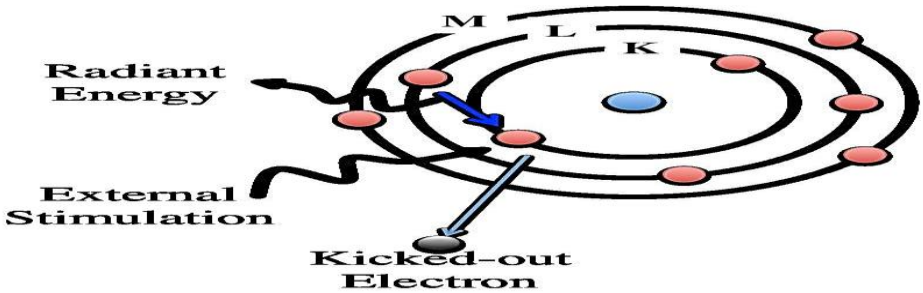

Figure 3.26. Diagram of Energy Dispersive X-ray spectroscopy (EDX) [221].

3.10.1. EDX Applications

EDX is widely used for purposes such as investigating the following:

- Product deformulation and competitor analysis;
- Adhesion, bonding, and delamination;
- Optical appearance, haze and colour issues;
- Legal cases and providing expert opinions;
- Machinery or equipment breakdowns and malfunctions;
- Catalyst quality, poisoning and elemental distribution;
- Product flaws and their underlying causes;
- Cases of corrosion and contamination;
- Issues related to quality assurance raw material and end product;
- Materials as fillers, and features such as pigment, fibre, additives, their degree of distribution and orientation;
- Plants and factories concerning particles and other forms of pollution; and
- Monitoring of construction and maintenance.

3.10.1.1. EDX Advantages

EDX offers a host of benefits to the industry among which we can refer to the following:

- Better management of quality and achieving added efficiency;
- Speedy determination of contaminants and likely origins;
- Added monitoring of the settings and the surrounding environment, pollutants, and other related subjects;
- Heightened assurance at workplace and improved productivity; and
- Pinpoint accuracy in problem-cause analysis in process chains [221,222,223].

3.11. TRANSMISSION ELECTRON MICROSCOPY (TEM)

These microscopes are of significant effect in the field of material engineering. By passing a beam of electrons with high energy through film specimens, one can investigate how the electrons and atoms behave to determine crystal forms and other characteristics such as displacements, grain boundaries, chemical combinations, layer development, material, and deficiencies in case of semiconductors. Advanced levels of resolution also enable experts to study the attributes, dimensions, forms, and degree of compactness within the quantum walls, wires and dots. TEM works in the same way as light microscopes, but uses electrons, instead, as they have a more limited wavelength, thus far exceeding light as regards optimal resolution and offering intricate details related to inner shapes and formations as small as a single atom [225,226].

A ray of electrons is concentrated with a gun with the help of condenser lenses and limited by another aperture to eliminate high-angle electrons. The ray hits the sample, and pass through in accordance to the depth and electron transparency of the sample's surface. This section within the sample is transformed into a picture by the objective lens on a phosphor screen or charge coupled device (CCD) camera. Alternatively, others segments can further improve the contrast by eliminating high-angle electrons. Later, the view travels the intermediate and projector lenses and becomes even bigger by doing so. TEM, compared to light microscopes, offers added resolution, which helps in examining in detail the inner structures of organelles, viruses and macromolecules and, in the same way, material specimens. The light microscope and TEM in combination are a part of all studies in the filed of material engineering [239].

Given the small dimensions of electrons and their higher likelihood of bouncing in case of hydrocarbons or gas molecules, vacuum settings are a must for electron beams. This is done using a number of pumps - rotary ones, referred to otherwise as roughing pumps, being the first in line and reducing pressure to 10^{-3} mm of Hg range inside the column where electrons move. Alternatively, diffusion pumps,

while capable of steadying the pressure, improve the vacuum by up to 10-5 mm; though they still require roughing pumps to complement them[224,225].

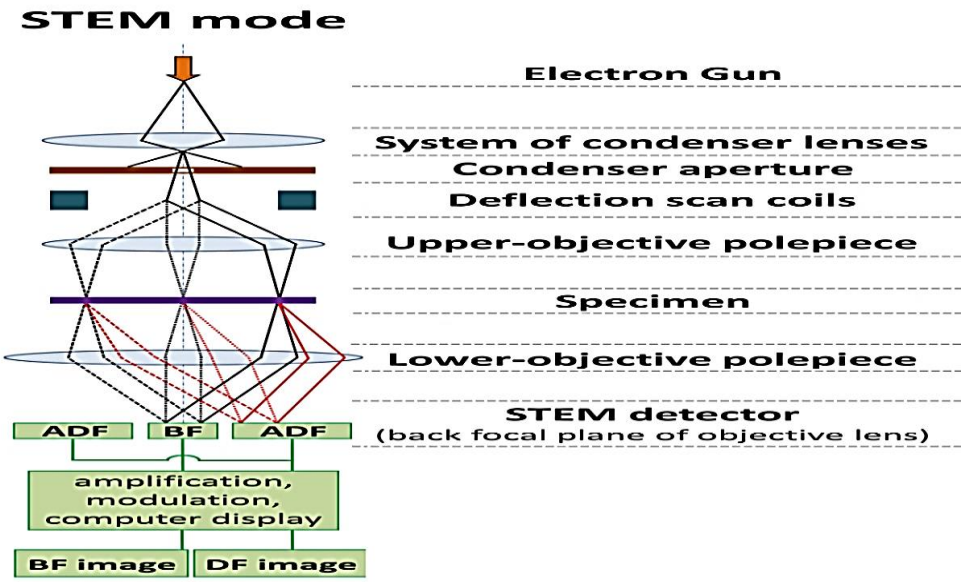

Figure 3.27. The organization of the transmission electron microscope (TEM) [226].

3.11.1. TEM Applications

There is a wide range of use for this microscopy. Here are some of them:

- In life sciences, nanotechnology, medical, biological and material research, forensic studies, gemology and metallurgy, not to mention industry and education;
- For studies related to topography, morphology, composition and crystalline structures;
- Examining specimens at molecular levels for structural and texture-related details;
- Crystal and metal analyses;
- Semiconductors, computers, and silicon chip research and manufacturing;
- In technology firms to detect deficiencies, cracks and other deformities at the micro level, paving the way to find solutions and achieve additional resistance and productivity;

- Shedding light on an entirely different perspective from the micro level with impressive depth and intricacy, and to observe a nano-sized world in incredible detail;
- Despite the need for orientation to use it, TEM can be also applied by students in research contributions to faculty; and
- Studies and projects carried out by academic establishments [224,225,226].

3.12. MEASUREMENT OF SURFACE ROUGHNESS

Solid surfaces – that is, boundaries being of solid–gas or solid–liquid – possess certain complicated features which rely on the type of material, the way they are made, and processes taking place between these areas and the surroundings. These attributes play a key role by impacting the actual contact zone, friction, wear, and lubrication. Apart from tribology, they are essential as regards optical, electrical and thermal functions, painting, and the way a work piece looks. Solid layers, regardless of the way they are made, can have disproportionalities and flaws related to geometry which can vary from physical deformity to the spaces among the constructing atoms. What remains is that machine processing, even at the most accurate level, can fail to create molecularly flat areas on standard materials, and the most even of all surfaces can still bear a certain degree of irregularity that transcends the interatomic spaces. Once intended for technological use, not only the macro features, but also the micro or nano-topography of these areas – also regarded as texture – can play a role. These flaws aside, a solid surface comprises many different areas of possibly different physical and chemical nature which are specific to the very material being worked with[227]. It is a key operation in numerous technical applications to assess surface roughness since it is a standard to determine the texture and the way a material behaves in a given surrounding, hence a mark of performance in mechanical pieces at work. Apart from this, roughness at certain degrees is not exactly a feature that is much sought after and can add to the production expenditure significantly. In theory, these calculations consider shape, surface finish and its profile roughness (Ra), and surface area roughness (Sa), texture, asperity, and finally structural attribution. In this respect, texture is defined as the continued or arbitrary divergence from the typical surface quality creating a 3D map of the surface. It

comprises roughness (both at the nano and micro level) waviness (at the macro level), lay, and flaws. Engineering disciplines mostly involve some form of assessing surface roughness in terms of performance so as to guarantee the expected standards within manufactured goods. To do this, a profile-meter is often applied along with a contact stylus. This instrument checks the surface profile in a precise and reliable manner, though certain drawbacks are present including added contact pressure and stylus erosion, causing probable scratch marks on the work piece. Another way is to use the computer-assisted method, which has been quite popular among specialists due to its advanced results. On the other hand, optical approaches to measurement are advantageous over mechanical ones given the degree of accuracy, added speed of operations, and others. In short, surface quality is key to guaranteeing the veracity of manufactured pieces. By extension, calculating the roughness can help to estimate due substitution of parts once they show signs of wear and tear – an occurrence quite common, especially in today's terms and requirements for machining operations [228,229,230].

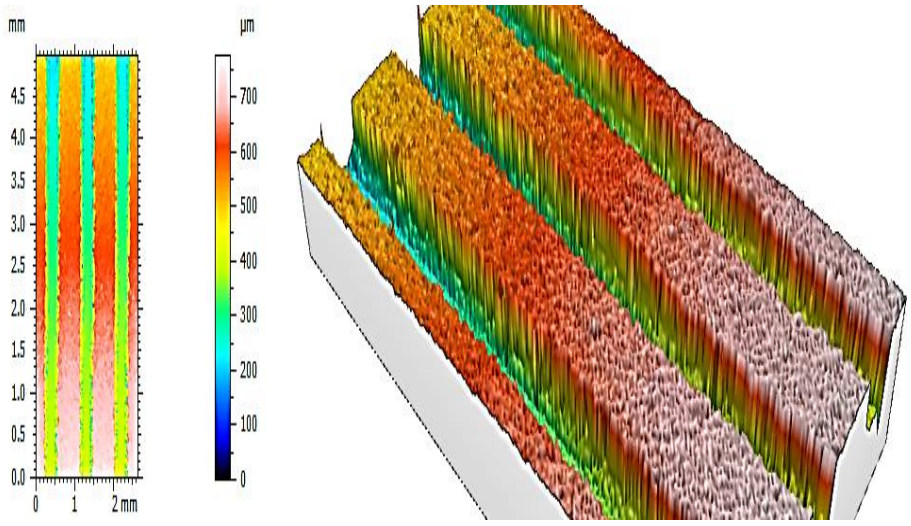

Figure 3.28. Micro machined surface roughness measurement [230].

3.13. SILVER NANOPARTICLE SYNTHESIS

Silver nanoparticles (AgNPs) continue to be employed extensively by experts in the field of medicine, nutrition, health sciences, consumer products, and industry alike because they possess exceptional physical and chemical properties – namely, optical,

electrical, thermal, and biological, as well as added conductivity. For this reason, the range of use for this nanoparticle is extensive and finds its way into other fields as manufacturing home appliances, coatings for sensitive machinery, detectors, cosmetics, drug production, foods and beverages, diagnostics, orthopedics, etc. In particular, metallic nanoparticles can transform the appearance, chemical and biological attributes quite significantly owing to surface-to-volume ratios [231,232].

Nanobiotechnology, as an increasingly expanding discipline for making the appropriate equipment, involves initially formation of NPs or nanoparticles based on alternative chemistries, dimensions, and textures as well as ideal distributions. This sector has evolved to become a basic branch out of modern nanotechnology to unite the incentives of material engineers worldwide given the variety of applications it can have. The science is quite multidisciplinary rooted in applying NPs within biology, biochemistry, chemistry, engineering, physics and medicine all in one place. Apart from this, the nanobio-technology offers an indispensable approach to creating clean, nontoxic, and environmentally acceptable operations to generate and stock metal NPs with inherent qualities to decrease metals thanks to very sophisticated metabolic processes. The added necessity for environmentally-conscious materials produced today without poisonous content – called also green synthesis – requires new visions toward creating mixed-valence polyoxometalates, polysaccharides, tollens, and employing other biological and irradiation approaches against the standard approaches that produce toxic chemicals. A good example is the choice of solvent medium and environment-friendly thinners or stabilizers and other similar agents, all of which can benefit greatly from NP made with green synthesis [232,233].

In other cases, such as in machining processes, cutting equipment are exposed to harsh plastic deformation under significant strain levels causing friction between the equipment and work piece, and eventually material loss. Cutting fluids, as a result, are key in decreasing both friction rates and heat, with the main purpose being proper lubrication and cooling at the areas of contact. Supplying the right material within the standard cutting fluids improves their thermal and tribological attributes. An effective material in this respect, nanomaterials are now on the spotlight in many

areas of study to serve as a supplement, all thanks to their significantly developed formula today. Nanofluids, as they are called now, are essentially designed as colloidal suspensions of nanoparticles (1-100 nm) in a base fluid [231,232,233].

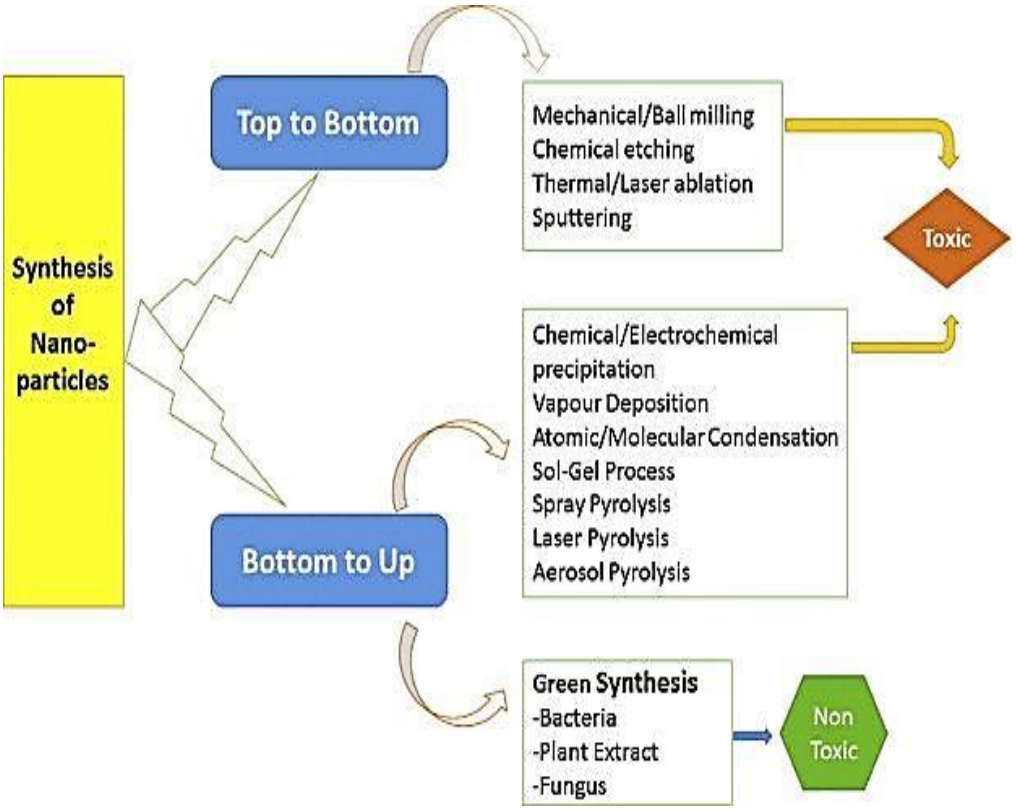

Figure 3.29. Different approaches of synthesis of silver nanoparticles [233].

3.14. MATERIALS AND SPECIMEN PREPARATION

Metallography is a field dealing with metal microstructures; in other words, examining chemical and atomic structures. For this reason, the field is important in terms of material endurance. Optical microscopy can, for this purpose, offer a general perspective, with yet better methods needed to enhance and prepare the surfaces. In this case, equipment such as SEM and TEM, X-Ray, electron diffractometers, and other alternative instruments come into the picture. Correctly preparing the samples positively affects microstructural examinations, thus calling for certain procedures to be carried out in order; these metallographic preparation steps are documentation, sectioning and cutting, mounting, planar grinding, rough

polishing, final polishing, etching, microscopic examination and analysis and hardness testing. The samples need to be maintained in a clean fashion and stages above gone through carefully so as to identify the microstructures correctly. Metallography examines microstructures, constitutions and structures of metals and alloys; for this reason, faulty steps can modify the actual information in this respect and generate inaccurate results, while professionalism in applying these steps calls for proper education and hands-on training [12,14,24].

In the end, these analyses offer information as to whether proper processing has been done for materials, and is therefore a major step in terms of reliability and establishing probable causes for failure. Metallographic specimens are commonly sectioned depending on the need and ease-of-handling. Material being of importance, this step is carried out using abrasive cutting to reduce damage, which could otherwise change microstructure and yield incorrect information. Appropriate cuts call for the right abrasive, bonding, and size apart from the suitable cutting speed, load and coolant [24,26,27].

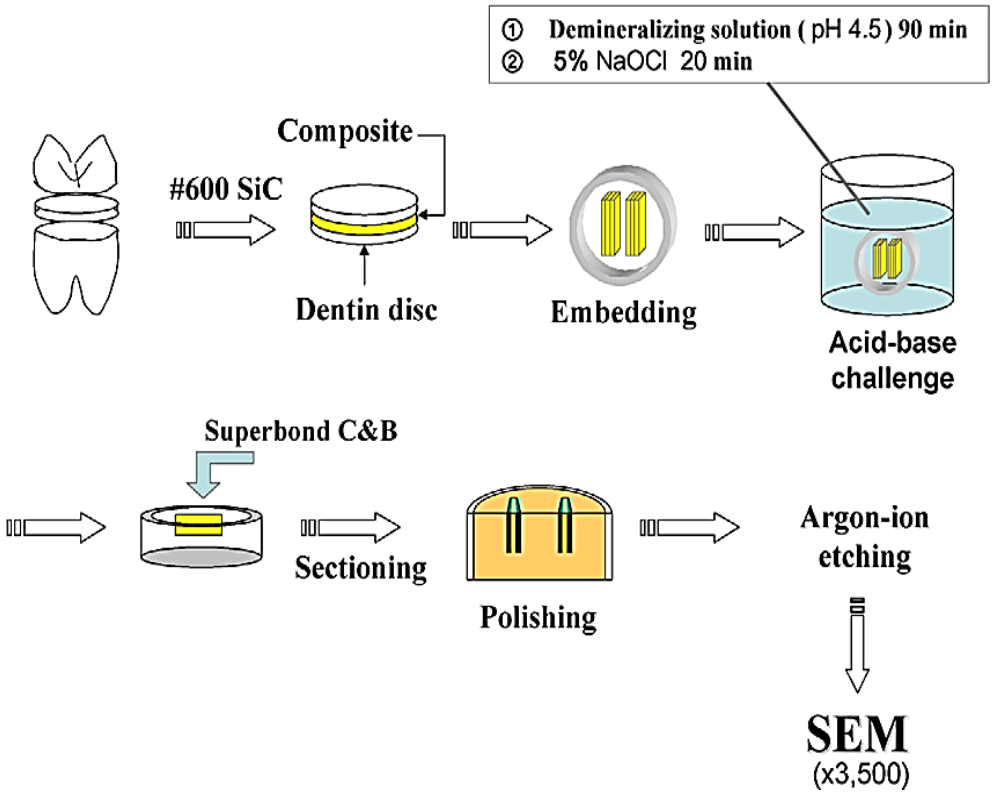

Figure 3.30. Specimen preparation for SEM observation [234].

3.15. METALLOGRAPHIC PROCEDURES

3.15.1. Sectioning and Cutting

A majority of metallographic specimens are sectioned to be handled with maximum ease, with the approach relying mostly on the material; hence, alternatives such as abrasive cutting, thin sectioning with a microtome, or diamond wafer cutting. All of these techniques help to reduce damage and improve accuracy in microstructural and analytic data. Once we cut a sample from a bigger piece, attention is to be paid so that the piece represents the same properties of the larger one to contain the information for intended features. Issues may arise as to the preparation altering the microstructure, for instance, by heating, chemical attack, or mechanical harm, whose degree can be relative to the technique employed. To illustrate, abrasive cutting generate a lot of damage, whereas low-speed diamond saws are less of an issue. Various cutting techniques exist, with some intended for certain materials [29,30,234].

Figure 3.31. Specimen Abrasive cutoff wheels for sectioning [235].

3.15.2. Mounting

Mounting helps to protect surface areas, fill the pores, and enhance the operation of irregular specimens, and can be done in different ways all relying on the material; for instance, compression mounting. Mounting is often crucial for easy handling and

reducing possible damage. The mounting material should not affect the samples by chemical or mechanical means, and it has to properly adhere. In case of subsequent electropolishing, the mounting material has to be naturally a conducting one. Samples may be hot-mounted by means of a press either in a thermosetting plastic – such as phenolic resin - or a thermos-softening plastic – such as acrylic resin. Should hot mounting change the sample structure, cold-setting resins are to be employed. Porous materials need impregnation using resin prior to mounting or polishing so as to avoid grit, polishing media or etchant stuck in pores, apart from maintaining the open structure. Mounted samples often possess a thickness of roughly half their diameter against movements while grinding and polishing take place. The edges of the sample are to be rounded to reduce harm to discs used for grinding and polishing [67,93,235].

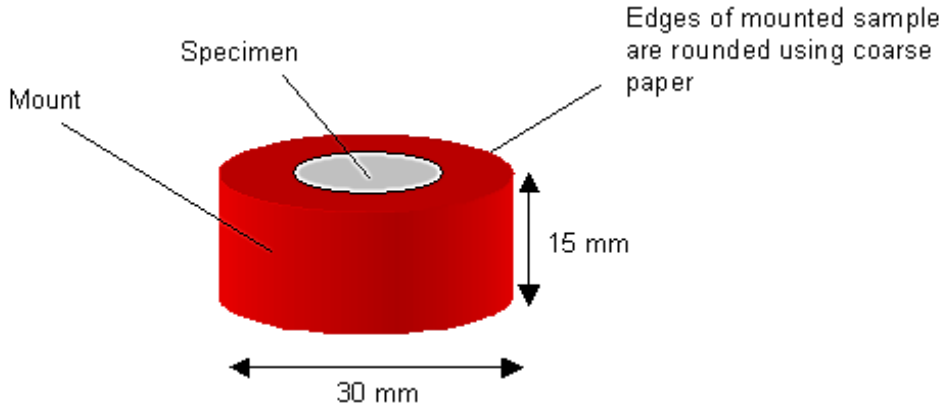

Figure 3.32. A mounted specimen (shows typical dimensions) [236].

3.15.3. Planar Grinding

This step is primarily intended for damage reduction due to former sectioning attempts. In the common sense, this entails the reduction of the particle size to prepare the material surface. Normally, the step calls for care not to inflict more damage than before to surface layers, which in damage cases require removal upon grinding. Mounted pieces are ground, as such, using rotating discs with abrasive paper, namely of wet silicon carbide. The grinding procedure involves several stages, using a finer paper (higher number) each time. Each grinding stage removes the scratches from the previous coarser paper. The process is carried out easily by

positioning the sample perpendicular to the former scratches. Between each grade, the sample is then cleaned up completely using soapy water to avoid contamination from coarser grit possibly remaining on the surface [95,234,236].

3.15.4. Polishing

Polishing aims to eliminate damage from cutting and planar grinding by means of diamond abrasion due to numerous tinier cutting edges for the least surface damage. Properly carried out, rough polishing is good enough a justification for the least time spent for subsequent polishing. The discs for this purpose are covered using soft cloth embedded with abrasive diamond particles and an oily lubricant or water lubricant. The particles have two different grades: a coarser one often of 6-micron particles for scratches caused by the finest grinding stage; and a finer one often of 1-micron particles for a smooth finish. Prior to this latter stage, the sample is cleaned up using soapy water and then alcohol against disc contamination. Next, drying with a hot air drier achieves quick results [99,236].

Final polishing eliminates surface damage and not the one inflicted by cutting and planar grinding. Should the damage from these two steps remain, rough polishing has to be carried out once again prior to subsequent steps. Mechanical polishing generally leaves behind a layer of disturbed material on the surface which may be taken away with electropolishing or chemical polishing [237,238].

Figure 3.33. Polishing steel parts [238].

3.15.5. Etching

This step is intended for optically improving the microstructural characters such as grain size, phase features, and others, using chemical etching as the widely used method, with other alternatives being molten salt, electrolytic etching, thermal etching, and plasma etching. Etching helps to expose the microstructure by targeted chemical processes; in case of alloys having over one phase, this step helps to form a contrast among various topographic zones and within the reflectivity of various phases. The etching rate is subject to crystallographic orientation; hence, the contrast created between grains, such as in in pure metals. The reagent, at the same time, preferentially etches high-energy spots including grain boundaries, thus causing surface relief for various crystal orientations, grain boundaries, phases and precipitates to be recognized without difficulty. To etch steel or copper and its alloys, a saturated aqueous solution of ferric chloride accompanied by a few drops of hydrochloric acid can be applied with a cotton bud rubbed repeatedly over the surface without over-etching [237,239].

Next, the samples are cleaned up quickly using alcohol and left to dry. after this step, many tiny etch pits may still remain as a result of localized chemical exchanges, mostly devoid of any microstructural features and appearing specifically in areas of advanced disorder such as highly-concentrated dislocations. In case of over-etching due to extended processing, pits like these often advance and block the dominant features to be investigated. The clean-up using ultrasonic baths helps as well, though not a condition. The surface subject to optical analysis is to be flat and level for the best results; otherwise, the viewing zone moving across the surface cannot remain in focus and, apart from this, the entire field of view cannot be materialized – with focused centres and unfocussed sides. Applying a levelling press to the sample can solve this issue by pushing the piece into plasticene on a microscope slide, thereby levelling it. A small piece of paper or cloth is applied to the surface against scratching [235,237,238].

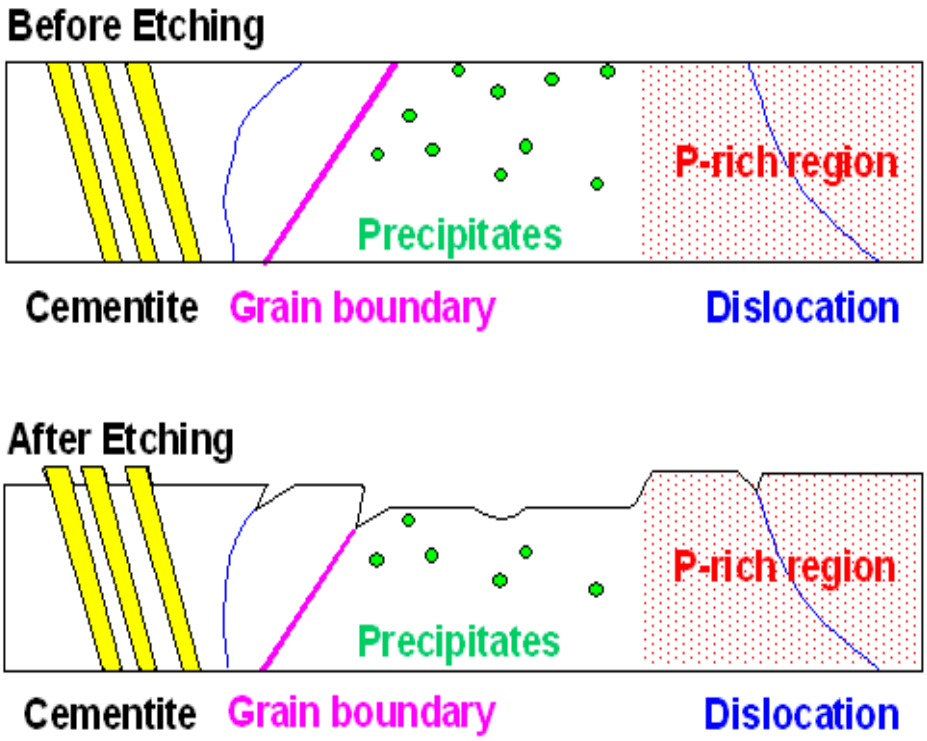

Figure 3.34. Structural of Steel Etching [239].

The metallographic analysis offers experts information concerning grain size, phase structure, solidification structure, and other features – a highly prioritized subject at present since materials including metals, ceramics, polymers, and others keep enhancing the quality of daily life as regards reliability, safety, and other measures. To optimally carry out such studies, hence, thorough testing and sample preparation is a pre-condition to learn about physical characteristics – including hardness, fracture toughness, and others. As a whole, the underlying purpose is reducing the damage as soon as possible in the microstructural preparation step [236,239].

PART 4

RESULTS AND DISCUSSION

4.1. BASIC INFORMATION

Hot work tool steels are used for industrial applications at temperatures of 200 °C and above. These tool steels contain Cr, Mo and V alloying elements and possess high hardness and toughness [240]. The H13 tool steels are generally used as hot extrusion, hot pressing, casting and moulding material [241]. These steels are subject to fatigue, creep, plastic deformation, thermal forces and wear, depending on the temperature of the environment in which they are used. Consequently, micro/macro cracks and deformations occur on the surface of the material [242]. Various surface hardening methods are used to minimise these deformations. In industrial applications, the boronizing (boriding) process is preferred in addition to surface hardening methods such as cementation, nitriding and carburising [243,244]. The boronizing process can be carried out in solid, liquid and gas phases. Boronizing is a thermo-chemical surface-hardening process usually carried out at 700–1200 °C in which penetrating boron atoms form a hard boron layer on the surfaces of iron-based and non-ferrous materials. This boron layer is highly corrosion-resistant, wear-resistant and quite hard [245]. Compared to other conventional surface hardening processes, the advantage of boronizing is that it achieves high surface hardness, low coefficient of friction and resistant to wear, corrosion and high-temperature oxidation [246,247]. Furthermore, one of the important properties of boronized surfaces is that they can sustain their surface hardness up to 1000 °C without losing their tribological properties [246]. There are a number of studies available in the literature reporting the effects of the boronizing process on wear resistance. Sahin and Meric [247] used the pack boronizing method to examine its effect on cast iron by boronizing grey iron, ductile iron and compressed graphite cast iron samples (10 mm in diameter and 7 mm in length). The metallographic examination results of the boronized samples

revealed that the structure of the boron layer formed was tooth-shaped and had a homogeneous distribution on the material surface. In addition, it was stated that the layer thickness increased with increasing process time and temperature. Moreover, when X-ray diffraction (XRD) analysis was applied to the layer, FeB, Fe_2B and Fe_3C phases were confirmed on the surface. The researchers also reported that the amount of FeB increased with increasing time and temperature. Among the three different types of cast iron, the thickest boron layer was observed on gray cast iron boronized at 930 °C for 6 h, while under the same conditions, ductile and compressed graphite cast iron had the same layer thickness. Microhardness values of non-boronized samples ranged from 289 to 247 HV, whereas the hardness of the boronized samples reached 2463–2683 HV. Thus, it was proven that the surface hardness of the samples was increased by ~ 10-fold by the boronizing process. Motallebzadeh et al. [248] evaluated the wear behavior of 31CrMoV9 and X40CrMoV5-1 steels under high temperature according to the phase structure of the boride layers. In the study, disc-shaped samples (35 mm in diameter, 6 mm in height) were subjected to boronization for 4 h at 900 °C and for 6 h at 950 °C. Wear tests were performed at room temperature (RT) and at 500 °C. At the end of the wear tests, a 2D optical profilometer detected wear marks on the surface and the surfaces were examined by scanning electron microscopy (SEM). As a result of the experiments, it was observed that the boride layers of the boronized steels consisted of FeB and Fe_2B phases with a thickness of approximately 65 μm. Similar frictional properties and superior wear resistance were observed at room temperature for both boronizing conditions, but the wear resistance decreased at 500 °C due to cracks in the contact zones. Taktak [249] applied the boronizing process to AISI H13 and AISI 304 steels and examined the mechanical properties of the borides. For the boronizing, parameters were applied for 3,5 and 7 h at 800, 850, 900 and 950 °C. The formation of FeB, Fe_2B, CrB and Ni_3B phases in the boride layer was determined by XRD. Using a Vickers microhardness tester, the hardness values of the AISI H13 and AISI 304 steels were measured as approximately 1860 and 2150 HV, respectively, and it was emphasized that these values were higher than for the base steels. In addition, they stated that the hardness values increased depending on the process temperature and time. An optical profilometer was used to measure the surface roughness of the coatings and the surface roughness of the boronized samples was found to increase with increasing

process temperature and time. In addition, the boride layer on the AISI 304 steel had a flat and smooth structure, whereas on the AISI H13 steel it had an irregular structure. He et al. [250] studied the low-temperature boronizing of high carbon steel (CPM® S90V) in terms of hardness change and wear resistance. Boronizing was carried out at 780 °C for periods of 2, 4, 12 and 24 h, and the boride layers were measured as 60, 130, 400 and 420 μm, respectively. It was thus determined that layer thicknesses increased with increasing boronizing time. According to the XRD diagrams, it was confirmed that FeB and Fe_2B phases were formed as a result of the boronizing. The surface hardness was measured with a Vickers hardness tester and indicated that the surface hardness of the sample had increased from 680 HV to 1070 HV due to the boronizing process. Another advantage of the boronizing was that the friction coefficient was reduced by 17% for steel-steel contact and by 65% for diamond-steel contact.

Another factor that provides wear resistance is the lubricant used in the wear environment. Accordingly, in order to minimize friction force in industrial applications and to prevent wear, there is a need to use lubricants between materials that come in contact with each other, including solid lubricants (graphite, MoS_2, boric acid, borax), liquid lubricants (synthetic hydrocarbons, organic esters, silicone) and gas lubricants (air, mineral gas) [251]. Additives such as oxidation inhibitors, high-pressure additives, and nanoparticles can be used to improve the mechanical and tribological properties of lubricants. The use of nanoparticles as friction-reducing and anti-wear additives is of great interest in tribology [251,252,253]. Using a ball-on-disc tribometer under loads of 7 and 10 N, Sanchez-Lopez et al. [252] studied the effects of the addition of Pd and Au nanoparticles (5 wt.%) with spherical diameters of approximately 2.2 nm as anti-wear lubricant additives on the friction and wear behavior between an AISI M2 steel disc and a 6-mm-diameter AISI 52 100 steel ball. According to SEM images, the nanoparticles formed a film layer against wear on the material surface. The best results were obtained using Pd nanoparticles under a 7-N load. The wear rate was determined as approximately 3.6×10^{-10} mm^3/Nm and the friction coefficient as less than 0.1. Ghaednia et al. [253] used a polyvinyl pyrolidone-stabilized silver nanoparticle-enriched polyethylene glycol (PEG) nanolubricant having an average spherical diameter of 5.6 nm at concentrations of 0,

1.5, 3 and 4.5 mM. The tribological performance was examined using a pin-on-disc tribometer (pin = 10 mm diameter, AISI 52100 chromium steel: disc = AISI 1080 carbon steel, 0.4 μm roughness). The PEG was used as both a nanoparticle reducing agent and a nano-lubricant in that study. As a result of the tribological test carried out under 10 N load, the friction coefficient and wear volume values of approximately 0.7 and 0.048 mm^3, respectively, decreased with increasing AgNP concentration. With the 4.5 mM concentration, friction coefficient and wear volume values were determined as approximately 0.43 and 0.034, respectively.

In the literature, the effect of boronizing on wear resistance has been investigated by many researchers [246,248–250,254,255]. Using the surface boronizing process is important for increasing the service life of tool steels working under friction and wear conditions. In addition, it is desirable to use tool steels together with cutting fluids in the working zone. Therefore, the wear behaviour of boronized surfaces should be examined in a lubricant environment. However, there is no study in the literature regarding the wear behaviour of boronized surfaces under different lubricated environment conditions. The performance of the coolant-lubricant fluids used in industry can be improved by additives. For this reason, the relationship between the wear behaviour of boronized surfaces and nanoparticle-doped lubricants was examined in detail in this study. The investigation of the wear characteristics of surface-boronized H13 steel in a nanoparticulate-added liquid environment is unique in the literature. Firstly, H13 steel was boronized at different temperatures and times, and its characteristics were determined via SEM imaging, energy-dispersive X-ray (EDX), XRD spectral analysis and microhardness measurements. In the second stage, boronized H13 steels were subjected to dry and lubricated wear tests. A nano-silver added colloidal suspension developed by coating with three different stabilising ligands was used in the liquid environment experiments. The investigation of the performance of the colloidal suspensions developed with different ligands as wear agents is second originality of the present study. The wear experiments were examined in terms of weight loss and friction coefficient measurement, 3D profile, SEM imaging and EDX spectral analysis methods.

4.2. MATERIAL AND METHODS

The purpose, generated hypothesis and methodology of the study are given in Figure 4.1 as a flow diagram. This study investigated the effect of surface coating and lubricants on the long-time usage of H13 steel.

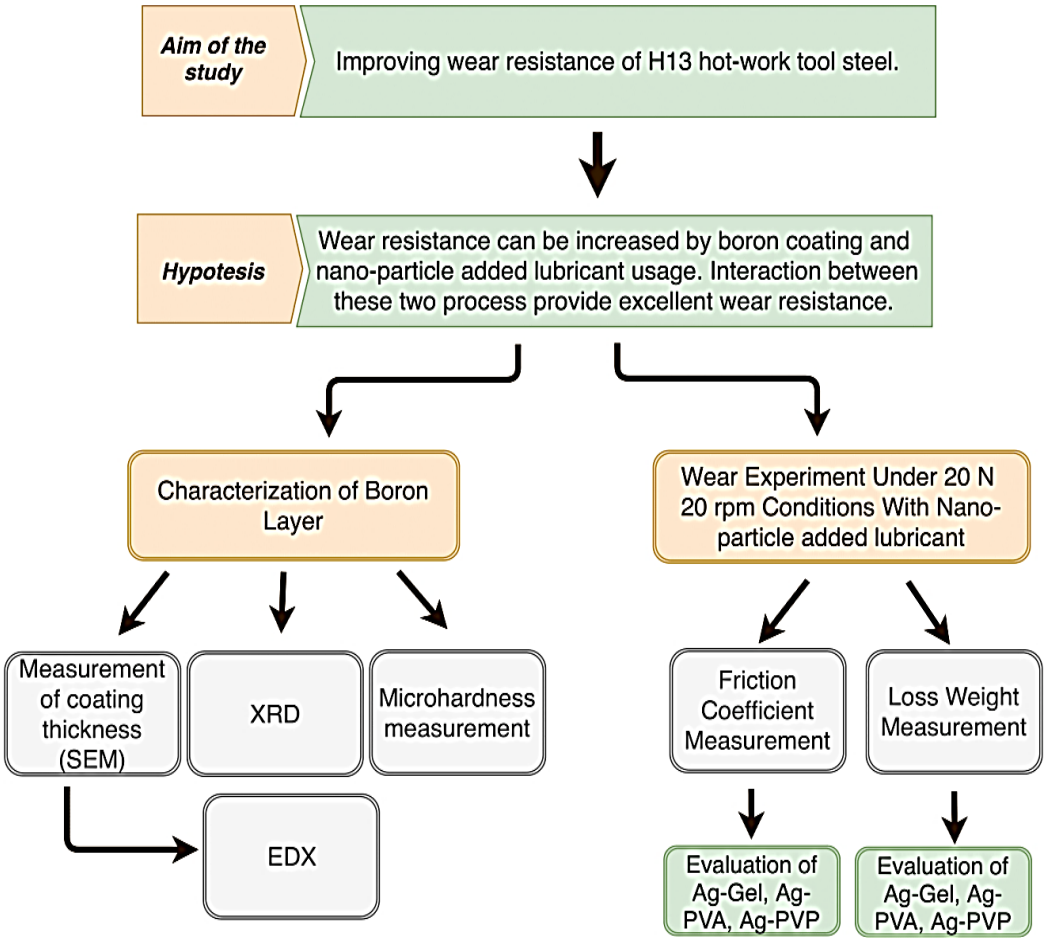

Figure 4.1. Flow diagram of the study

4.2.1. H13 Hot Work Tool Steel and Boronizing Process

This study used H13 hot work tool steel which is extensively used in mould production and exposed to wear continuously. The chemical composition of H13 steel is given in Table 4.1. This steel has high toughness, a tensile strength of 1500 MPa, and a hardness value of ~ 45 HRC. The H13 steel cylindrical samples were cut to 9 mm in diameter and 2 mm in length and prepared for boronizing. The pack

boronizing method was selected for the study because the equipment is easily supplied and operated, and it results in a smooth surface [254].

Table 4.1. Chemical composition of AISI H13 hot work steel (wt.%).

Chemical Composition (%)	**C**	**Cr**	**Mo**	**V**	**Si**	**Mn**
	0.39	5.10	1.30	1.00	1.00	0.40

For the boronizing heat treatment, the usual choices for the source of boron are B_4C, $Na_2B_4O_7$, and H_2B_6 [244,250] along with KBF_4 [256] as the activating agent. The activating agent ensures steady growth of the formed layer, while the fillers retain oxygen at the established processing temperature [244]. A single-phase (Fe_2B) or dual-phase (FeB and Fe_2B) boride layer is formed on the surface of the material, depending on conditions such as the temperature after boronizing, time duration and chemical composition of the samples [245,247]. When the SEM images of the materials are examined, a needle-like structure can generally be seen going inward from the surface [257]. FeB phase is undesirable on the surface of the material because, in these structures, the FeB phase is harder, but has lower toughness than the Fe_2B phase [246,255,258]. The formation of the FeB phase on the surface affects the material under high stresses by causing brittleness and crack formation [259].

The boronizing process, shown schematically in Figure 4.2, consisted of heat treatment applied at 700, 800, and 900 °C for 4 h and at 800 °C for 2, 4, and 8 h in a ~ 1800 °C capacity heat treatment furnace. In the boronizing process, 95% by volume of nano boron powder was used as the boron source and 5% KBF_4 as the activating agent. At the beginning of the firing process, a 1-cm-thick layer of nano boron powder was spread in the stainless steel container, and the samples were placed on this powder at approximately 2 cm intervals. After placement, the nano boron powder was filled to a height of 2 cm over the samples, and the remaining space in the container was filled with the activator. After the container was sealed airtight, the firing process was carried out according to the specified parameters. After firing, the container was removed from the oven and cooled to room temperature.

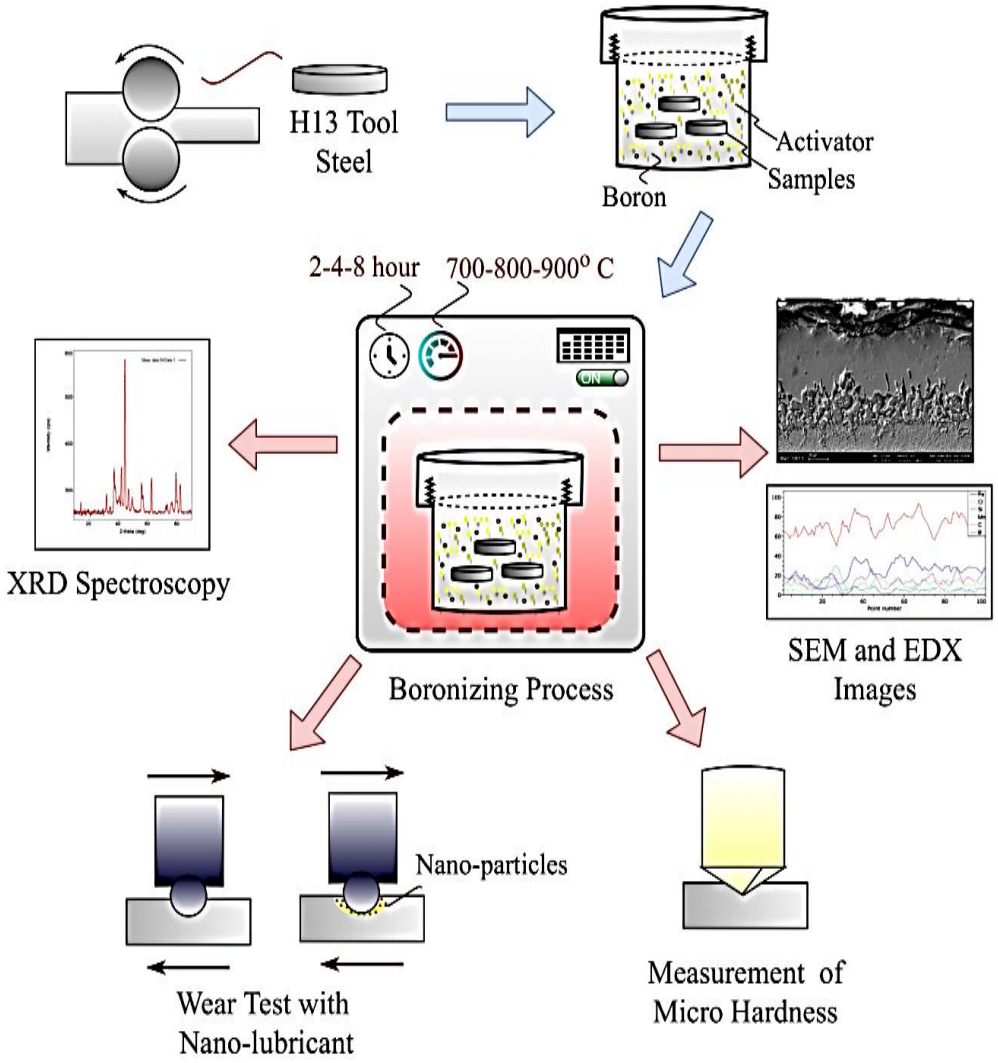

Figure 4.2. Boronizing process

The boronized samples were subjected to cutting, grinding, polishing and etching for metallographic and visual analyses. After etching, the coating thickness and hardness values of the samples were measured, and the phases formed on the surface of the material were determined. Vickers hardness (HV) measurements were made using a Bruker-UMT microhardness tester under a 50-g load for a period of 15 s. The surface hardness values of the layers were determined by measuring from eight different points. The boride phases were determined by XRD spectrometry using a Rigaku Ultima IV with Cu Kα radiation (scanning speed: 20 °/min; voltage: 40 kV; scanning angle: 20 - 90 °; current: 30 mA). The coating thickness was measured by SEM (Carl Zeiss Ultra Plus Gemini FESEM), and the morphology of the worn surfaces was

examined. In addition, images were obtained using a 3D optical profilometer (Phase View Optic Profilometer) to determine the surface quality of the samples.

4.2.2. Synthesis of Silver Nanoparticles

In this study, silver nanoparticle (AgNPs) suspensions obtained using three different ligands were used. The AgNP suspensions were synthesised using the Tollens' process with gelatin as the stabilising ligand [260]. According to this process, 2.5×10^{-2} M, 10 mL of sodium borohydride ($NaBH_4$, Sigma-Aldrich) and 0.2 g of gelatin (Fluka) were placed in a beaker. Following this, 1.25×10^{-2} M, 20 mL ammonia (NH_3, Sigma-Aldrich) and 5.10^{-2} M sodium hydroxide (NaOH, Merck) were added to it. This mixture was placed over a magnetic stirrer and mixed in an ice bath until it had cooled down to 5 ℃. Next, 2.5×10^{-3} M, 10 mL of silver nitrate ($AgNO_3$, Sigma-Aldrich) solution was dripped into the cooled mixture at a rate of 1 drop/s. The mixture was stirred for a further 5 min at room temperature and then kept in a cool, dark place.

Furthermore, the AgNP suspensions were synthesised using PVA and PVP stabilising ligands as follows. First, 0.2 g of polyvinylalcohol / polyvinylpyrrolidone (PVA / PVP, Sigma-Aldrich) was added to 6.25×10^{-3} M, 40 mL of sodium borohydride solution. This mixture was placed on the magnetic stirrer and mixed in an ice bath until it had cooled down to 5 ℃. Next, 2.5×10^{-3} M, 10 mL of silver nitrate ($AgNO_3$, Sigma-Aldrich) solution was dripped into the cooled mixture at a rate of 1 drop/s. The mixture was stirred for a further 5 min at room temperature and then kept in a cool, dark place.

The optical properties of the synthesised AgNP suspensions were characterised using the Agilent Cary 60 UV-Vis spectrometer. The size and morphology of the nanoparticles were characterized via a Philips CM 300 FEG / UT transmission electron microscope (TEM).

4.2.3. Wear Experiments under Dry and Lubricated Conditions

Experiments were carried out under lubricated and dry sliding conditions to investigate the wear performance of the boronized H13 steel. Three different nanoparticle-doped lubricants were used in the experiments performed under the lubricated sliding condition. Wear tests were carried out under a constant 20 N load [261] at a sliding speed of 20 rpm for 2 h (1000 m) [261] on a ball-on-plate wear apparatus (Fig. 4.3). The parameters were determined according to preliminary tests and literature by considering the parameters in which the wear marks could be seen clearly. The abrasive material used was 6-mm-diameter AISI 52100 (100Cr6), having a hardness of 55 HRC [278]. The friction coefficient and weight-loss parameters were measured to analyse the wear tests. All tests were repeated three times, and the mean value was taken. Friction coefficient data were continuously recorded during the wear test. A 10^{-4} g precision balance was used for weight loss measurements of the samples subjected to wear testing. The experimental design model for the coating and wear tests is given in Table 4.2. Ethylene glycol (EG) was used to the carriage of nano-particles to the wear zone.

Figure 4.3. Ball-on-plate wear apparatus

Table 4.2. Experimental design.

Boronizing Process			**Wear Experiments**		
Temperature (°C)	**Time (h)**	**Load (N)**	**Speed (rpm)**	**Lubricant Additive**	**Quantity (ml)**
700	4	20	20	AgNP@Gel	250 ml Ethylene Glycol + 50 ml AgNP@GEL
800	2, 4, 8			AgNP@PVA	250 ml Ethylene Glycol + 50 ml AgNP@PVA
900	4			AgNP@PVP	250 ml Ethylene Glycol + 50 ml AgNP@PVP

4.3. ANALYSIS OF RESULTS

4.3.1. Microstructural Analyses of Boron Layer

Boron atoms react with the base material to form boride layers on the surface of the material. Whether the layer is single-phase (Fe_2B) or dual-phase (FeB and Fe_2B) depends on the chemical composition of the base material [249,256]. The microstructures of the samples boronized for 4 h at 700, 800, and 900 °C and for 2, 4, and 8 h at 800 °C were examined by SEM and the resulting images are given in Figures 4.4,5,6 and 4.7,8,9. The figures show that the thickness of the boride layer increased due to the increases in both temperature and test time. The layer thicknesses of the samples boronized at 700, 800, and 900 °C for 4 h were approximately 3, 9 and 26.5 μm, respectively, while those of the samples boronized at 800 °C for 2, 4, and 8 h were measured as 7, 9 and 11.5 μm, respectively. According to these values, boronizing temperature is more effective on the boride layer thickness than boronizing time. In the study conducted by Cimenoglu et al.

[246], boronizing 4140 steel at 750 and 800 °C resulted in the formation of only a single-phase (Fe_2B) layer on the surface, whereas at 850 and 900 °C, the double-phase (Fe_2B and FeB) layers were formed. Similarly, Erdogan [259] boronized H13 steel under dry sliding conditions and observed that a single-phase boride layer was formed at 800 °C, while a dual-phase boride layer was formed on the samples boronized at 900–1000 °C. In Figures 4.4,5,6 and 4.7,8,9, single-phase layer formation is seen at 700 and 800 °C, while FeB and Fe_2B phases are formed together at 900 °C. The dark-coloured layer in Figure 4.4c shows the FeB phase and the lighter region shows the Fe_2B phase. When the microstructures formed under other conditions were examined, no contrasting separation was evident in the boride layers. However, the XRD graph given in Figure 4.18.d shows a small amount of FeB phase formation in the boronized sample at 800 °C for 2 hours. In addition, the number of FeB peaks increased with increasing boronizing time (Figures 4.16 and 4.19). According to the results, the FeB phase increases for H13 steel at 800 °C with boronizing times over 2 hours. While FeB phase is observed closest to the surface, Fe_2B phase is formed between FeB phase and main material according to Figure 4.6. In Figures 4.4,5,6-4.7,8,9,boride layers of 900 °C, 4h and 800 ° C, 8h boronized samples (Figure 4.6, Figure 4.9) had saw tooth morphology [240,262], while a smooth and regular morphology was obtained in other parameters [263].

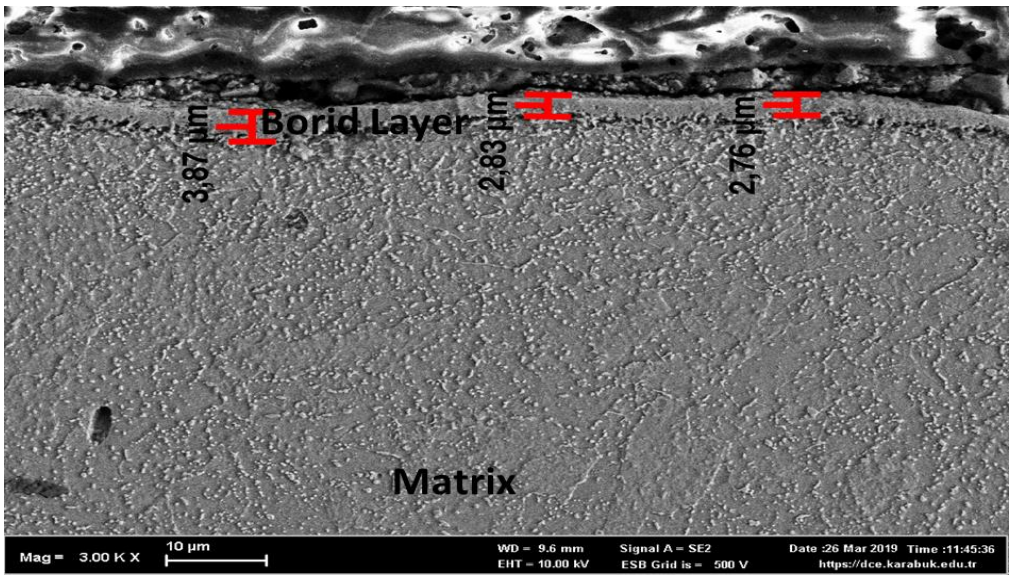

Figure 4.4. SEM microstructure of H13 steel boronized for 4 h at 700 °C.

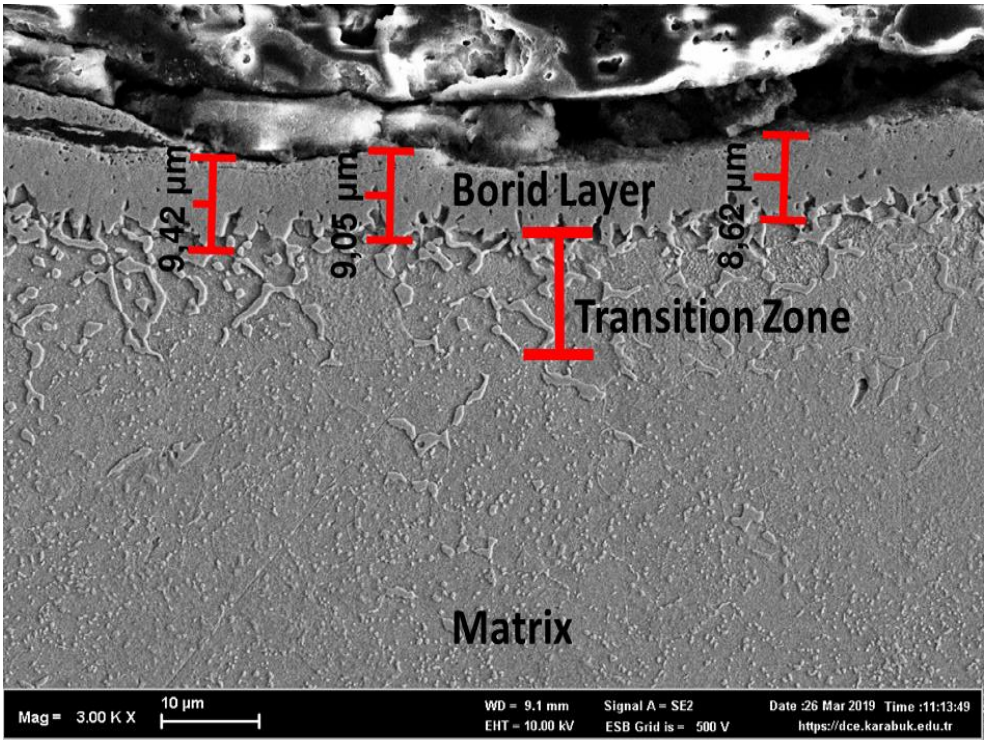

Figure 4.5. SEM microstructure of H13 steel boronized for 4 h at: 800 °C.

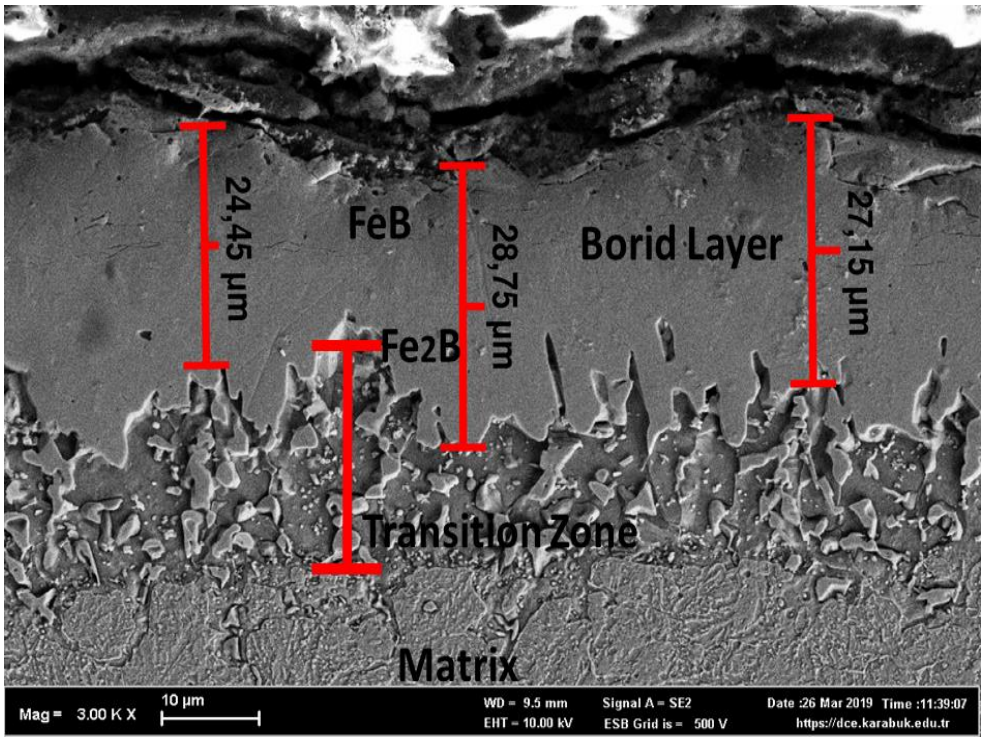

Figure 4.6. SEM microstructure of H13 steel boronized for 4 h at: 900 °C.

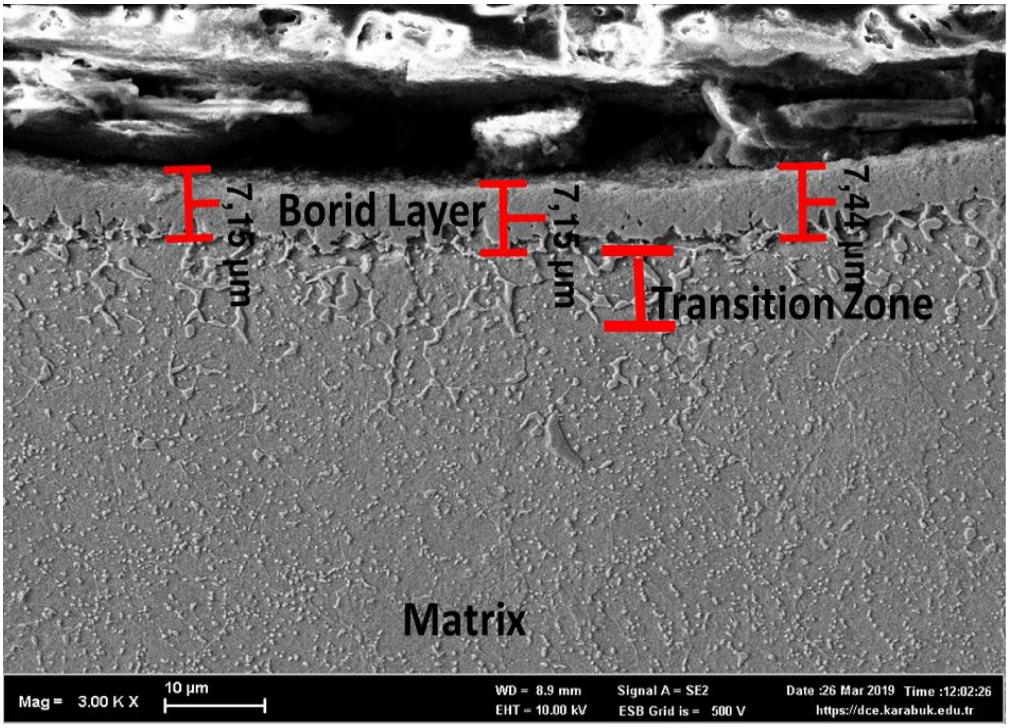

Figure 4.7. SEM microstructure of H13 steel boronized at 800 °C for 2 hours.

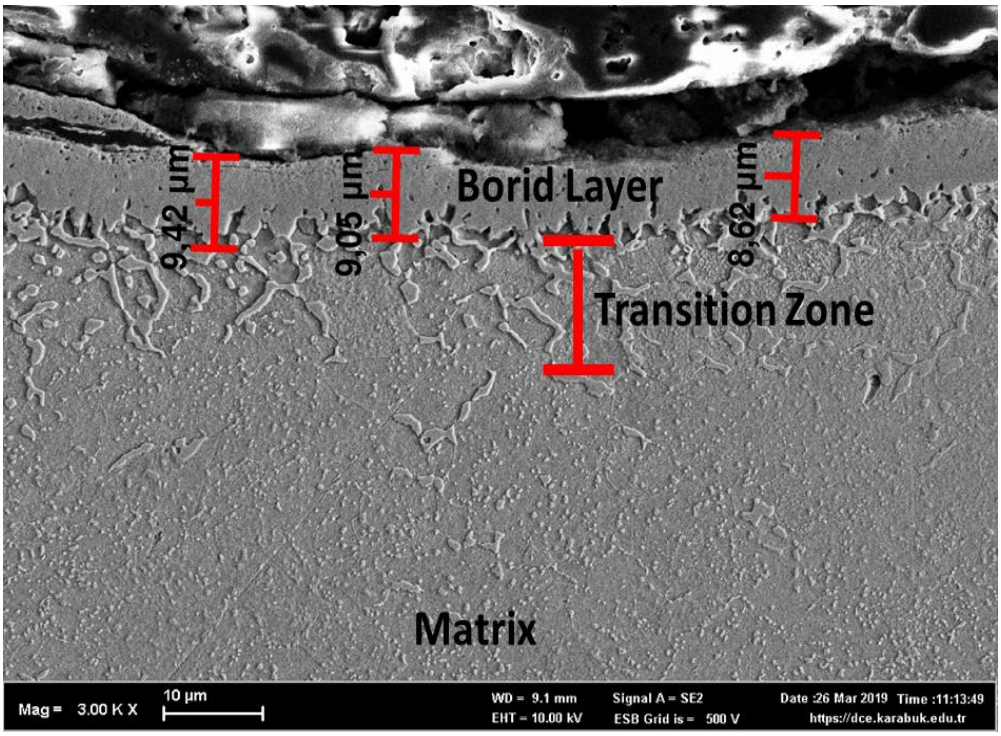

Figure 4.8. SEM microstructure of H13 steel boronized at 800 °C for 4 hours.

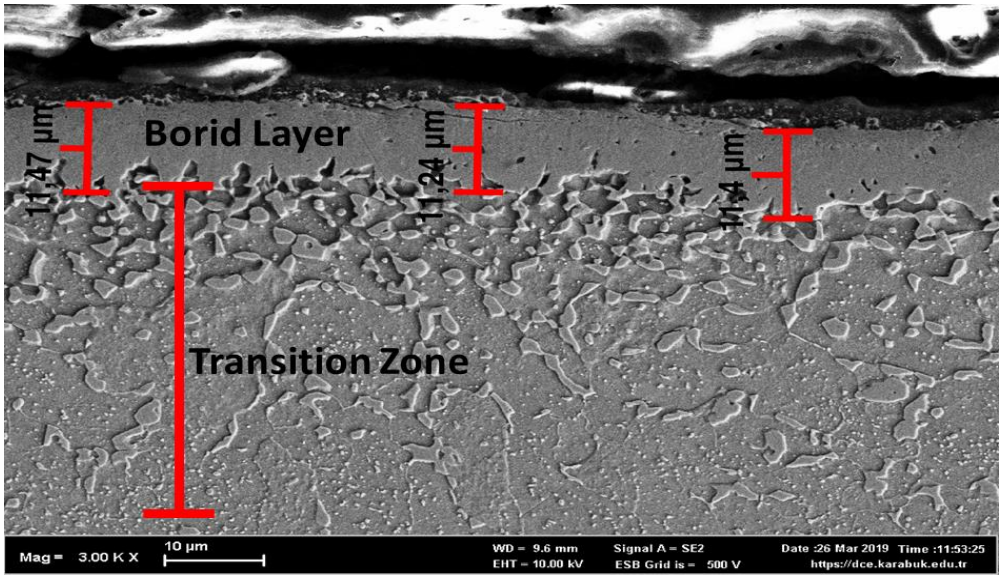

Figure 4.9. SEM microstructure of H13 steel boronized at 800 °C for 8 hours.

Figures 4.4,4.5,4.6 and 4.7,4.8,4.9, show that boride layers of different thicknesses were formed on the sample surfaces as a result of the boronizing. The composition of the chemical elements in these layers was analysed by EDX and XRD. Among the study parameters, the best layer thickness was observed in the sample boronized for 4 h at 900 °C. The EDX image of this sample is given in Figure 4.10, which shows the elements of Fe, Cr, Si, Mn, C and B in the boride layer, (this result as per the compare between figures 4.11- 4.14).

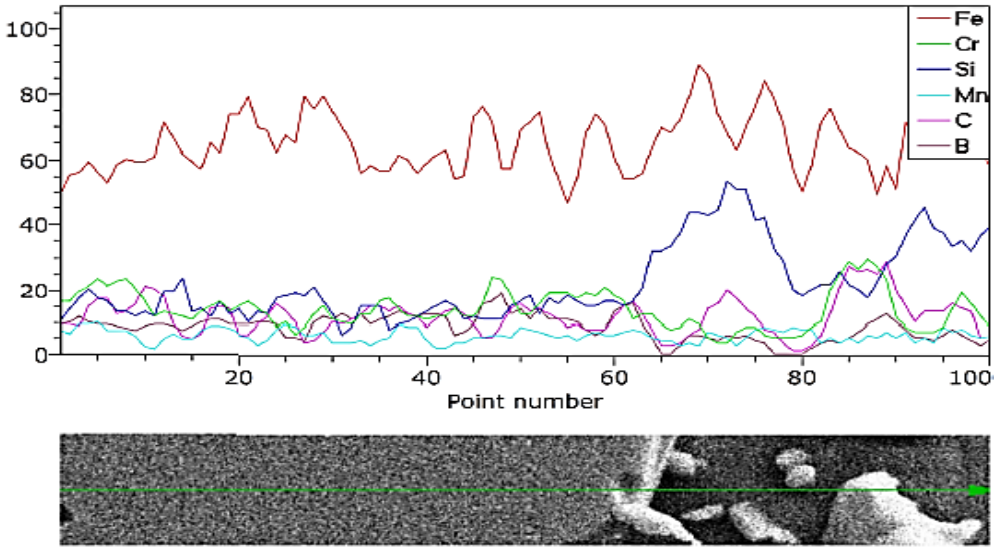

Figure 4.10. EDX image of 4-h boronized sample at 900 °C.

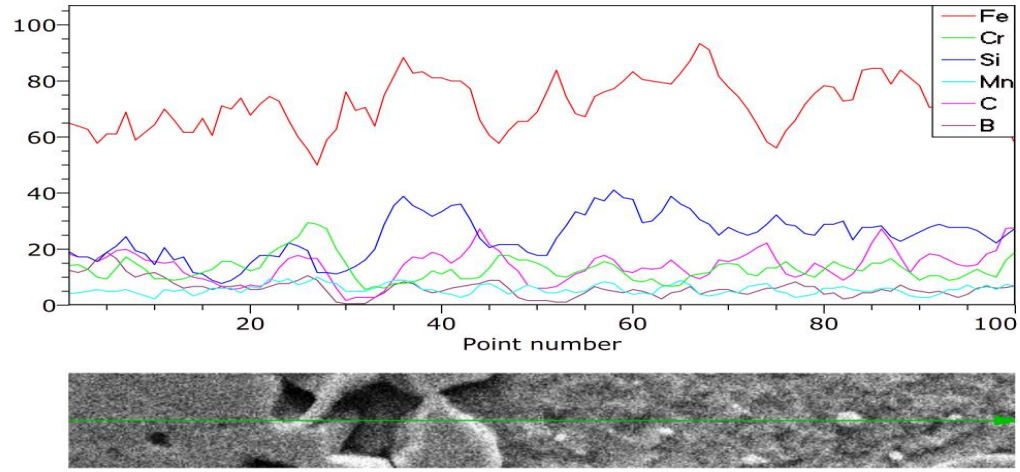

Figure 4.11. EDX image of 4-h boronized sample at 800 °C.

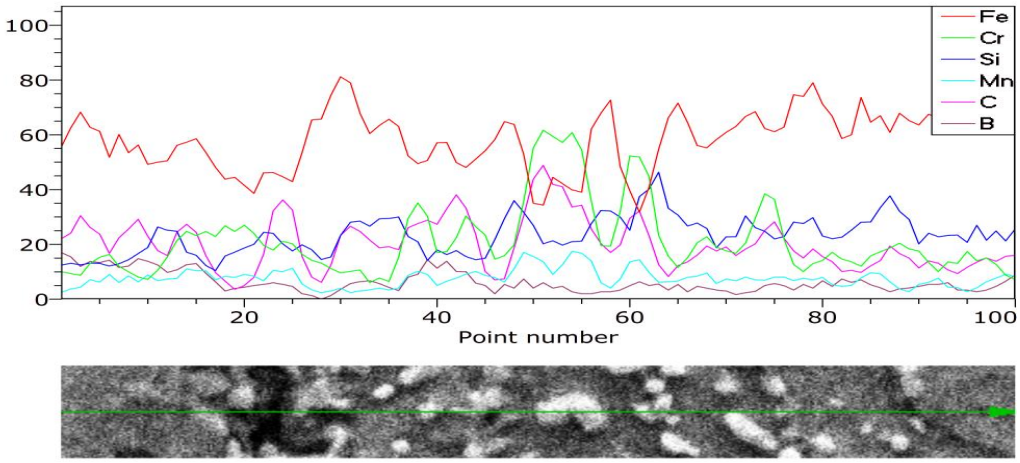

Figure 4.12. EDX image of 4-h boronized sample at 700 °C.

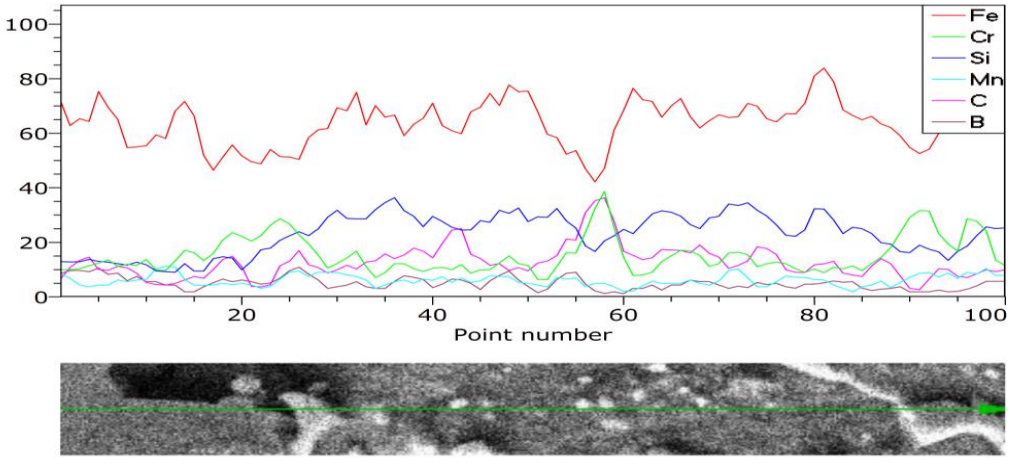

Figure 4.13. EDX image of 2-h boronized sample at 800 °C.

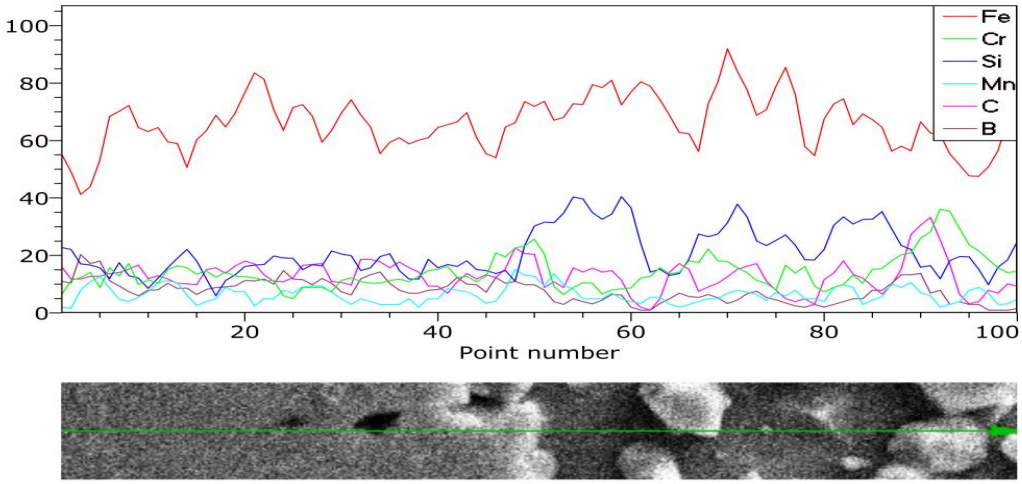

Figure 4.14. EDX image of 8-h boronized sample at 800 °C.

The XRD analysis (Figures 4.15–19) show that the boride layer consisted of Fe2B, FeB, CrB and MnB phases [259]. The amounts of these phases varied according to the coating parameters. In general, it is seen that with increasing boron temperature and time, Fe2B phase decreases and FeB phase increases in the boride layer. It is seen in Figures (4.15–19) that boride layers mostly consist of dual-phase (Fe2B and FeB) [248,263] rather than a single phase. Thanks to these phases, the mechanical properties of boride layers can be defined [258,263]. In the Fe2B and FeB phases, the iron was replaced by chromium and manganese (CrB, MnB) in the coating. However, even when MnB reached its maximum concentration, it was clear that it occurred at a lower density than the FeB and Fe2B phases.

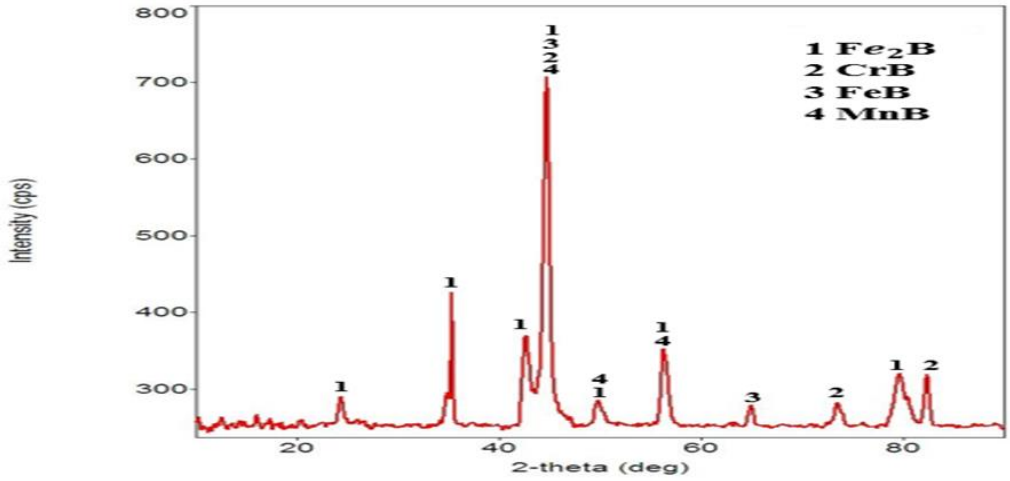

Figure 4.15. XRD analysis of the compound: 700 °C for 4 h.

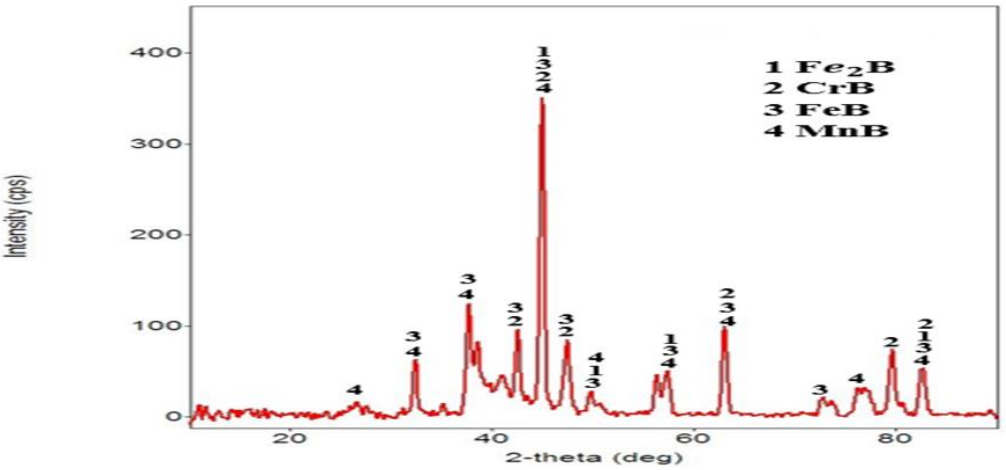

Figure 4.16. XRD analysis of the compound: 800 °C for 4 h.

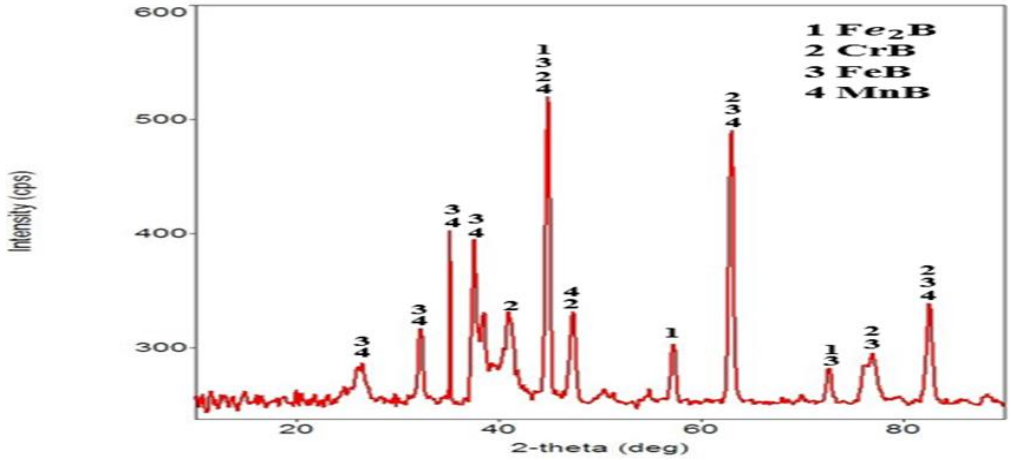

Figure 4.17. XRD analysis of the compound: 900 °C for 4 h.

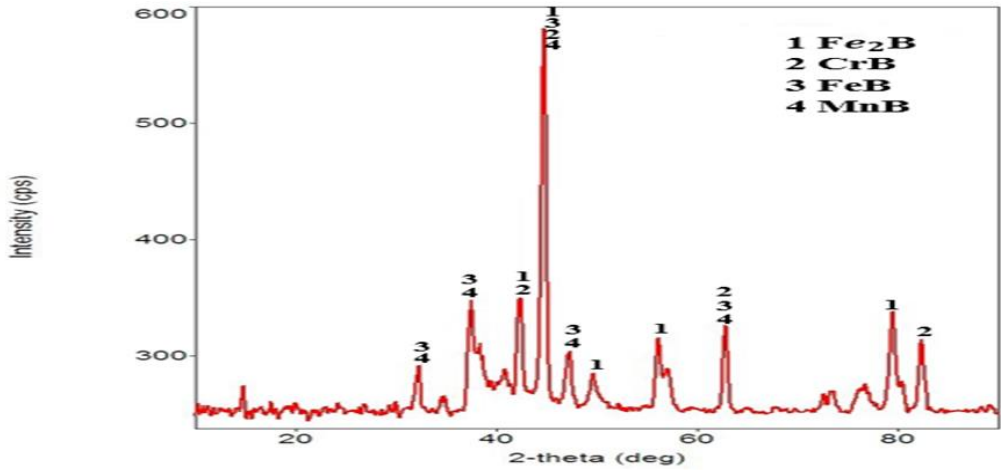

Figure 4.18. XRD analysis of the compound: 800 °C for 2 h.

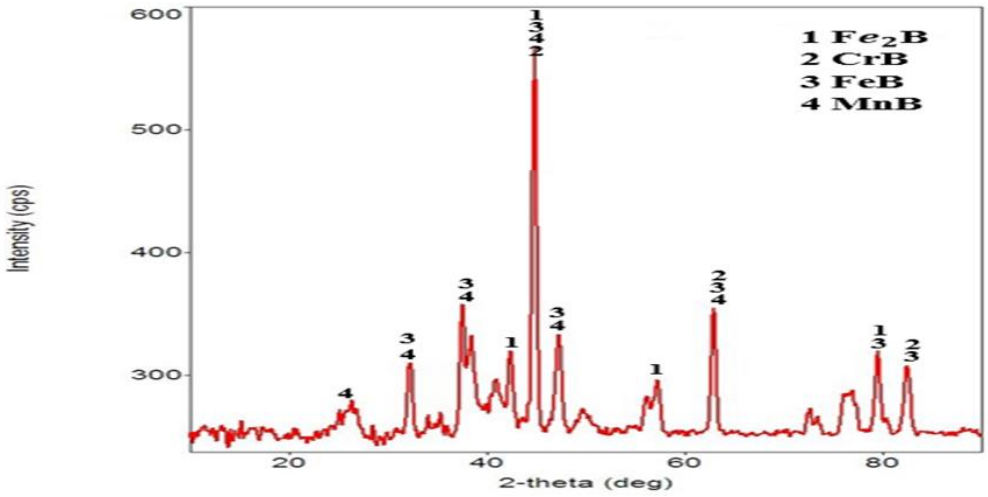

Figure 4.19. XRD analysis of the compound: 800 °C for 8 h.

4.3.2. Microhardness Analyses of Boron Layer

The best advantage obtained by the boronizing method is hardness [247]. With this method, carbon steels can reach a hardness of 1800–2000 HV, alloy steels 2500–2800 HV and high-speed steels 2800–3300 HV [245]. The heat generated by the friction in the boron layers is not expected to reduce the wear resistance of the material. Because a structure with a hardness value of 2000 HV can maintain its surface hardness even at 900–1000 °C, and among surface diffusion processes, this feature is a property of boronizing only [244,245].

The surface hardness values of boronized H13 steel are given in Figure 4.20. Hardness changes were measured at seven different points from the outermost surface to the inner surface of the material at a depth of 70 µm. Figure 4.20 shows that the surface hardness values of the samples boronized at 700, 800, and 900 °C for 4 h and 800 °C for 2, 4, and 8 h increased depending on the processing time and temperature. It is stated in the literature that if the boronizing process is carried out at a high temperature and for a long time, a harder layer is obtained due to the FeB phase [240,259,264]. In this study, the surface hardness values of the samples boronized at 700, 800, and 900 °C for 4 h were 1758 HV, 1887 HV and 2001 HV, respectively. Surface hardness values of the samples boronized at 800 °C for 2, 4, and 8 h were measured as 1376 HV, 1887 HV and 1923 HV, respectively. It can be

seen in Figure 4.20 that the hardness decreased as the boride layer moved towards the base material, and thus, the boronizing process substantially increased the material hardness. The highest surface hardness value at 900 °C can be explained by the FeB phase formed in the coating layer (Fig. 4.6). Since the FeB phase was harder than the Fe_2B, the hardness had reached maximum values. The results obtained are consistent with the studies in the literature [240,254,259,264].

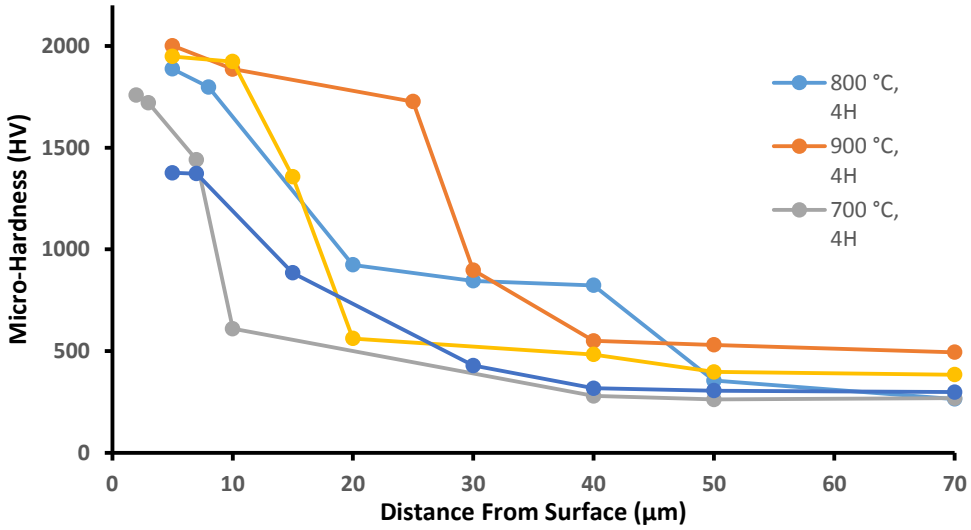

Figure 4.20. Microhardness profile of the boronized H13 steel.

4.3.3. Characterisation of Silver Nanoparticles Coated with Different Ligands

The Figures 4.21,22,23, show TEM images of the AgNP suspensions prepared using different ligands. From the literature, we know that AgNPs can be synthesised in different morphological structures (rod, octahedral, tetrahedral, etc.) using different ligands [265]. However, with the three ligands used in this study, the nanoparticles were synthesised in a similar spherical morphology. The size of the nanoparticles obtained by using gelatin, PVA and PVP as stabilising ligands were 12.24 ± 1.73, 12.39 ± 3.18 and 16.39 ± 4.30 nm, respectively. A comparison of the standard deviations of the AgNPs showing both their size and size distributions revealed that the smallest particle size and the closest (monodisperse) particle size distribution were obtained by using gelatin. With the use of PVP, both the size and standard deviation values of the particles reached the maximum.

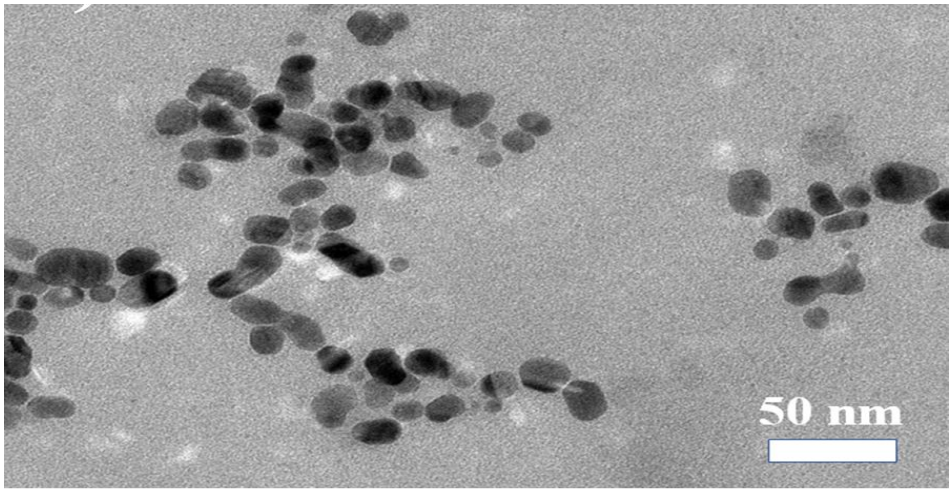

Figure 4.21. TEM images of silver nanoparticles: Ag@Gel.

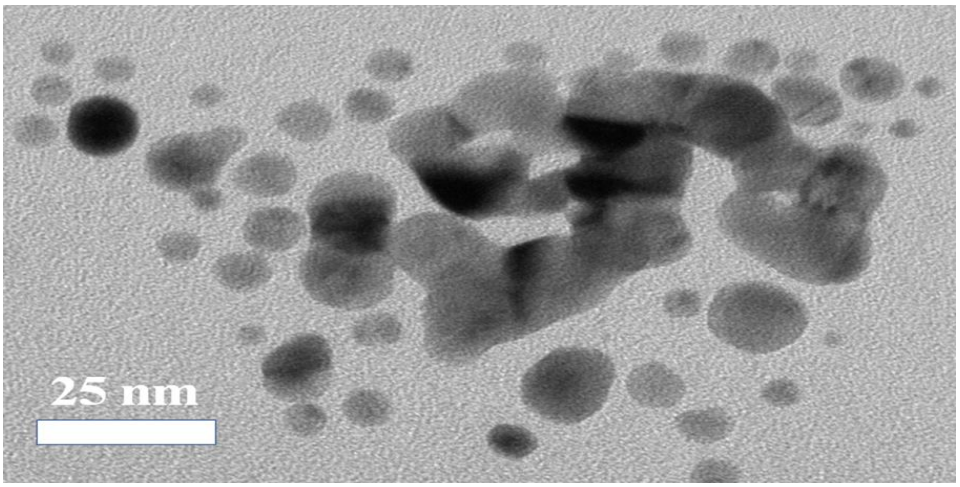

Figure 4.22. TEM images of silver nanoparticles: Ag@PVA.

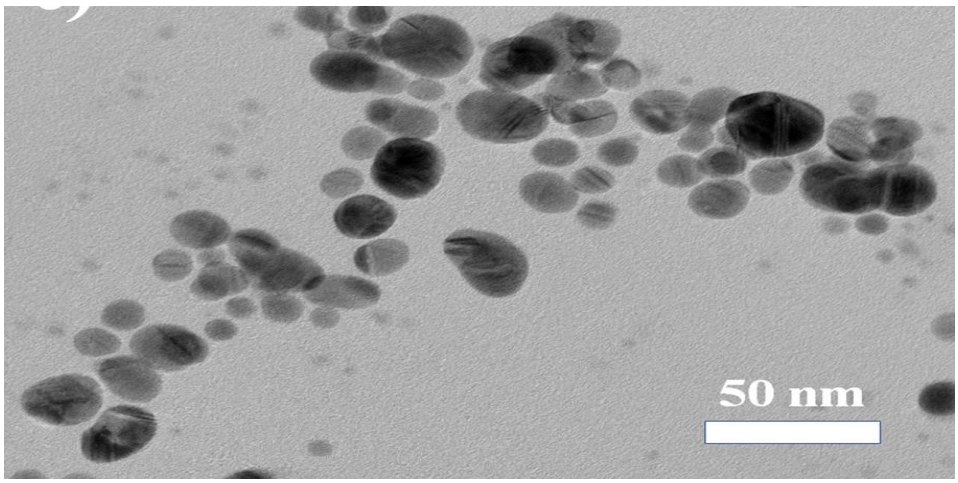

Figure 4.23. TEM images of silver nanoparticles: Ag@PVP.

The AgNPs with spherical morphology gave absorbance peaks at wavelengths of about 390–420 nm depending on varying sphere diameters [266]. From the literature, we know that with reduced particle size, the absorbance peak shifts to lower wavelengths [267]. When the UV-Vis analyses of the AgNP suspensions were examined, the absorbance peaks of all three ligands were very close to each other at wavelengths of 401–403 nm. As determined from the TEM analysis results, the suspensions with very small particles produced absorbance peaks at low wavelengths.

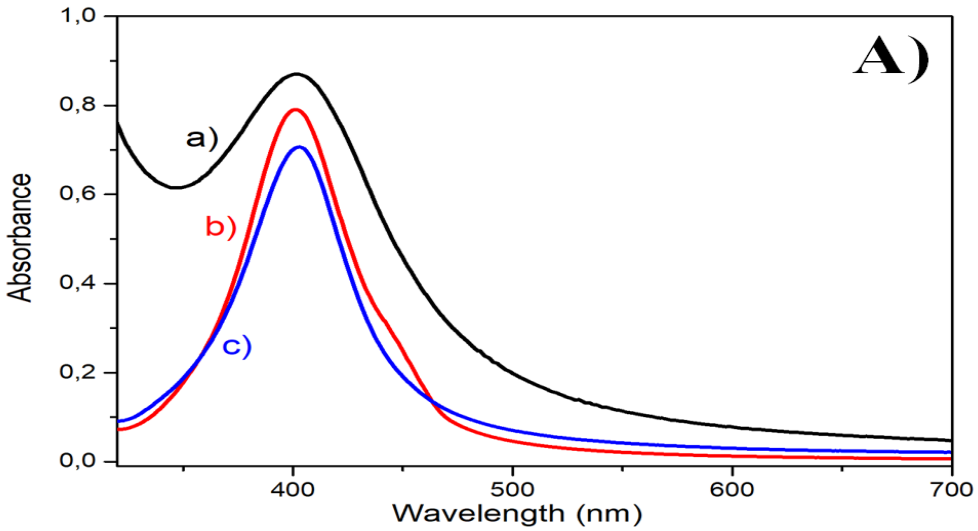

Figure 4.24. A) Pre-wear UV spectra of AgNP suspensions.

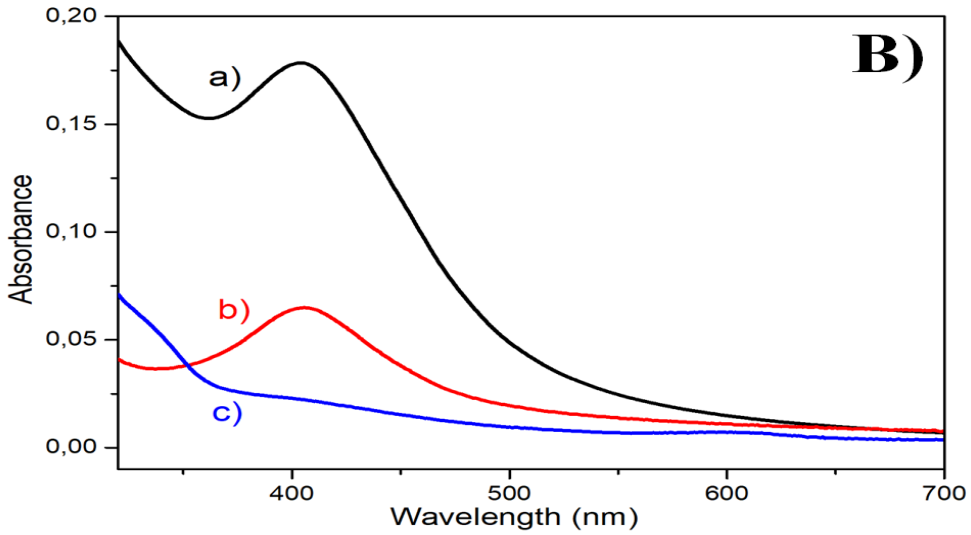

Figure 4.25. B) Post-wear UV spectra of AgNP suspensions.

Metal nanoparticles in a solvent, over time, tend to come together and precipitate [268]. Metal nanoparticles are coated with stabilising ligands to reduce or prevent this tendency. These ligands have different functional groups which can influence the stability of metal nanoparticles to different degrees [269]. The UV spectra of the AgNP suspensions in the study are shown after wear in Figure 4.25/B. Accordingly, all AgPVP nanoparticles were agglomerated after wear and grew larger than the nanoscale size (Fig. 25/Bc). With the use of PVA as a stabilising ligand, small amounts of AgNPs were found to be nano-sized (Fig. 25/Bb). When gelatin was used, more AgNPs were found to be nano-sized compared with the PVA and PVP (Fig. 25/Ba). According to these results, the stability of the AgNP suspensions used as lubricants ranged from low to high for PVP, PVA and gelatin, respectively. As explained in detail in the following sections, both the friction coefficient and the wear weight loss of the samples were reduced with the increasing stability of the AgNPs due to the reduced particle size and, more importantly, the effect of the ligand used.

4.3.4. Friction and Wear Behavior

Wear tests were applied on samples boronized at 700, 800, and 900 °C for 4 h and 800 °C for 2, 4, and 8 h using three different nano-silver-doped lubricants (AgNP@Gel, AgNP@PVA, AgNP@PVP) and under dry conditions. The friction coefficients obtained during the wear test are shown in Figure 4.26.The figure shows that there is no meaningful relationship between boronizing parameters and friction coefficients. This result is consisted with the literature. Yazıcı and Yılmaz [270] studied the wear behavior of heat-treated of R260 rail steel with high power diode laser at 1100 °C, 1200 °C and 1300 °C process temperatures. Initially, the hardness of the untreated sample was 277 HV, while the hardness of the samples treated at 1100 °C, 1200 °C and 1300 °C reached to 836 HV, 851 HV and 889 HV, respectively. The friction coefficients were 0.4 in the untreated sample while the friction coefficients of the treated samples were 0.56, 0.53 and 0.57, respectively, with increasing process temperature. Due to the increase in surface hardness, it was observed that the coefficient of friction and wear rate of laser-treated samples were expected to decrease, but these values increased. Cuao-Moreu et al. [271] boronized

the CoCrMo casting alloy at temperatures of 1223, 1248 and 1273 K for 6, 8 and 10 hours, respectively. During abrasion tests, the lowest friction coefficient was obtained in the untreated sample, contrary to expectations. In the boronized samples, the friction coefficient varies between 0.46 and 0.52, while the highest friction coefficient was obtained in 1273 K-10h boronized samples. Cimenoglu et al. [246] applied the boronizing process to the 4140 steel at 750, 800, 850 and 900 °C for 12 h. The hardness of the boronized surfaces was measured as ~ 1500 HV (single-phase) at 750 and 800 °C and ~ 1850 HV (dual phase) at 850 and 900 °C. Wear tests were performed at room temperature, 300 °C and 500 °C. It was stated that the friction coefficients of the samples with double-phase layered (850-900 ° C) were lower than the single-phase samples (750-800 ° C) for all three conditions. In addition, it is stated that samples boronized at 850-900 °C provide better wear resistance than boronized samples at 750-800 °C. In literature, it is seen that there is inconsistency between the boronizing parameters and frictions coefficients. In this study, friction coefficients were evaluated according to liquid and dry environment conditions since there was no significant relationship between boronizing parameters and friction coefficients.

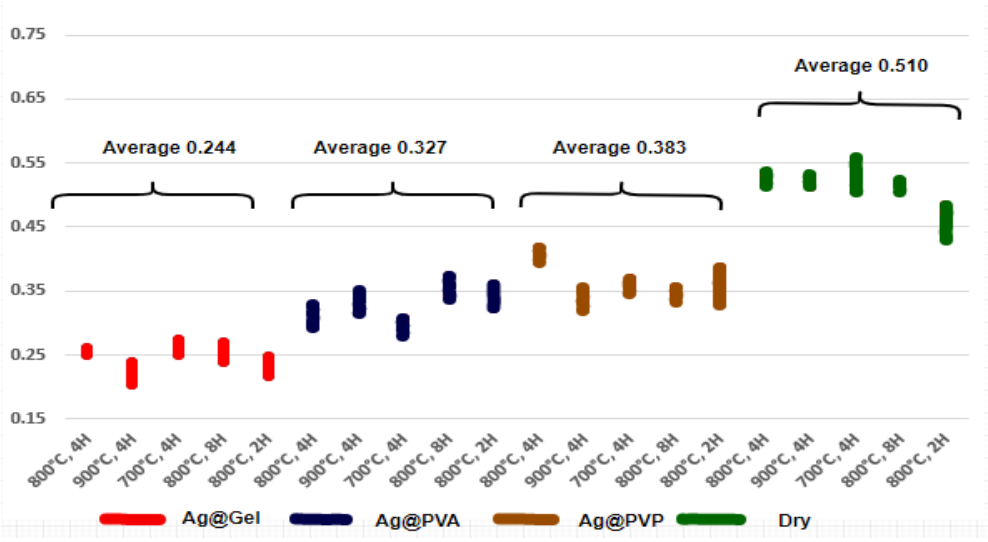

Figure 4.26. Friction coefficients of treated samples.

The average friction coefficient values were evaluated according to lubricated and dry conditions and the friction coefficient values for the AgNP@Gel, AgNP@PVA and AgNP@PVP were 0.244, 0.327 and 0.383, respectively, while the average

coefficient of friction for the dry medium tests was 0.510 (Fig. 4.26). This proves that the nano-silver-doped lubricants reduced the coefficient of friction. It was expected that the amount of heat transferred from the wear zone would increase with the use of nano-silver particles in the experiments carried out under lubricated conditions, and thus, that the friction coefficient would decrease [272]. Erdogan [259] stated that the coefficient of friction would increase as the wear environment temperature increased. In addition, Motallebzadeh and Cimenoglu [246,248] examined the tribological behaviour of boronized surfaces at high temperatures and stated that the coefficient of friction increased and deeper wear marks occurred with increasing wear temperature. The fact that low friction coefficients were obtained under the experimental conditions using AgNPs confirmed that the nano-silver particles had produced significant results in terms of decreasing the wear environment temperature by increasing the heat transfer. At the same time, the particles helped to reduce the coefficient of friction by acting as a solid lubricant by forming a film layer on the sample [252,273].

The friction coefficient of 3 different liquids used in the study can correlate with the particle sizes. Wu et al. [273] determined that smaller nanoparticles were more likely to interact with the contact regions to form an anti-wear surface film and to reduce friction. In terms of particle size, those of the AgNP@Gel were smaller than those of the AgNP@PVA, and the AgNP@PVA particles were smaller than those of the AgNP@PVP. As a result, it was determined that wear was significantly reduced in the experiments carried out under the lubricated conditions compared to those under the dry environment and that more efficient results could be obtained in studies by using an AgNP@Gel nanoparticle-doped lubricant.

According to the experimental results, the agglomeration behaviour of the nanoparticles was effective on the wear coefficient. By deforming the ligand layer, the nanoparticles which exhibited agglomeration and precipitation behaviour showed lower performance in the wear environment. It is seen in the post-wear UV graphs shown in Figure 4.26 that the PVA-coated nano-silver particles exhibited a higher rate of agglomeration and precipitation behaviour than the gelatin-coated nano-silver particles, whereas those coated with PVP exhibited a higher rate of precipitation and

agglomeration behaviour than the PVA. There is a significant relationship between the results obtained in terms of friction coefficients and agglomeration behaviour.

The Figures 4.27,28,29,30, show the weight loss of boronized samples tested for wear with AgNP@Gel, AgNP@PVA, AgNP@PVP and under dry conditions. The average weight losses depending on different wear environments were taken into account since no significant relationship was found between weight change values depending on boronizing parameters. The average weight loss in the dry wear environment was 0.01636 g, in the AgNP@ Gel medium 0.00191 g, in the AgNP@PVA medium 0.00395 g and the AgNP@PVP medium 0.01068 g. When the weight losses were evaluated according to lubricated and dry environmental conditions, the lowest wear was observed in the AgNP@Gel nanoparticle-doped lubricant environment and the highest under the dry environmental conditions. The weight loss parameter and the coefficient of friction yielded similar results. Verification of both parameters is important for the reliability of the test results. Ghaednia et al. [253] determined that the concentration ratio of nano-silver varies in direct proportion with the friction and wear parameters. The results obtained were consistent with the literature. The agglomeration and precipitation behaviour with the colloidal suspension lubricant prepared with AgNP@Gel was minimal compared to the other wear conditions, indicating that the nano-silver particles could retain their functionality during the wear process and thereby minimise friction-related weight loss.

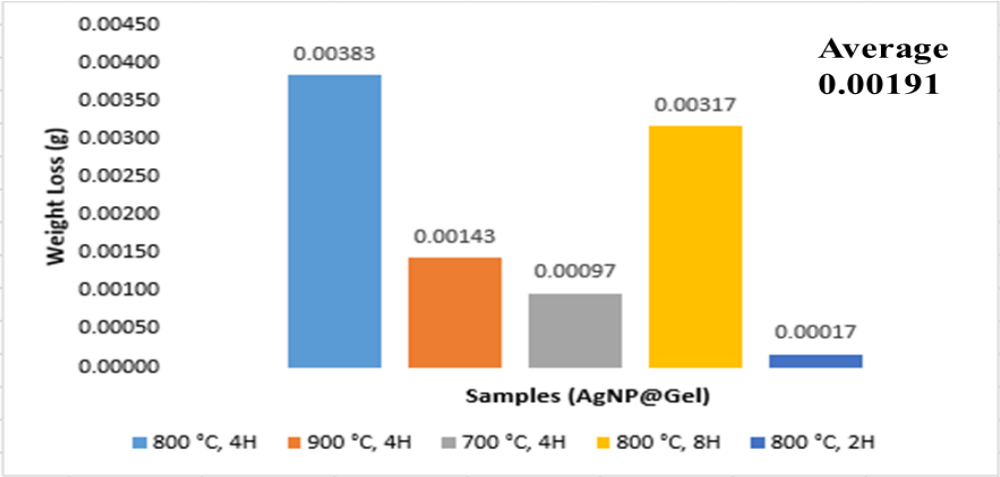

Figure 4.27. Weight loss measurements: Ag@Gel.

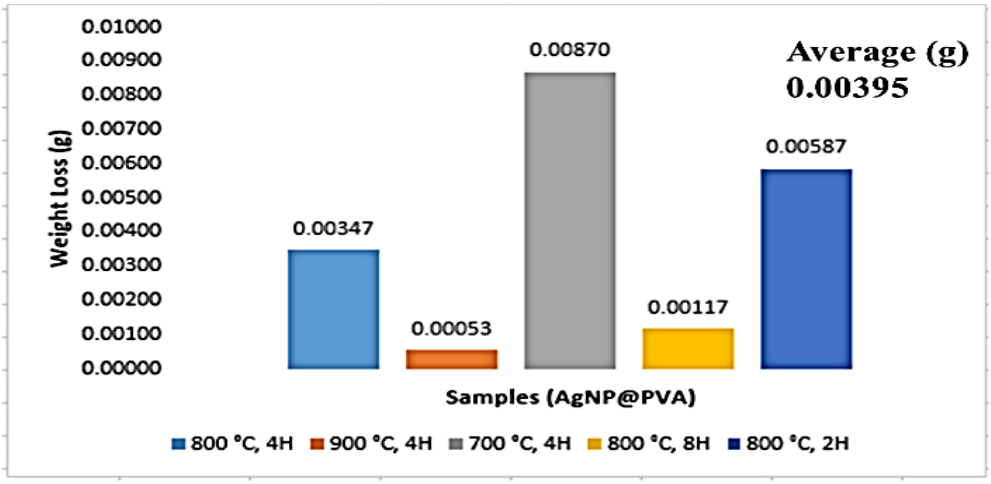

Figure 4.28. Weight loss measurements: Ag@PVA.

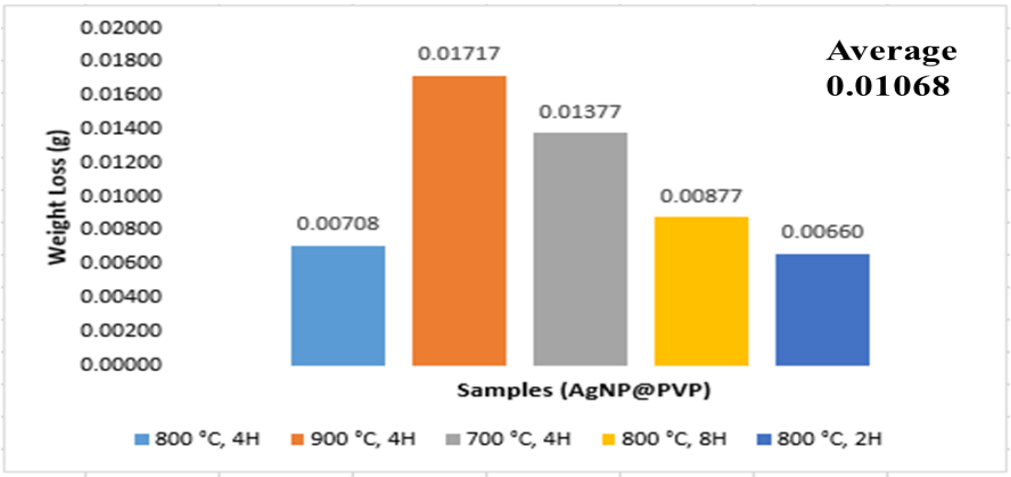

Figure 4.29. Weight loss measurements: Ag@PVP.

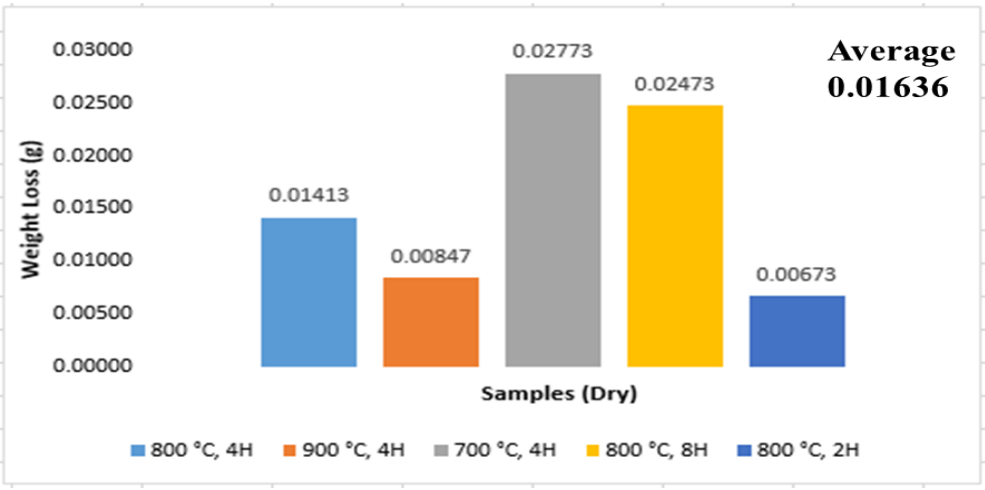

Figure 4.30. Weight loss measurements: Dry.

Roughness and form defects occur on surfaces subjected to wear. The surface quality causes characteristic properties such as friction, wear, lubrication, fatigue resistance to change. It is important to use a lubricated environment to improve the surface quality of parts subject to wear. The temperature associated with wear causes the surface form to deteriorate. Fluctuations and roughness occur when the heat is not distributed homogeneously on the surface of the material. When used as a lubricating oil additive, nanoparticles form a film layer on the surface and increase the amount of heat transfer [252,273]. Thus, it is expected that the deformation in surface form would be minimized. Images of the surface topography of the worn samples were measured by a 3D optical profilometer and are shown in Figures 4.31-50, when the topographical images were examined; the number of waves of the samples worn in the nanoparticle-reinforced lubricant medium was seen to decrease. The surface roughness (R_a) values obtained from the profilometer images given in Figure 4.51 show that the AgNP@Gel colloidal suspension yielded the best R_a value under all conditions, while the worst R_a value was seen under dry wear conditions. The surface topography of the samples worn under dry sliding conditions is shown in Figures 4.34,38,42,46,50. The very high fluctuations under the dry sliding conditions can be explained by the fact that the heat generated in the wear zone was not homogeneously distributed on the surface. According to Figure 4.51, under all conditions the Ag@PVA and Ag@PVP colloidal suspensions performed better than the dry wear condition but worse than the AgNP@Gel. The images obtained for the Ag@Gel-reinforced lubricant wear environment in Figures 4.31,35,39,43,47 exhibit better surface quality than those of the Ag@PVA and Ag@PVP media. At the same time, when the roughness values are examined according to boronizing parameters, the best surface roughness was found with the samples boronized at 700 °C for 4 h (Fig. 4.39-42). It is stated in the literature that the surface roughness of boronized samples increases with increasing boronizing temperature and time [249]. The results obtained in this study are consistent with the literature. In addition, the different performances of the nanoparticles coated with different ligands in the wear environment showed that the coating technique had a significant effect on the wear performance.

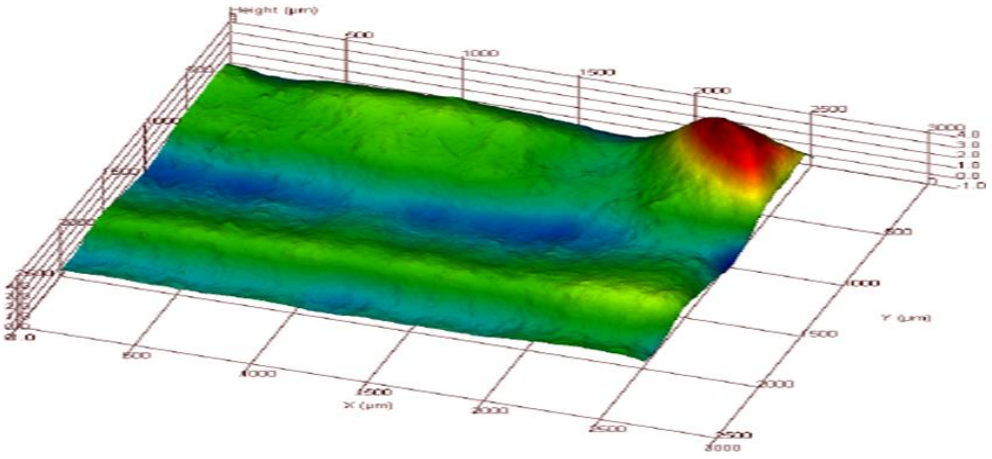

Figure 4.31. Topographical images of worn surfaces: 800 °C, 4 h - Ag@Gel.

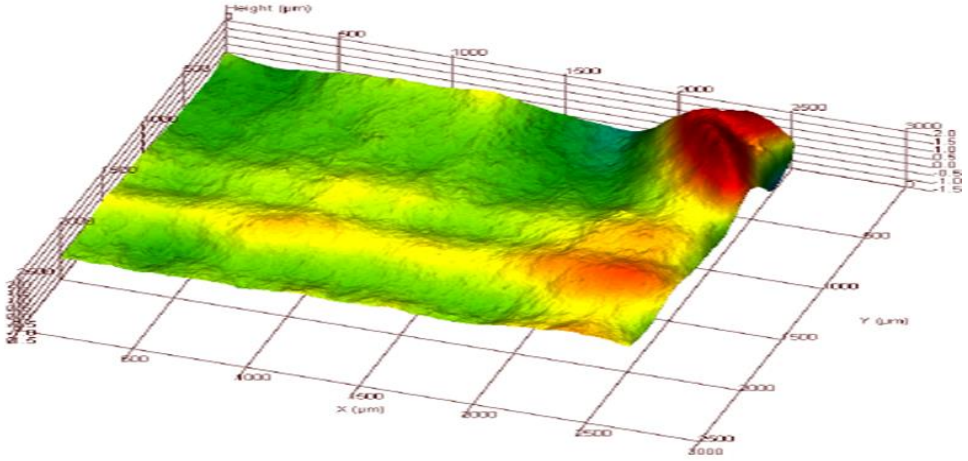

Figure 4.32. Topographical images of worn surfaces: 800 °C, 4 h - Ag@PVA.

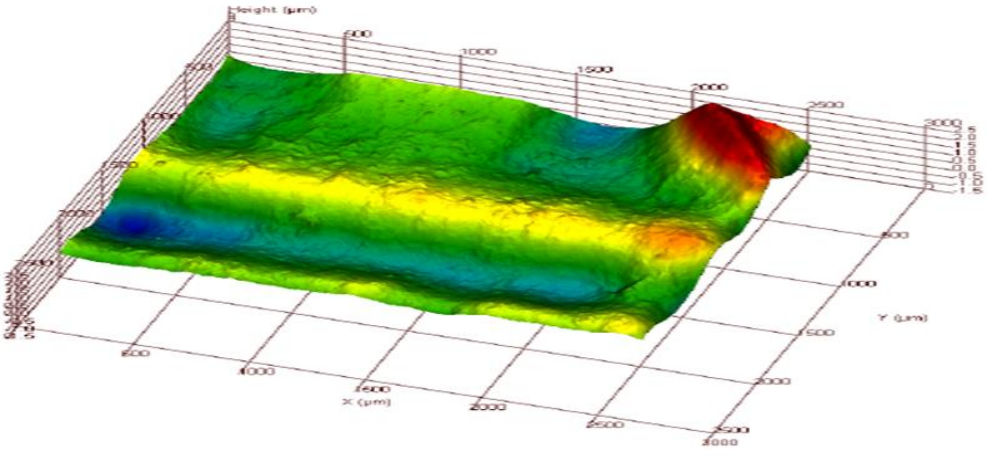

Figure 4.33. Topographical images of worn surfaces: 800 °C, 4 h - Ag@PVP.

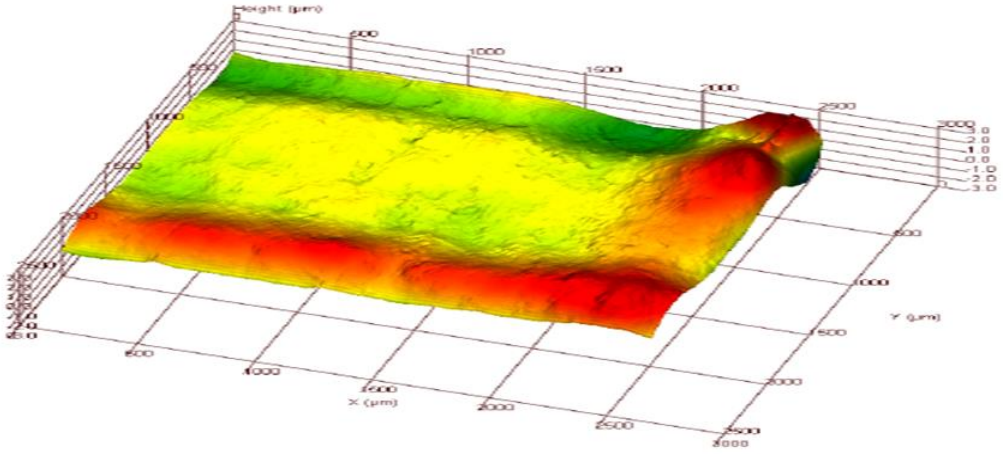

Figure 4.34. Topographical images of worn surfaces: 800 °C, 4 h – dry.

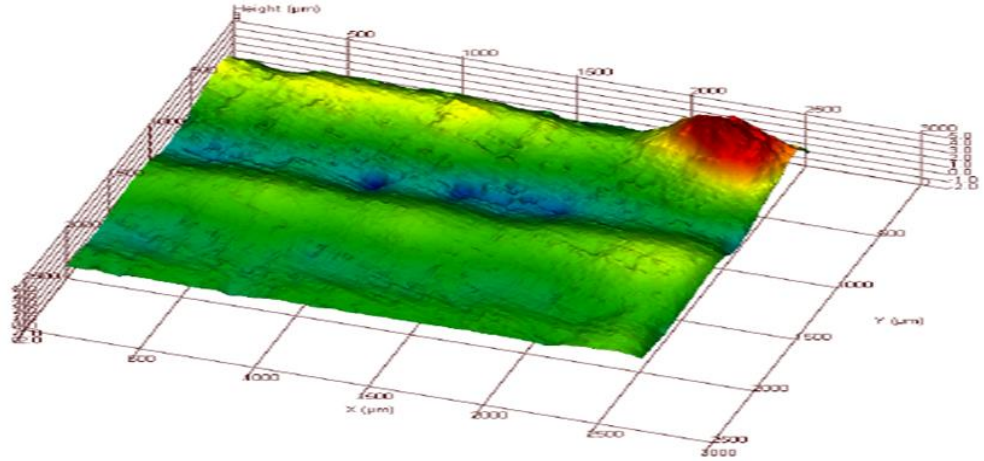

Figure 4.35. Topographical images of worn surfaces: 900 °C, 4 h - Ag@Gel.

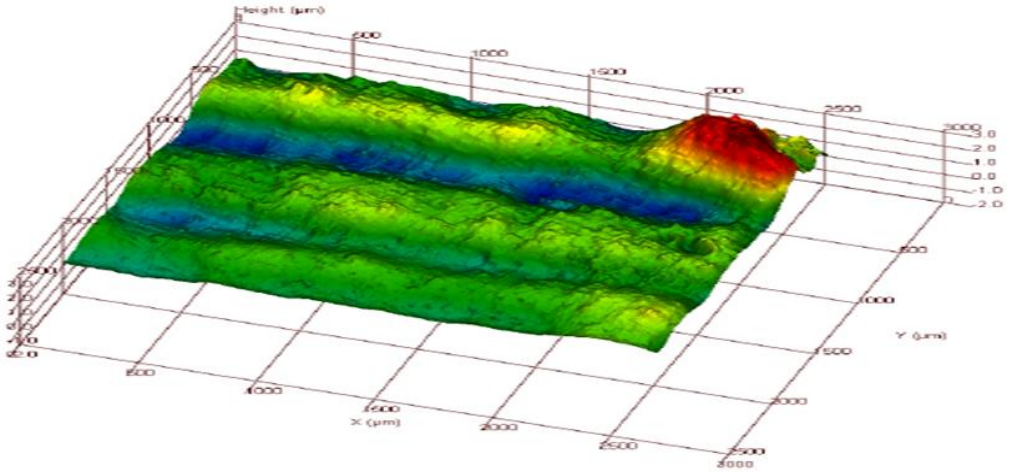

Figure 4.36. Topographical images of worn surfaces: 900 °C, 4 h - Ag@PVA.

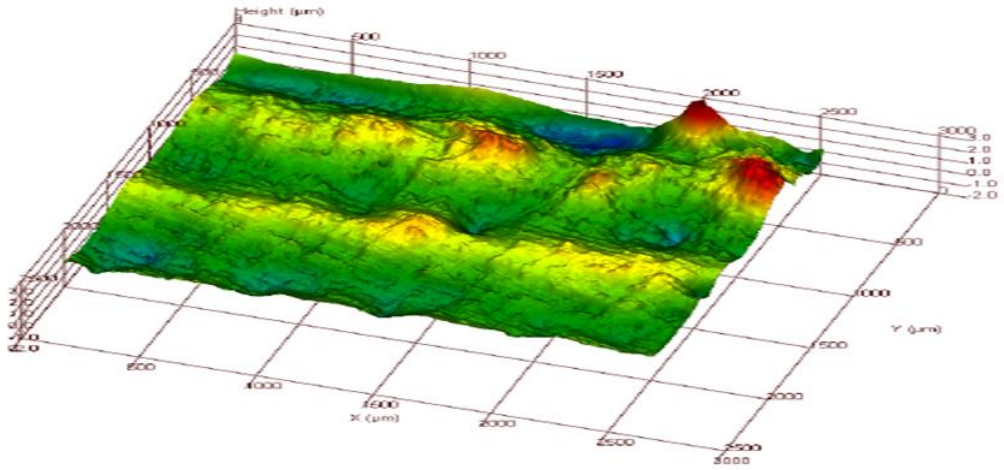

Figure 4.37. Topographical images of worn surfaces: 900 °C, 4 h - Ag@PVP.

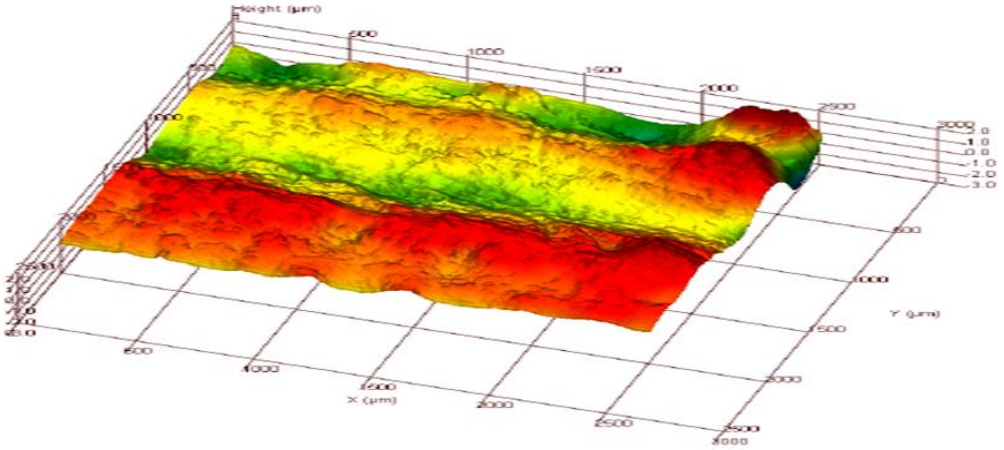

Figure 4.38. Topographical images of worn surfaces: 900 °C, 4 h – dry.

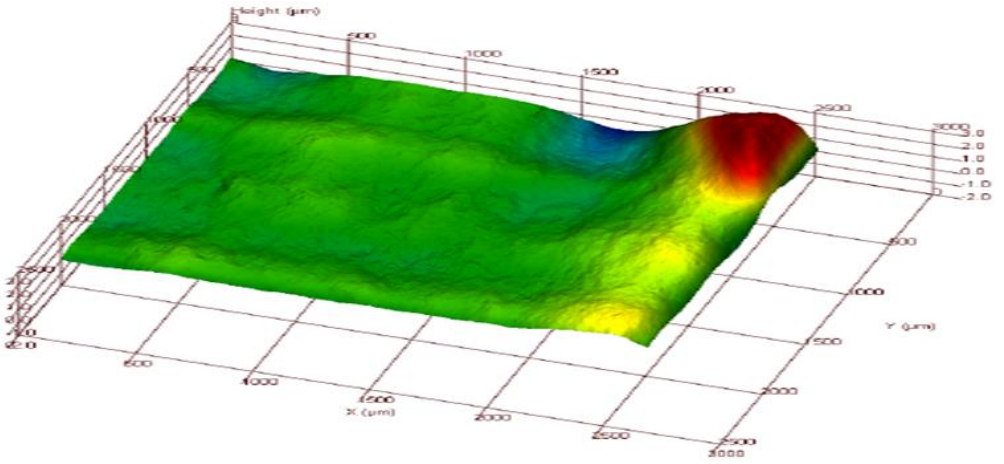

Figure 4.39. Topographical images of worn surfaces: 700 °C, 4 h - Ag@Gel.

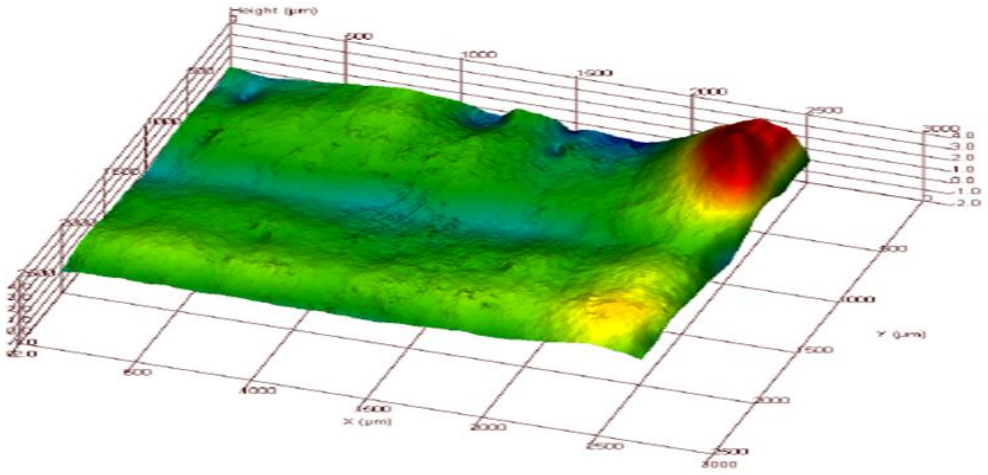

Figure 4.40. Topographical images of worn surfaces: 700 °C, 4 h - Ag@PVA.

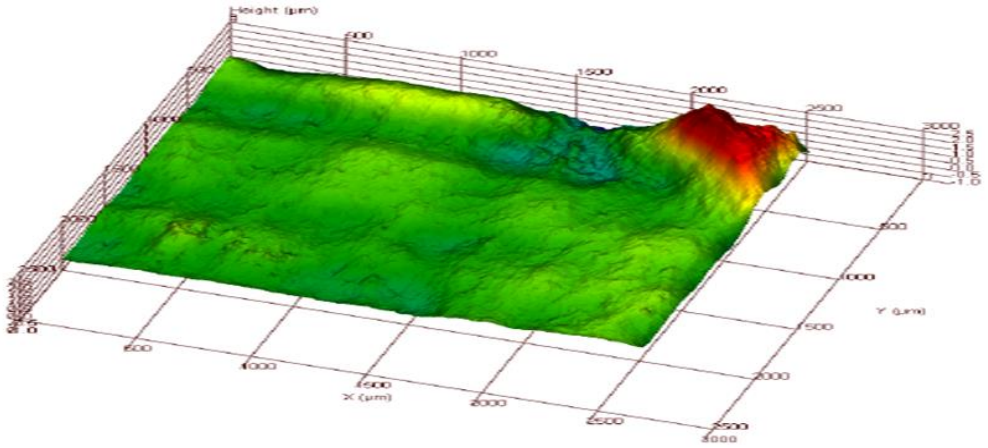

Figure 4.41. Topographical images of worn surfaces: 700 °C, 4 h - Ag@PVP.

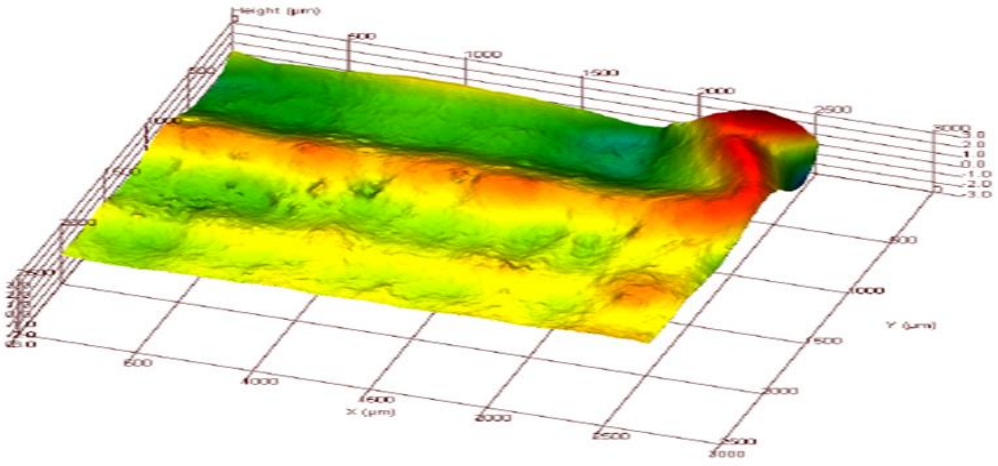

Figure 4.42. Topographical images of worn surfaces: 700 °C, 4 h – dry.

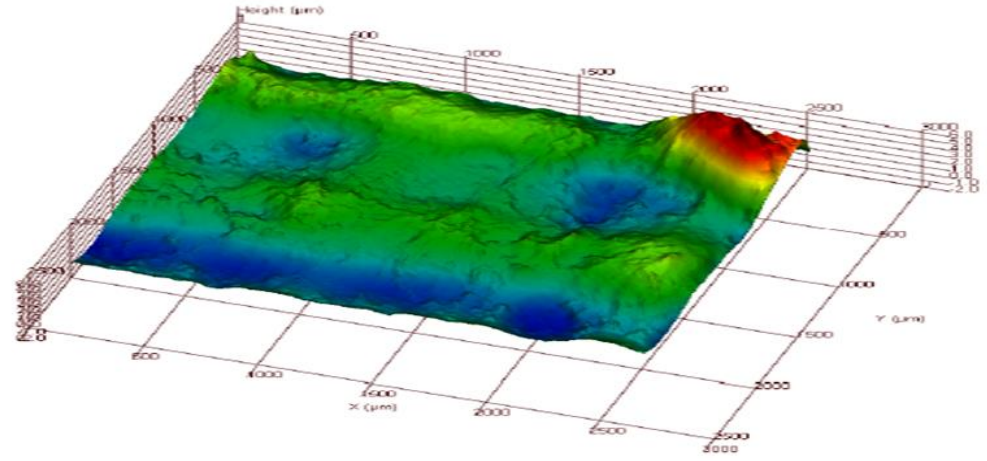

Figure 4.43. Topographical images of worn surfaces: 800 °C, 8 h - Ag@Gel.

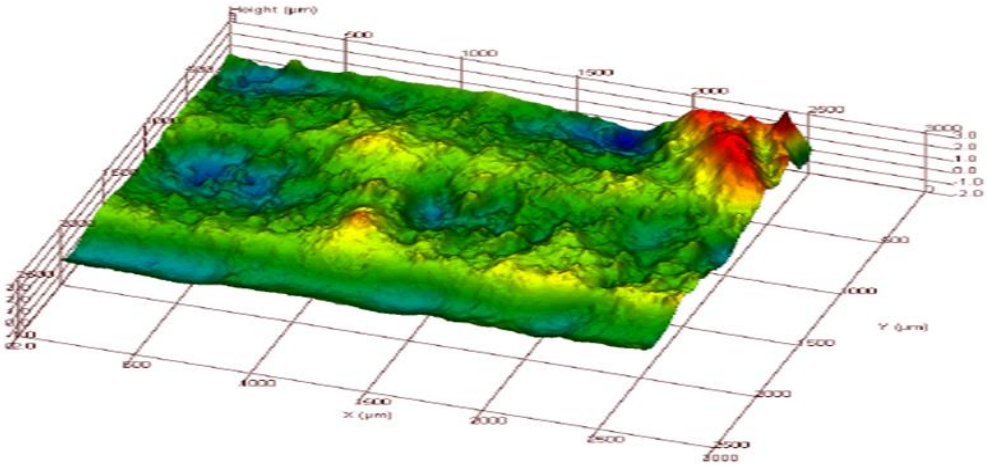

Figure 4.44. Topographical images of worn surfaces: 800 °C, 8h - Ag@PVA.

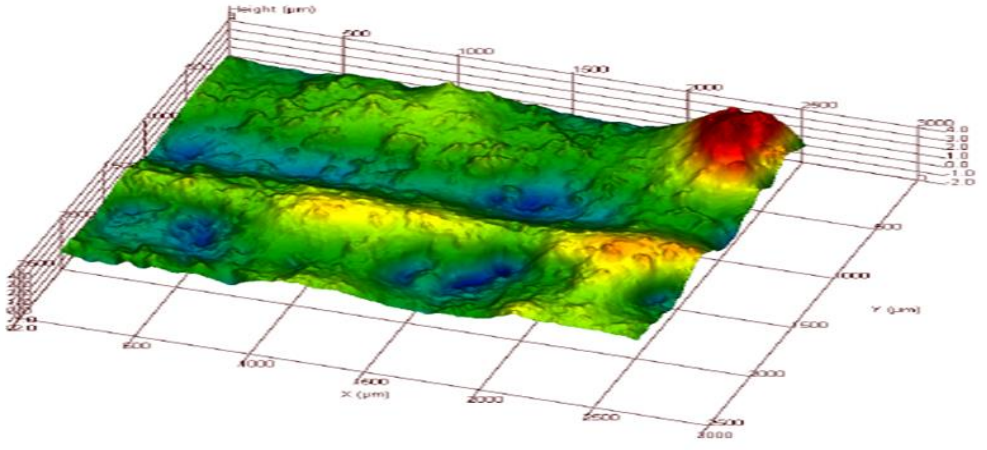

Figure 4.45. Topographical images of worn surfaces: 800 °C, 8 h - Ag@PVP.

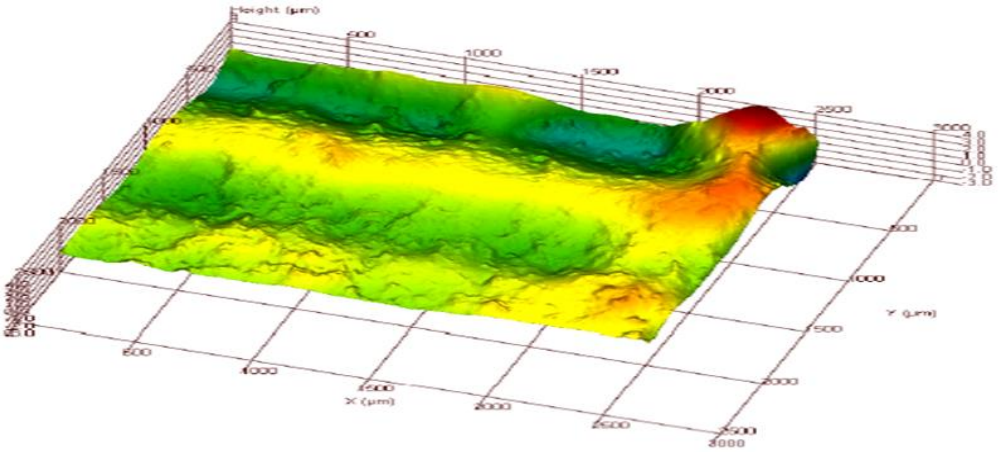

Figure 4.46. Topographical images of worn surfaces: 800 °C, 8 h – dry.

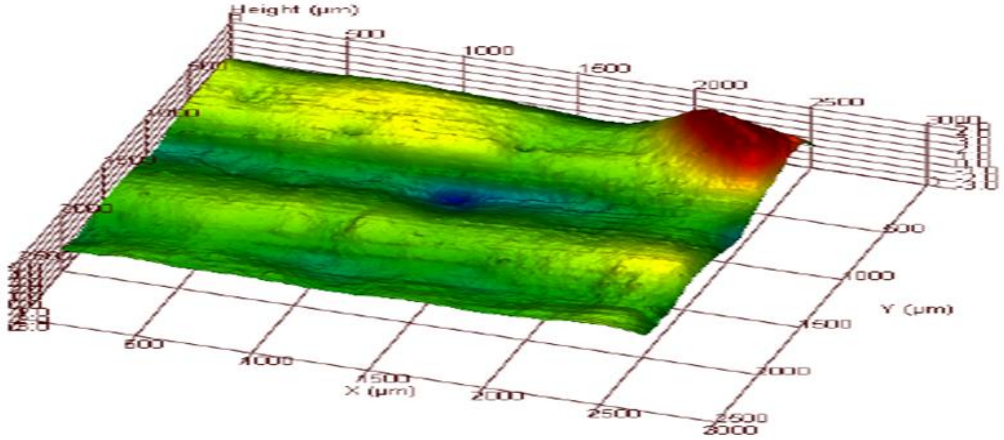

Figure 4.47. Topographical images of worn surfaces: 800 °C, 2 h - Ag@Gel.

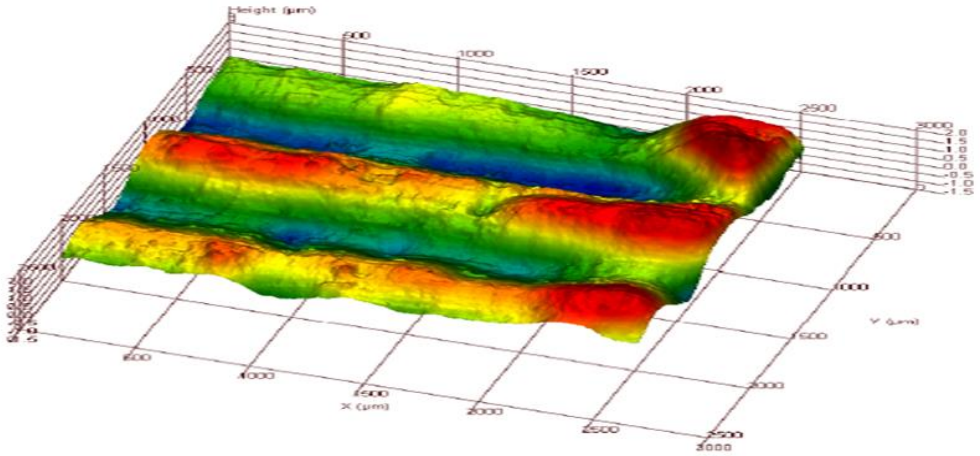

Figure 4.48. Topographical images of worn surfaces**:** 800 °C, 2 h - Ag@PVA.

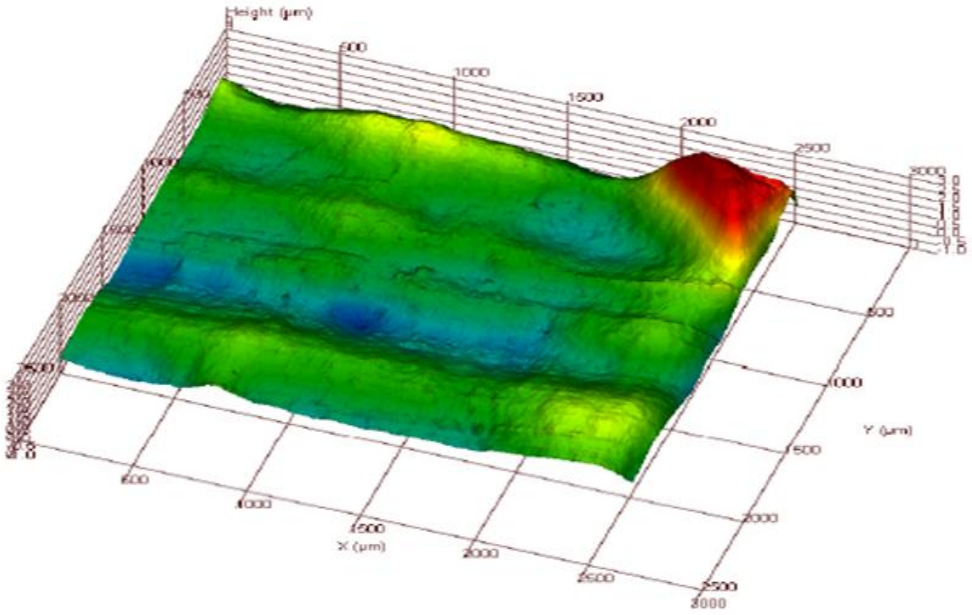

Figure 4.49. Topographical images of worn surfaces: 800 °C, 2 h - Ag@PVP.

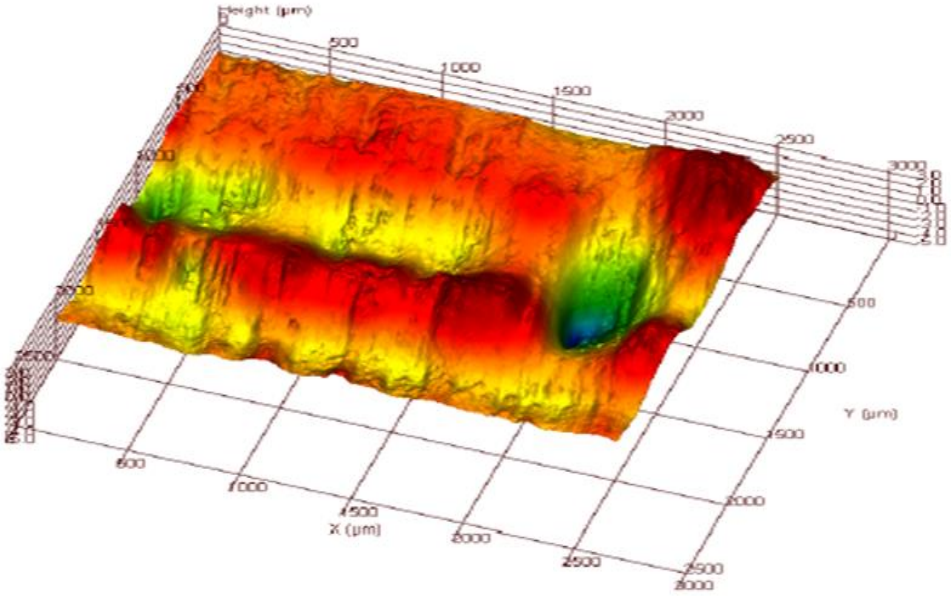

Figure 4.50. Topographical images of worn surfaces: 800 °C, 2 h – dry.

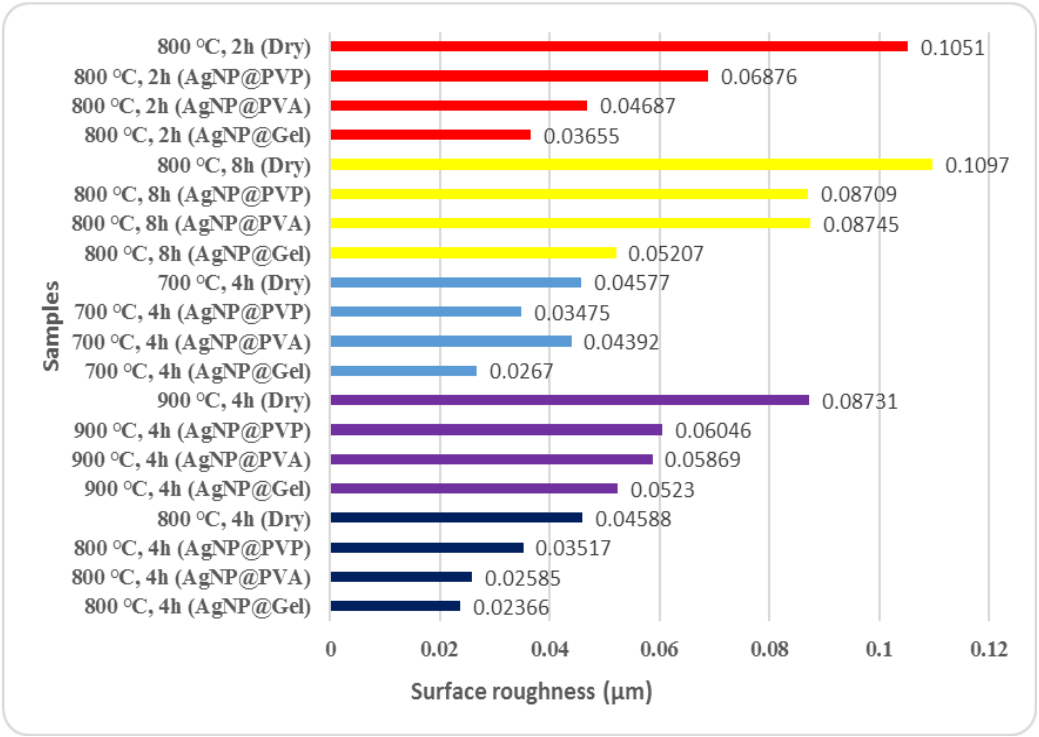

Figure 4.51. R_a (µm) Results for dry and nano-silver-doped lubricant conditions.

The SEM (500×) images of the worn surfaces were obtained for surface quality research. When the wear images were examined, no apparent adhesions or microcrack formations were found in any of the surface images for all wear conditions. At 700 °C for 4 h and 800 °C for 2 - 4 h, the direction of the wear marks was evident, but there were no signs of wear at 800 ° C for 8 h or at 900 °C for 4 h. The 700 °C / 4 h parameter (Fig. 4.52-55) resulted in surface deformations with uneven borders formed in the wear layer. These deformations were more distinct under dry wear conditions. With the AgNP@Gel medium, there were much fewer deformation zones than with the AgNP@PVP and AgNP@PVA media. The SEM images of the samples boronized at 800 °C for 2h (Fig. 4.56-59) show superficial deformations with linear characteristics formed in the wear direction. Wear lines are numerically expressed on the SEM image. In Figures 4.56-58 three wear lines in are shown for the AgNP@Gel, four for the AgNP@PVA and five for the AgNP@PVP. Since the surface was completely formed of these deformation lines under dry condition (Fig. 4.59), it was not shown numerically. As a result, it is clearly seen that the fewest deformations were in the gelatin environment and the most in the dry environment. There was no significant surface deformation in the samples boronized

at 800 °C for 4 h (Fig. 4.60-63). The only differences existed in the depth and clarity of the wear lines. Although the wear lines were superficial with the AgNP@Gel, the line depth and number for this parameter increased moving towards the dry wear conditions. The dry wear image (Fig. 4.63) shows that ploughing wear occurred on the surface. On the SEM images of samples boronized for 8 h at 800 °C and 4 h at 900 °C (Fig. 4.64-67 and 4.68-71), no surface deformation or wear lines are present, and there is no significant difference between the different lubricated conditions. In general, we can say that abrasion wear occurred on the surfaces. Dry wear conditions at 800 °C for 8 h and at 900 °C for 4 h produced a surface form similar to that of the lubricated conditions. As a result, it was seen that the wear resistance of the materials increased significantly as the boronizing temperature and time increased.

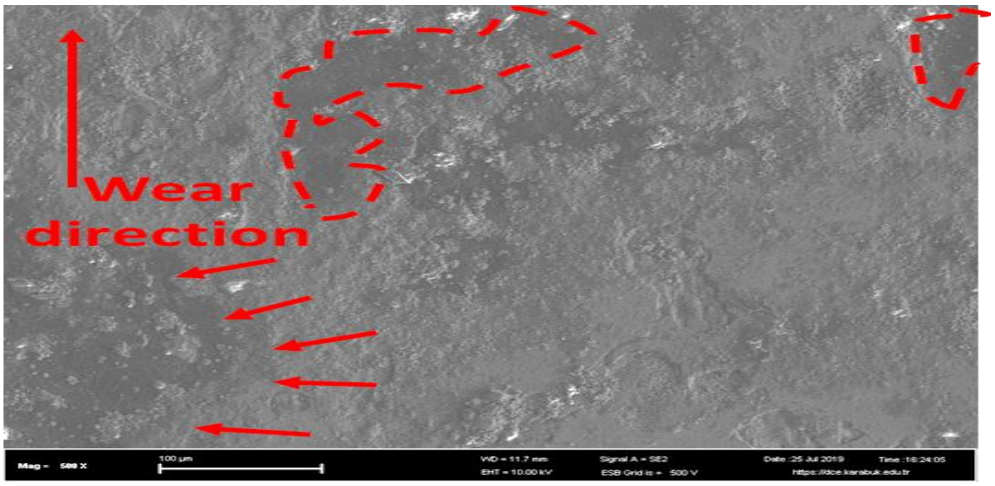

Figure 4.52. SEM images of wear marks: 700 °C, 4h - Ag@Gel.

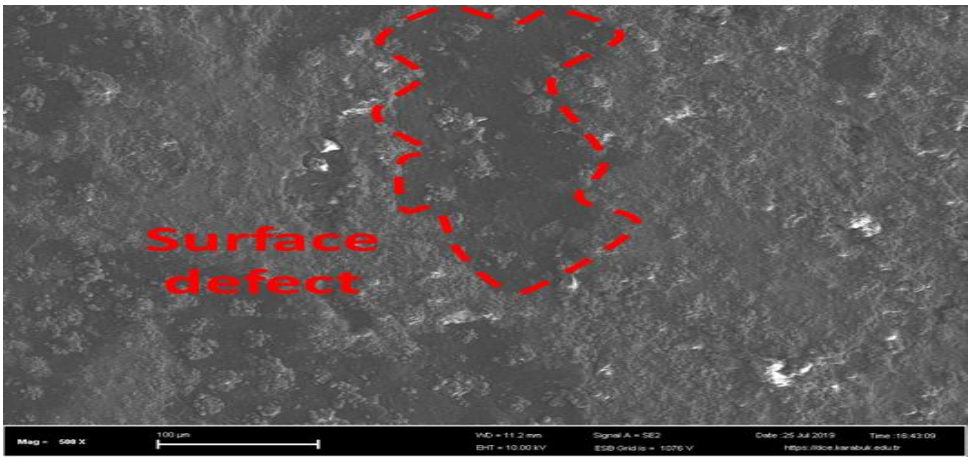

Figure 4.53. SEM images of wear marks: 700 °C, 4h - Ag@PVA.

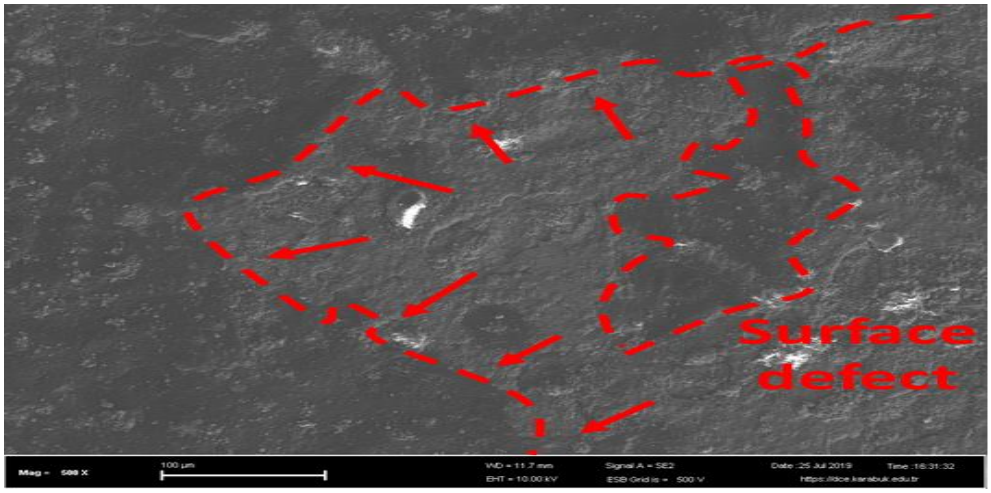

Figure 4.54. SEM images of wear marks: 700 °C, 4h - Ag@PVP.

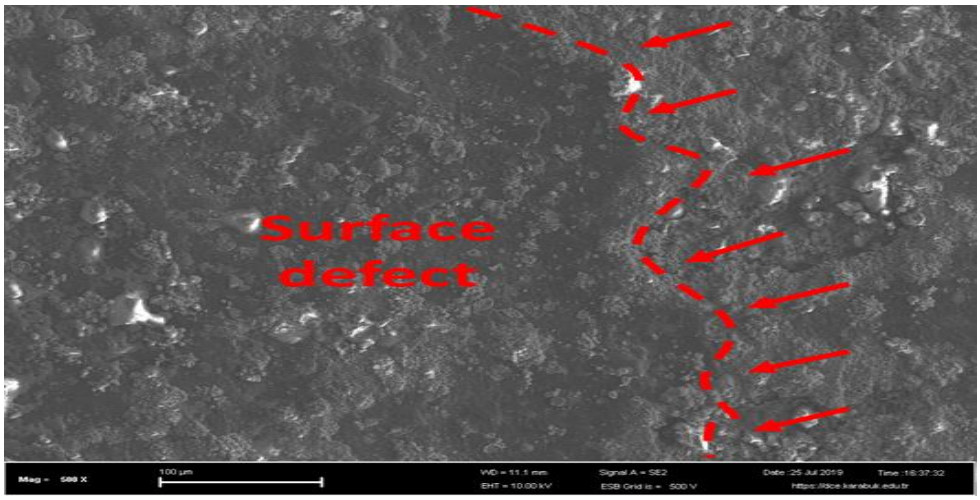

Figure 4.55. SEM images of wear marks: 700 °C, 4h – dry.

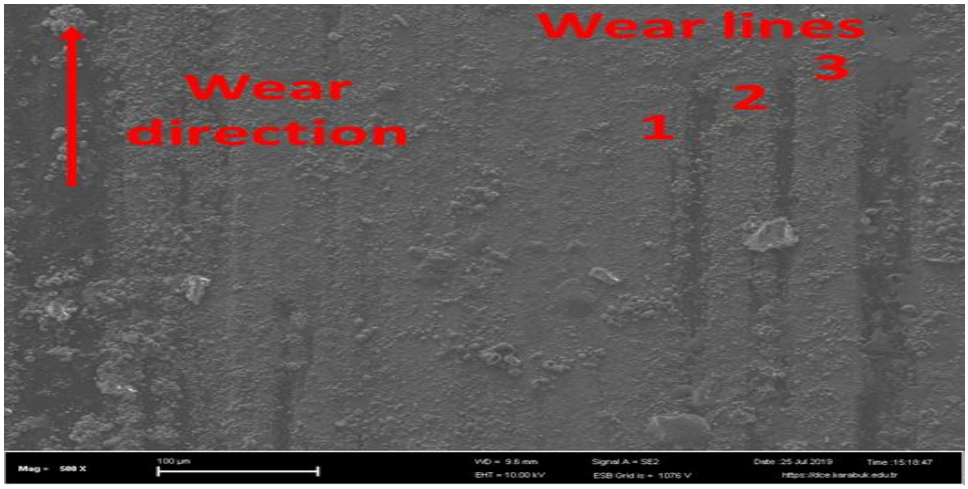

Figure 4.56. SEM images of wear marks: 800 °C, 2h - Ag@Gel.

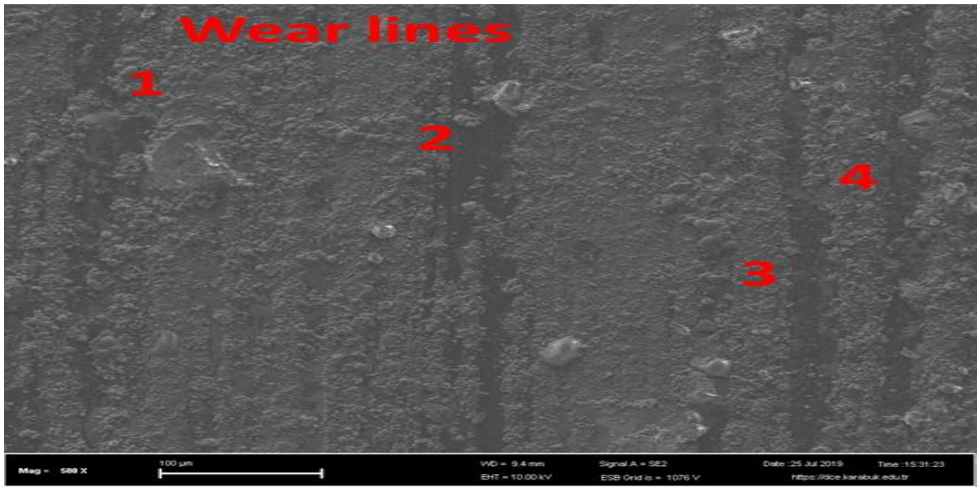

Figure 4.57. SEM images of wear marks: 800 °C, 2h - Ag@PVA.

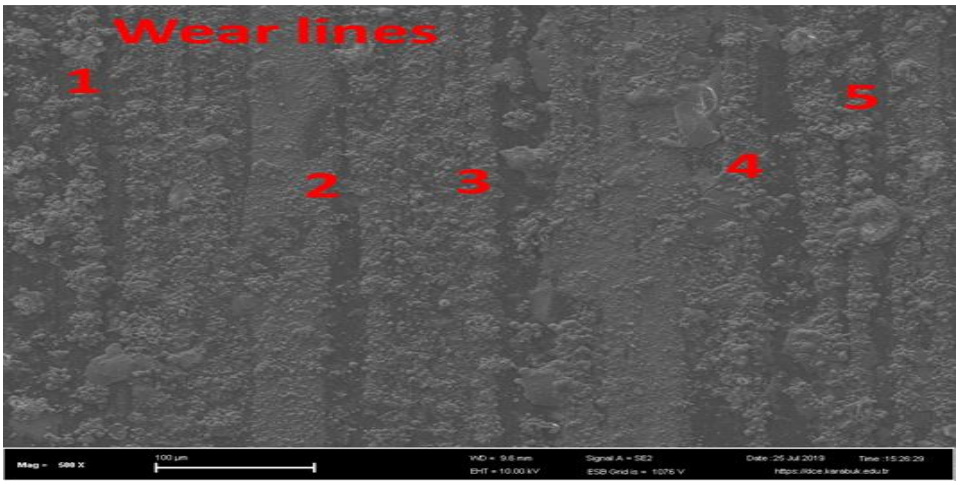

Figure 4.58. SEM images of wear marks: 800 °C, 2h - Ag@PVP.

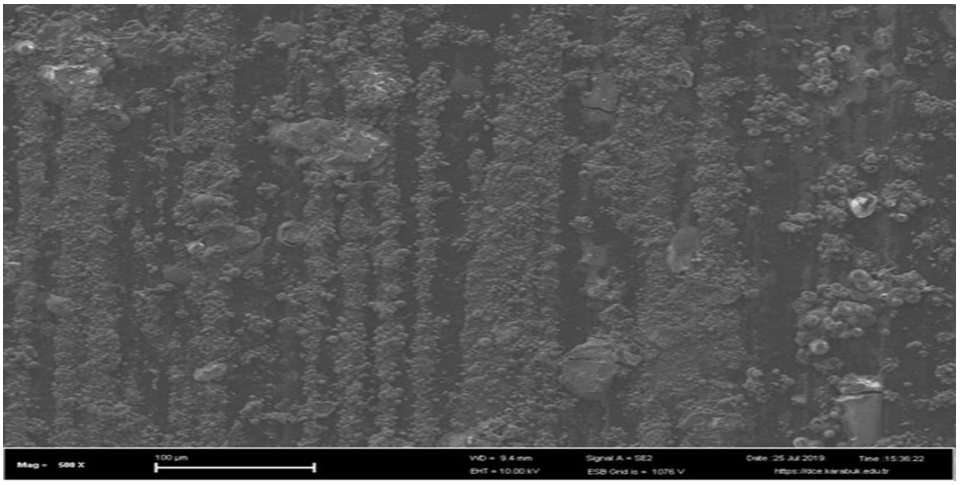

Figure 4.59. SEM images of wear marks: 800 °C, 2h – dry.

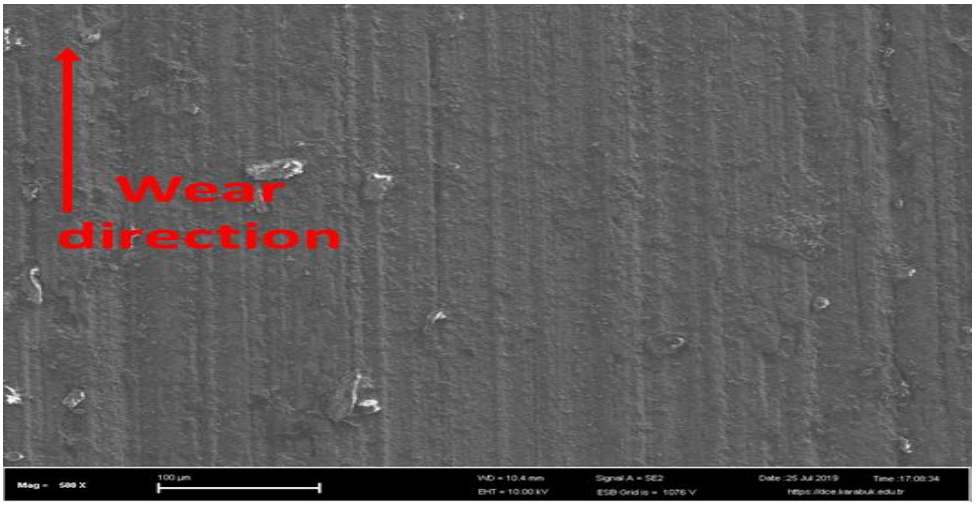

Figure 4.60. SEM images of wear marks: 800 °C, 4h - Ag@Gel.

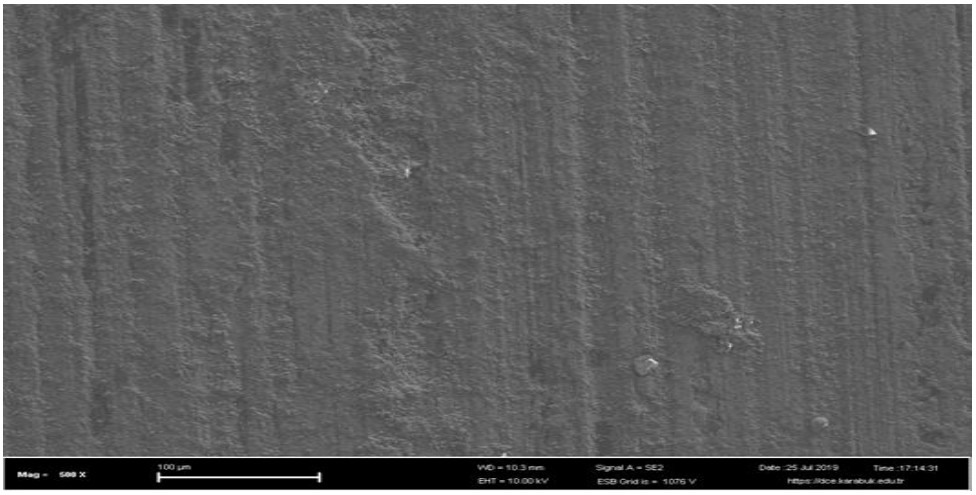

Figure 4.61. SEM images of wear marks: 800 °C, 4h - Ag@PVA.

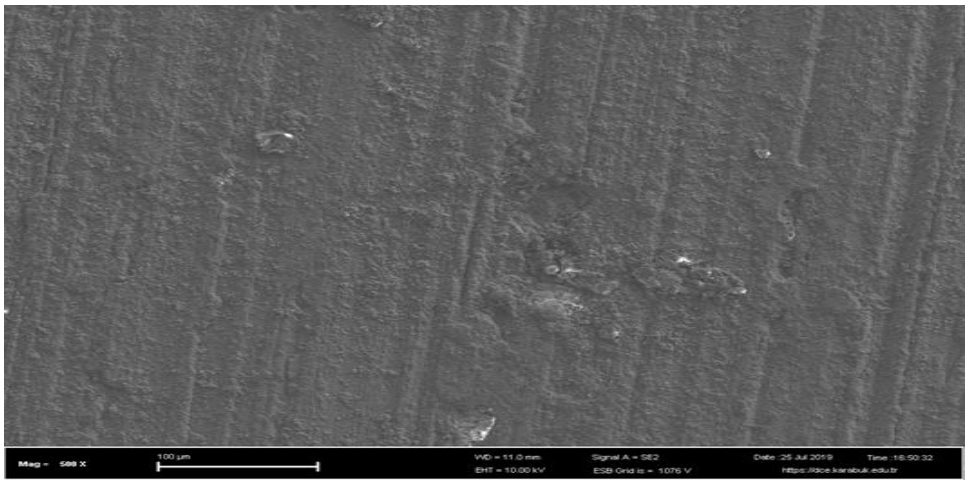

Figure 4.62. SEM images of wear marks: 800 °C, 4h Ag@PVP.

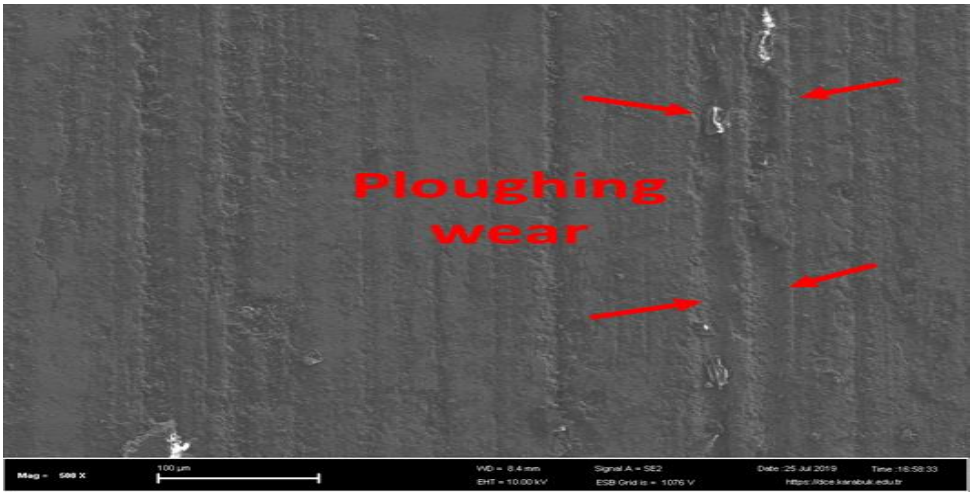

Figure 4.63. SEM images of wear marks: 800 °C, 4h – dry.

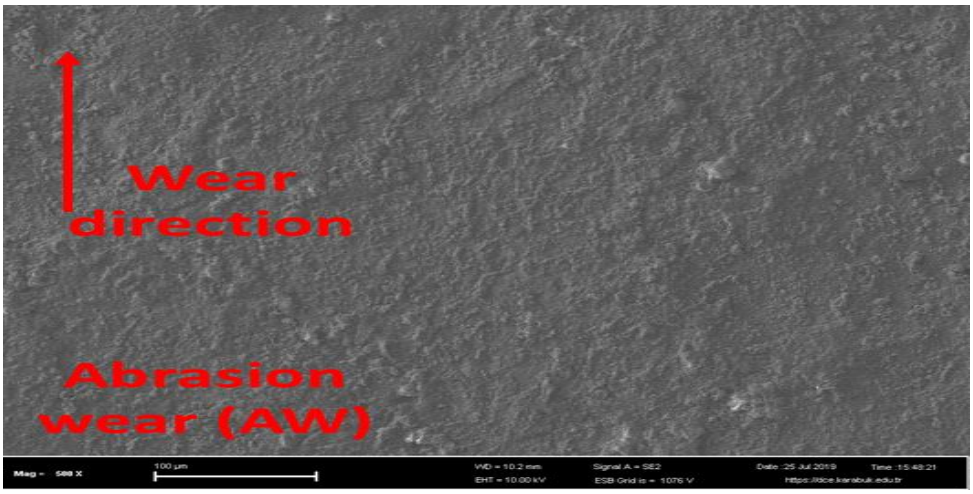

Figure 4.64. SEM images of wear marks: 800 °C, 8h - Ag@Gel.

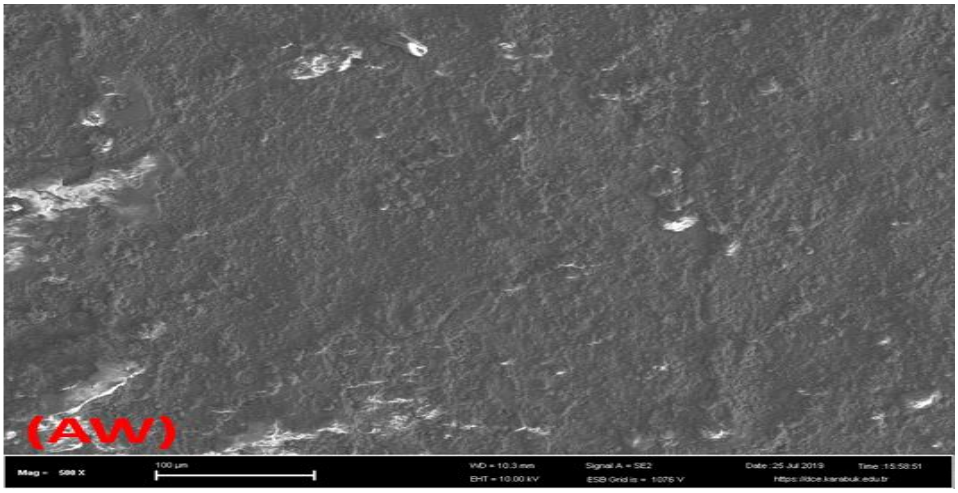

Figure 4.65. SEM images of wear marks: 800 °C, 8h - Ag@PVA.

Figure 4.66. SEM images of wear marks: 800 °C, 8h - Ag@PVP.

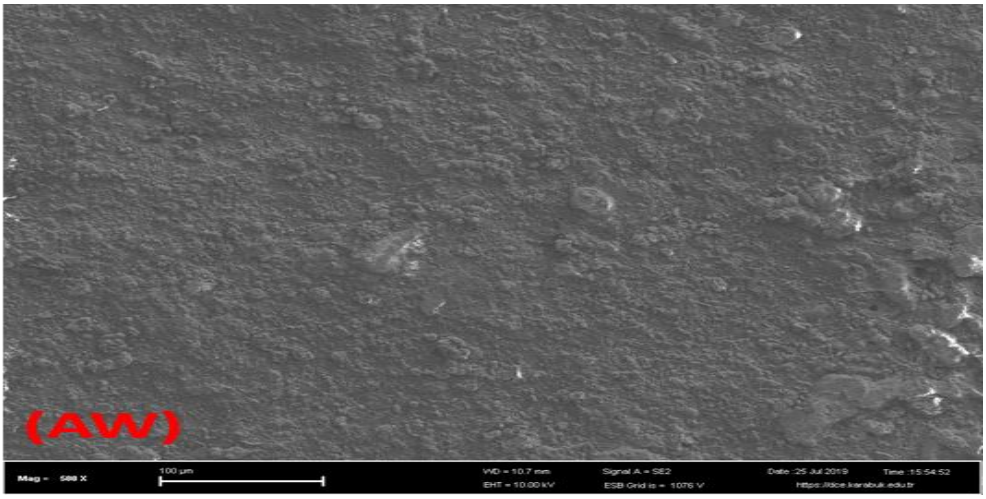

Figure 4.67. SEM images of wear marks: 800 °C, 8h – dry.

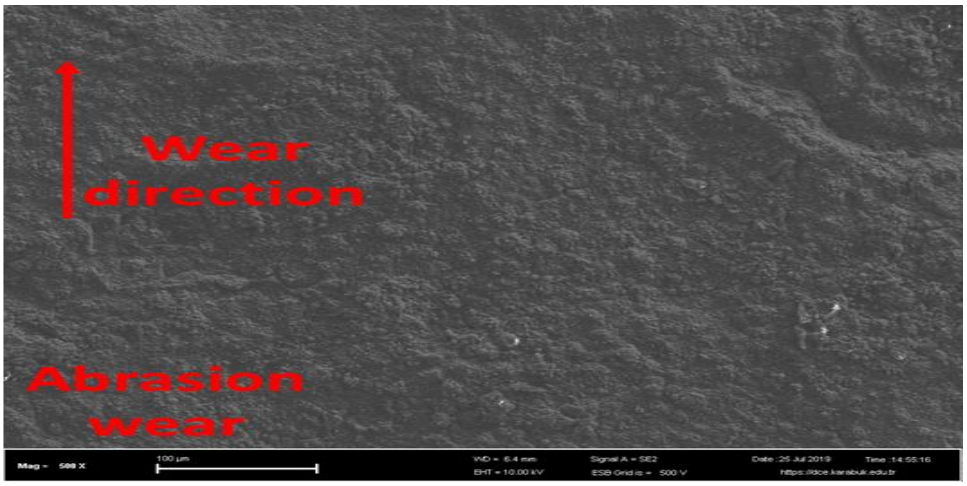

Figure 4.68. SEM images of wear marks: 900 °C, 4h - Ag@Gel.

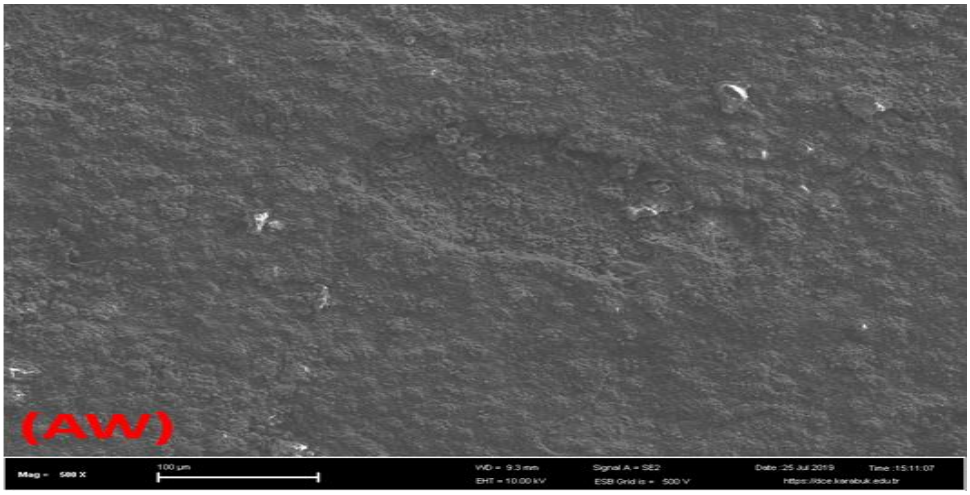

Figure 4.69. SEM images of wear marks: 900 °C, 4h - Ag@PVA.

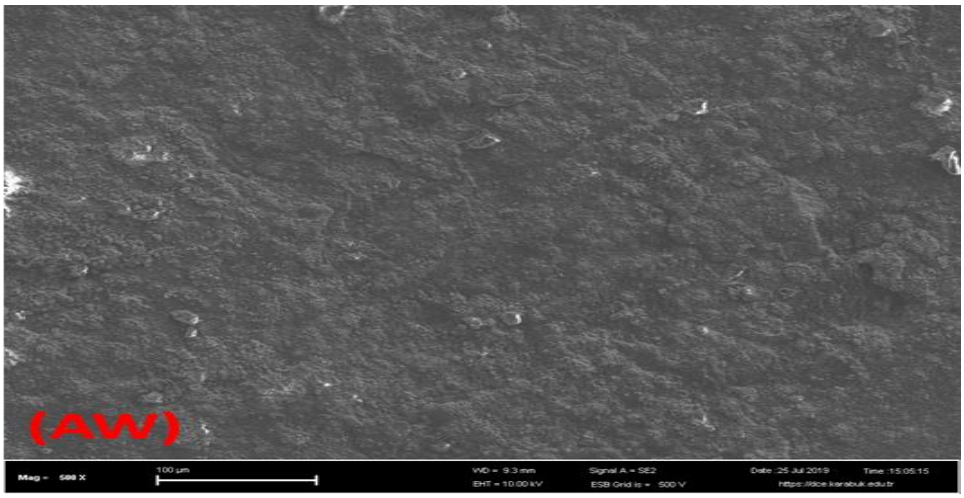

Figure 4.70. SEM images of wear marks: 900 °C, 4h - Ag@PVP.

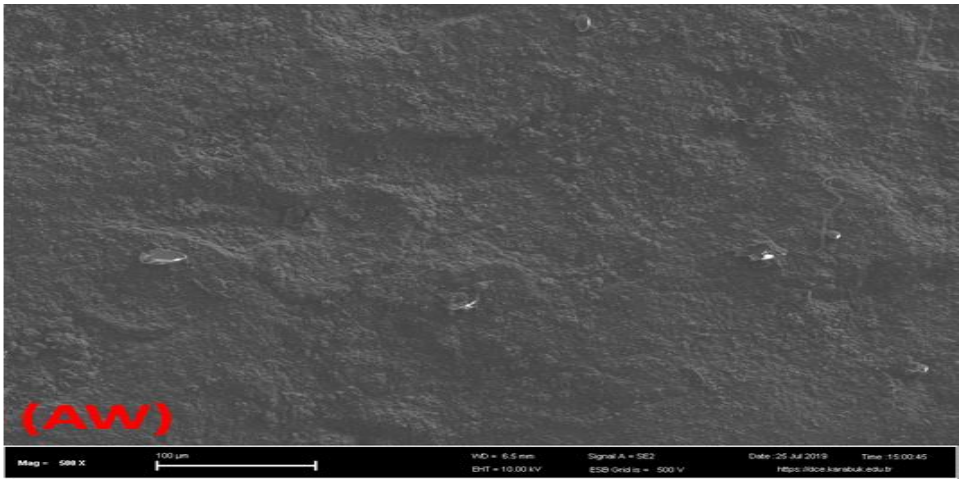

Figure 4.71. SEM images of wear marks: 900 °C, 4h – dry.

4.4. RESULTS ANALYSIS OF CORROSION RESISTANCE

4.4.1. Background Information

Corrosion is a thermochemical process in which oxidized or sulfurous compounds are formed on the surfaces of metals due to electrochemical reactions [106]. In the corrosion test, the investigated metal material is in contact with the electrolyte and acts as an electrode [107]. Two metals in contact with the electrolyte liquid generate an electrochemical circuit [109]. Electrochemical corrosion event occurs after the circuit is completed.

Corrosion and wear are mechanical problems that begin on the surfaces of the materials and progress to the interior of the materials over time. For this reason, it is primarily necessary to make the material surfaces resistant to wear and corrosion. Surface modifications such as boron coating, galvanizing, metal spraying, physical vapour deposition (PVD), chemical vapour deposition (CVD) are among the methods used for this purpose [274].

Boronizing process (700-1100 ° C), which is a thermochemical surface treatment, is considered as one of the most effective surface modification methods to improve the corrosion resistance and mechanical properties of steel surfaces and metals [275]. Thanks to boron diffusion, hard iron borides are formed on the substrate surface. FeB phases occur in the outermost region of this surface, and Fe_2B phases occur in the inner part of the surface. In addition, these bores give better tribological results than other conventional surface treatments [275]. These phases increase the strength of the steels and affect their corrosion resistance in friction and wear environments [274,111,119].

The corrosion resistance of boronized steels varies depending on whether the boride layer is a single or double phase, and the surface is in the porous and microcrack form [276]. Porous or cracked surfaces in the wear zone allow the abrasive particles to penetrate the boride layer into the base material, which can cause the layer to separate with the substrate [121].

H13 hot work tool steel [240], which is used in industrial applications at temperatures of 200 °C and above, is exposed to intense wear and corrosion due to working conditions (mould manufacturing, hot pressing, casting etc.) [277,241]. In the literature, Kariofillis et al. [274] have bored AISI H13 hot work tool steel for 6 hours at 950 ° C and examined the corrosion resistance of H13 steel. Corrosion tests were carried out in two ways, both immersion and potentiodynamic polarization test. Acid solutions of 5% by volume HCl, 5% by volume H_2S0_4 and 30% by volume H_3PO_4 were used in the immersion test. Samples were weighed before immersion, and after immersion, weight losses were recorded by weighing at certain time intervals. Potentiodynamic polarization tests were carried out in atmospheric weather conditions, in the same acid solutions, in a standard apparatus. Polarization was started with −1000 mV cathodic overvoltage, and the scan rate was determined as 10 mV/min. Typical potentiodynamic polarization curves are obtained for each corrosion environment. It was determined by the researchers that the H13 steel in the short-term immersion tests increased corrosion resistance in H2SO4 and H3PO4 solutions, and in the long immersion tests, the corrosion behaviour of H13 steel in all H2SO4, H3PO4 and HCl environments was decreased. Considering the potentiodynamic polarization curves, the corrosion potential (Ecor = −219 mV) of boronized H13 steel was found to be more electro-positive than unbonded H13 steel (Ecor = −400 mV). According to this result, they stated that the boronizing process served as a protection barrier for H13 steel. In general, when the corrosion performance of boronized samples is characterized, it is stated that the highest corrosion resistance occurs in HCl solution and the lowest corrosion resistance occurs in H2SO4 solution. Kayalı et al. [255] bored AISI D2 steel by plasma paste boronizing method and examined the wear and electrochemical corrosion behaviour of AISI D2 steel. Corrosion experiments were done with Gamry reference 600 potentiostat/galvanostat ZRA and Echem Analyst program. Before starting the experiments, the samples were cleaned and dried in an ultrasonic bath at 15 °C with 15 minutes of acetone, 15 minutes of ethanol and 15 minutes of double-distilled water. As a result of the experiments, it was observed that the polarization current density values of boron-free samples were 0.983 $\mu A/cm^2$, while the polarization current density values of boronized samples varied in the range of 0.245-0.474

$\mu A/cm^2$. The researchers stated that the corrosion resistance of boiled AISI D2 steel increases with boron coating.

The present study aims to investigate the electrochemical corrosion behaviour (in 3.5% NaCl solution) of H13 steel boronized at different temperatures and times and to compare the corrosion resistance in different layer thicknesses obtained by boronizing.

4.5. MATERIAL AND METHOD

In this study, H13 hot work tool steel, which is widely used in mould production and exposed to continuous wear, is used. Cylindrical samples of H13 steel were cut to 9 mm in diameter and 2 mm in length, and spheroidizing annealing was carried out at 850 °C for 2 hours in accordance with the literature [275,255]. Annealed samples were polished and ultrasonically cleaned before boronizing [259].

Boronizing was done at 700, 800 and 900 ° C for 2, 4 and 8 hours. In the boronizing process, 95% by volume nano-boron powder was used as a boron source, and 5% KBF4 was used as an activator. All samples were placed in a stainless-steel box together with nano-boron powder and activator for the boronizing process, and the box was hermetically sealed. Then, the firing was carried out under atmospheric conditions in the specified parameters. After firing, the container was removed from the oven and cooled to room temperature.

After the cross-section of the samples was prepared metallographically, the thickness of the boron layers obtained was measured with the help of scanning electron microscope (Carl Zeiss Ultra Plus Gemini FESEM).

Tafel Extrapolation Method, one of the electrochemical corrosion measurement methods, was used for corrosion experiments. The Tafel method was preferred in terms of determining meagre corrosion rates, obtaining corrosion current densities and speeds in a short time, and the accuracy of the data obtained is equivalent to

traditional weight loss methods [106]. The electrochemical corrosion process is shown schematically in Figure 4.72.

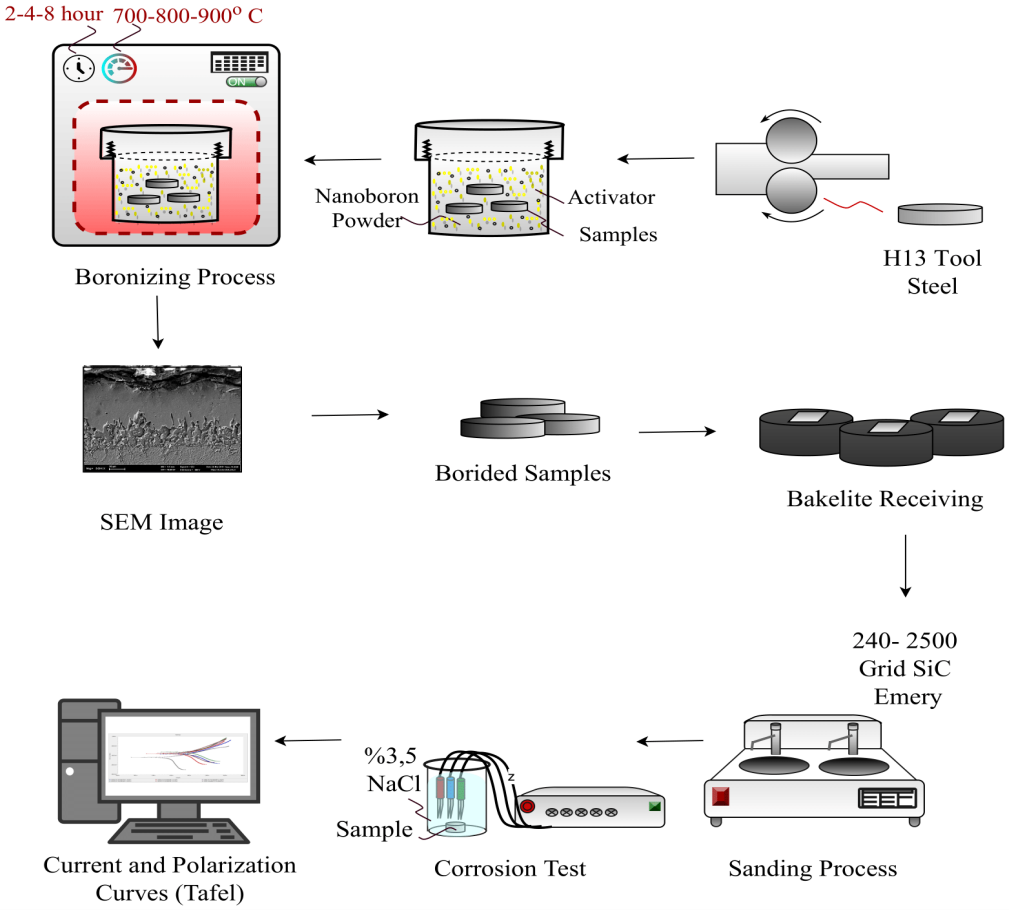

Figure 4.72. Boronizing process and corrosion test.

Corrosion experiments were carried out in 3.5% NaCl solution at room temperature. Corrosion test surface was grinded with 240-2500 grid SiC before the experiment, and it was placed in the set-up by making a connection with the electrode. Each corrosion test was applied to the surface area of ~1 cm^2. An electrochemical cell, electrode (solution treated UNS32205), reference electrode (Ag / AgCl electrode) and counter electrode (platinum plate) were used for the experimental setup. The potential was applied between -250 mV and 250 mV (5 mV/s scan rate) after 15 minutes immersion times. Tafel curves were obtained using Gamry Echem Analyst software. Ikor and Ekor values were determined from these curves, and the corrosion rate was calculated based on these data. The following equation is used for the corrosion rate calculation [122].

Corrosion rate (mpy) = $\lambda . i_{corr} . (E.W.)/d$

(1)

λ = 0.1288 (mpy.g)/(μA.cm) metric conversion factor

E.W.= Equivalent weight

d = Density (g/cm^3)

4.6. RESULTS AND DISCUSSIONS OF CORROSION TEST

In H13 steel, which is boronized at different temperatures and times, the boron layer thicknesses that occur after boronizing are examined with SEM, and the images are shown in Figures 4.73,74,75,76,77. It was observed that the thickness of the boride layer increased due to the increase in both the temperature and the duration of the experiment. The layer thicknesses of samples boronized at 700 ° C, 800 ° C, 900 ° C for 4 hours are approximately 3 µm, 9 µm and 26.5 µm, respectively. Layer thicknesses of samples boiled at 800 ° C for 2 and 8 hours were measured as 7 µm and 11.5 µm, respectively.

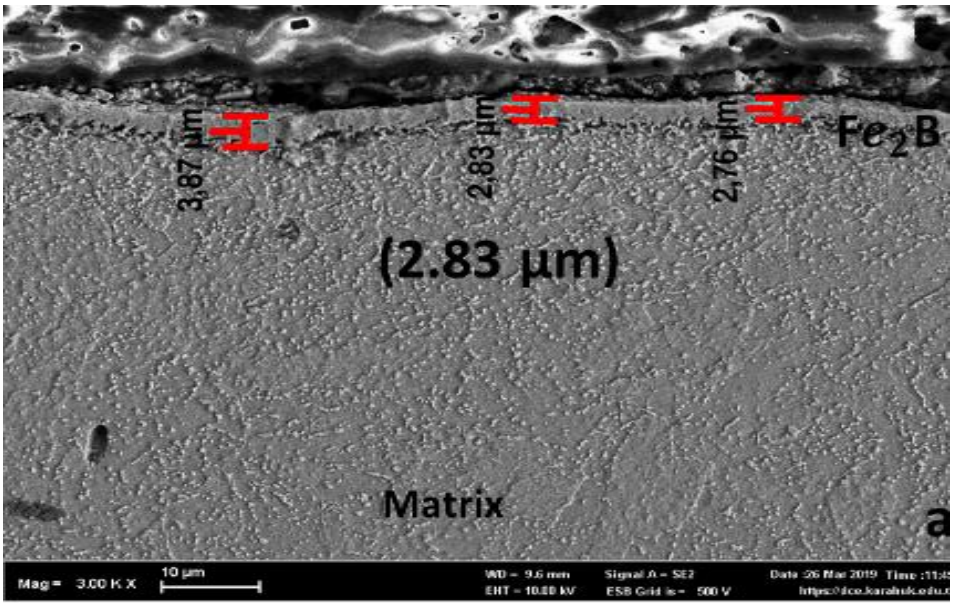

Figure 4.73. Microstructure and bored layer of bored H13 steel at 700 ° C 4h.

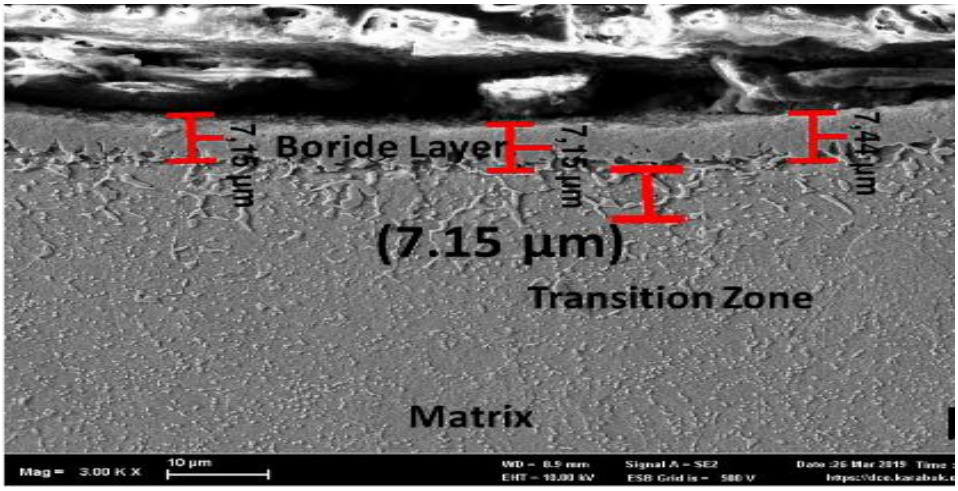

Figure 4.74. Microstructure and bored layer of bored H13 steel at 800 ° C 2h.

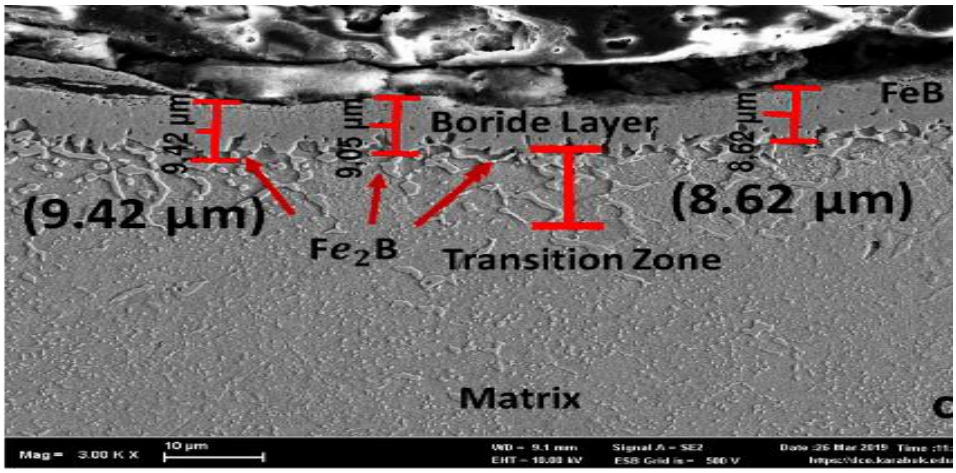

Figure 4.75. Microstructure and bored layer of bored H13 steel at 800 ° C 4h.

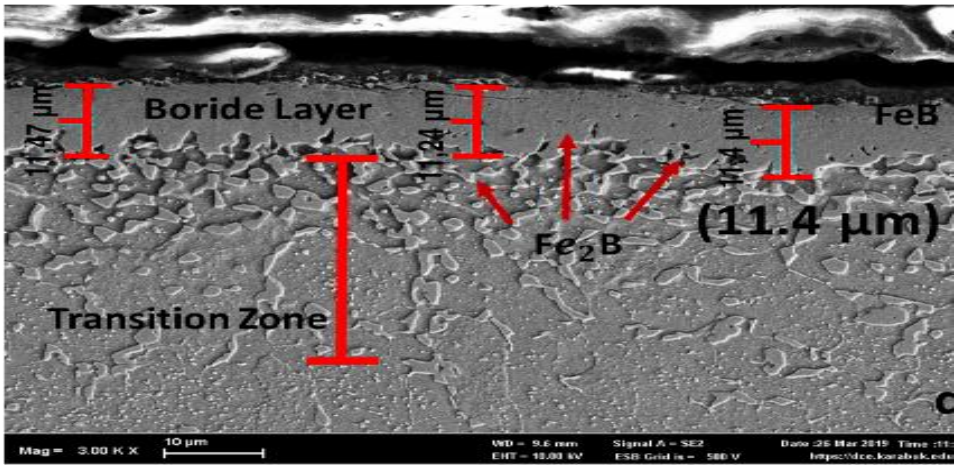

Figure 4.76. Microstructure and bored layer of bored H13 steel at 800 ° C 8h.

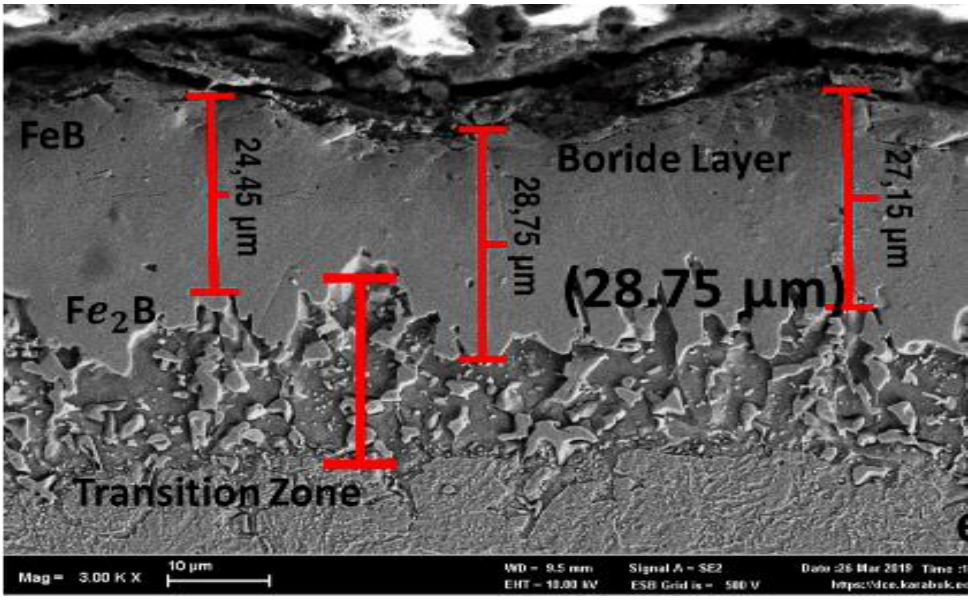

Figure 4.77. Microstructure and bored layer of bored H13 steel at 900 ° C 4h.

Corrosion potential and corrosion current values are obtained by Tafel curves, which show the relationship between current density and potential logarithm. In Tafel curves, the potential and current values at the intersection of the linear lines drawn on anodic and cathodic curves give the corrosion potential (Ekor) and the corrosion current (Ikor), respectively. Corrosion current density is found by dividing the corrosion current into the surface area and gives us information about the corrosion rate. The lower the corrosion current density, the higher the corrosion resistance. In addition, when the Ekor value shifts to more negative potentials, the corrosion resistance is low [245].

After the corrosion tests on 3.5% NaCl solution, the corrosion current density (Ikor) and corrosion potential (E_{corr}) values determined by Tafel polarization method and the corrosion rates calculated according to Equation 1 are given in Table 4.3. The current Tafel curves are shown in Figures 4.78,79,80,81,82. Corrosion data of the uncoated H13 steel given in Table 4.3 were taken from the study of Gunen et al. [275].

Table 4.3. Corrosion values in 3.5% NaCl Solution.

Sample	E_{corr} (mV) corrosion potential	I_{corr} (A/cm^2) 10^{-6} corrosion current	Corrosion Rate (mpy)
Uncoated	-632	90	91
700 °C, 4h	-371	189	39
800 °C, 2h	-365	145	30
800 °C, 4h	-351	133	28
800 °C, 8h	-329	124	25
900 °C, 4h	-352	111	23

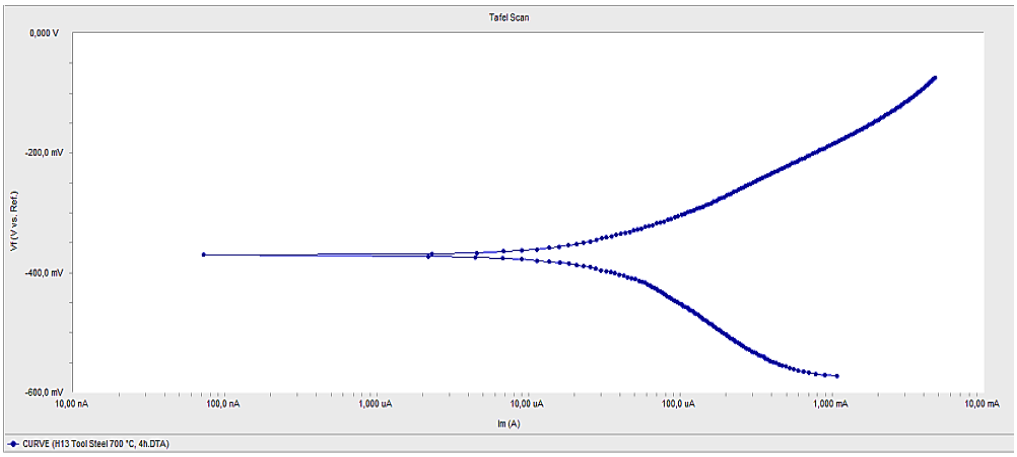

Figure 4.78. Tafel curve of H13 steel boronized for 4 h at 700 ° C.

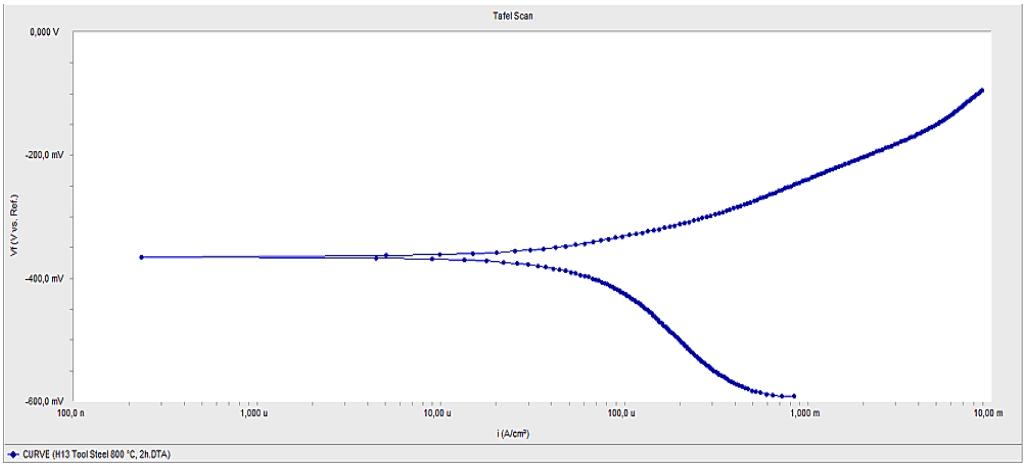

Figure 4.79. Tafel curve of H13 steel boronized for 2 h at 800 ° C.

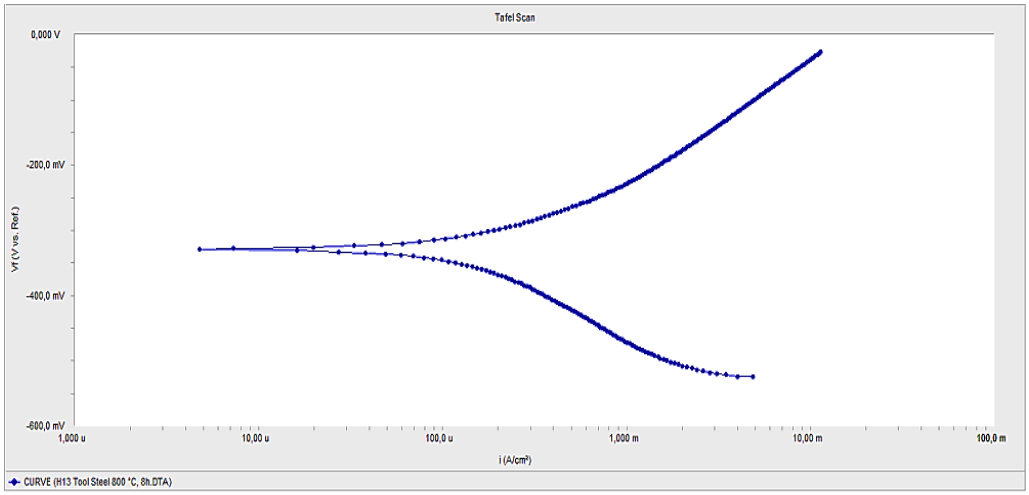

Figure 4.80. Tafel curve of H13 steel boronized for 4 h at 800 ° C.

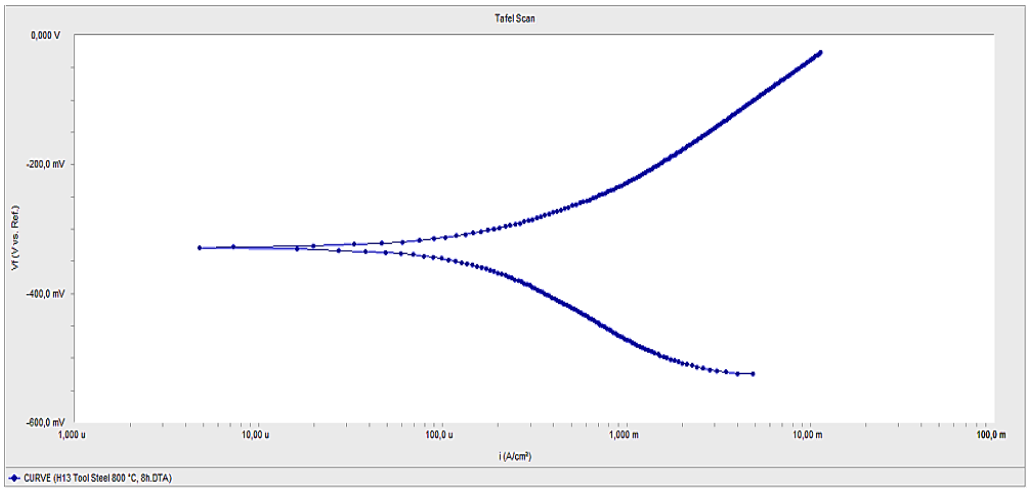

Figure 4.81. Tafel curve of H13 steel boronized for 8 h at 800 ° C.

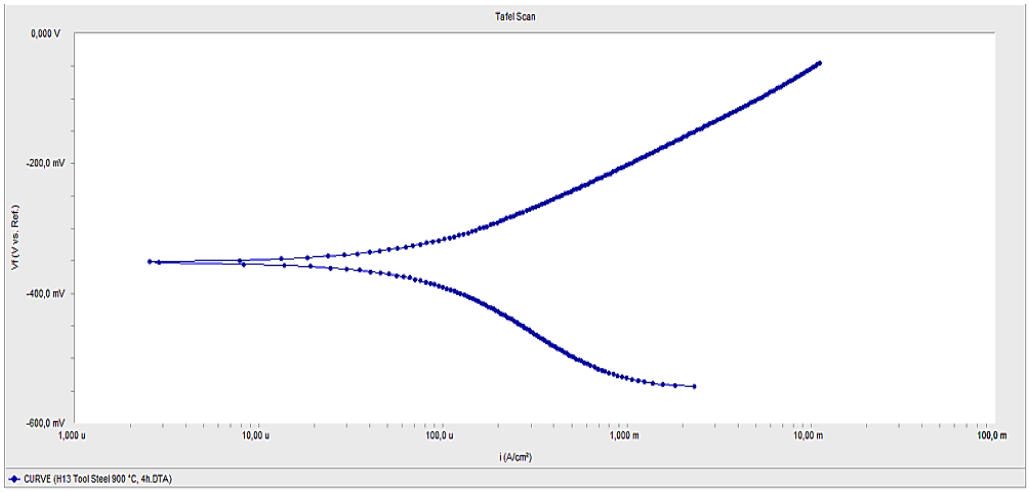

Figure 4.82. Tafel curve of H13 steel boronized for 4 h at 900 ° C.

When the Tafel curves obtained in corrosion experiments performed in 3.5% NaCl environment are examined, it is understood from the corrosion current and corrosion potential values (Table 4.3) that the corrosion rate in the coating layer is much lower than the base material, except for the sample, which is boronized for 8 hours at 800 °C. According to the table, the sample in which the corrosion potential (Ekor) the most negative is the uncoated sample. This situation caused the corrosion rate to be high. The layer thickness obtained with the boronizing process was observed at the lowest 700 °C, while the highest thickness was obtained at 900 °C. When Table 4.3 is examined, it can be seen that the increase of layer thickness at the sample boronized at 800 °C for 8 h, enables the corrosion rate to be reduced.

The morphology and phase structure of the boride layers vary depending on the sample used, the chemical composition of the boron powders, the environment, temperature and duration of the boronizing process [245,247]. FeB and Fe_2B phases have different thermal expansion coefficients (23×10^{-6} °C^{-1} and 7.85×10^{-6} °C^{-1}). For this reason, cracks will likely form on the material surfaces, and the corrosion resistance will decrease [275].

Excessive boronizing time in the samples coated may cause cracking in the coating layer, and this caused the corrosion rate to increase. It has also been noted that corrosion rate differences can be caused by factors such as the amount and dispersion of iron carbides in the microstructure and stresses occurring in the material [122].

PART 5

CONCLUSIONS

Based on the different conclusions in the course of the present study, it can be stated that the mechanical properties may change based on the type of surface treatment. For this reason, given the characteristics and areas of use, the proper treatment can be chosen. It is well known that engineering materials cannot achieve ideal and theoretical strength in lab conditions – with the main reasons behind their failure being design faults, improper choice of materials, production defects, going beyond design limits, overloading, and insufficient repair work and maintenance. Flaws can initiate stress values leading to early failure in components. As a general rule, sharp corners create high amounts of stress, eventually causing early failure. Apart from this, creep failure relies on not just temperature, but stress as well.

It is paramount that most steel types today have the highest level of resistance toward wear and corrosion – to which end, certain treatments are at hand now that improve this quality in components. The early 2000s bore witness to the awareness that the industry can produce very strong and corrosion-immune surfaces using the boriding process – the expression implying thermal treatment using boron in a thermochemical way. In detail, boron atoms are carried upon thermal energy into the lattice of the material at issue to later generate boride in combination with atoms constituting the parent material.

This treatment is carried out at high temperatures in many hours, during which period the layer and coat are formed on the outer surface in accordance to the boron potential. As a result, boron spreads within steel at speeds that are subject to the lattice type – that is, whether faced-centered or body-centered. Once achieving an ideal intensity of boron on the surface, Layered Crystal start to form nuclei which creates a layer below which, in turn, a large boron area appears.

The boride layer affects both the mechanical and the chemical conduct the underlying steel component in accordance to the boriding operational temperature, period of treatment, boron potential at the surface layer, and steel chemistry in detail. As for the kinetic factors for growth, they are subject to boron dispersion at the boride coats; apart from this, the mentioned coat expands due to boron dispersion in a vertical angle against the surface of the sample, with the values of intensity staying unchanged in the boride layer while treatment. Next, a horizontal profile is formed inside each boride layer, in this way making more room for improved resistance against wear and abrasion in comparison to other alternative thermochemical modes of treatment like carburising and nitriding.

The depth of the boride layer was about 60 μm, with high hardness values, which would decline as the depth advanced. a different set of borided samples were processed with heat in the conventional manner, they were initially heated and later cooled using air current. The entire operation was conducted in an argon setting to do away with the oxidation factor. The point worthy of attention is that the boride layer attributes of hardness and depth managed to remain unchanged even after heat tempering, with yet an added degree of substrate hardness.

Boriding has been shown to significantly improve resistance against wear and corrosion among ferrous materials in the presence of non-oxidizing dilute acids and alkali mediums, while thermochemical surface treatments develop hard iron borides triggered by boron dispersion at high temperatures. The FeB within the outside area and the Fe2B on the inside layer get shaped and, owing to advanced hardness, strengthen and elongate the life steel components exposed to friction and wear. The H13 steel has also been seen, upon boriding, to possess more resistance against wear as opposed to other variations finished with nitriding, carburizing, and transformation hardening.

This study investigated the wear and corrosion behaviour of AISI H13 hot work tool steel boronized with nano-boron powder at 700, 800, and 900 °C for 4 h and 2 and 8 h at 800 °C, under dry sliding conditions and with three different silver nanoparticle-doped lubricants (AgNP@Gel, AgNP@PVA, AgNP@PVP). Since AISI H13 is a hot

work tool steel, it must have high wear resistance. The study aimed to increase the wear resistance of H13 steel by boronizing the surface and using nano-silver-doped fluid in the wear environment.

In all, based on the tests carried out for the purpose of the work at hand, and some conclusions can be made. The results obtained were as follows:

- As boronizing time and temperature increased, a thicker boride layer was obtained. The maximum boride layer of 26.5 μm was achieved under conditions of 900 °C for 4 hours.
- In the boron layer, while Fe_2B phase was dominant at 700 ° C-4h and 800 ° C-2h, FeB phase intensified and the layer became dual phase with increasing boronizing time and temperature. In addition to iron borides, MnB and CrB phases were also determined in the boron layer.
- FeB phase is formed near the surface, and Fe_2B phase is formed between FeB phase and main material.
- The hardness of the boride layer increased with the increase of the boronizing time and temperature. The highest hardness value was measured as 2001 HV in the sample boronized at 900 °C for 4 h.
- The best wear resistance was obtained for samples boronized at 800 °C for 8 h and 900 °C for 4 h. These two parameters showed similar characteristics and no deformation or wear marks were observed on the surface.
- Among the average friction coefficients of the samples, the highest (0.510) was observed for the samples tested under dry conditions, and the lowest coefficient of friction (0.244) was obtained for the samples tested using the AgNP@Gel.
- Analysis of the 3D optical profilometer and SEM images showed the best results to be from the samples wear-tested using theAgNP@Gel medium.
- When the performance of silver nanoparticles coated with different ligands in the wear environment was compared, the most successful colloidal suspension was found to be AgNP@Gel.
- The fact that the Gel is dimensionally smaller than PVP and PVA has increased the wear resistance of the boron layer.

- Boriding process enhanced surface properties and better resistance toward friction, and this impact the surface layer material in a peculiar way as the microscopic analyses have revealed.
- Treatment is shown to greatly enhance surface texture by creating depressions within the profile and minimizing such parameters leading to roughness.
- Thermal treatment has effects, namely forming residual stress, adding to strain hardening, and changing the surface morphology to comprise dimple-shaped indentations.
- Assessing surface roughness can help in improving the related parameters for the as-built condition.
- This treatment enhances strength at the surface level, not to mention resistance against abrasive. Given the correct factors, and can reduced frictional energy losses.
- Upon the comparative analyses of approaches within the present study, it can be stated that thermal surface treatment is effective to enhancing and improve the fatigue life in the field.

5.1. RECOMMENDATION FOR FUTURE WORK

Boronizing process has been originally deployed to improve several properties of steel substrate, boronizing is initially used to optimize a number of attributes including protection against wear, oxidation, and corrosion.This is done through creating a boronized layer on the steel , and by forming boronized coating on steel substrate. However, in some environments that endure, and certain settings subject to high degrees of wear and tear, added temperature oxidation, and advanced degrees of high corrosion, boronized layers for coating cannot be considered as enough protection.

Many researchers and industries have been developing and studying to add other elements, for this reason, numerous studies have targeted the addition of other material for multi-component boronizing to further strengthen the degree of resistance, also to increase those properties, according to the experimental data and

mechanical attributes, our future attempts are aimed toward some endeavors, and based on the data , and with this background, and according to the experimental results and the proven and ideal mechanical properties, exhibited excellent properties. Therefore, attempts are aimed toward some efforts, and our future work will include the following aspects:

- Test surface mechanical treatment on other variations of steels, so that their mechanical properties are improved;
- Try to enhance and improve of corrosion resistance of H steel family, using mechanical and thermal surface treatments;
- Model and Simulation of relationship of grain size, and different structures composed of planar defects, to further optimize and development the combination of strength and ductility;
- Further work on the field surface treatment, improving it in case of other materials and chemical configurations, and examining the impacts on untested samples and materials;
- Variation of heat treatment and testing parameters is required to find ways for further improvement and to optimize the process;
- Investigated the effect of other microstructural parameters – namely, phase distribution and volume variation by finite element model tools after surface treatment;
- Investigate in the field of H steel further, Although work had been done by other researchers, and despite the already present other works, and there are some problems related to H steel are still open to question;
- We must offer a promising approach, and Come up with practical methods to assess alternative materials under conditions which involving concurrent impacting and sliding;
- Further examine the wear and failure mechanisms of coated systems under impact-sliding wear conditions, and these tests are another interesting research interest;
- Moreover optimization of powder composition and surface finish to achieve clean, powderless surfaces with added thickness for coating;

- Conduct additional corrosion experiments given the advanced failure rate of these tests caused by flaking;
- Preferably attempt to carry out corrosion tests in flow rates identical to erosion and erosion-corrosion experiments;
- Further study particles in the material plume and attempt to decrease particle size to obtain smoother film surfaces and enhance the wear properties, and More films should also be tested for wear-resistance;
- Attempt to improve our notions regarding the physical metallurgy of surface treatment, and study the impact of treatment process parameters on transforming hardness and microstructure;
- Concentrate on developing the multi-component boronizing process to optimize the coating attributers by means of applying own original powder mixtures;
- Examine two detailed diffusion approaches regarding multi-component boronizing in accordance to the periodic table categories of the additional second elements. In case of transition metals in Group VB and VIB, boron diffusion is dominant at the preliminary phase and the coating thickness is controlled in accordance to the diffusion rate of the additional second elements. As to the transition metals in Group IVB, chemical affinity is dominant at the afore-mentioned phase, developing the metal carbide and inhibiting boron diffusion;
- Supply other elements into boronizing – which effort might trigger deformation of crystal structures depending on the atomic size related to the group and period on the periodic table;
- Improve multi-component boronizing to enhance corrosion resistance more than the standard boronized coatings. According to tests, Tungsten and Molybdenum are good alternatives as second elements in processing for high corrosion-resistance implementations;
- Increase oxidation –resistance by multi-component boronizing by applying Niobium as the ideal second elements, for oxidation resistant applications for a wide range temperature up to 800 °C. Hafnium and titanium can be added for such resistance less than 600 °C;

- Involve in studying the chemical composition of powder mixtures in case of boron, second elements and activators, and also the durations and temperatures required for heat treatment;
- Monitor phase compositions within coating to avoid fractures, thereby enahcing the attributes required for resistance against wear, oxidation, corrosion, and micro-hardness;
- Investigate oxidation kinetics and mechanisms in case of second elements for multi component boronizing,and further study to investigate behaviors of oxidation process;
- Create a novel ternary diffusion method for use in the industry for added surface hardness, deep case depth, and added protection against corrosion;
- Description the new process for kinetics, microstructure, and the outcome attributes essential for use-specific scenarios, and work toward their efficiency in industrial and technological terms;
- Optimize processing parameters for sequential diffusion to reduce case degradation, enhance hardness, effective case depth, and protection against corrosion. Further concentrate on reducing case defects to improve performance;
- Enhance modeling softwares, and focus upon improving the capabilities of simulation software to further expand the scope of conductible tests at lower costs and time;
- Study intermediate and advanced elastic pre-stress scenarios throughout the treatment process to determine the ideal values for different residual stress profiles;
- Re-conduct certain tests for added accuracy by means of adding to the specimens employed for assessment. For instance, using other steel variations to study the impact of mechanical and thermal surface treatments;
- Implement the findings and data in participation with the industry;
- Determine the elements and processes involved in die failure and wear;
- Methodology for the selection of die materials on the basis of material properties, and define methods to choose die materials in accordance to

ideal attributes and predicted thermal fatigue performance in certain environments and under selected process conditions.

- Collaboration between industry and academia to development and produce better mechanical and thermal surface treatment methods;
- Application of accurate and practical prediction and development methods for wear and corrosion resistance;
- Come up with efficient temperature assessment tools for added accuracy in induction heat-treatment;
- Investigate in detail the trade-off in fatigue performance in compressive residual stressing and cracking of precipitate particles, thereby mproving our understanding of the wear and failure mechanisms of coated systems under impact-sliding wear;
- Control the wear behavior of the developed steels based on both hardness and the differences between the yield strength and the tensile strength;
- Conduct other fretting wear tests in elevated temperatures to find the exact thermal stability limits;
- Carry out load/contact stress-related wear tests to see precise impacts on the wear rate;
- Estimate all related mechanical properties – among them, ductility and fracture toughness to see precise impacts on wear rates;
- Examine other lubrication for wear tests to see their impact on material behavior;
- Carry out real-life wear tests to accurately resemble the industrial conditions of service;
- Development of cases and applications within the industry ranging in surface hardness, deep case depth, and high corrosion resistance;
- From a scientific viewpoint additional research is required to gain a better scientific insight into the process of initiation and concerns regarding new steel alloys;
- Work further toward understanding corrosion propagation behavior since any other study in this respect can tell us whether or not corrosion induced concrete damage can essentially take place in corrosion-resistant steel;

- Highly recommended to creating surfaces with added corrosion resistance, thus necessitating better surface texturing as an option for other metals;
- More studies can be performed on metals with different alloying elements or compositions and within various corrosive solutions;
- Additional study is needed to link the predicted amount of micro segregation reduction to the expected mechanical properties to generate guidelines for heat treatment to achieve the best mechanical properties. If quantitatively formed, these relations can help in developing the right heat treatment cycle in accordance to the expected property specifications and, thus, reducing cost;
- Attempt to harden H tool steels in a controlled protective atmosphere furnace followed by air cooling;
- Further examine strain hardening behavior of this steel;
- Focus on the microstructural changes in H13 steel to develop specially-tailored heat treatment regimes for precise and intended microstructures with different values of each constituent in the content;
- Work further to determine alternative degrees of formability parameters, such as by stretch-bend testing to identify the viability of these steels for manufacturing applications;
- Carry out additional mechanical tests on heat-treated specimens to achieve better statistics and reproducibility of the observed mechanical property outcomes; and
- It is necessary to adopt thermochemical treatment technique to improve their surface properties, such as thermal fatigue resistance.

REFERENCES

1. J. W. Martin, "Concise Encyclopedia of the Mechanical Properties of Materials", ***Elsevier Science & Technology, Oxford, United Kingdom*** (2010).

2. Val Ivanoff, "Engineering Mechanics", ***McGraw-Hill Education / Australia*** (2011).

3. Bert Verlinden, Julian Driver, Indradev Samajdar, Roger D. Doherty, "Thermo-Mechanical Processing of Metallic Materials: Volume 11", ***Elsevier Science & Technology, Oxford, United Kingdom*** (2009).

4. Henry Tindell, "Engineering Materials", ***The Crowood Press Ltd, Ramsbury, United Kingdom*** (2014).

5. Uday Shanker, Narayanan, R. Ganesh, "Strengthening and Joining by Plastic Deformation", ***Springer Nature Switzerland*** *(2016).*

6. Bhaduri,, Amit, "Mechanical Properties and Working of Metals and Alloys", ***Springer Nature Switzerland*** (2018).

7. Hume-Rothery William, "The structure of metals and alloys", ***Metals & Metallurgy Trust; 5th edition*** (2003).

8. Internet: Jeff Grill hails, "Guide to the Mechanical Properties of Metals", **https://weldguru.com/mechanical-properties-of-metals/** (2019).

9. Internet: Mechanical Booster, "Mechanical Properties Of Materials", **https://www. mechanical booster.com/2016/08/mechanical-properties-of-materials.html** (2020).

10. Lindsay, J., Coatings and coating processes for metals, ***ASM International, Metals Park, OH,*** (2010)

11. Internet: Surjeet Sankararaj, "Mechanical Properties of a Metal", **http:// mechteacher. com/mechanical-properties-of-metal/** (2019).

12. Bhushan, B. and Gupta, B. K.. Handbook of Tribology: ***Materials, Coatings, and Surface Treatments. McGraw-Hill, New York*** **(**2003).

13. Rickerby, D.S. & Matthews, Advanced Surface Coating- ***Handbook of Surface Engineering*** (2009).

14. Ed: Satas, D. & Tracton, A., ***Coatings technology handbook, 2nd edition.*** (2006)

15. C W Lung, Norman H March, ***"Mechanical Properties of Metals", Amazon Products*** (2009).

16. Chattopadhyay, R. Surface Wear: Analysis, Treatment, and Prevention. ***ASM International. Materials Park, OH*** (2007).

17. Holmberg, K. and A. Matthews. "Tribology of Engineered Surfaces." Wear: Materials, Mechanisms, and Practice. ***Ed. Gwidon W. Stachowiak. John Wiley and Sons, Ltd. Hoboken,*** NJ. p.123 (2009)

18. Internet: Flame Treating Systems, "Flame Hardening", **https:// flame treating systems .com/gear-flame-hardening/** (2019).

19. Chattopadhyay, R. Surface Wear: Analysis, Treatment, and Prevention. ***ASM International. Materials Park, OH*** (2007).

20. Internet: Viktor Pocajt, "Mechanical Properties of Metals", **https://www.totalmateria.com/Article53.htm** (2019).

21. Internet: graham fry, sandra fry, ryan clifford, dennis okwuonu "an overview of the mechanical properties of metals", **https://technoweld.com.au/2019/06/11/mechanical-properties-of-metals/** (2019).

22. Fuqian Yang , James . Li, "Micro and Nano Mechanical Testing of Materials and Devices", ***Springer-Verlag New York Inc., New York, NY, United State*****s** (2012).

23. Ndt Resource Center.i, "Introduction to Materials and Processes", **https://www.ndeed.org/EducationResources/CommunityCollege/Materials/cc_mat_index.htm** (2019).

24. Joshua Pelleg, "Mechanical Properties of Materials", ***Springer Science & Business Media, United Kingdom*** (2012).

25. Philip A. Schweitzer, P.E., "Metallic Materials: Physical, Mechanical, and Corrosion Properties", ***CRC Press, United Kingdom*** (2008).

26. D. Wigley, "Mechanical Properties of Materials at Low Temperatures", ***Springer-Verlag New York Inc., New York, NY, United States*** (2012).

27. Wole Soboyejo, "Mechanical Properties of Engineered Materials", ***CRC Press, United Kingdom*** (2019).

28. C. Suryanarayana, "Experimental Techniques in Materials and Mechanics", ***CRC Press, United Kingdom*** (2011).

29. George Dieter, “Mechanical Metallurgy”, ***McGraw-Hill Education / Australia*** (2004).

30. Murr, Lawrence E., “Handbook of Materials Structures, Properties, Processing and Performance”, ***Springer Science & United Kingdom*** (2015).

31. Internet: Russell, "Mechanics of Materials", **https:/ /mechanicalc. com/reference/ mechanical-properties-of-materials** (2019).

32. Internet: Melbourne Freelance, "Mechanical Properties Every Mechanical Engineer.ShouldKnow", **https://www.freelancer. Com/ community/ articles / mechanical- properties-every-mechanical-engineer-should-know** (2019).

33. J. Edwards, “Coating and Surface Treatment Systems for Metals: A Comprehensive Guide to Selection”, ***Sciences, Technology & Medicine (Books)*** (2003).

34. Tadeusz Burakowski, Tadeusz Wierzchon, “Surface Engineering of Metals: Principles, Equipment, Technologies”, ***Materials Science & Technology*** (2008).

35. Sina Ebnesajjad Cyrus Ebnesajjad, “Surface Treatment of Materials for Adhesive Bonding”, 1st Edition, ***Elsevier Science & Technology, Chadds Ford, PA, USA*** (2006).

36. Sina Ebnesajjad Cyrus Ebnesajjad, “Surface Treatment of Materials for Adhesion Bonding”, 2nd Edition, ***Elsevier Science & Technology, Chadds Ford, PA, USA*** (2013).

37. Internet: Tantec, "Surface Treatment of metals", **https://tantec.com/surface-treatment-of-metals.html** (2019).

38. Internet: Keller Technology Corporation, "Metal Surface Finishing Treatment Processes", **https:// www.kellertechnology.com/blog/8-common-types-of-surface-treatments-for-metal-parts/** (2019).

39. Internet: Vanchem Performance Chemicals, "The process of metal surface treatment", **http://www.vanchem.com/metal-surface-treatment/** (2019).

40. Internet: Figeac Aero, “Surface TreatmenT”, **https://www.figeac-aero.com/en/surface-treatment** (2019).

41. Internet: Misumi Corporation, "Surface Treatments and the Methods", **https:// www. misumi-techcentral.com/tt/en/surface/2012/08/127-types-of-surface-treatments-and-the-methods.html** (2019).

42. Internet: European Commission, “The Surface Treatment of Metals and Plastics",**https://aida.ineris.fr/sites/default/files/directive_ied/stm_bref_0806. pdf** (2019).

43. Internet: Minifaber,"Metal surface treatments", **https://www .minifaber. com/ sheet-metalworking/metal-surface-treatments** (2019).

44. Internet: Surface Treatment, **https://www.hcintalm. com.tw/en/ service/ Surface -Treatment/Surface-Treatment.html** (2020).

45. Tubal Cain," Hardening, Tempering and Heat Treatment", ***Special Interest Model Books, Hemel Hempstead, United Kingdom*** (2009).

46. Herbert James, "Effect of Heat Treatment on the Mechanical Properties of 1 Per Cent Carbon Steel", ***Wentworth Press*** (2016).

47. Internet: Machine Design, "A Quick Look at Heat Treating Processes for Metals",**https://www.machinedesign.com/materials/metals/article/21832107/ a-quick-look-at-heat-treating-processes-for-metals** (2019).

48. B. Zakharov, "Heat Treatment of Metals", ***University Press of the Pacific*** (2012).

49. wilhelm wiederholt, "Chemical Surface Treatment of Metals", ***Materials Science & Technology*** (1998).

50. Internet: American Machine Tools Corp, "HEAT TREATMENT OF METALS",**https://www.americanmachinetools.com/heat_treating_metals.htm** (2019).

51. Sankara Narayanan, "Thermochemical Surface Engineering of Steels",1st Edition, ***Elsevier Science & Technology, United Kingdom*** (2014).

52. Erik Oberg, "Heat-Treatment of Steel: A Comprehensive Treatise on the Hardening, Tempering, Annealing", ***(Classic Reprint) Engineering (Books)*** (2012).

53. Internet: Octal, "Heat Treatment Method in Steel Pipe Industry", https:// **www. octalsteel.com/faq/heat-treatment-method-for-steel-pipe.html** (2019).

54. Internet: Bodycote, "Heat treatment services", **https://www. bodycote. com / services/heat-treatment/** (2019).

55. Erik Oberg, "Heat-Treatment of Steel", Special Interest Model Books, United Kingdom.George E. Totten, ***"Steel Heat Treatment Handbook", CRC Press*** (2016).

56. Internet: Heat treating (or heat treatment)", **https:// www. yeguang special steel. com/ ?p=339** (2020).

57. George E. Totten, "Steel Heat Treatment Handbook", ***Metallurgy and Technologies, CRC Press*** (2006).

58. Internet: Bright Hub Engineering, “Heat Treatment of Steels & Metals", **https:// www.brighthubengineering.com/manufacturing-technology/30476-what-is-heat-treatment/** (2019).

59. Internet: AZOM, “Heat Treated Metals and Their Uses", **https://www. azom. com / article.aspx?ArticleID=14896** (2019).

60. Abdel Salam Makhlouf, Mahmood Aliofkhazraei , “Handbook of Materials Failure Analysis with Case Studies from the Chemicals, Concrete and Power Industries”, ***1st Edition, Elsevier Science & Technology*** (2015).

61. Ashok Choudhury, “Failure Analysis of Engineering Materials”, ***1st Edition, Mc Graw-Hill Companies*** (2007).

62. R. H. Jones, “Materials Failure Analysis”, ***Materials Science & Technology Monographs*** (2003).

63. Charlie R. Brooks, Ashok Choudhury, “Metallurgical failure analysis”, ***McGraw-Hill Companies*** (1998).

64. Neville W. Sachs , “Practical Plant Failure Analysis”,***1st Edition, Dekker Mechanical Engineering*** (2009).

65. E. Gdoutos, K. Pilakoutas, Chris Rodopoulos, “Failure Analysis of Industrial Composite Materials”, ***McGraw-Hill Companies*** (2008).

66. Kannadi Palankeezhe Balan, “Metallurgical Failure Analysis”,***1st Edition, elsevier science & technology*** (2018).

67. Abdel Salam Makhlouf, Mahmood Aliofkhazraei , “Handbook of Materials Failure Analysis With Case Studies from the Construction Industries”, ***Butterworth-Heinemann*** (2018).

68. Internet: Arcelormittal, “Wear resistant steels", **https://industeel.arcelormittal. com/products/wear-resistant-steels/** (2019).

69. Internet: Research Gate, “wear testing machine."**https://www.researchgate. net/figure/Pin-On-Disc-wear-testing-machine_fig1_267944198** (2019).

70. Ellis Horwood series, “Coatings and surface treatment for corrosion and wear resistance”, ***Halsted Press*** (1998).

71. Internet: Surface Engineering, “Wear Testing and Wear Measurement”, **http://emrtk.unimiskolc.hu/projektek/adveng/home/kurzus/korsz_anyagtech/1_konzultacio_elemei/wear_testing_measurement.htm** (2019).

72. B G Mellor, “Surface Coatings for Protection Against Wear”,***1st Edition, Woodhead Publishing Series in Metals and Surface Engineering*** (2008).

73. I.Saravanan, A.Devaraju, Ganesh babu, “Investigation of Surface Treatment process on stainless steel and its effects for tribological applications”, ***Materials Today: Proceedings,*** Volume 22, Part 3 (2020).

74. Xue Han, Zhenpu Zhang, Jiayu Hou, “Tribological behavior of surface treatment/ austempered AISI 5160 steel”, ***Tribology International***, Volume 145, (2020).
75. Internet: Surface hardening technology, “Wear resistance on stainless steel", **https://www.expanite.com/surface-hardening-of-stainless-steel/wear-resistance-results/** (2019).

76. Gwidon W. Stachowiak, “Wear – Materials, Mechanisms and Practice”, ***John Wiley & Sons, Ltd*** (2005).

77. AL-Mokhtar O.Mohamed, Zoheir Farhat, Andrew Warkentin, “Effect of a moving automated peening parameters on surface integrity of Low carbon steel”, ***Journal of Materials Processing Technology***, Volume 277 (2020).

78. P.J.Blau and R.G.Bayer, “Wear of Materials”, ***Materials Science and Technology*** (2005).

79. Erfan Maleki, Okan Unal, Kazem Reza, “Surface layer nano crystallization of carbon steels subjected to surface treatment: Analysis and optimization”, ***Materials Characterization,*** Volume 157 (2019).

80. A. Devaraju, “A critical review on different types of wear of materials”, Volume 6, Issue 11, ***International Journal of Mechanical Engineering and Technology*** (2015).

81. Koji Kato,Koshi Adachi, “Wear Mechanisms”, ***Tohoku University, Tribology series, Elsevier*** (2013).

82. Internet: Springer Nature Switzerland AG, “Mechanisms of wear”, **https://www.substech.com/dokuwiki/doku.php?id=mechanisms_of_wear** (2020).

83. Internet: Apex Shears, “Wear Resistance of Steels”, **http://apexshears.com/technical _resources.html** (2019).

84. Internet: Surface Engineering, “Wear and Wear Mechanism”, **http://emrtk.uni-miskolc.hu/projektek/adveng/home/kurzus/korsz_anyagtech/1_konzultacio_elemei/wear_and_wear_mechanism.htm** (2020).

85. J. K. Lancaster, “Wear Mechanisms of Metals and Polymers”, Volume 56, - Issue 1, ***The International Journal of Surface Engineering and Coatings*** (2017).

86. Amrita Bag,Dorian Delbergue,Jihane Ajaja, “Effect of different surface treatment on the fatigue life of 300 M steel submitted to high stress amplitudes”, ***International Journal of Fatigue,*** Volume 130 (2020).

87. H.Kovacı, I.Hacısalihoglu, A.celik, “Effects of shot peening pre-treatment and plasma nitriding parameters on the structural, mechanical and tribological properties of AISI 4140 low-alloy steel”, ***Surface and Coatings Technology,*** Volume 358 (2019).

88. Ian Hutchings, Philip Shipway, “Tribology: Friction and Wear of Engineering Materials”, ***Spedizione Gratis & Amazon*** (2017).

89. Theo Mang, Kirsten Bobzin, “Industrial Tribology: Tribosystems, Wear and Surface Engineering, Lubrication”, ***Spedizione Gratis & Amazon*** (2010).

90. Dmitrij Lyubimov, “Micromechanisms of Friction and Wear: Introduction to Relativistic Tribology”, ***Spedizione Gratis & Amazon*** (2015).

91. Internet: Slide Share, “Wear measurement”, **https://www. slideshare. net/veeresh232/ wear-measurement** (2019).

92. Bin Liu, Bo Wang,Xudong Yang, Xingfeng Zhao, “Thermal fatigue evaluation of AISI H13 steels surface modified by gas nitriding with pre- and post-shot peening”, ***Applied Surface Science,*** Volume 483 (2019).

93. Amrita Bag, Martin Levesque, Myriam Brochu, “Effect of surface treatment on short crack propagation in 300M steel”, ***International Journal of Fatigue,*** Volume 131, (2020).

94. George E. Totten, “Handbook of Lubrication and Tribology: Volume I Application and Maintenance”, ***Spedizione GRATIS & Amazon*** (2006).

95. Bharat Bhushan, “Modern Tribology Handbook”, ***Spedizione Gratis & Amazon*** (2002).

96. Internet: Machinery Lubrication, “Wear Analysis Strategy”, **https://www.machinery lubrication.com/Read/382/wear-analysis** (2020).

97. Internet: researchgate, “Tribological properties of ptfe cookware coatings”, **https:// www.researchgate.net/figure/Schematics-of-linear-reciprocating-wear-test_fig2_ 276294389** (2019).

98. Okan Unal, Erfan Maleki, Ibrahim Kocabas ,Haluk Yilmaz, “Investigation of nanostructured surface layer of severe shot peened AISI 1045 steel via response surface methodology”, ***Measurement,*** Volume 148 (2019).

99. V. Kragelsk, “Tribology Handbook: 1”, ***Spedizione Gratis & Amazon*** (2015).

100. J Furustig, A Almqvist, L Pelcastre, “A strategy for wear analysis using numerical and experimental tools, applied to orbital type hydraulic motorsy”, ***Sage Journals,*** Volume: 230 issue: 12, page(s): 2086-2097 (2016).

101. Internet: research gate, **https://www.researchgate.net/figure/Flow-chart-diagram-of-optimal-strategy-for-identification-of-wear-mode-of-engineering_fig10_268074489** (2020).

102. Internet: Quora, “coefficient of static friction”, **https://www.quora.com/Can-coefficient-of-static-friction-vary** (2019).

103. Kirill Dolgopolov, “Friction; An introduction to tribology”, ***The science study series*** (2014).

104. Jung-chul Thomas Eun , “Handbook of Engineering Practice of Materials and Corrosion”, ***Spedizione Gratis & Amazon*** (2018).

105. Internet: Corrosion of metals, “Corrosion theory for metals”, **https://xapps.xyleminc.com/Crest.Grindex/help/grindex/contents/Metals.htm** (2020).

106. Philip A. Schweitzer, “Corrosion Resistance Tables: Part B (Corrosion Technology)”, ***Crc Press; 5th Rev and Expanded ed. edition*** (2006).

107. S.D. Cramer and B.S. Covino, J., "New Literature Corrosion : Fundamentals , Testing , and Protection , Volume Thermal Spray 2003 : Advancing", ***Journal Of Thermal Spray Technology,*** 459–463 (2003).

108. Michael Schutze, Roman Bender, Karl-Gunther Schutze , “Corrosion Resistance of High-Performance Materials”, ***Wiley-VCH; 1 edition*** (2012).

109. Mejia-Caballero, Martinez Trinidad, J., Romero-Romo, M., Perez Pasten-Borja, and Campos-Silva, "Corrosion behavior of AISI 316L borided and non-borided steels immersed in a simulated body fluid solution", ***Surface And Coatings Technology,*** 280: 384–395 (2015).

110. Michael Schütze, Ralf Feser, Roman Bender, “Corrosion Resistance of Alloys”, ***Wiley-VCH; 1 edition*** (2011).

111. Amir Poursaee, “Corrosion of Steel in Concrete Structures”, ***1st edition, Elsevier Science*** (2016).

112. Internet: Total Materia, “Corrosion Fatigue”, **https://www.total materia .com/ page. aspx?ID=CheckArticle&site=kts&LN=HU&NM=441** (2020).

113. Internet: Corrosion Testing, “Standing up to Environmental Conditions”,**https://www.labtesting.com/services/materialstesting/corrosion-testing/** (2020).

114. R. Winston Revie, “Uhlig's Corrosion Handbook”, ***Third Edition,John Wiley & Sons, Inc*** (2011).

115. Internet: Schneider Electric Blog, “Prepare for the Winter Corrosion Speedup”, **http s://blog.se.com/power-management-metering-monitoring-power-quality/ 2017/ 11/14/ prepare-winter-corrosion-speedup/** (2020).

116. Philip A. Schweitzer, “Handbook of Corrosion Resistant Piping”, ***Crc Press; 5th Rev and Expanded ed. edition*** (2014).

117. Internet: Research Gate, “corrosion testing in a stainless steel", **https://www.research gate.net/figure/Schematic-for-immersion-corrosion-testing-in-a-stainless-steel-autoclave-type-corrosion_fig1_285578029** (2019).

118. Internet: Market Info, “Global Corrosion Monitoring System Market Advances with.Technology-driven Operations”,**https://marketinfo247.wordpress.com/ 2017/06/26/global-corrosion-monitoring-system-market-advances-with-technology-driven-operations-says-report/** (2020).

119. Jiang, J., Wang, Y., Zhong, Q., Zhou, Q., and Zhang, L., "Preparation of Fe2B boride coating on low-carbon steel surfaces and its evaluation of hardness and corrosion resistance", ***Surface And Coatings Technology,*** 206 (2–3): 473–478 (2011).

120. Internet: Petersen Stainless Rigging Limited “Relative corrosion resistance of stainless steels", **http://www.petersen-stainless.co.uk/technical-data/relative-corrosion-resistance.html** (2019).

121. Palomar-Pardave, M., Amador, A., VillaVelazquez,"Corrosion behavior of boride layers evaluated by the EIS technique", ***Applied Surface Science,*** 253 (23): 9061–9066 (2007).

122. ASTM International, "Astm Designation G102: Standard Practice for Calculation of Corrosion Rates and Related Information from Electrochemical Measurements", ***Annual Book Of ASTM Standards*** 66: 37–39 (2012).

123. Internet: Research Gate, “Corrosion Risk Analysis, Risk based Inspection”, **https://www.researchgate.net/figure/below-gives-the-effectiveness-of-various-inspection-techniques-for-detecting-different_tbl2_271714263** (2020).

124. Internet: vecor pipe line, **https://vecor-pi.com/index.php/3-columns-default/item/16-corrosion** (2020).

125. Internet: Corrosion Engineering: Principles and Practice, “Corrosion Resistance to Atmospheric Corrosion”, **https://corrosion-doctors.org/Corrosion-Atmospheric/Corrosion-resistance.htm** (2020).

126. Vicente Braz TrindadeI, Rodrigo Borin, “High-temperature oxidation of pure Fe and the ferritic steel 2.25Cr1Mo”, ***Mat. Res.*** vol.8 No.4. (2005).

127. Internet: Stee Construction.info, “Corrosion of structural steel”, **https:// www. steelconstruction.info/Corrosion_of_structural steel** (2020).

128. Anonymous, “Testing the Hardness and Durability of Metals”, ***Sagwan Press*** (2015).

129. Internet: Merriam-Webster, “Definition of hardness”, **https://www.merriam-webster.com/dictionary/hardness** (2020).

130. Internet: Brystar metrology Tools, “Vickers Microhardness Tester", **https: //www.brystartools.com/phase-ii-vickers-microhardness-tester-900-391e-auto-x-y-axis-auto-turret-video-auto-measurement-software-900391e/** (2020).

131. Internet: Wikipedia, “Measuring hardness”, **https:// en. wikipedia .org/wiki/ Hardness** (2020).

132. Internet: corrosion pedia, “Hardness of Materials”, **https://www. Corrosion pedia.com/definition/620/hardness-of-materials-material-resistance** (2020).

133. Internet: engineering clicks, “Hardness Test: What it is and how it’s measured, **https://www.engineeringclicks.com/vickers-hardness-test/** (2020).

134. Internet: ispatguru, “Material hardness and hardness testing”, **https:// www. ispatguru.com/material-hardness-and-hardness-testing/** (2020).

135. Internet: Azo Materials, “Materials and Hardness Testing - The Importance of its Applications”, **https://www.azom.com/article.aspx?ArticleID=15122** (2020).

136. D. Tabor, “The Hardness of Metals”, ***CRC Press; Oxford University Press, Amazon.co.uk*** (2004).

137. Konrad Herrmann, “Hardness Testing: Principles and Applications”, ***CRC Press; Oxford University Press*** (2011).

138. Internet: TWI Ltd, Cambridge, UK, “Hardness testing part one", **https:// www. twi-global.com/technical-knowledge/job-knowledge/hardness-testing-part** (2020).

139. Internet: Materials Guide, “STEEL”, **https://www. knives from japan. co.uk /materials-guide-i22** (2020).

140. Internet: Nano science, “ Microhardness Testing", **https://www.nanoscience. com/techniques/mechanical-testing/microhardness-testing/** (2020).

141. Internet: Science Direct, “Micro hardness”, **https://www.Science direct .com/ topics/materials-science/microhardness** (2020).

142. Internet: ScienceDirect, “Microhardness Testing”, **https://www. sciencedirect. com/topics/materials-science/microhardness-testing** (2020).

143. Internet: Corrosionpedia, “Definition - What does Microhardness mean?” **https://www.corrosionpedia.com/definition/775/microhardness** (2020).

144. Internet: Nano Science, “Microhardness Testing”, **https://www.nanoscience. com/techniques/mechanical-testing/microhardness-testing/** (2020).

145. Internet: Copyright Gordon England, “Microhardness Test”, **https://www. gordonengland.co.uk/hardness/microhardness.htm** (2020).

146. Anton F. Mohrnheim, “Microhardness Testing and Hardness Numbers”, ***Springer Nature Switzerland AG*** (2012).

147. Internet: Merriam Webster, “Definition of microhardness”, **https://www. merriam-webster.com/dictionary/microhardness** (2020).

148. Q. Jane Wang, Yip-Wah Chung, “Encyclopedia of Tribology”, ***Springer-Verlag New York Inc*** (2013).

149. FilipIlie, “Tribological behaviour of the steel/bronze friction pair (journal bearing type) functioning with selective mass transfer”, ***International Journal of Heat and Mass Transfer,*** Volume 124, (2018).

150. R. Autay, M. Kchaou, K. Elleuch, “Tribological behaviour of carbon and low alloysteels: effect of mechanical properties andtest conditions”, ***Research Gate GmbH. All rights reserved*** (2011).

151. G. Pantazopoulos, “An Overview on the Tribological Behaviour of Nitro Carburised Steels for Various Industrial Applications”, ***Tribology in Industry*** (2013).

152. Sergej Mozgovoy , Jens Hardell , Liang Deng , Braham Prakash, “Tribological Behavior of Tool Steel Under Press Hardening Conditions Using Simulative Tests”, ***Journal of Tribology,*** Volume 140, Issue 1 (2017).

153. S. Ghorpade, H. Gawande, “Tribological Behaviors of Steel and Al Alloys for Hydroforming Components”, ***Journal of Bio- and Tribo-Corrosion,*** volume 4, (2018).

154. Internet: M. Nilsson, M. Olsson, “Tribology in Metal Working”, **https://www. diva-portal.org/smash/get/diva2:58943 /Fulltext01.pdf** (2020).

155. Internet: Martini Research Group, Fundamental Tribology, “Introduction to Tribology”, **https://faculty.ucmerced.edu/amartini/tribology.shtml** (2020).

156. Internet: Research Gate, “International standardization and organizations in the field of tribology”, **https://www.researchgate.net/figure/Graphic-description-of-tribology-interacting-with-other-sciences_fig1_235636782** (2020).

157. Internet: The functional configuration of surfaces, “Tribology and surface design”,**https://www.iwm.fraunhofer.de/en/why-fraunhofer-iwm/core-competencies-technical-possibilities/tribology-and-surface-design.html** (2020).

158. Internet: HEF Group, “Tribology Testing Overview”, **https://www. hefusa .net/tribology_testing/overview.html** (2020).

159. Internet: Machinery Lubrication, “Tribology Explained”, **https://www. machinerylubrication.com/tribology-31340** (2020).

160. H.k.d.h. Bhadeshia, “Some phase transformations in steels”, ***Materials Science and Technology*** (2013).

161. Internet: Slide Share, “Phase Transformation Lecture equilibrium, Phase Diagram”,**https://www.slideshare.net/MuhammadAliSiddiqui6/phasetransformation-lecture-equilibrium-phase-diagram** (2020).

162. Internet: Metal supermarkets, “tool steel applications and grades”, **https:// www.metalsupermarkets.com/tool-steel-applications-grades/** (2020).

163. Internet: Hitachi Metals, “tool steels”, **https://www.hitachi-metals.co .jp/ e/ products/auto/ml/pdf/yss_tool_steels_d.pdf** (2020).

164. Internet: Azo Materials, “Tool Steel Classifications”, **https://www. azom. com/ article.aspx?ArticleID=6138** (2020).

165. Internet: Wikipedia, “Steel production”, **https://en.wikipedia.org/wiki/Steel** (2020).

166. Internet: C & W Hardware, “Stainless Steel”, **https://cwhardware.com/ products/stainless-steel/** (2020).

167. Internet: World Steel Association, “About Steel”, **https://www.worldsteel. org/about-steel.html** (2020).

168. Internet: Encyclopaedia Britannica, “Properties of Steel”, **https://www. britannica.com/technology/steel** (2020).

169. Internet: Research Gate, “The effect of heat treatment on the hardness and impact properties of medium carbon steel”, https://www.researchgate.**net/figure/ Chemical-Composition-of-Medium-Carbon-Steel_tbl1_296686341** (2020).

170. Internet: Dictionary.com, “Definition of Steel”, **https://www.dictionary. com/ browse/steel** (2020).

171. Internet: Otai Special Steel, “What Is Tool Steel? (Six Groups with Details)”, **http://www.astmsteel.com/steel-knowledge/what-is-tool-steel/** (2020).

172. Internet: purohit steels. Hot work tools steel **http://www. purohit steels. com/ Hot%20work.aspx** (2020).

173. Internet: Azom Materials, “Hot-Work Steels”, **https://www. azom. com/ article.aspx?ArticleID=6213** (2020).

174. Internet: Hudson Tool Steel, “H13 Tool Steel”, **https://www .hudson tool steel.com/technical-data/steel H3** (2020).

175. Internet: Azom Materials, “H13 Tool Steel - Chromium Hot-Work Steels”, **https://www.azom.com/article.aspx?ArticleID=9107** (2020).

176. Internet: Mat Web, “AISI Type H13 Hot Work Tool Steel”, **http://www.mat web.com/search/datasheet_print.aspx?matguid** (2020).

177. Internet: Otai Special Steel, “H13 Tool Steel (chromium hot work tool steel)”, **http://www.astmsteel.com/product/h13-tool-steel-x40crmov5-1-skd61-hot-work-steel/** (2020).

178. Internet: Songshun Steel, “Application of H13 hot die steel in hot extrusion die”, **http://www.songshunsteel.com/news_show_27_22_82.html** (2020).

179. Internet: Markforged, “What is H13 Tool Steel?)”, **https://markforged. com/ blog/introducing-h13-tool-steel/** (2020).

180. Internet: Metal Suppliers Online, “h13 tool steels material property data sheet, **https://www.suppliersonline.com/propertypages/H13.asp** (2020).

181. Internet: Metal Supermarkets, “Tool Steel H13”, **https://www. metal super markets.com/metals/tool-steel/tool-steel-h13/** (2020).

182. Internet: West Yorkshire Steel, “H13 Tool Steel”, **https://www. west yorks steel.com/tool-steel/h13/** (2020).

183. Internet: Wikipedia, “Boriding”, **https://en.wikipedia.org/wiki/Boriding** (2020).

184. Internet: Science Direct, “Boriding - an overview”, **https://www.sciencedirect. com /topics/engineering/boriding** (2020).

185. Internet: indiamart, “Boron Powder, Packaging Type”, **https://www. india mart.com/proddetail/boron-powder-7471752948.html** (2020).

186. Internet: Bodycote, “Boriding”, **https://www.bodycote.com/services/heat-treatment/case-hardening-with-subsequent-hardening-operation/boriding/** (2020).

187. Xingliang He, Huaping Xiao, M. Fevzi Ozaydin, Karla Balzuweit,"Low-temperature boriding of high-carbon steel ", ***Surface and Coatings Technology,*** Volume 263, Pages 21-26 (2015).

188. Internet: IBC Coatings Technologies, Inc, “Boriding / Borinizing (DHB)”, **https://www.ibccoatings.com/boriding-boronizing-dhb** (2020).

189. Internet: BorTec GmbH & Co. KG, Inc, “Boriding vs. Nitriding”, **https:// bortec.de/en/blog/boriding-vs-nitriding/** (2020).

190. Internet: BorTec GmbH, Inc, “Overview of the different boriding agents”, **https://bortec.de/en/blog/boriding-agents/** (2020).

191. Q. Jane Wang, Yip-Wah Chung, “Boronizing”, ***Encyclopedia of Tribology, Springer Link*** (2013).

192. Internet: TD Coating, Inc, “Boriding / Boronizing”, **http://www.td.co. za/boronising/** (2020).

193. Internet: Total Material, Inc, “Boriding/Boronizing of Steel Materials”, **https://www.totalmateria.com/page.aspx?ID=CheckArticle&site=kts&NM= 496** (2020).

194. Internet: Total Material, Inc, “Boriding Surface Treatments”, **https://www. totalmateria.com/page.aspx?ID=CheckArticle&site=kts&NM=490** (2020).

195. M. Ortiz-Domínguez, A. Gómez-Vargas, G. Torres-Santiago, “Modeling of the Growth Kinetics of Boride Layers in Powder-Pack Borided ASTM A36 Steel Based on Two Different Approaches”, ***Advances in Materials Science and Engineering,*** Volume 2019 |Article ID 5985617 (2019).

196. Internet: Manufacturing Guide, Inc, “Boriding process”, **https://www. manufacturingguide.com/en/boriding** (2020).

197. V.I. Dybkov, “Basics of Formation of Iron Boride Coatings”, Institute of Problems of Materials Science, National, ***Academy of Sciences of Ukraine,*** (2016).

198. Internet: Mehmet Yorulmaz, “An investigation of boriding of medium carbon steels”, Marmara University, faculty of engineering, **http://mimoza .marmara. edu. tr/~ekalafatoglu/pdf/Dokuman/Boriding_medium_carbon_steels.pdf** (2020).

199. Internet: Carla Martini, “Mechanism of Thermochemical Growth of Iron Borides on Iron”, **https://www.researchgate.net/publication**

/226491317_Mechanism_of_Thermochemical_Growth_of_Iron_Borides_on_Iron (2020).

200. Turker Turkoglu, Irfan Ay, "Analysis of boride layer thickness of borided AISI 430 by response surface methodology" ***An International Journal of Optimization and Control: Theories & Applications,*** Vol.9, No.3 (2019).

201. Edgar Cardenas, Roger Lewis, "Characterization and wear performance of boride phases over tool steel substrates", ***Advances in Mechanical Engineering (AIME)*** (2019).

202. Junji Morimoto, Taisuke Ozaki, "Some properties of boronized layers on steels with direct diode laser", ***Surface and Coatings Technology*** (2012).

203. Internet: Research Gate, "Some mechanical properties of borides formed on AISI 8620 steel", **https://www.researchgate.net/publication/283809589_Some_mechanical_properties_of_borides_formed_on_AISI_8620_steel** (2020).

204. Internet: Total Materia, "Boriding/Boronizing of Steel Materials", **https://www.totalmateria.co/page.aspx?ID=CheckArticle&site=kts&NM=496** (2020).

205. Internet: Geochemical Instrumentation and Analysis, "Scanning Electron Microscopy (SEM)", **https://serc.carleton.edu/research_education/geochemsheets/ techniques/SEM.html** (2020).

206. Internet: Nano Science, "Scanning Electron Microscopy", **https://www.nanoscience.com/techniques/scanning-electron-microscopy/** (2020).

207. Internet: Department of Earth & Atmospheric Sciences, "Scanning Electron Microscope Laboratory", **https://www.eas.ualberta.ca/sem/** (2020).

208. Internet: Thermo Fisher Scientific, "What is SEM? Scanning electron microscope technology explained", **https://blog.phenom-world.com/what-is-sem** (2020).

209. Internet: Encyclopaedia Britannica, "Scanning electron microscope (SEM)", **https://www.britannica.com/technology/scanning-electron-microscope** (2020).

210. Internet: Nano Images, "SEM Technology Overview", **https://www.nanoimages.com/sem-technology-overview/** (2020).

211. Internet: Science Direct, "Scanning Electron Microscopy", **https://www.sciencedirect.com/topics/medicine-and-dentistry/SEM** (2020).

212. Internet: Thermo Fisher Scientific, "SEM: Types of Electrons" **https://www.thermofisher.com/blog/microscopy/sem-types-electrons-and-the-information-they-provide/** (2020).

213. Internet: Microscope Master, "SEM Imaging Components and Applications" **https://www.microscopemaster.com/scanning-electron-microscope.html** (2020).

214. Internet: Azo Materials, "Applications of Scanning Electron Microscopes", **https://www.azom.com/article.aspx?ArticleID=5528** (2020).

215. Internet: research gate, **https://www.researchgate.net/figure/XRD-analysis-of-gold-nanoparticles-Crystalline-nanoparticles-represented-by-four-peaks_fig6_269414028** (2020).

216. Internet: Yale University, "X-ray diffraction (XRD)" **https://ywcmatsci. yale.edu/xrd** (2020).

217. Internet: Technology of Materials, "Analysis of Materials by XRay Diffraction (XRD)" **http://www.xraydiffrac.com/xraydiff.html** (2020).

218. Internet: Physics Open Lab, "XRD Analysis of some Metals" **http://physicsopenlab.org/2018/02/21/xrd-analysis-of-some-metals/**(2020).

219. Internet: Rigaku corporation and its global subsidiaries, "X-RAY Diffraction (XRD)" **https://www.rigaku.com/techniques/x-ray-diffraction-xrd** (2020).

220. Internet: LSAI Labs, "X-RAY Diffraction (XRD)" **https://www.lsailabs .com/ XRD.html** (2020).

221. Internet: The Prashant Laboratory, "Energy Dispersive X-RAY Spectroscopy (EDX)" **https://www3.nd.edu/~kamatlab/facilities_physchar.html** (2020).

222. Internet: Intertek Group, "Energy Dispersive X-Ray Analysis (EDX)" https:// **www.intertek.com/analysis/microscopy/edx/** (2020).

223. Internet: Science Direct, "Energy Dispersive X Ray Analysis" **https://www. sciencedirect.com/topics/materials-science/energy-dispersive-x-ray-analysis** (2020).

224. Internet: Encyclopaedia Britannica, "Transmission Electron Microscopy (TEM)" **https://www.britannica.com/technology/scanning-tunneling-microscope/ Applications** (2020).

225. Internet: Microscope Master, "Transmission Electron Microscopy" **https:// www.microscopemaster.com/transmission-electron-microscope.html** (2020).

226. Internet: Wikipedia, “Scanning transmission electron microscopy”, **https://en.wikipedia.org/wiki/ Scanning _transmission_ electron_ microscopy** (2020).

227. Internet: Mitutoyo, “Quick guide to surface roughness measurement” **https:// www.mitutoyo.com/wp-content/uploads/2012/11/1984 _Surf_ Roughness** (2020).

228. Internet: Vista Instrument, “Surface roughness measurement in the lab” **https://wms2.vistainstrument.com/index.php/contour-form-roughness-measurement-machine** (2020).

229. Internet: Encyclopedia of Microfluidics and Nanofluidics, “Measurement of Surface,Roughness”**https://link.springer.com/referenceworkentry/10.1007%2F978-0-387-48998-8_1506** (2020).

230. Internet: Think Focus Grou, “Micro machined surface roughness measurement **http://en.think-focus.com/yyal/&pmcId=101.html** (2020).

231. Internet: NCBI Resources, “Synthesis of silver nanoparticles: chemical, physical and biological methods” **https://www.ncbi .nlm.nih.gov/pmc/ articles/ PMC4326978/** (2020).

232. Internet: Wikipedia, “Silver nanoparticle” **https://en.wikipedia.org/wiki/ Silver_nanoparticle** (2020).

233. Internet: Research Gate, “Different approaches of synthesis of silver Nano particles” **https://www.researchgate.net/figure/Different-approaches-of-synthesis-of- silver-nanoparticles_fig1_275015459** (2020).

234. Internet: Research Gate, “Specimen preparation for SEM observation” **https://www.researchgate.net/figure/Specimen-preparation-for-SEM-observation_ fig1_26651499** (2020).

235. Internet: Kemet International Ltd, “Wet Abrasive Cut off Machines for Metallographic Samples” **https://www. kemet.co.uk/ products/ metallography /abrasive-cut-off-machines/wet-abrasive-cutting-machine** (2020).

236. Internet: Optical Microscopy and Specimen Preparation, “Metallographic Specimen Preparation” **http://www.icbl.hw.ac.uk/learnem/ doitpoms/ Optical Microscopy/metallography.htm** (2020).

237. Internet: Lap Master, “Abrasive Discs – Paper – Wet/Dry” **https://www. Lap master-wolters.com/metal/mets-papr-200-0120-200-mm-plain-backed-silicon-carbide -abrasive-paper-discs** (2020).

238. Internet: Louis, “Polishing metal parts on your motorcycle” **https://www. louis.eu/rund-ums-motorrad/schraubertipps/metall-polieren** (2020).

239. Internet: Science, “Etching Steel” **https://www.tf.uni-kiel.de/matwis/ amat iss/kap_7/illustr/s7_1_2.html** (2020).

240. M. Gok, Y. Kucuk, M. Oge, E. Kanca, A. Gunen, Dry sliding wear behavior of borided hot-work tool steel at elevated temperatures, ***Surface & Coatings Technology,*** 328: 54–62 (2017).

241. J. Lee, J. Choe, J. Park, J. H. Yu, S. Kim, I.D. Jung, H. Sung, Microstructural effects on the tensile and fracture behavior of selective laser melted H13 tool steel under varying conditions, ***Mater. Charact.*** 155 109817 (2019).

242. Y. Sert, Investigation of Tribological Properties of TiAlZrN Coated on Nitrided H13 Steel. ***Karadeniz Technical University The Graduate School of Natural and Applied Sciences Mechanical Engineering Graduate Program*** (2016).

243. K. Yıldızlı, D. Odabaş, F. Nair, Investigation of Erosive wear of The Borided ***AISI 1020 Steel, Balıkesir Univ. J. Inst. Sci. Technol.*** 5, 130–140 (2003).

244. O. Akbayır, H. Gasan, Abrasive Wear Properties of Borided AISI 1030 Steel, J. Fac. ***Eng. Archit. Eskisehir Osmangazi Univ.*** 21,71–85 (2008).

245. U. Er, B. Par, The Investigation on Abrasive Wear Resistance of Surface Hardened AISI 1030 and AISI 1050 Steels By Boronizing, J. Fac. ***Eng. Archit. Osmangazi Univ.*** 17 (2004).

246. H. Cimenoglu, E. Atar, A. Motallebzadeh, High temperature tribological behaviour of borided surfaces based on the phase structure of the boride layer, Wear. ***Surface & Coatings Technology,*** 309, 152–158 (2014).

247. Sahin, S. and Meric, C., "Investigation of the effect of boronizing on cast irons", ***Materials Research Bulletin,*** 37 (5): 971–979 (2002).

248. A. Motallebzadeh, E. Dilektasli, M. Baydogan, E. Atar, H. Cimenoglu, Evaluation of the effect of boride layer structure on the high temperature wear behavior of borided steels, ***Wear.*** 328–329, 110–114 (2015).

249. S. Taktak, Some mechanical properties of borided AISI H13 and 304 steels, ***Mater. Des.*** 28 ,1836–1843 (2007) .

250. X. He, H. Xiao, M. Fevzi Ozaydin, K. Balzuweit, H. Liang, Low-temperature boriding of high-carbon steel, ***Surf. Coatings Technol.*** 263, 21–26 (2015).

251. Y. Imece, O. Erdem, B. Tuc, Investigation of Tribological Properties of MoS2 and Graphite Coatings Under Different Environmental Conditions, ***J. Fac. Eng. Archit. Gazi Univ.*** 33, 995–1012 (2018).

252. J.C. Sanchez-Lopez, M.D. Abad, L. Kolodziejczyk, E. Guerrero, A. Fernandez, Surface-modified Pd and Au nanoparticles for anti-wear applications, ***Tribol. Int.*** 44, 720–726 (2011).

253. M.S. Hossain, R.L. Jackson, Tribological Performance of Silver Nanoparticle–Enhanced Polyethylene Glycol Lubricants, ***Tribol. Trans.*** 59, 585–592 (2016).

254. C. Meric, S. Sahin, B. Backir, N.S. Koksal, Investigation of the boronizing effect on the abrasive wear behavior in cast irons, ***Mater. Des.*** 27, 751–757 (2006).

255. H. Yang, X. Wu, G. Cao, Z. Yang, Enhanced boronizing kinetics and high temperature wear resistance of H13 steel with boriding treatment assisted by air blast shot peening, ***Surface And Coatings Technology,*** 307: 506–516 (2016).

256. A. Gunen, E. Kanca, M.S. Karakas, M.S. Gok, M. Demir, Effect of borotitanizing on microstructure and wear behavior of Inconel 625, ***Surf. Coatings Technol.*** 311,374–382 (2017).

257. M. Kulka, N. Makuch, A. Piasecki, Nanomechanical characterization and fracture toughness of FeB and Fe2B iron borides produced by gas boriding of Armco iron, ***Surf. Coatings Technol.*** 325, 515–532 (2017).

258. L.G. Yu, X.J. Chen, K.A. Khor, G. Sundararajan, FeB/Fe2B phase transformation during SPS pack-boriding: Boride layer growth kinetics, ***Acta Mater.*** 53, 2361–2368 (2005).

259. A. Erdogan, Investigation of high temperature dry sliding behavior of borided H13 hot work tool steel with nanoboron powder, Surf. ***Coatings Technol.*** 357, 886–895 (2019).

260. M. Sivera, L. Kvitek, J. Soukupova, A. Panacek, R. Prucek, R. Vecerova, R. Zboril, Silver nanoparticles modified by gelatin with extraordinary pH stability and long-term antibacterial activity, ***PLoS One.*** 9 (2014).

261. M.E. Turan, Y. Akgul, Y. Turen, H. Ahlatci, The effect of GNPs on wear and corrosion behaviors of pure magnesium, ***J. Alloys Compd.*** 724, 14–23 (2017).

262. O. Perez-Acosta, E. Lorenzo-Bonet, P. Zambrano-Robledo, The effect of a boride diffusion layer on the tribological properties of AISI M2 steel, ***Wear.*** 426–427, 1667–1671(2019).

263. Y. Kayali, I. Gunes, S. Ulu, Diffusion kinetics of borided AISI 52100 and ***AISI 440C steels, Vacuum.*** 86,1428–1434 (2012).

264. U. Sen, S. Sen, S. Koksal, F. Yilmaz, Fracture toughness of borides formed on boronized ductile iron, ***Mater. Des.*** 26, 175–179 (2005).

265. Y. Wan, Z. Guo, X. Jiang, K. Fang, X. Lu, Y. Zhang, N. Gu, Quasi-spherical silver nanoparticles: Aqueous synthesis and size control by the seed-mediated Lee-Meisel method, ***J. Colloid Interface Sci.*** 394, 263–268 (2013).

266. R. Desai, V. Mankad, S.K. Gupta, P.K. Jha, Size distribution of silver nanoparticles: UV-visible spectroscopic assessment, Nanosci. Nanotechnol. ***Lett.*** 4, 30–34 (2012).

267. L.M. Liz-Marzan, Tailoring surface plasmons through the morphology and assembly of metal nanoparticles, ***Langmuir.*** 22, 32–41(2006).

268. V. Hirsch, S. Balog, D. Urban, C. Jud, B. Rothen-Rutishauser, M. Lattuada, A. Petri-Fink, Nanoparticle colloidal stability in cell culture media and impact on cellular interactions, ***Chem. Soc. Rev.*** 44, 6287–6305 (2015).

269. F. Gambinossi, J.K. Ferri, Aggregation kinetics and colloidal stability of functionalized nanoparticles, Adv. ***Colloid Interface Sci.*** 222, 332–349 (2015).

270. O. Yazici, S. Yilmaz, Investigation of effect of various processing temperatures on abrasive wear behaviour of high power diode laser treated R260 grade rail steels, ***Tribol. Int.*** 119, 222–229 (2018).

271. C.A. Cuao-Moreu, M. Alvarez-Vera, E.O. Garcia-Sanchez, A. Perez-Unzueta, M.A.L. Hernandez-Rodriguez, Tribological behavior of borided surface on CoCrMo cast alloy, ***Wear.*** 426–427, 204–211 (2019).

272. F. Chinas-Castillo, J. Lara-Romero, J.F. Jimenez-Jarquin, Tribological Characteristics of Protected Silver Nanoparticles in Oil, ***J. Dispers. Sci. Technol.*** 35,1665–1674 (2014).

273. Y.Y. Wu, W.C. Tsui, T.C. Liu, Experimental analysis of tribological properties of lubricating oils with nanoparticle additives, ***Wear.*** 262, 819–825 (2007).

274. Kariofillis, G. K., Kiourtsidis, "Corrosion behavior of borided AISI H13 hot work steel", ***Surface And Coatings Technology,*** 201 (1–2): 19–24 (2006).

275. Gunen, A., Karahan, I. H., Karakas, M. S., Kurt, B., Kanca, "Properties and Corrosion Resistance of AISI H13 Hot-Work Tool Steel with Borided B4C Powders", ***Metals And Materials International,*** (0123456789) (2019).

276. Telasang, G., Dutta Majumdar, and J., Padmanabham, "Wear and corrosion behavior of laser surface engineered AISI H13 hot working tool steel", ***Surface And Coatings Technology,*** 261: 69–78 (2015).

277. Koneshlou, M., Meshinchi Asl, K., and Khomamizadeh, F., "Effect of cryogenic treatment on microstructure, mechanical and wear behaviors of AISI H13 hot work tool steel", ***Cryogenics,*** 51 (1): 55–61 (2011).

278. H. Ahlatci, Wear and corrosion behaviours of extruded Al-12Si-XMg alloys, ***Mater Lett.*** 62, 3490–3492 (2008).

RESUME

HAMDI ABDULHAMID HASAN RAGHS was born in Darnah in Libya and he graduated first and elementary education in this city. He completed high school education in Osta Omar High School, after that, he started undergraduate program in Sirte University Department of Mechanical Engineering,and he obtain the Bachelor degree in Mechanical and Production Engineering, after that, he started graduate programs in Sheffield Hallam University Department of Mechanical Engineering in October 2007, and he obtain Degree of master of science in Advanced Mechanical Engineering, after that, he started graduate programs in Karabuk University Department of Mechanical Engineering, and he obtain Degree of PhD in Mechanical Engineering in September 2020.

CONTACT INFORMATION

Address: Naci Cakir Mahallesi 753 Sokak 6/7 Dikmen
Cankaya - Ankara - Turkey

Mobile phone: 00905070497431

E-mail: hamdiraghis@yahoo.com